Faculty of medicine and health sciences

Ghent University

2018

TREATMENT of HYDROCEPHALUS with the VENTRICULO-SINUS SHUNT
TECHNICAL and THROMBOTIC CHALLENGES

Edward Baert

Promotor: prof. dr. Dirk Van Roost

Co-promotor: prof. dr. Filip De Somer

prof. dr. Jean-Pierre Okito Kalala

Thesis submitted to fulfill the requirements for the degree of Doctor in Medical Sciences

PROMOTOR

prof. dr. Dirk Van Roost Ghent University, Belgium

Administratively responsible promoter until 30/09/2018

CO-PROMOTOR

prof. dr. Filip De Somer Ghent University, Belgium

prof. dr. Jean-Pierre Okito Kalala Ghent University, Belgium

Administratively responsible promoter from 01/10/2018

DOCTORAL ADVISORY COMMITTEE

prof. dr. Paul Boon Ghent University, Belgium

prof. dr. Rudy Van Coster Ghent University, Belgium

prof. dr. Marleen Praet Ghent University, Belgium

prof. ir. Pascal Verdonck Ghent University, Belgium

EXAMINATION AND READING BOARD

prof. dr. Johan Vande Walle – chairman Ghent University, Belgium

prof. dr. André Grotenhuis Radboud University, Netherlands

prof. dr. Frank Van Calenbergh Leuven University, Belgium

prof. dr. Koen Paemeleire Ghent University, Belgium

prof. dr. Barbara De Moerloose Ghent University, Belgium

prof. dr. Patrick Van De Voorde Ghent University, Belgium

Aan Ellen, Reinhart, Robbrecht en Ophelia

TABLE OF CONTENTS

LIST OF ABBREVIATIONS

ACT	activated clotting time
AE	air embolism
AKA	also known as
ASAH	acute subarachnoid hemorrhage
AV	arachnoid villus
CFD	Computerized fluids dynamic
CM	cisterna magna
CNS	central nervous system
CONG	congenital
C_{out}	conductance
CP	choroid plexus
CR	clot rate
CSF	cerebrospinal fluid
CSH	chronic subdural hematoma
CT	computer tomography
CTRL	control
CVA	cerebrovascular accident
CVP	central venous pressure
DSA	digital subtraction angiography
DVS	dural venous sinus
DVSAD	dural venous access device
EC	endothelial cell
EM NN	electromagnetic neuronavigation
η	viscosity
F	female
FR	CSF formation rate
G	Gauge
HC	hydrocephalus
IC	interpeduncular cistern
ICP	intracranial pressure
ICU	Intensive Care Unit
IJV	Internal jugular vein
IIH	idiopathic intracranial hypertension
IJV	internal jugular vein
IM	intramuscular
IOF	industrieel onderzoeksfonds
IV	intravenous
IZ	impact zone
LP	lumbar puncture
LPS	lumbo-peritoneal shunt
M	male

MMC	myelomeningocele
MR	magnetic resonance
NN	neuronavigation
NNS	neonatal sepsis
NPH	normal pressure hydrocephalus
obstr.	obstruction
$\mathbf{P_{aCO2}}$	arterial partial pressure of carbon dioxide
pat.	patient
PF	platelet function
$\mathbf{P_{IE}}$	dynamic pressure of impact effect
$\mathbf{P_{IZ}}$	impact zone pressure
$\mathbf{P_{SSS}}$	superior sagittal sinus pressure
PU	polyurethane
$\mathbf{P_V}$	venous pressure
Q	infusion rate
ρ	density
reop.	reoperation
RL	Ringer's lactate
ROI	region of interest
$\mathbf{R_{out}}$	resistance to (CSF) outflow
RPM	rotations per minute
RVSS	retrograde ventriculo-sinus shunt
SAS	subarachnoid space
SC	subcutaneous
SEM	surface electron microscopy
SI	Steerable Instruments (company)
SSC	sagittal sinus catheter
SSS	superior sagittal sinus
SST	sagittal sinus thrombosis
ST	survival time
t	time
T	tumor
TBI	traumatic brain injury
TINA	there is no alternative
TJ	tight junction
TR	tumor resection
US	ultrasound / ultrasonography
V	velocity
VAS	ventriculo-atrial shunt
VC	ventricular catheter
VPS	ventriculo-peritoneal shunt
VSS	ventriculo-sinus shunt
$\mathbf{V_{tot}}$	(total) vascular volume or volume of circuit
WZ	wake zone
$\mathbf{\Delta P}$ / $\mathbf{\Delta_P}$	differential pressure / pressure difference

LIST OF FIGURES

CHAPTER 1. CEREBROSPINAL FLUID (CSF) ANATOMOPHYSIOLOGY

CHAPTER 2. HYDROCEPHALUS TREATMENT

CHAPTER 3. VENTRICULO-SINUS SHUNT (VSS)

CHAPTER 4. PROTOTYPING NOVEL 'DURAL VENOUS ACCESS DEVICE'

CHAPTER 5. ANIMAL IN-VIVO STUDY

CHAPTER 6. DISCUSSION & FUTURE OF VSS PROJECT

LIST OF TABLES

CHAPTER 1. CEREBROSPINAL FLUID (CSF) ANATOMOPHYSIOLOGY

CHAPTER 2. HYDROCEPHALUS TREATMENT

CHAPTER 3. VENTRICULO-SINUS SHUNT (VSS)

CHAPTER 4. PROTOTYPING NOVEL 'DURAL VENOUS ACCESS DEVICE'

CHAPTER 5. ANIMAL IN-VIVO STUDY

CHAPTER 6. DISCUSSION & FUTURE OF VSS PROJECT

LIST OF MANUSCRIPTS & PUBLICATIONS SUPPORTING Ph. D.

1. PUBLICATION [Proc Inst Mech Eng H., A1, Q2, IF 0,566, published[1,2], 2008;222(4):455-464]

   Experimental and numerical modeling of the ventriculo-sinus shunt (El Shafei shunt)

   K Van Canneyt[1*†], J Kips[1,2†], G Mareels[1], E Baert[3], D Van Roost[3] and P Verdonck[1]

   [1]Institute Biomedical Technology (IBiTech), Ghent University, Ghent, Belgium

   [2]Department of Pharmacology, Ghent University, Ghent, Belgium

   [3]Department of Neurosurgery, Ghent University Hospital, Ghent, Belgium

2. PUBLICATION, original paper [World Neurosurgery, A1, Q2, IF 2,592, published[3], June 29, 2018]

   Treating Hydrocephalus with Retrograde Ventriculo-sinus Shunt - Prospective Clinical Study

   E. Baert, F. Dewaele, J. Vandersteene, G. Hallaert, J-P. O. Kalala and D. Van Roost

   Department of Neurosurgery, Ghent University Hospital, Ghent, Belgium

3. PUBLICATION [IJ of Artificial Organs, A1, Q2, IF 2,403, published[4], November 04, 2018]

   A new dynamic model for in vitro evaluation of intravascular devices

   E J Baert[1], J Vandersteene[1], F Dewaele[1], A Vantilborgh[3], D Van Roost[1] and F De Somer[2]

   Department of Neurosurgery[1], department of Cardiac Surgery[2], department of Hematology[3] of Ghent University Hospital, Ghent, Belgium

4. PUBLICATION [US Patent No: US 9,402,982 B2, published[5], August 2, 2016]
   Minimally-Advancing Luminal Catheter
   Edward Baert, Frank Dewaele

5. MANUSCRIPT [Veterinary Research Communications, A1, Q1, IF 1,696, submitted[6] and under revision]
   A hydrocephalic goat experimental model to evaluate the efficacy of hydrocephalus treatments
   E. Baert[1], S. Schauvliege[2], J. Vandersteene[1], K. Vandevelde[2], F. Dewaele[1], F. De Somer[3], D. Van Roost[1]
   [1] Department of Neurosurgery, Ghent University Hospital, Belgium
   [2] Faculty of Veterinary Medicine, Ghent University, Belgium
   [3] Department of Cardiac Surgery, Ghent University Hospital, Belgium

6. PUBLICATION [Laboratory Animals, A1, Q1, IF 1,532, published[7], January 2018]
   A non-hydrocephalic goat experimental model to evaluate the ventriculo-sinus shunt
   J. Vandersteene[1], E. Baert[1], S. Schauvliege[2], K. Vandevelde[2], F. Dewaele[1], F. De Somer[3], D. Van Roost[1]
   [1] Department of Neurosurgery, Ghent University Hospital, Belgium
   [2] Faculty of Veterinary Medicine, Ghent University, Belgium
   [3] Department of Cardiac Surgery, Ghent University Hospital, Belgium

7. PUBLICATION [J. Neurosurgery, A1, Q1, IF 4,059, published[8], April 28, 2018]
   The influence of cerebrospinal fluid on blood coagulation and the implications for ventriculo-venous shunting
   J. Vandersteene[1], E. Baert[1], G. Planckaert[2], T. Van Den Berghe[2], D. Van Roost[1], F. Dewaele[1], M. Henrotte[2] and F. De Somer[3]
   [1] Department of Neurosurgery, Ghent University Hospital, Belgium
   [2] Faculty of Medicine and Health Sciences, Ghent University, Belgium
   [3] Department of Cardiac Surgery, Ghent University Hospital, Belgium

INTRODUCTION

Hydrocephalus (HC) is a very common, brain damaging and life-threatening disease. All age groups, from the premature neonatal to the geriatric, may be involved. Only since the late 1950's, with the introduction of cerebrospinal fluid (CSF) shunts in general neurosurgical practice, a reliable and life-saving therapy for many thousands of hydrocephalic patients worldwide became available. At present, the vast majority of these CSF shunts drain towards the peritoneal cavity (about 80 % of shunts are ventriculo-peritoneal or lumbo-peritoneal shunt[9]) or towards the right cardiac atrium (about 10 % of shunts are ventriculo-atrial shunt[9]), a small minority towards the pulmonary pleural cavity, the gallbladder or urinary bladder. In general, these shunts offer correct treatment concerning the devastating CSF accumulation and subsequent threat of brain or optic nerve damage. The risks of the required surgery and possible surgical revisions of the CSF shunt do not outweigh the huge benefits of these CSF shunts. However, a minority of patients (about 3,5% of operative shunt revisions[9]) remains experiencing medical complications requiring multiple reoperations and complaints invalidating social and professional life because of non-physiological intracranial pressures (ICP). The main cause of the inability of present CSF shunts to drain physiologically, concerns the gravitational siphoning effect of their distal catheter when the patient is in an erect (sitting or standing) position. Despite the invention of programmable resistance shunt valves, flow regulating shunt valves and anti-siphon devices, this non-physiological drainage remains an issue. A revival of endoscopic neurosurgery, thanks to technical advancements in the 1980's, made endoscopic third ventriculo-cisternostomy a safe procedure, restoring the physiological CSF absorption in the minor subgroup (8 % of HC surgeries) of 'obstructive' or 'non-communicating' HC patients. But the medical wellbeing of the majority of patients (92% of HC surgeries), suffering of a 'communicating' HC, remains fully dependent of the CSF shunt. Since the beginning of the twentieth century, the neurosurgical community[10] is

aware that shunting CSF towards the dural venous sinuses (DVS) would guarantee a physiological drainage, as this type of shunt would benefit of the anti-siphoning role of the internal jugular vein (IJV). Only, realizing a long-lasting ventriculo-sinus shunt (VSS) remains challenging. Inspired by the retrograde VSS of El Shafei[11,12] and the SinuShunt® of Børgesen and Gjerris[13-15], we wondered why the VSS did not become standard clinical practice. This wondering and the need of a more physiological shunt in our clinical practice, were our main incentives to start the present experimental and clinical work.

CHAPTER 1. CEREBROSPINAL FLUID (CSF) ANATOMOPHYSIOLOGY

1.1 CSF production and absorption

1.1.1 CSF composition and function

In humans, the central nervous system (CNS, i.e. the brain, cerebellum and spinal cord) is embedded in a water bath. This brain water is called cerebrospinal fluid (CSF). Macroscopically, CSF looks like pure spring water, as it is almost acellular (< 5 leucocytes/µl, 0 red blood cells and thrombocytes/ Table 1). Although CSF derives from plasma, their ionogram, protein content, amino acids level and glucose concentration differ significantly.

Table 1. Components of CSF

Average concentrations of various solutes (mEq/kg, unless otherwise specified) in plasma and lumbar CSF of normal human subjects [Source: Adapted from Davson H, Segal MB. Physiology of the CSF and Blood-Brain Barriers. Boca Raton, FL: CRC press, 1996]

Solute	Plasma	CSF	Ratio CSF/plasma
Na^+	150.0	147.0	0.98
K^+	4.36	2.86	0.62
Mg^{2+}	1.61	2.23	1.39
Ca^{2+}	4.70	2.28	0.49
Cl^-	99.0	113.0	1.14
HCO_3^-	26.8	23.3	0.87
amino acids	2.62	0.72	0.27
total protein (mg/dl)	6987.2	39.2	0.0056
glucose (mg/dl)	96.2	59.7	0.62
osmolality (mOsm/kg)	289.0	289.0	1.00
pH	7.397	7.300	-
pCO_2	41.1	50.5	-

1.1.2 CSF functionality

The CSF serves several purposes:

- CNS organogenesis

  During the organogenesis, the CSF pressure is important for the development of the ventricles (Table 2) after formation of the neural tube out of the neural placode[16] and supports the expansion of the brain.

Table 2. Steps of the development of CSF spaces

SAS: subarachnoid space; CP: choroid plexus; SSS: superior sagittal sinus [Source: adapted from L. Saka and J. Chazal[8]]

time after conception	event
1st month	closure of rostral (25th day) and caudal (27th day) neuropores – closure of neural tube, CSF pressure increases in neural tube with increase of the volume of the cephalic extremity → prosencephalon (at 35th day telencephalon and diencephalon), mesencephalon, rhombencephalon and lumen of spinal cord (later canalis centralis)
32nd day	appearance of SAS (only in mammals) at the ventral aspect of the rhombencephalon, later extending caudally and dorsally
41st day	- opening of fourth ventricle and start of CSF circulation - appearance of first CP, in fourth ventricle; the epithelium of the CP is continuous with the ependyma and derived from the neural tube, the leptomeningeal axis is derived from the paraxial mesoderm
14th week	differentiation of the three meningeal layers
26th week	cerebral veins dilate at their outlets in the SSS
35th week	formation of arachnoid villi: the arachnoid stroma lined with endothelium protrudes into the lumen of the SSS via a defect in the dura mater
39th week	appearance of arachnoid granulations, developing until the age of 18 months

- Protection:
    - The CSF offers the CNS a **hydro-mechanical** protection. As a shock absorber it dampens and retards the brain's and the spinal cord's movements caused by the frequent mechanical shocks and jolts in daily life.
    - It provides the brain's **buoyancy**, preventing the weak brain from being compressed under its own weight, as the brain has no internal nor external carrying structure. This neutral buoyancy prevents from compression of blood supply or neurons in the lower sections of the brain. The average weight of the adult brain is 1400 – 1500 g, but suspended in the CSF bath, its relative weight is only 25 – 50 g.
    - The CSF can **compensate for sudden or chronic fluctuations in ICP**, as stated in the Monro-Kellie doctrine (Table 3). During acute ICP rise due to Valsalva maneuver or an acute intracranial hemorrhage, the cranial CSF can extrude from the cranial vault to the spinal intrathecal sac, through the foramen magnum. In case of a progressive intracranial mass (e.g. tumor), the total CSF volume can diminish equally. On the contrary, loss of brain volume will be compensated by an increase of CSF volume.

Table 3. Monro-Kellie doctrine

Monro-Kellie doctrine	**[vol_{brain} + $vol_{intracranial\ blood}$ + vol_{CSF} = constant]**
In a closed skull the intracranial volume is constant due to the fixed cranial dimensions. Or To maintain normal ICP in a closed skull, increase in one of the volumes requests equal decrease of the others.	

- Transport and homeostasis:
    - The metabolic by-products (active molecules and catabolic waste) generated by the activity of the neuronal and glial cells are distributed or evacuated by the CSF flow. The CSF is not only a waste eliminator, but also a distributor of substances. An example of distribution all over the CNS surfaces of biologically active substances as neuroendocrine factors is given by the thyrotropin-releasing hormone from the hypothalamus[17].
    - After its trans-ependymal perfusion towards the ventricles, extracellular fluid is drained via the CSF pathways.
    - The CSF circulation (Figure 1) plays an important role in the electrolyte balance regulation. Not only as a buffer, but also as an afferent conduit of signals that alters regional brain activity: CSF contacting neurons in the circumventricular organs respond to changes in CSF composition[18]. Thus, in mice, changes in CSF sodium (Na^+) concentrations alter water and sodium intake behaviors through the actions of specialized Na^+ channels expressed on neurons in the subfornical organ[19].

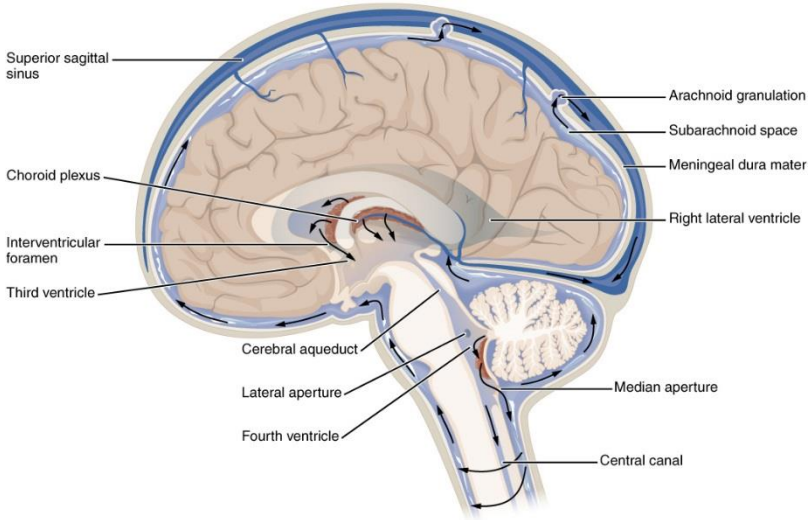

Figure 1. CFS Circulation

[Source: Textbook OpenStax version 8.25, Anatomy and Physiology published May 18 2016]

1.1.3 CSF production

There's a constant refreshment of CSF, at a CSF formation rate of about 0,35 ml/min ± 0,02 ml/min or 504 ml/d. The CSF formation rate is relatively independent of short-term alterations in ICP over a range of 0 – 200 mm H_2O[20]. As CSF is constantly produced, it needs also to be constantly absorbed.

The CSF is produced in the brain's cavities, called ventricles. It's produced by active and passive means:

1.1.3.1 Choroid plexus

The most important production site is the choroid plexus (CP), responsible for **80 – 90%** of CSF production[21-23]. The CP consists of villous folds lined by epithelium, continuous with the ependymal layer, with a central core of highly vascularized connective tissue, with fenestrated capillaries and venules. As the CP is present in all ventricles, CSF is produced in all the brain's cavities covered with ependymal layer.

- The first step of the CP CSF secretion consists of a passive filtration of plasma from the fenestrated capillaries towards the interstitial compartment of the CP. Small molecules like water and ions readily diffuse through the CP vessels but are prevented from reaching the CSF by junctional complexes connecting the epithelial cells.
- Active transport from the interstitial compartment to the ventricular cavity across the choroid epithelial layer is responsible for the second step of the CP CSF secretion. The choroidal epithelial cells produce CSF using active transport dependent upon (1) intracellular carbonic anhydrase process and (2) ATP-driven Na^+/K^+ ion pump at the apical epithelial cell membrane (Figure 2).

  Carbonic anhydrase is an intracellular enzyme that catalyzes the conversion of H_2O and CO_2 into HCO_3^- and H^+. The HCO_3^- and H^+ ions produced are then swapped via the Na^+/H^+ and Cl^-/HCO_3^- exchangers at the basolateral membrane of the

epithelial CP layer. The carbonic anhydrase process can be blocked by acetazolamide (Diamox©), a carbonic anhydrase inhibitor[24,25].

The secretion of the CSF at the apical membrane of the epithelial CP layer is directly influenced by the intracellular Na^+ and Cl^-. At this apical membrane, the active, one-way flux of ions from one side of the epithelial layer to the other, creates an osmotic gradient that is accompanied by the movement of water through aquaporin channels, driven by:

- sodium-potassium-adenosine triphosphatase or Na^+/K^+ ATPase pumps transporting three Na^+ ions out of the cell in exchange of two K^+ ions via energy provided by ATP hydrolysis[26]; this Na^+/K^+ ATPase pump can be blocked by ouabain[25].
- A $Na^+/K^+/2Cl^-$ co-transporter that moves all three of these ions out of the cell and is driven by the intracellular Cl^- gradient.
- Channels for the selective secretion of K^+ and HCO_3^-.

This netto effect of one-way efflux of NaCl and $NaHCO_3$ through the apical membrane of the CP epithelium towards the ventricles, creates an osmotic gradient allowing H_2O outflow through the aquaporins in the basolateral and apical membranes of the CP epithelium into the ventricles.

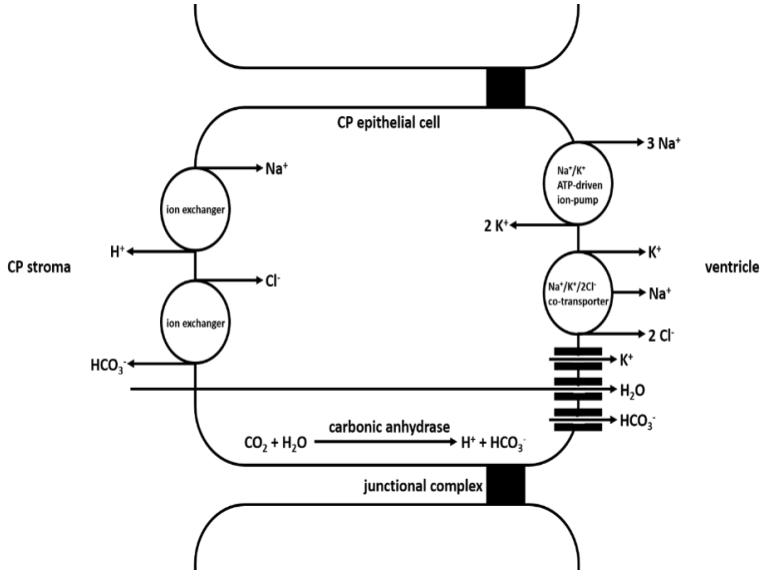

Figure 2. Carbonic anhydrase process

Schematic drawing of carbonic anhydrase process and ionic and water exchanges at the cell membranes of the CP epithelium

The CP CSF secretion volume and composition are finely tuned by several pathways[22,23]:

Increase in ICP will result in decrease of the differential pressure across the fenestrated capillaries in the choroidal stroma, influencing the plasma filtration. However, several studies showed an insignificant influence on the CSF production rate until the ICP becomes markedly elevated. Therefore, CSF formation rate is considered independent of pressure.

The CP receives both cholinergic and adrenergic autonomic nerve fibers. The adrenergic fibers originate almost entirely from the superior cervical sympathetic ganglia and adrenergic stimulation leads to an acute reduction of CSF production of 30 percent. Parasympathetic cholinergic stimulation can increase CSF production up to 100 percent.

Multiple receptors for monoamines and neuropeptides have been identified on the apical choroidal epithelial surface and will influence CSF production and/or absorption at CP level: dopamine, serotonin, melatonin, atrial natriuric peptide and arginine vasopressin receptors. E.g., atrial natriuric peptide and arginine vasopressin decrease CP CSF production.

1.1.3.2 Extra-choroidal CSF source

The extra-choroidal CSF source is responsible for about **10 – 20 %** of the CSF production and arises as a bulk flow of the cerebral interstitial/extracellular fluid and cerebral capillaries[23]. There's a constant diffusion of fluids through the ventricular wall, called the ependymal layer[27,28]. The ependymal layer lacks resistance to free exchange between the ventricular and extracellular fluid. Furthermore, the extracellular and ventricular fluid have a similar composition. This diffusion process is bidirectional. In HC CSF can be diffused from the ventricles to the extracellular layer causing trans-ependymal diffusion, recognized as trans-ependymal drainage on CT scan or MR imaging, with signal changes in the white matter around the frontal and occipital ventricular horns.

The total CSF volume in healthy adults (Table 4) is about 140-270 ml, in newborns approximately 50 ml. About 25 percent of this CSF volume fills the ventricular system, the rest circulates in the subarachnoid space, the basal cisterns, and around the spinal cord in the thecal sac of the spinal canal.

Table 4. Intracranial volumes

Intracranial volumes (in ml), based on MR imaging of 42 schizophrenic patients and 43 normal controls (Gur RE et al.)[29]

total cranial volume	**1051,7 ± 86,9 SD**	**range 939 – 1183**
total cranial CSF volume	164,5 ± 47,8 SD	range 62,2 – 267
intraventricular volume	31,9 ± 17,8 SD	range 7,49 – 70,5
third ventricle volume	0,95 ± 0,62 SD	range 0,26 – 2,40
subarachnoid volume	132,6 ± 43,2 SD	range 54,7 – 220,8

1.1.4 CSF circulation

As the CSF is produced in all four ventricles, it has to flow from the left and right lateral ventricles through both foramina of Monro to reach the third ventricle. From the third ventricle the CSF passes through its longest and narrowest pathway, the aqueduct of Sylvius, into the fourth ventricle which possesses 3 foramina (median foramen of Magendie and bilateral foramina of Luschka) to then stream out of the ventricular system into the SAS of the posterior fossa[30]. In the SAS part of the CSF will pass the foramen magnum down to the spinal thecal sac and part will stream around the brainstem into the arachnoid cisterns and further cranially towards the SAS of the external cerebral surface, the supratentorial arachnoid cisterns and finally towards the

arachnoid villi and granulations, where it will be absorbed in the venous system. Mixed with the venous blood, further evacuation happens through the DVS, towards the jugular bulbs, bilateral IJV, superior caval vein and finally in right cardiac atrium. Part of the CSF that streamed towards the spinal thecal sac will return cranially, part will be absorbed at spinal level.

The principal powers of this CSF propulsion are the differential pressures between the ventricles, between the intraventricular cavities and SAS and between the SAS and the venous system. This differential pressure is generated by the continuous production of CSF and the points of resistance on the pathway (foramina of Monro, aqueduct of Sylvius, foramina of Luschka and foramen of Magendie), ensuring a slight differential pressure between the ventricles itself, each time in favor of the more proximal ventricle. This combination is responsible for the net direction of the flow from the ventricles towards the SAS and arachnoid villi and granulations.

The flow rate and dynamics are heavily influenced by the brain's pulsations caused by the systolic arterial dilatation[31,32].

1.1.5 CSF absorption

1.1.5.1 Arachnoid villi and granulations

Absorption of the CSF occurs mainly through the arachnoid villi and the arachnoid granulations. Arachnoid villi are microscopic arachnoid epithelium protuberances not only into the DVS but also into the cerebral cortical veins proximal to their injection in the DVS and the radicular veins to the spinal venous plexus[33,34]. The arachnoid granulations (a.k.a. bodies of Pacchioni or pacchionian bodies) are macroscopic arachnoid epithelium protuberances into the dural venous sinuses, mainly the superior sagittal sinus (SSS). These arachnoid villi and granulations allow bulk flow of the subarachnoid CSF towards the venous blood stream. The only proven force responsible for this CSF efflux is the differential pressure between the subarachnoid space (i.e. the

ICP) and the venous structure (i.e. the SSS pressure or P_{SSS}). To initiate and maintain this bulk flow, the required pressure gradient is between 50 - 70 mm H_2O in favor of the CSF compartment[35]. The combination of constant CSF secretion and the constant resistance to CSF outflow creates the basal ICP, which is 'disturbed' by both the arterial pulse and the changes in thoracic pressure due to respiration (Figure 6).

Also the arachnoid villi in spinal subarachnoid space, along spinal nerve root dural sheets, protruding into spinal root venous branches and into the spinal venous complex, play an important role in CSF evacuation. With radionuclide cisternography by lumbar puncture (LP) in 34 healthy young adults, spinal CSF absorption was estimated 0,11 – 0,23 ml/min, with an increased spinal absorption activity in the active group versus the resting[33]. In man, the spinal villi are probably absorbing 15 % of the CSF[36].

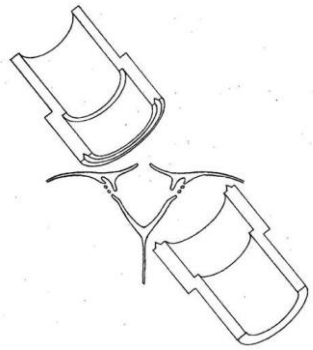

Figure 3. Drawing of the test of flow direction

Test of flow direction over the presumed arachnoidal microscopic valves, of differential pressure required to open the valves [measuring their resistance to CSF outflow] and of the (linear) relationship between differential pressure and flow rate) [Source: Welch K., Friedman V.[23]]

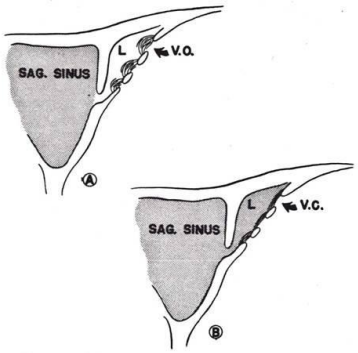

Figure 4. Arachnoidal microscopic valvular action

Schematic drawing - interpretation of the presumed arachnoidal microscopic valvular action at the venous lacunae of the SSS (L: lacuna; VO: open valves; VC: closed valves) [source: Welch K, Friedman V.[35]]

As the arachnoid villi and granulations are fully covered by the venous endothelium, with very resistant intercellular tight junctions, the question how the trans-endothelial CSF efflux was established, lived for decades. The discussion whether an osmotic filtration or seepage process[37,38], a microscopic valved canalicular system[35] (Figure 3 and Figure 4) or a transcellular vacuolization action responsible for the CSF absorption at the arachnoid villi and granulations level, lasted until 1974, in favor of the transcellular vacuolization process[39,40]. Electron microscopic studies proved this transcellular vacuolization process resulting in endothelial intracellular vacuoles and even trans-endothelial pores, up to a width of 1 – 2 µm. Also was proved that raised differential pressure increased the number and size of the vacuoles and pores and vice versa, that no vacuoles nor pores were evident at negative or reduced differential pressure[40].

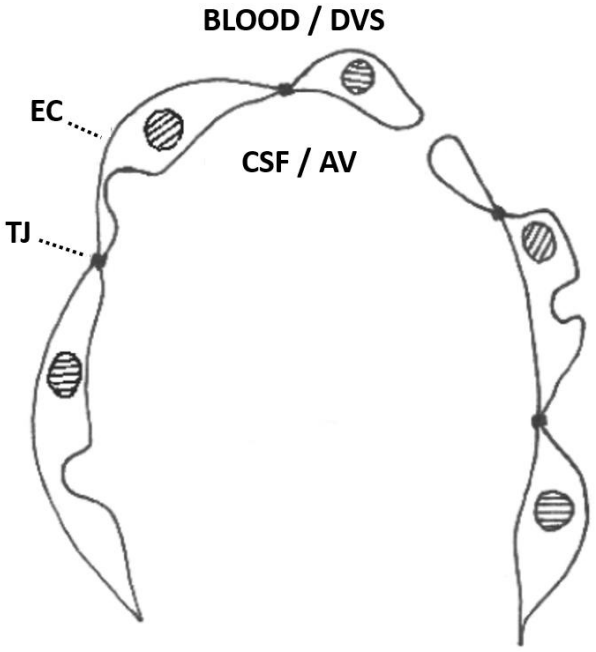

Figure 5. Endothelial vacuolization process at arachnoid villus

Schematic drawing of dynamic vacuolization process at the endothelial layer of arachnoid villus (AV: arachnoid villus; EC: endothelial cell; TJ: tight junction; DVS: dural venous sinus; CSF: cerebrospinal fluid) - [personal adaptation of Tripathi & Tripathi[39]].

1.1.5.2 Alternative mechanisms of CSF absorption

Although the CNS is considered devoid of a **lymphatic system**, in mammals and humans a CSF evacuation towards extra-cranial lymphatic vessels (at paranasal, cervical and paraspinal levels) has been proven[41]. The subarachnoid space is continuous with the dural sleeves around the olfactory, optic, trigeminal, acoustic and spinal nerves. CSF is able to pass into the connective tissue around the cranial and spinal nerve roots and is then absorbed by local lymphatic channels. This lymphatic CSF drainage pathway has been extensively studied in mammals and is considered to be responsible for up to 30 – 50 % of the CSF absorption. In humans, the relative importance of this lymphatic seems less important and needs further investigation to be determined. In humans the CSF-nasal lymph connection - at the nasal submucosa - through the cribriform plate of the ethmoid bone, was nicely confirmed[42]. As in fetus and neonates the arachnoid villi and granulations are still non- or underdeveloped (Table 2), extra-cranial lymphatic vessels may play an important role in CSF absorption[43].

The **CP** is not only a source of CSF, it's also capable of absorbing specific compounds from the CSF[21]. In vitro and in-vivo studies demonstrated the evacuation of penicillin and organic acids injected into the subarachnoid space and specific CP membrane carriers have been recognized.

There's ample evidence that CSF and interstitial fluid continuously interchange. This exchange of fluids is facilitated by 2 processes:

- Slow **transependymal** diffusion process depending on hydrostatic and osmotic forces.
- Rapid convective processes at the **glymphatic system**[44,45] play the role of the CNS devoid *lymphatic* system and the astrocytic *glial* cells form its boundaries. In the latter, the CSF of the cortical SAS is driven along the perivascular space of the brain penetrating arterioles and capillaries in between the vessel's wall and the surrounding pia mater. At vascular branching points, the perivascular space widens

and forms Virchow-Robin spaces. These perivascular spaces are surrounded and delineated by astrocytic vascular endfeet. At the level of capillaries and venules, where fluids and metabolites exchange happens, an extracellular matrix is formed by a basal lamina, surrounded by astrocytic vascular endfeet expressing aquaporin-4. The major role of the glymphatic system seems to be clearance of excess of interstitial fluid and transport of metabolites and solutes, e.g. the evacuation of beta-amyloid and tau. The concept of glymphatic system is recent and still under investigation. Along the perivenous glymphatic system metabolites and fluids are evacuated towards the meningeal lymphatic vessels (e.g. lymphatic vessels alongside the SSS) through the cribriform plate towards the paranasal submucosal lymphatic system[46].

1.2 Intracranial Pressure (ICP)

Creating ICP is a dynamic process that is due to the combination of continuous CSF production and constant resistance to CSF outflow towards venous and lymphatic systems. Because the differential pressure between the SAS and the dural veins remains stable in every physiological state, the dural venous pressure - determined by the abdominal, thoracic and cervical venous pressure - is the most determining factor of the absolute ICP value. Some authors refer to this as the Monro-Kellie doctrine 2.0[47].

Table 5. Literature review of ICP, CSF formation and absorption, rate and P_{SSS}

Summary of ICP, CSF Formation rate, P_{SSS}, CSF absorption rate studies in patients or normal individuals. Authors state no sex differences in variables nor any age dependence

	Masserman (1934)	Masserman (1935)	Spina-Franca (1963)	Tourtelotte (1964)	Cutler[20] (1968)	Shulman (1964)	Ekstedt[48] (1978)	Børgesen[49] (1982)	Albeck[50] (1991)	Edsbagge[33] (2004)	Avery[51] (2010)
	284 normal humans	200 normal humans	1500 patients	105 normal humans	11 patients 4-13y		58 patients 15-83y	80 NPH patients	8 normal young adults	34 healthy humans 21-35y	197 patients 1-18y
	(LP)	(LP)	(cisterna magna)	(LP)	(V-LP)		(LP)	(V-LP)	(LP)	(LP)	(LP)
ICP ($cm\ H_2O$)	14,8 ± 0,2	15,1 ± 0,2	11,9 range: 4,1 - 19,7	15,0 ± 3,3		14,7	14,08 ±1,9		14,9 6	13,6 ± 3,1	19,8 ± 6,8 P90: 25 P10: 11,5
CSF formation rate (ml/min)					0,35 ± 0,02		0,4 ± 0,08			0,34 ± 0,13	
ICP - P_{SSS} differential pressure ($cm\ H_2O$)							3,77 ± 1,02				
sagittal sinus pressure ($cm\ H_2O$)						9,03 torcular: 4,6	10,2 ± 2,04				
minimal ICP pressure to start CSF absorption ($cm\ H_2O$) [if ICP increases up to 25 → linear AR increase up to 1,5 ml/min]					6,8 FR = AR at 11,2						
spinal CSF absorption rate (ml/min) [more pronounced in active than in resting individuals]										0,11 – 0,23	
R_{out} ($mm\ Hg \times min \times ml^{-1}$)							< 8,33	< 12,05	< 9,10		

1.2.1 Measuring ICP

At present, we have 3 - invasive - methods to reliably measure ICP (compared to the atmospheric pressure):

1.2.1.1 Lumbar puncture

Allows measurements for a short period, through a LP needle (more reliable) or through an intrathecal catheter (less reliable) introduced through the LP needle. The LP needle or the intrathecal catheter can be connected with a manometric water column for very short term measurement or with an external pressure transducer to allow longer periods and registration of the measurements (Figure 6), or to perform infusions during measurements, e.g. to determine the resistance to CSF outflow (R_{out}) (Table 5).

Advantages

- Minimal invasive and cost effective
- Requires only short hospitalization (1 day clinic or 1 night of stay-over).

Disadvantages:

- Only indicated for measurements of a short period, especially when the LP needle is used.
- Risk of overestimation of the ICP, especially in case of using a LP needle, due to inadequate "relaxation" of the patient (pain, anxiety, forced positioning).
- Risk of underestimation of the ICP, especially in case of using an intrathecal catheter, due to possible leakage of CSF in between the catheter and the punctured dural sac.
- The patient has to remain in a horizontal position, lateral recumbent or supine.
- Possible 'post-puncture' cranial hypotension complications.
- In cases of intracranial hypertension due to tumor or edema, risk of causing uncal or tonsillar herniation and therefore potentially life-threatening in these indications.

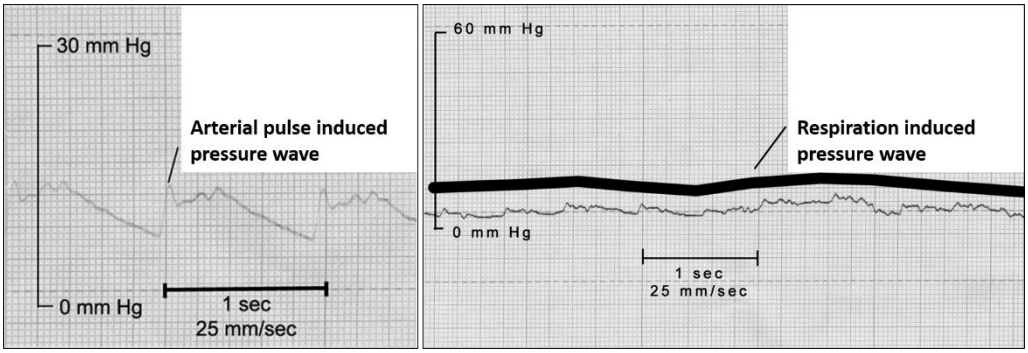

Figure 6. 'Old school' ICP registration on thermic paper

Nicely demonstrates ICP being influenced by respiration and by cardiac-arterial pulsations.

1.2.1.2 Ventricular catheter

Ventricular catheter connected with an external pressure transducer (Figure 7).

Advantages

- Long-term reliable ICP-measurement (up to periods of weeks), allowing evacuation of CSF in cases of intracranial hypertension; therefore, extremely useful in an ICU setting both as a therapeutic and monitoring mean.
- Patient can be positioned as required (pressure transducer and dripping chamber need to remain positioned in level with the reference point = center of the head; in our hospital we use the external acoustic meatus, for ease of use).
- Frequent and rapid recalibration of the system in relation to the atmospheric pressure.
- Can be applied and life-saving in cases of severe intracranial hypertension due to tumor, bleeding, edema, …, reducing the risk of uncal or tonsillar herniation.

Disadvantages

- More invasive (requires surgical procedure, including a skull bone burr hole and a transcerebral trajectory) and prone to complications (e.g. intracranial hemorrhage).

- Higher risk of CNS infection, especially when long-term (i.e. 8 days or more) monitoring on ICU and in case of frequent CSF sampling[52-54]. Most common pathogens causing meningitis are coagulase negative Staphyloccus (56%), followed by Staphyloccus Areus (25%), Staphylococcus epidermidis and others.
- Agitated and inadequate patients may pull out the catheter.

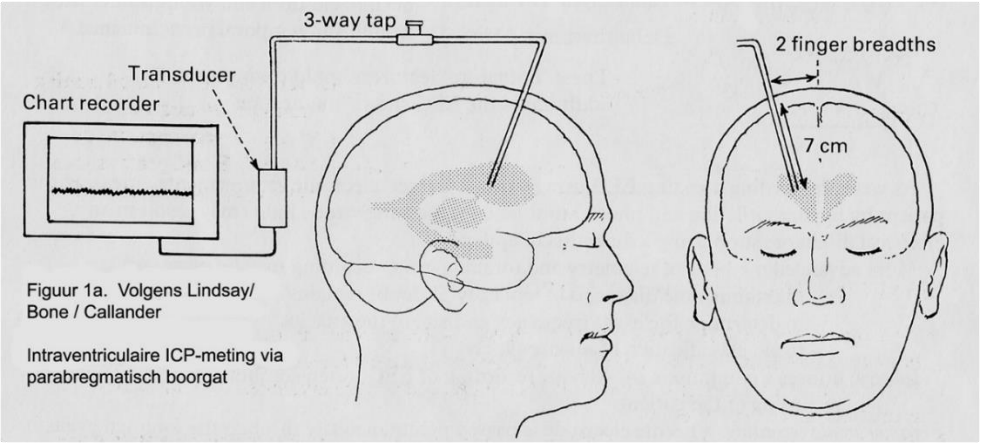

Figure 7. Drawing position frontal external ventricular drain for ICP monitoring
[Source: Lindsay / Bone / Callander]

1.2.1.3 Parenchymal micro-sensor

e.g. Codman MicroSensor®, Integra Camino® (Figure 8), Sophysa Pressio®):

Advantages

- Do not require intraventricular positioning, intrathecal cranial position (most often in right cerebral frontal lobe) is sufficient; thus, can be used in cases of reduced ventricular sizes (severe cerebral edema, severe brain shift …).
- These sensors have a smaller diameter and a shorter intracerebral trajectory than the ventricular catheter. Consequently, they are less invasive and less prone to the risk of intracranial hemorrhage, interesting in patients with clotting disorder.

Figure 8. Camino parenchymal ICP sensor in right frontal lobe

In horizontal supine position ICP 8, in 30° flexed supine position -4 and in sitting position -7 mm Hg were measured, indicating correct CSF shunt functioning.

Disadvantages

- Their high cost (in Belgium: above € 400,00 taxes excluded and not refunded by our social security system, RIZIV / INAMI).
- Not reliable in the long term:
  - Present sensors are fragile, rapid internal mechanical interruption can occur.
  - They allow no recalibration; only at the moment of surgical introduction, calibration with the atmospheric pressure is possible.
  - Parenchymal micro-sensors do not allow evacuation of CSF for diagnostic or therapeutic reasons.

1.2.1.4 Telematic readable micro-sensors

Since a few years, telematic readable and fully implantable ICP measurement devices were made commercially available.

Advantages

- Measurements can be registered in any position or during any physical activity of the patient, hospitalized or discharged.
- As the devices are fully implanted, risk of infection is reduced (estimated at the same level as of a CSF shunt procedure).
- Measurements can run over much extended periods – in case of the Neurovent-P-tel of Raumedic® (Figure 9), the device has to be removed within 1 month after implantation; in case of the Miethke-Aesculap® Sensor Reservoir (Figure 10), the device can remain implanted and correct measurement is guaranteed for a period of 3 years.
- In case of the Miethke-Aesculap® Sensor Reservoir, the device can be integrated as a Rickham reservoir in a CSF shunt system, which is not the case for the Raumedic® Neurovent-P-tel.

Disadvantages

- Both devices have a very high cost (around € 3000,00 TVA excluded) and are not RIZIV / INAMI reimbursed).

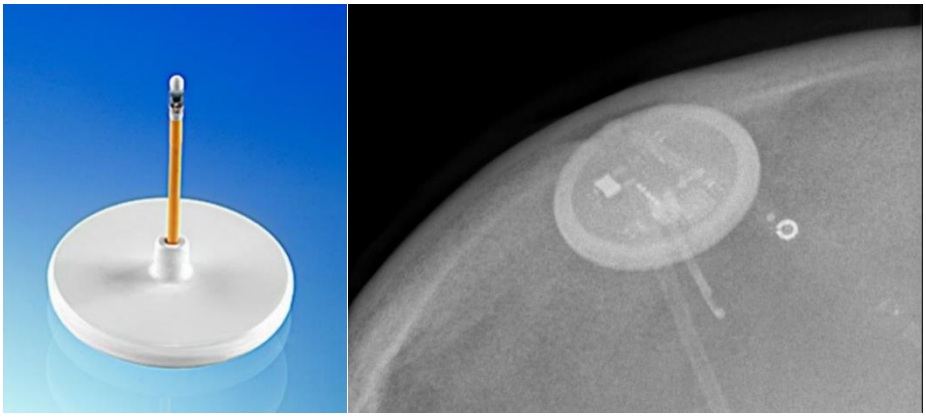

Figure 9. Raumedic© Neurovent-P-Tel parenchymal ICP micro-sensor

(Left) photograph of the device [source: Raumedic©, Germany] and (right) X-ray of implanted device

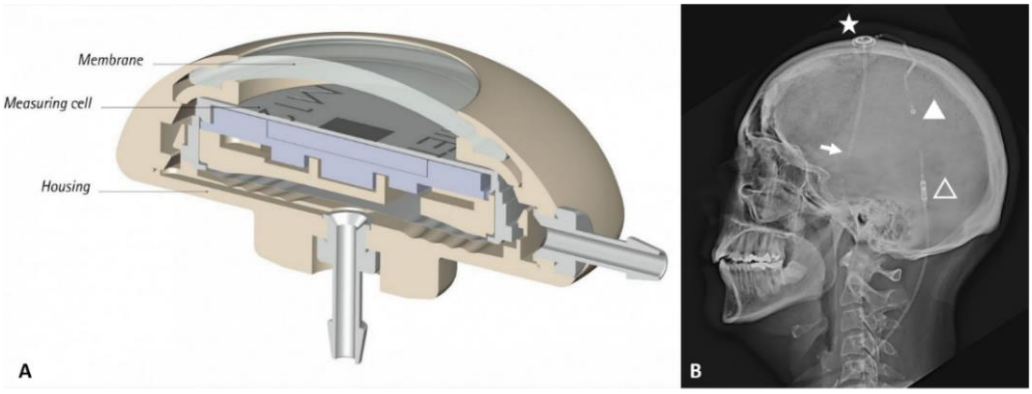

Figure 10. Miethke-Aesculap© Sensor Reservoir

(A) Technical drawing [source: Miethke-Aesculap©] and (B) skull X-ray of in CSF shunt integrated Sensor Reservoir (white asterisk: Sensor Reservoir; white arrow: tip of ventricular catheter; solid white triangle: Codman Hakim programmable CSF shunt valve; open white triangle: Miethke antisiphon device, ShuntAssistant)

1.2.2 Correlation between ICP and CSF formation / absorption

As the CSF absorption flow rate is proportional to the pressure gradient between the SAS and the DVS[20] (in a linear relation), it follows Poiseuille's law (Table 6), leading to the following equation[36,55,56]:

Table 6. Poiseuille's law of flow rate

FR = CSF formation rate, expressed in ml/min; $\Delta \boldsymbol{P}$ *= differential pressure between start and end of a tube, expressed in mm Hg, i.e. differential pressure between ICP and* P_{SSS} *(pressure in superior sagittal sinus);* $\boldsymbol{\pi}$ *= mathematical number pi; r = radius of a tube; l = length of a tube;* $\boldsymbol{\eta}$ *= viscosity of the fluid (CSF); 8 = constant;* R_{out} *= resistance to CSF outflow, expressed in mm Hg × min ×* ml^{-1} *[i.e. the reciprocal value of conductance to CSF outflow (*C_{out}*) or* $R_{out} = 1 / C_{out}$*]; ICP -* P_{SSS} *equals the differential pressure*

$$\text{flow rate} = \frac{\Delta P \times \pi \times r^4}{l \times \eta \times 8}$$

which means that:

$$\frac{\pi \times r^4}{l \times \eta \times 8} = C_{out} \text{ or its reciprocal value } \frac{1}{R_{out}}$$

which concludes that in a ventriculo-subarachnoid system:

$$\textbf{CSF flow rate} = \frac{\mathbf{ICP - P_{sss}}}{\mathbf{R_{out}}}$$

CSF production and absorption have to remain in balance in order to maintain a correct ICP. This balance is clearly expressed by the Davson[55] equation (table 7).

Table 7. Davson[55] equation

FR (CSF formation rate) expressed in ml/min and equals the AR (CSF absorption rate) in the normal (i.e. non-hydrocephalic)

$$ICP = (FR \times R_{out}) + P_{SSS} = (AR \times R_{out}) + P_{SSS}$$

During a LP on a patient in lateral recumbent position using a manometer connected on the LP needle and performing an infusion test, the ICP and R_{out} can easily be measured[36,49,57,58]. Even an estimation of the FR can be realized, using the Masserman[59] manometric technique. The first and simplest LP infusion test, the constant rate infusion test, a.k.a. Katzman test[57], allows to calculate the R_{out} with the simple equation (Table 8).

Table 8. R_{out} equation during Katzman test

P_1 = opening ICP, before start of infusion test; P_2 = new ICP during the infusion, reached when formation rate and absorption rate balance re-established [both P-values expressed in mm Hg]; $\boldsymbol{FR_1}$ = formation rate before the start of the infusion; $\boldsymbol{FR_2}$ = formation rate during the infusion test [both FR-values expressed in ml/min]; $\boldsymbol{FR_2 - FR_1}$ equals the infusion rate, as is observed that the CP CSF formation rate remains stable during short periods of ICP modulation

$$R_{out} = \frac{P_2 - P_1}{FR_2 - FR_1}$$

1.3 Pathophysiology of hydrocephalus (HC)

1.3.1 Definition of HC

It's already mentioned that the balance between CSF production and CSF absorption is essential in preserving and determining physiological ICP. In HC this balance is disturbed in disfavor of the absorption of CSF, meaning that the formation overwhelms the absorption. In almost all cases (> 99 %), HC is caused by a absorption impediment, as in normal physiological conditions, the absorption capacity is 4 to 5 times higher than the standard CSF production rate[20].

This leads to the definition of HC:

Active HC is a medical condition in which the balance between CSF production and CSF absorption is disturbed, the production overwhelming the absorption, causing a *progressive* increase of the ICP and a *progressive* dilatation of the ventricular dimensions.

It is important to state that dilated ventricles congenital or due to loss of brain tissue (arrested/treated HC, brain atrophy, post-CVA brain loss, post-surgery …) is not a HC condition, but a 'ventricular dilatation ex vacuo'. In many cases of ex vacuo ventricular dilatation, certainly in general brain atrophy, also a widening of the cerebral sulci and the SAS occurs (Figure 11 and 12). On the contrary, small or normal sized ventricles do not exclude active HC.

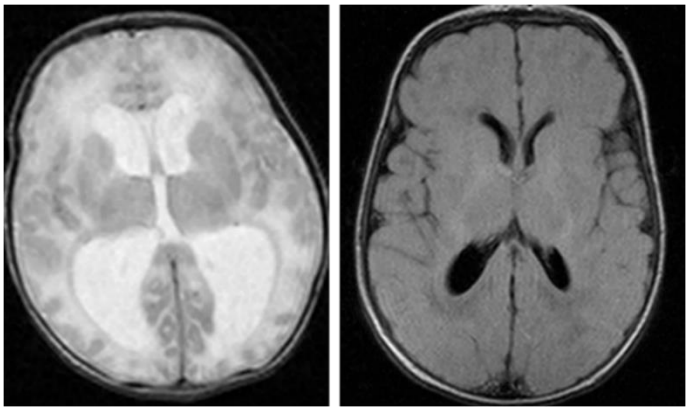

Figure 11. MR scan of 2 patients suffering HC
(Left) with clearly widened ventricles; (right) only slightly ballooned; it is not the size but the evolution of ventricles that's indicative of active HC.

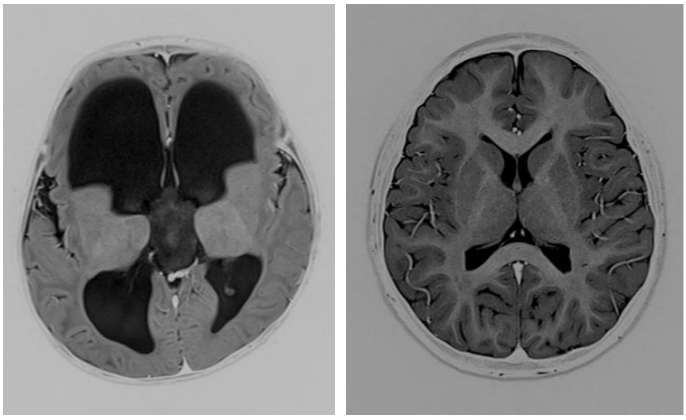

Figure 12. MR scans of 2 patients free of HC
(Left) dilated ventricles, but not ballooned, in a patient with cured HC thanks to an endoscopic third ventriculo-stomy; (Right) normally sized and non-ballooned ventricles of normal individual

1.3.2 Classification of HC

Some authors[60] state that the in general used terms of communicating and obstructive or non-communicating HC[30,61,62] are misleading, though in clinical practice very useful. In agreement with Rekate's provocation to debate, the following classification is suggested (Table 9):

Table 9. Classification hydrocephalus (personal suggestion)

CLASSIFICATION OF HYDROCEPHALUS	AKA
TYPE A HC by **A**rachnoid CSF flow impediment	communicating HC
TYPE V HC by **V**entricular outflow obstruction	obstructive HC
TYPE AV HC by combined **A**rachnoid and **V**entricular flow obstruction	complex HC
TYPE C HC without obstruction	HC by **C**horoid plexus pathology

1.3.2.1 HC by arachnoid CSF flow impediment

This group represents by far the largest group, around 84,3 %[63] of HC patients. As the name suggests, these patients have a free outflow of the CSF out of the ventricles, but are touched by an impediment of the CSF circulation in the SAS or by an obstruction of the CSF through the arachnoid villi and granulations. Classical examples are the patients with acquired HC because of a subarachnoid, intraventricular or traumatic intracranial hemorrhage, because of an intracranial bacterial / fungal / yeast infection, and the majority of the patients with postoperative HC.

Subgroups:

- Premature neonates suffering of an intraventricular 'matrix' hemorrhage, suffering of temporary or ongoing HC. At our institution, these patients are initially treated with evacuative CSF punctures through a Rickham reservoir connected to a ventricular catheter. The majority develops a 'spontaneous' recovery of the CSF absorption, the minority will need the placement of a CSF

shunt (possibly because of the ongoing development of the arachnoid villi and granulations until the age of 18 months).

- congenital CNS malformations with high incidence of HC
    - spina bifida aperta (myelomeningocele, encephalomeningocele)
    - Dandy-Walker malformation
- At the other end of the life-spectrum, are the normal pressure HC (NPH) patients. Up to now etiological questions remain, rather indicating multifactorial answers. The conditions we rely on to indicate a CSF shunt are:
    - progressive development of the Hakim triad (broad based gait disturbance / balance problems + short term memory dysfunction + urinary incontinence)
    - MR and/or CT scan indicative of NPH (dilated supratentorial ventricles + signs trans-ependymal CSF drainage at frontal and posterior ventricular horns, absence of distinct generalized cerebral atrophy)
    - evacuative LP with temporary improvement of the Hakim triad manifestations
    - infusion test through LP indicative for raised R_{out} (i.e. > 14 mm Hg × min × ml^{-1})
    - absence of evidence for: other type of dementia, pronounced cardiovascular / hepatic / pulmonic / renal / oncologic disease or clotting disturbance

1.3.2.2 HC by ventricular CSF outflow obstruction

This group, about 15,7 %[63] of HC patients, is very inhomogeneous. The outflow obstruction can be congenital, tumoral / cystic, intra- or extra-ventricular … Classic examples are (non-limitative list):

- aqueductal stenosis
    - congenital (X-linked)
    - diffuse peri-aqueductal brainstem glioma

    - tumor or cyst in supra-quadrigeminal cistern / pineal region compressing the aqueduct
    - tumor or cyst in posterior part of third ventricle, at proximal opening of aqueduct

- stenosis of foramen of Monro (uni- or bilateral)
    - colloid cyst on third ventricular roof
    - widened cavum septum pellucidi or cavum septum virgae
    - tumor in anterior part of third ventricle (e.g. germinoma)
    - suprasellar arachnoid cyst

- third ventricular obstruction
    - thalamic tumor
    - lateralized lesion with important mass effect (hemorrhage, tumor, sylvian arachnoid cyst, cerebral edema, …)

- fourth ventricular obstruction
    - large posterior fossa tumor or cyst with obliteration or compression of ventricle
    - arachnoidal occlusion of foraminal outflow of fourth ventricle
    - compression of fourth ventricular foramina (e.g. pronounced Chiari-malformation or Arnold-Chiari-malformation, osteopetrosis of the skull, achondroplasia, …)

- localized (partial) ventricular obstruction:
    - cystic (e.g. choroidal cyst in temporal or posterior ventricle horn)
    - tumor (e.g. central glioma or meningioma at trigone of lateral ventricle in adults, supratentorial ependymoma or ATRT or CP tumor in young children)

1.3.2.3 HC by combined SAS and ventricular CSF outflow obstruction

This is a complex form of HC as encountered in patients who suffered severe meningitis combined with ventriculitis, especially those caused by fungal or Escheridia Coli-like bacterial contaminations. Typical examples are patients with infected external ventricular drains, patients suffering bacterial sepsis because of colonized cardiac valves, colonized arteriovenous anastomosis for hemodialysis, uncontrolled osteomyelitis. Typical pediatric patients are those with a breakthrough mastoiditis or sinusitis, exacerbating pneumococcal or hemophilus influenza subdural empyema, congenital cutaneo-thecal fistula (sacro-lumbal, naso-ethmoido-frontal …). Rarely important hemorrhagic incidents with intraventricular extension or breakthrough are responsible for such complex HC.

The treatment of this group requests in most cases a combination of endoscopic fenestrations of the intraventricular occlusive reactive septa followed by a CSF shunt. The endoscopic fenestrations aim to reduce the required number of ventricular catheters, preferentially to a single one (Figure 13). One of the most challenging example of this group, is the trapped fourth ventricle HC[64,65]. In most cases, the availability of optimal preoperative MRI study and operative neuronavigation guidance is essential for success.

Figure 13. X-Ray of multilocular hydrocephalus treated with multiple ventricular catheters

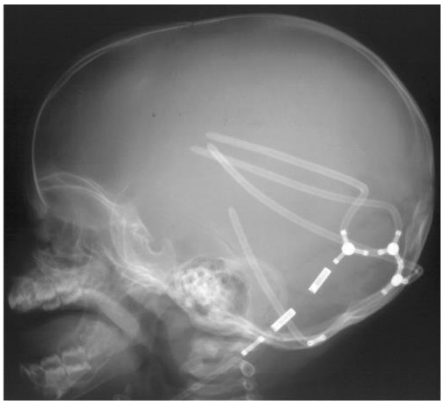

1.3.2.4 HC without obstruction

Only the very rare group of patients suffering villous hypertrophy of the CP, or CP tumor can develop HC caused by a CSF production rate surpassing the physiological capacity of CSF absorption. In our patients groups even the CSF shunt drainage capacity was overwhelmed by the CSF overproduction.

Not to be included in the condition of HC are:

- *benign external HC*

  These infants do not suffer of HC, but have a raised compliance of the cranial structures, possibly combined with a not yet optimal development of the arachnoid villi and granulations, leading to a too rapid expansion of the head circumference. Their prognosis is excellent, not requesting surgical intervention. Important tools to recognize this condition are:

  - On imaging a (very) wide SAS is recognized, generally with normal or only slightly enlarged ventricles.
  - On clinical examination and follow-up: normal psychomotorical evolution, absence of clinical and hetero-anamnestic signs of intracranial hypertension, stagnation of the progressive deviation on the head circumferences (mostly between 14 - 18 months of age).

- *pseudotumor cerebri or idiopathic intracranial hypertension (IIH)*

  This group of patients have a proven intracranial hypertension without any sign of HC on medical imaging. Most often with clinical manifestation of visual impairment due to papillary edema, quite often with complaints of headache, fatigue, concentration and learning impairment and sometimes with tinnitus, vertigo or dizziness. Treatment with a CSF shunt is an option if medication fails[66-68].

1.3.3 Clinical aspects of HC

The clinical aspects of HC are age-dependent (Table 10). The infant group with absence of fused cranial sutures (high compliance of cranial structures) should be differentiated of the pediatric & adult group with closed cranial vault (low compliance of cranial structures and following the Monro-Kellie hypothesis (Figure 1).

As long as an expansion of one of the three volumes is compensated by an equal reduction of the 2 other volumes, the patient's ICP remains under control and the auto-regulation system of the cerebral blood perfusion functions. However, these volume shifts provide limited compensation and increasing ICP leads to decreasing compliance (Figure 14). Once the compensation mechanisms are exhausted (e.g. venous compression impeding cerebral venous outflow towards SSS), a little extra volume expansion will cause an uncontrollable ICP raise, with loss of the auto-regulation and putting the cerebral blood perfusion pressure into jeopardy[69,70].

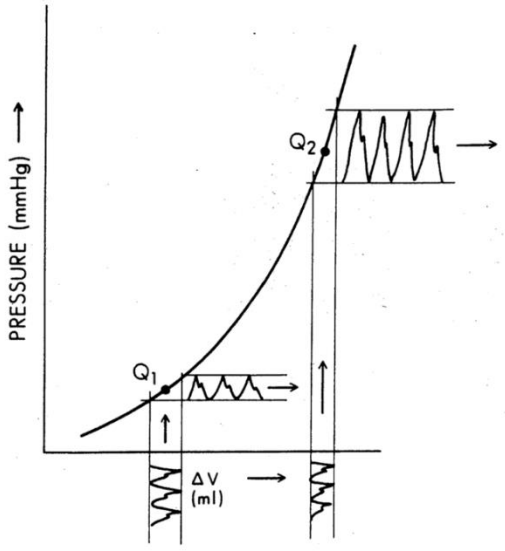

Figure 14. Volume-pressure curve

Q_1 represents the initial resting pressure level, Q_2 the resting pressure level at an increased steady-state ICP. Because of the reduced compliance at Q2, the pulsatile components of the ICP increase in magnitude. [source: Marmarou A. et al, J. Neurosurg., vol. 43, Nov. 1975]

This shift in volumes plays an major role in the cranial compliance. The cranial compliance is expressed / measured by the raise of the ICP caused by the raise of one

of the intracranial volumes[71,72]. This compliance can be estimated by rapid infusion of a fixed volume of CSF through a LP needle or an intraventricular catheter:

$$\textbf{compliance} = \frac{\Delta \mathbf{V}}{\Delta \mathbf{P}}$$

Table 10. Symptoms occurring with ongoing ICP increase in uncontrolled HC (personal suggestion)

List of symptoms during observation and clinical examination - this list is indicative, not limitative.

INFANT (open fontanel and sutures) rather slowly progressive symptoms (cited from mild till life-threatening)	**CHILD & ADULT (fused cranial sutures) rather fast progressive symptoms (cited from mild till life-threatening)**
diminished appetite	headache
irritability - frequent crying - uncomfortable	fatigue, concentration disturbance
(full anterior fontanel)	reduced appetite, nausea
vomiting - intake refusal	vomiting
less active - passivity	visual complaints: double vision, blurred vision; less frequent: sunrise phenomenon
eye movement disturbances e.g. sunrise phenomenon or sign of Parinaud	agitation, restlessness, passivity, loss of interest
full and tense anterior fontanel engorgement of scalp veins	mild cognitive deficit, GCS < 15/15
progressive somnolence – stupor reduction in AVPU score	progressive somnolence, further GCS reduction
increased arterial pressure, first tachycardia	
coma, increased arterial pressure, bradycardia	

CHAPTER 2. HYDROCEPHALUS TREATMENT

2.1 Present hydrocephalus treatment options

Table 11. Guideline for surgical options in the treatment of HC

[personal suggestion]

CLASSIFICATION OF HYDROCEPHALUS	TREATMENT OPTIONS
Type A / communicating HC	CSF shunt [*rarely*: endoscopic CP coagulation]
Type V / obstructive HC	depending on etiology: - removal of etiological factor - endoscopic fenestration of cyst - endoscopic 3rd ventriculostomy - only if TINA: CSF shunt
Type AV / complex or combined HC	endoscopic fenestration + CSF shunt [preferably under neuronavigation]
Type C / CP pathology	depending on etiology: - CP hypertrophy: endoscopic CP coagulation - CP tumor: surgical resection

2.1.1 The rise of CSF shunts

The era of present **cerebrospinal fluid shunting** rises in 1949, as Frank Nulsen and Eugene B. Spitz successfully implant shunt into the superior caval vein using a one-way differential pressure valve, with two 'ball-in-cone' valves with platinum helix springs with interposed rubber pumping chamber (Figure 15). They are the first to implant successfully a ventriculo-venous cerebrospinal fluid shunt and are the fathers of the later ventriculo-atrial shunt. In the 1950's different groups develop other simple differential pressure valves (ball-in-cone valves, proximal and distal slit valves, diaphragm valves) and silicone is invented, which will revolutionize shunt material development and will lead to a worldwide therapeutic breakthrough. By 1955 the first commercially available valves are the Nulsen – Spitz ball-in-cone and the Spitz – Holter slit valves (Figure 16). John Holter, a technical engineer, became father of Charles Casey, born in 1955 with a myelomeningocele and HC. He developed his successful and at that era the most reliable valve, urged by his son's condition (Figure 17). Neurosurgeon Robert Pudenz took care of the medical aspects[73]. Reports of ventriculo-pleural and ventriculo-peritoneal shunts were published in 1952 and 1953[74,75]. All other body cavities were tried out. Lumbo-peritoneal shunts were reported since 1969 as acceptable alternative[68,76-78]. At present, ventriculo-peritoneal shunting is the standard practice, the ventriculo-atrial the second option.

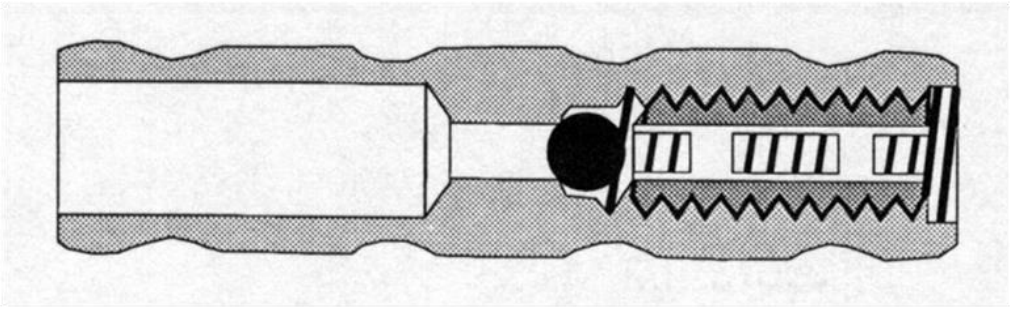

Figure 15. Ball-in-cone valve

Frank Nulsen (°1916 - †1994) and Eugene Spitz (°1919 - †2006) ball-in-cone valve, 1949

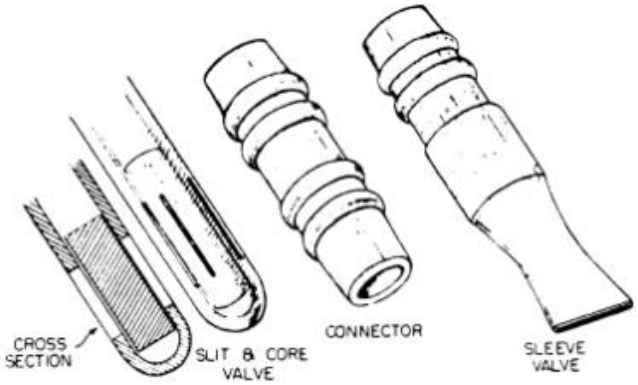

Figure 16. Slit-valves on catheter's end and connector for silicone tubes

Robert Pudenz (°1911 - †1998) and Ted Heyer slit-valves on catheter's end and connector for silicone tubes, 1955

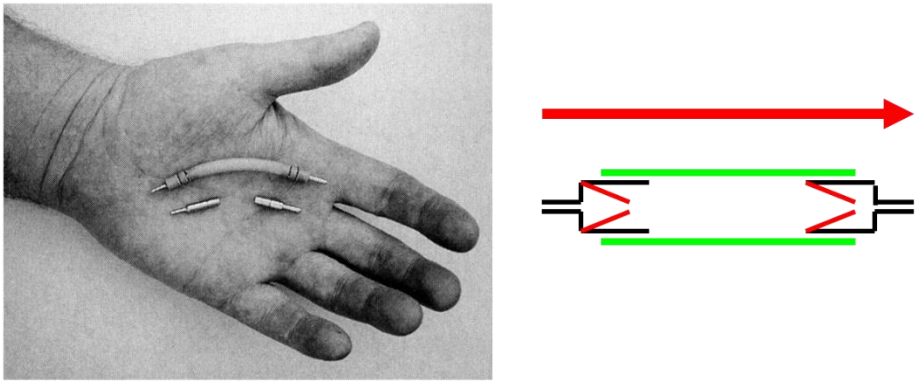

Figure 17. Slit valve design

John Holter's (°1916 - †2003) and Robert Pudenz (°1911 - †1998) slit valve design, with two serial valves in silicone cylindrical housing; digital percutaneous compression of the housing created a 'pumping' effect and evaluates proximal and distal shunt patency

2.1.2 Choroid plexus coagulation or extirpation

CP coagulation or extirpation (choroid plexectomy) techniques were first performed by V. D. Lespinasse[79] in 1910, performing endoscopic cauterization of the choroid plexus with the use of a urinary cystoscope. In 1918, W. E. Dandy[80] (°1886 - †1946) also executed endoscopic CP cauterization and surgical CP extirpation. However, due to their technical limitations, success rate was very low and complication rate high, avoiding these techniques to become standard practice.

2.1.3 Ventriculostomy - ventriculocisternostomy

In the treatment of 'obstructive' HC, early **ventriculostomy** attempts were performed by Anton (1908) and later by W. E. Dandy (1922) either by pterionic or subfrontal (with midline splitting of the optic chiasm) approach, also with low success and high complication rate. In 1939, Arne Torkildsen[81,82] (°1899 - †1968) developed a shunt between the lateral ventricle and the cisterna magna to treat aqueductal stenosis, which remained standard practice until the renaissance of the intraventricular endoscopic neurosurgery in the 1980's. A physical engineer, Harold Hopkins[79] (°1918 - †1994) was responsible for the endoscopic revival, inventing the single rod glass lens (patented 1959), a giant leap forward in visual quality and clarity. These endoscopic improvements (Figure 18 and Figure 19) obtained a high success rate with low complication rate in the treatment of obstructive HC with third ventriculostomy, recreating physiological CSF absorption without the need of a shunt or implant in this group of HC patients[83].

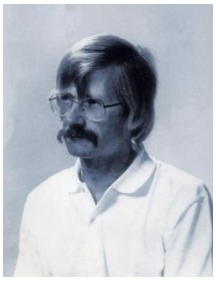

Figure 18. Prof. Dr. Jacques Caemaert

Pioneer in the worldwide implementation of endoscopic intra-ventricular endoscopic surgery into standard practice[84-88]. He created a dedicated ventricular endoscope (in co-operation with Richard Wolf©) in the 1980's. Head of department of Neurosurgery UZ Gent from 1996-2004.

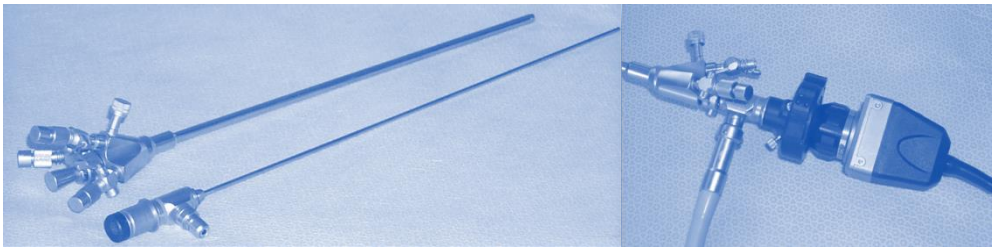

Figure 19. Caemaert ventricular endoscope (Richard Wolf©)

(Left) shaft and optic element; (right) optic element, glass fiber light cable and camera mounted onto shaft. Besides excellent for performing 3rd ventriculostomy, the Caemaert endoscope proved successful in fenestration or removal of cystic lesions, resection of small intraventricular tumors (e.g. colloid cysts, craniopharyngioma), tumor biopsy or debulking of pineal lesions, aqueductoplasty, evacuation of intracerebral hemorrhages. It remains a fundamental pillar of the neurosurgical practice at our and other departments, either free hand or guided with electromagnetic neuronavigation.

2.2 Complications of present CSF shunts

Although revolutionizing HC treatment and life-saving many thousands of HC patients worldwide on a yearly basis, the present ventriculo-peritoneal (VP), ventriculo-atrial (VA) and lumbo-peritoneal (LP) shunts know well recognized complications and a reduced survival time, leading to a high reoperation rate[89-96]. 50% Shunt survival times from 1 year (low pressure valves in neonatal patient group) to 5 years are reported in large review studies[78,92,95,97-104]. In the UK some 3000 shunt operations are performed on a yearly base; about 50 % of those operations are shunt revisions[9]. VA, VP and LP shunt complications are:

2.2.1 Shunt obstruction

The majority (49,3 %[9]) of obstructions finds place at the level of the ventricular catheter (CP aspiration, blood clot), at the distal catheter (21,5 %) or at the valve (15,8 %)

(cerebral debris, blood clot, protein flakes or membranes). The CP aspiration into the ventricular catheter seems highly related to the siphoning effect of a standard VA or VP shunt.

2.2.2 Shunt infection

Figures variate from around 3% per shunt procedure up to more than 10%! Shunt infection requires shunt removal, if necessary temporary treatment with external ventricular drain and, once infection cured, shunt re-implantation. A shunt infection is responsible for several surgical procedures, extended hospitalization on ICU (high social security costs) and –if complicated- brain damage with functional loss (high and lifelong individual costs). The vast majority of shunt infections are induced in the peri-operative phase due to dermal bacteria as Staphylococcus Epidermidis, Staphylococcus Aureus, Propionibacterium Acnes. Less frequent are post implantation infections. Most common group of these are the colonization of a VP shunt by intra-abdominal flora (e.g. E Coli bacterium) as a complication of an abdominal procedure. VA shunts are colonized at the atrial catheter due to hemodialysis or venous infusion lines or cardiac surgery complicated with infection.

2.2.3 Siphoning effect

In a VA or VP shunt patient in the upright position, the CSF fluid column in the distal catheter is orientated vertically. This vertically orientated fluid column is attracted by gravity, like a piston that falls into a cylinder, and thus exerts aspiration. This phenomenon will be addressed as the siphoning effect (Figure 20). Siphoning effect can lead to a variety of complications, difficult to treat:

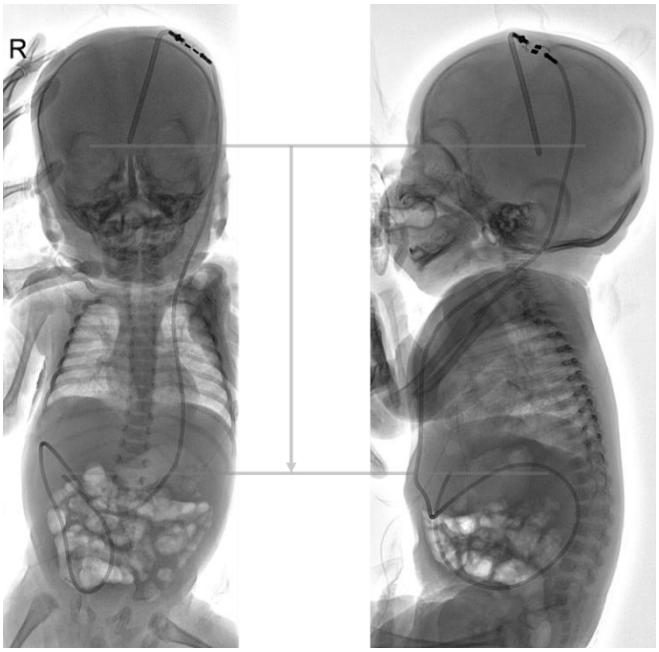

Figure 20. The height of the CSF column determines the siphoning effect caused by gravitational hydrostatic pressure.

X-ray of toddler with VPS; at this age, clinically relevant siphoning effect is infrequent. Evidently, in larger children and adults, siphoning effect increases.

2.2.3.1 Ventricular collapse and subdural hematomata

Siphoning can cause uni- or bilateral collapse of the ventricles causing acute / chronic uni- /bilateral subdural hematoma over the cerebral hemispheres(Figure 21).

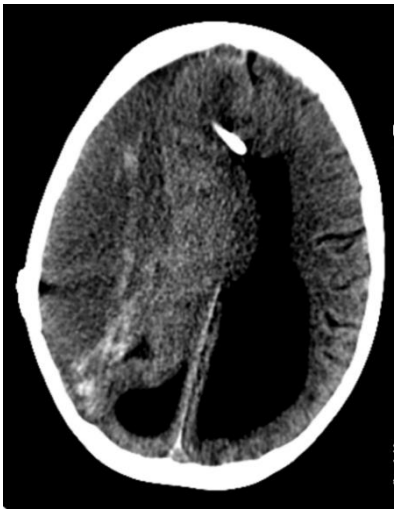

Figure 21. CT scan of collapsed right lateral ventricle and semi-acute subdural hematoma

The ventricular collaps is associated with obstruction of the ventricular catheter and of the left lateral ventricle.

2.1.3.2 Secondary craniosynostosis and microcephaly

Siphoning can cause premature closure of the cranial bone sutures (secondary craniosynostosis) leading to microcephaly with inadequate growth of cranial vault to harbor the developing cerebral structures and chronic intracranial hypertension (Figure 22). Secondary craniosynostosis is a rare overdrainage manifestation (3,5 %[9]).

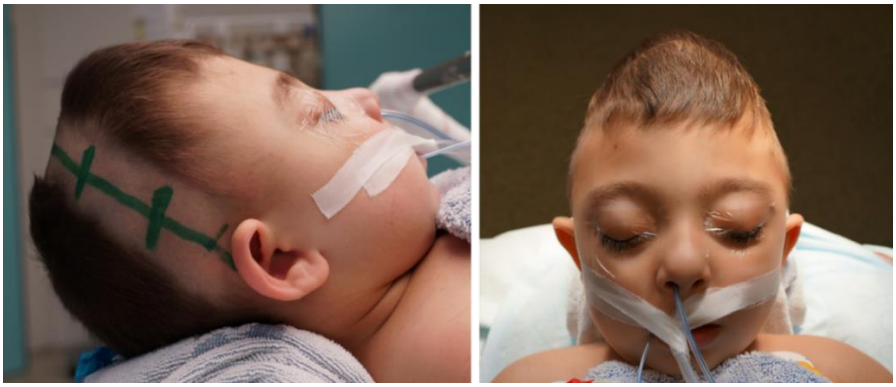

Figure 22. Turrencephaly with raised ICP

Pansynostotic micro-vault (turrencephaly), secondary proptosis due to shallow orbits and raised ICP due to the pressure of the cerebral growth [parental consent obtained].

2.2.3.3 Slit ventricle syndrome

The supratentorial ventricles become slit-like. This is the most common to treat overdrainage symptom (49 %[9]). These patients experience a yo-yo-effect between episodes of intracranial hypotension during the ventricular collapse into slits and episodes of hypertension when the ventricular catheter is blocked by the ependymal wall and the intraventricular pressure needs to increase highly to re-expand the ventricles. According to the law of Laplace, a high intracranial pressure is required to re-expand ventricles with a very narrow diameter (Table 12, Figure 23 and Figure 24).

Table 12. law of Laplace - phenomenon of the 'stiff ventricle'

F equals the tension on the wall, in case of HC the disruptive force enlarging the ventricular size; π is the mathematical pi; r is the ventricular radius; P stands for the transmural pressure, which is in direct relation to the ICP. As the disruptive wall tension is in relation to the square radius of the ventricle, in very small ventricles a very high ICP is required to start ventricular dilatation and the wider the ventricle becomes, the lower the required ICP increase for progressive dilatation. This explains the phenomenon of the so called 'stiff ventricle'.

Law of Laplace

$$\mathbf{F = \pi \times r^2 \times P}$$

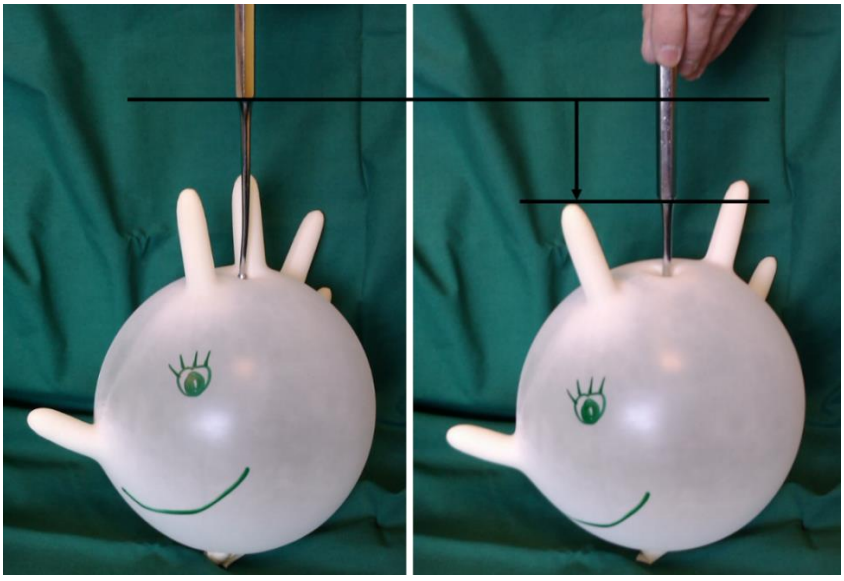

Figure 23. Demonstration of law of Laplace

Inside the digital extensions and palm compartment of the glove, the pressure is equal but the wall tension is impressively lower on the digital extensions with small radius than on the palm compartment with wide radius.

2.2.3.4 Chronic intracranial hypotension

Chronic intracranial hypotension is an invalidating condition in which patients suffer of general malaise, fatigue and chronic headache and nausea, sometimes vomiting. In general, these complaints worsen in upright and ameliorate in horizontal supine position (Figure 24).

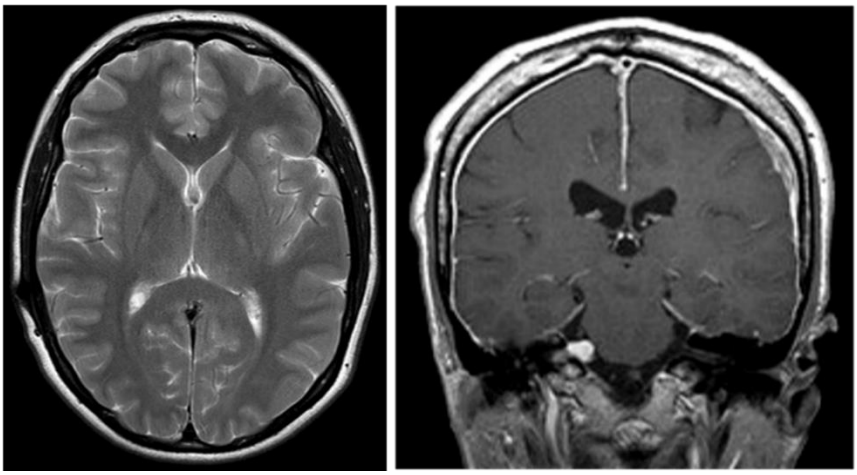

Figure 24. MR-imaging of slit ventricle syndrome and chronic intracranial hypotension

(left) MR-T2 sequence of slit ventricle syndrome; (right) MR-T1 with gadolinium IV of chronic intracranial hypotension with clear pachydural enhancement and even small subdural hematoma (on left convexity)

2.2.4 Disconnection or dislocation of the shunt material

Considering disconnection or dislocation of the shunt material, anything is possible. Evidently surgical correction is required. Typical etiology of disconnection concerns the mechanical stress on the shunt material because of the growing child or because of physical activity and possible elongation forces on the cervical-thoracic-abdominal trajectory.

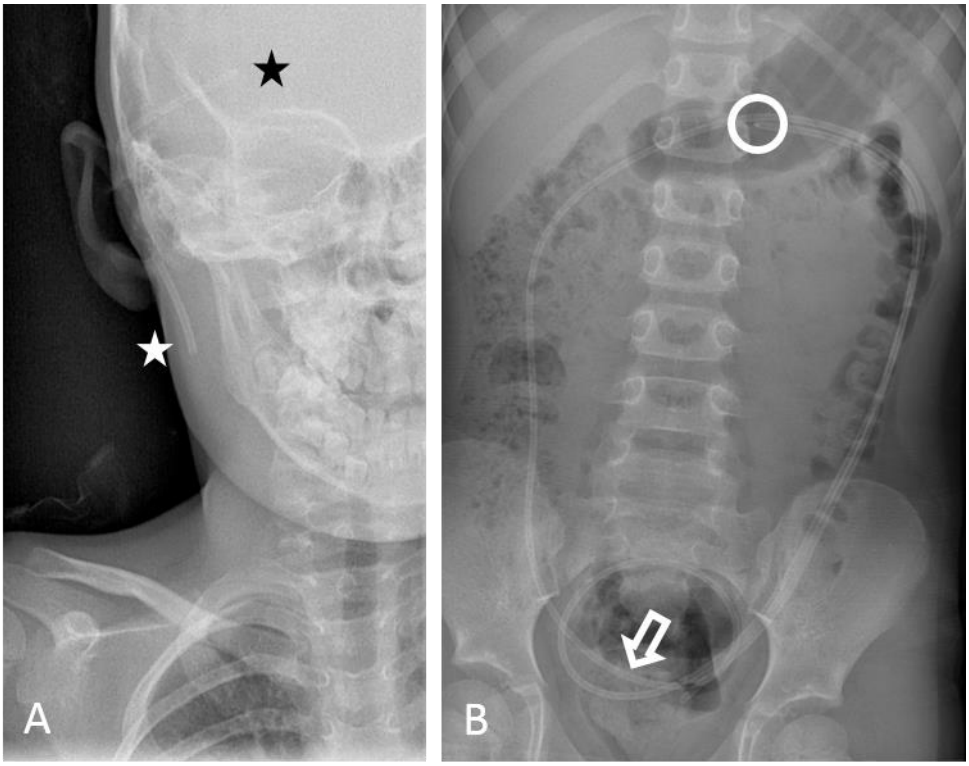

Figure 25. X-ray of disconnected VP shunt

[A] interruption at the proximal segment of the peritoneal catheter [white star: end op proximal remnant of peritoneal catheter; black star: tip of the ventricular catheter]; [B] accumulation of distal end of peritoneal catheter intraperitoneally [white circle: distal end of peritoneal catheter; white open arrow: accumulation of proximal end of migrated peritoneal catheter in lower pelvis]

2.2.5 Pulmonary hypertension

In VA shunts specifically, a risk of developing arterial pulmonary hypertension is not illusive, due to chronic formation of small emboli formed at the tip of the atrial catheter being shot towards the pulmonary arteries and arterioles[105-107]. The arterial pulmonary hypertension induces right cardiac overload and if ongoing, atrial fibrillation, decompensation, possibly lethal. Recognizing this ongoing pulmonary hypertension is of vital importance. Also, in case of an inadequately treated infected atrial catheter,

septic emboli might permanently damage the cardiac valves, septic emboli might cause renal colonization and functional loss, putting again the patient's life at risk. These uncommon but very severe possible complications of the VA shunt are the main reason of the "popularity" of the VP shunt.

2.2.6 Chiari-malformation

In the case of LP shunts, secondary Chiari-malformation is a possible complication [97,108,109]. If such, the LPS needs to be converted into a VPS or VAS (Figure 26).

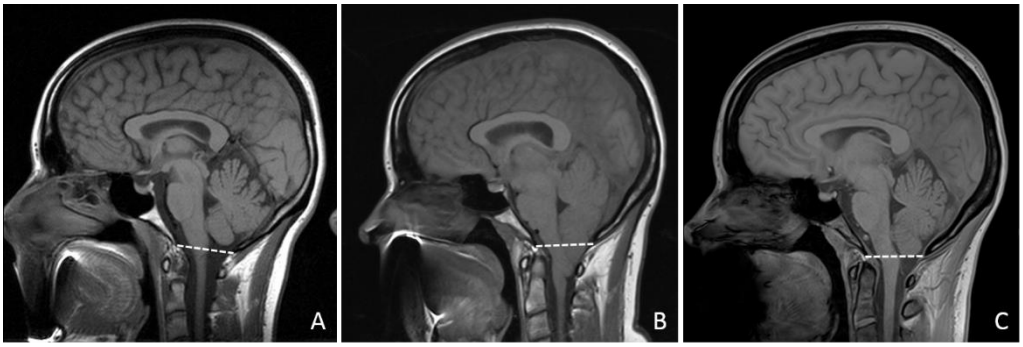

Figure 26. MR-T1 sagittal imaging of secondary Chiari-malformation to LP shunt in patient with idiopathic intracranial hypertension

(A) Before implantation of the LP shunt; (B) pronounced tonsillar herniation in combination with clear sunken brainstem with functional LP shunt; (C) 1 year after conversion of LP shunt into VP shunt

2.3 Shunt devices developed to prevent siphoning

Already in the late 1960's, beginning 1970's the problem of siphoning effect was well recognized[100] and numerous attempts to prevent siphoning with the present VPS, VAS and LPS were performed. Although very ingenious, technically outstanding but also fragile devices at a high development and production price, the siphoning remains a challenge to treat. A subgroup of shunt-dependent HC patients remains refractory for the complaints caused by siphoning, nevertheless the application of programmable valves and anti-siphon devices, invalidating and in conflict with their daily life. Moreover, the use of these sophisticated and expensive shunt devices, did ameliorate shunt results, but not the 50% shunt survival period of about 5 years[99,110].

An arsenal of shunt devices has been developed and marked over the last 4 decades:

2.3.1 Programmable opening pressure valves

Standard valves have a fixed opening pressure. This means: if the differential pressure between the ventricles and the distal organ (peritoneum or right cardiac atrium) exceeds the opening pressure, the valve is open; if not, it remains closed. When putting in a CSF shunt, the surgeon has to decide between a valves of a very low, low, medium, high or very high opening pressure. However predicting the adequate opening pressure for a specific patient is impossible. Also, in infants, the requested opening pressure, might need to increase as they grow up and later sit up, stand up and walk. Therefore, since the nineties, valves with programmable opening pressure were marketed, all programmable with a non-invasive and painless (electro)magnetic programming unit. Some of the most common types are shown here below (Figure 27, Figure 28 and Figure 29). Some are not MR-scan stable (= can be accidently reprogrammed during MR-scan) some remain MR-scan stable. They are all MR scan compatible. Theoretically, programmable opening pressure valves are not able to compensate for the siphoning-

effect. In practice however, many patients are fine with their CSF shunt with only a valve set at the adequate opening pressure.

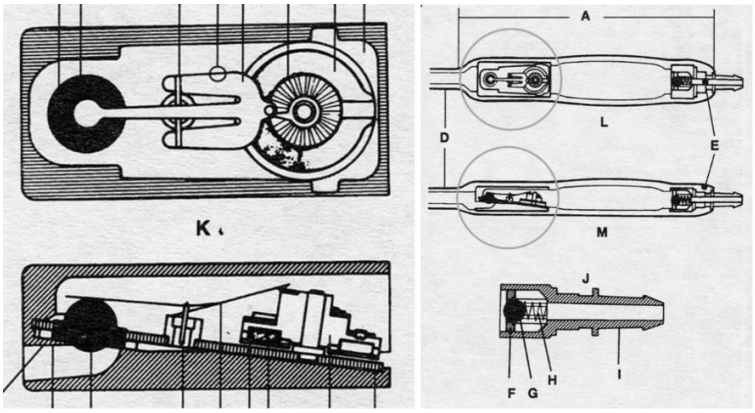

Figure 27. Hakim - Codman© valve [source: adapted from Codman©]

(Right) technical drawing of the programmable Hakim - Codman© valve, with the programmable valve on its left / inlet end and a ball-in-cone anti-reflux valve on its right / outlet end; (Left) detail of the programmable valve part, with its rotational round staircase , pivoting spindle in the center of the feather for the lever effect. Thus a higher staircase step creates an increased pressure on the ball-in-cone valve.

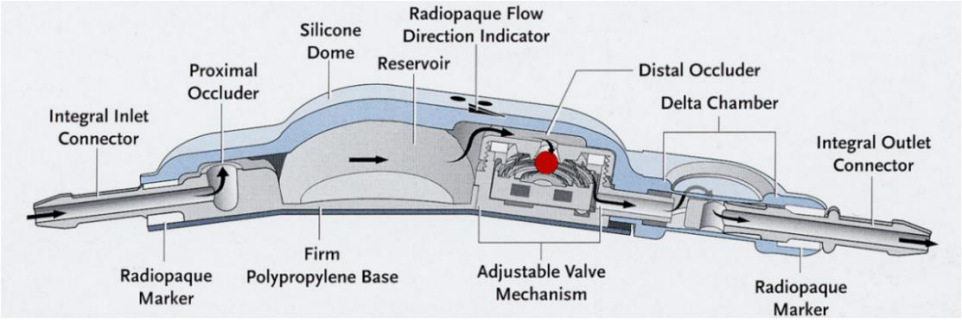

Figure 28. Medtronic© Strata valve [source: Medtronic©]

Technical drawing of Strata valve with its programmable opening pressure valve and included anti-siphon device (Delta Chamber) working on the Bernoulli principle, to impede flow rate (see also Figure 33).

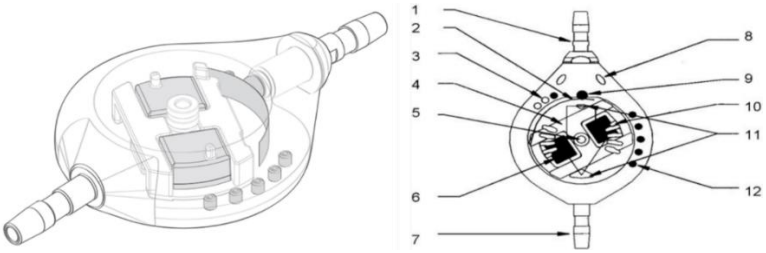

Figure 29. Sophysa© Polaris valve [source: Sophysa©]

on both sides the Sophysa© Polaris valve is drawn. A central rotor pushes on a feather in a position further from the ball-in-cone valve (less lever and less pressure on the ball) or closer (more pressure on ball). Five different opening pressures are programmable and Sophysa© merchandised Polaris valves with 4 different ranges, to accord all specific needs. The big advantage of this valve is its MR-stability, in contrary with the Codman Hakim and Medtronic Strata valves. The more recently merchandised Codman© Certas Plus and Aesculap-Miethke© proGAV-2 are MR-stable programmable valves.

2.3.2 Gravitational valves

Gravitational valves (Figure 30) use the horizontal or vertical position of the patient to include the gravitational forces of metal balls to create extra (in vertical position) or no extra opening pressure (in horizontal position) above the included ball-in-cone valve with fixed opening pressure. Difficulty with these valves is their correct implantation along the vertical axis.

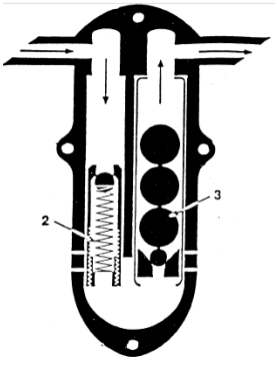

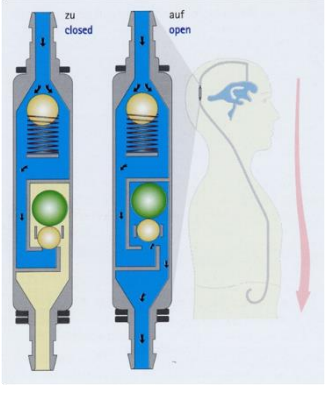

Figure 30. Cordis©-Hakim horizontal/ vertical valve (left); Aesculap Miethke© Gravity Control valve (right) [sources: Cordis© and Aesculap-Miethke©]

2.3.3 Flow-regulating valve

Only 1 flow-regulating valve is commercially available, the Integra© Orbis-Sigma valve (Figure 31). It uses a membrane with included diaphragm, moving up or down according actual differential pressure, along a central conical piston. This results in a constantly variable opening and therefore resistance, regulating the CSF flow. 3 different models are available, working with the same principle, to accord to the needs of pediatric, adult and NPH HC patients.

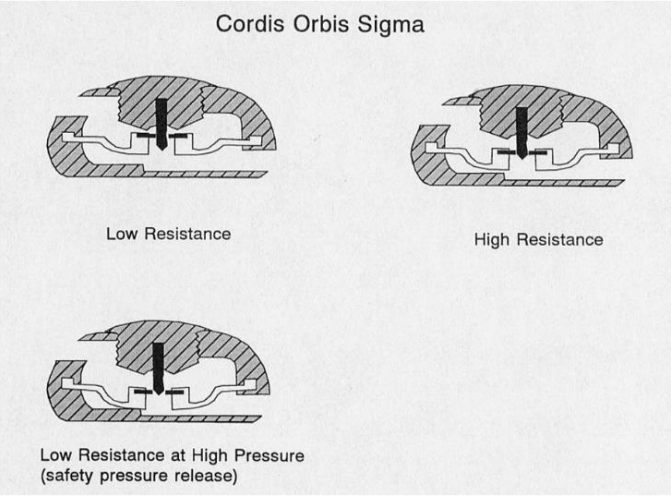

Figure 31. Orbis-Sigma-valve [source: Integra©] *Technical drawing of valve, commercialized as the OSV II & OSV II low profile, both set at a flow rate of 18 - 30 ml/h, and the Flow Regulating Low Flow & Low Flow Mini model, both set at 8 - 17 ml/h.*

2.3.4 Anti-siphon devices

Anti-siphon devices are included in a CSV shunt, in serie with its valve. Anti-siphon devices have been developed by 3 different principles:

2.3.4.1 Gravitational principle

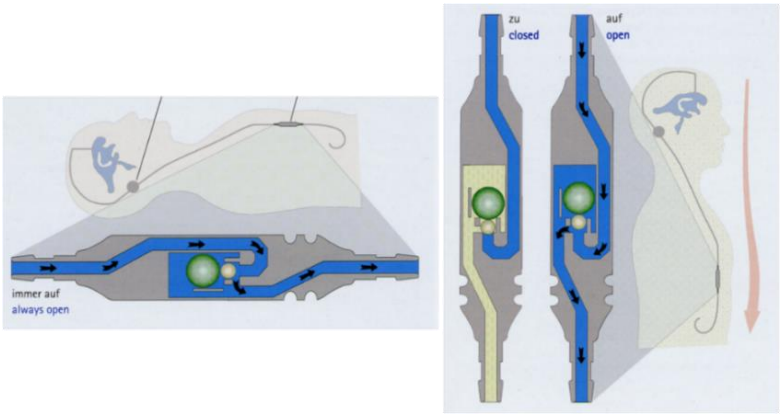

Figure 32. Aesculap-Miethke© ShuntAssistant anti-siphon device

This device is highly dependent on the correct orientation of the valve in the vertical axis of the patient. (Left) no increased resistance in horizontal position; (right) extra gravitational resistance (depending on the weight of the included balls) in the vertical, or better, non-horizontal position

2.3.4.2 Bernoulli's principle

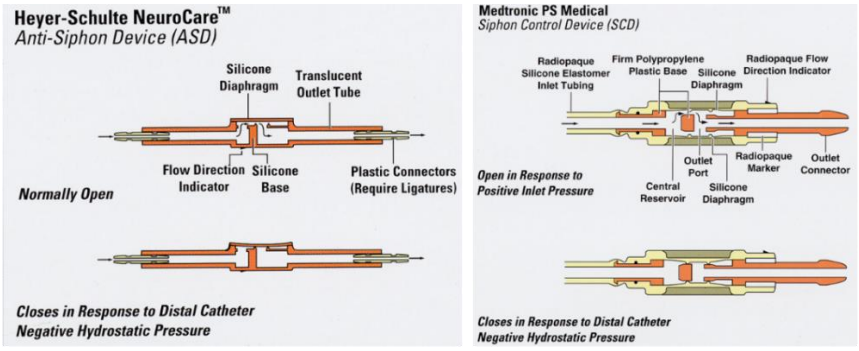

Figure 33. NeuroCare and PS Medical anti-siphon devices [sources: Heyer-Schulte© and Medtronic©]

(Left) Heyer-Schulte© NeuroCare and (right) Medtronic© PS Medical anti-siphon devices. As in the Medtronic© Delta Chamber (see Figure 28). According to Bernoulli's principle, a membrane is progressively attracted towards the chamber's opening as the flow rate increases, reducing the rate.

2.3.4.3 Flow impeding techniques according to Poiseuille's law

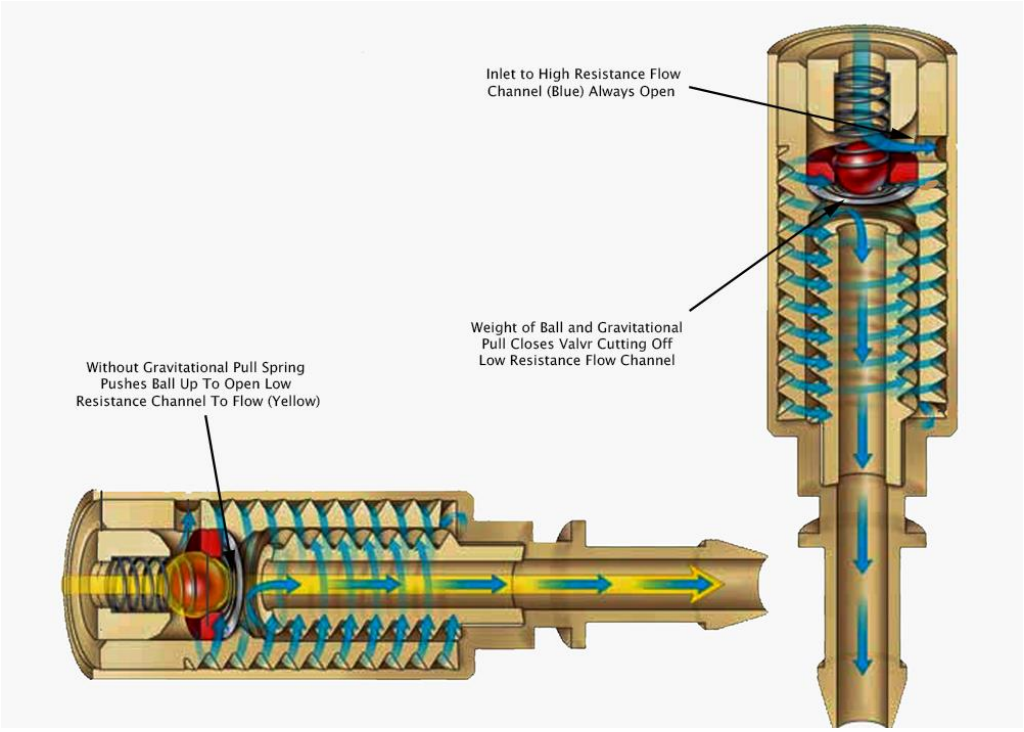

Figure 34. Codman© SiphonGuard anti-siphon device [source: Codman©]

In case of high flow rate and the presence of gravitational focus (vertical orientation), the wide and central opening is closed by the ball-in-cone valve and the CSF flow deviated towards a long and narrow - helicoidal - trajectory, strongly impeding flow rate according to the law of Poiseuille (Table 6).

CHAPTER 3. VENTRICULO-SINUS SHUNT (VSS)

3.1 Rationale and expected advantages of the VSS

An essential and clarifying question is: 'Why is there no CSF siphoning in normal physiological conditions?'. It has been proven (see above in CSF absorption) that the cranial CSF drainage systems act as a (low) resistance valve (with differential opening pressure of about 6,8 cm H_2O or 5 mm Hg[20]). CSF / blood mixture is then further evacuated via a wide venous tube (dural venous sinuses → jugular bulb → internal jugular veins → superior caval vein) down to the right cardiac atrium. A situation very similar to that of a VAS.

This question was very nicely addressed by Ismail Lofty El Shafei (°1928 - †2009) and El-Rifaii in their experimental study on the role of the internal jugular vein as a physiological anti-siphon device[111]. The IJV is able to adjust continually its diameter and therefore its flow rate in according to whatever physical condition, thanks to its extreme compliance answering any transmural pressure change (Figure 35). The transmural pressure represents the differential pressure between the intravascular and the extravascular pressure or equals $P_{intravascular}$ - $P_{extravascular}$. The $P_{intravascular}$ is the sum of the static venous blood pressure and the dynamic venous pressure. The $P_{extravascular}$ is the pressure created by the surrounding, para-venous, structures such as the cervical muscles.

Realizing that this very delicate physiological anti-siphon device can never be fully imitated by whichever human made technical shunt device, El Shafei and many other neurosurgeons[10,112-115] were convinced that a CSF shunt should drain proximally to the IJV, i.e. to a dural venous sinus. We also were convinced that deriving CSF towards a dural venous sinus or a ventriculo-sinus shunt (VSS) has the capacity to obtain near-

physiological CSF drainage, respecting the differential pressures and in balance with the CSF production. As a consequence, the possible advantages of VSS were:

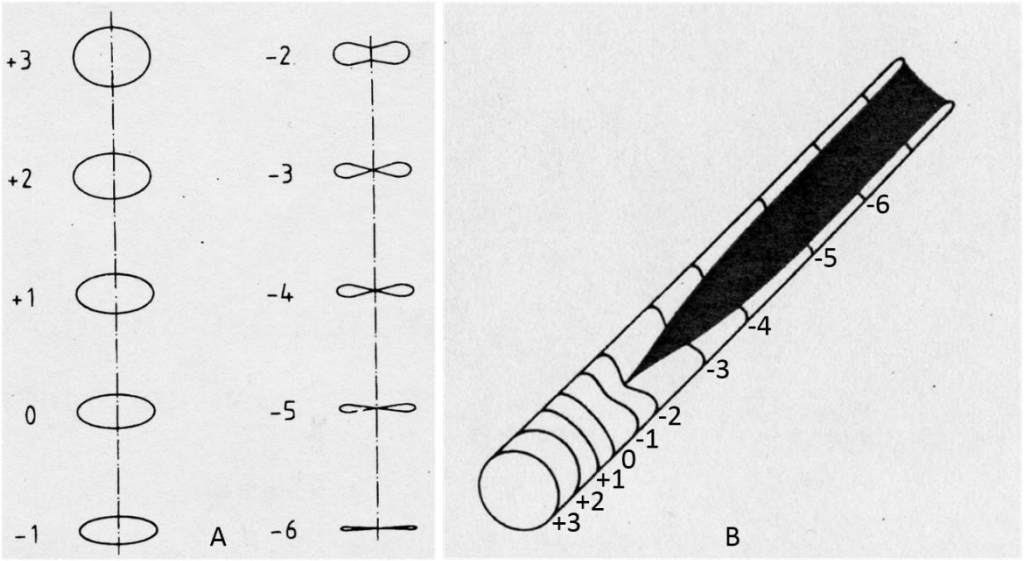

Figure 35. El Shafei's drawing of the collapsibility of the IJV [source: El Shafei and El-Rifaii, adapted]

El Shafei's drawing of the collapsibility of the IJV acting as physiological anti-siphon device[111]. (A) The numbers represent the transmural pressure registered during the experimental setting (in cm H_2O. (B) besides them the evolution of the IJV aperture: Already at an angle of 40° away from the horizontal position, the pressure above the 'IJV' representing the cranial venous pressure was stabilized and did not decrease with further inclination upon the vertical axis.

3.1.1 Longer shunt survival and less shunt complications

Significant increase in shunt survival time is expected by:

- As siphoning effect is annihilated, a significant reduction of ventricular catheter obstruction by CP aspiration is to be expected.

- The VSS trajectory is limited to the skull, resulting in a much shorter surgical trajectory. A smaller surgical field can reduce the risks of shunt infection, of wound healing problems. The very limited surgical field would even allow VSS implantation under local anesthesia.
- Thanks to the shunt's limitation to the cranial region, an important reduction in mechanical shunt problems due to growth in the pediatric population is to be expected. In other patient groups is would reduce the mechanical stress on the shunt trajectory to almost zero.
- The shunt devices are straightforward, 2 catheters and a standard very low resistance one-way valve; the less the complexity, the lower the chances of technical problems.

3.1.2 Reduced costs for patient and society

- Only a standard one-way valve (anti-reflux) with very low, fixed, resistance is needed, apart from the ventricular and dural venous sinus catheter. This standard and technically not complex material is very cost effective.
- The expected longer shunt survival and reduced complication incidence will also create a significant cost benefit.

3.2 Børgesen vs El Shafei

In 2004 we decided to study the theoretical principles and surgical aspects of VSS. A literature search revealed VSS clinical study publications in the 20th century starting with Payr E.[10,116] in 1908. Payr transplanted autologous veins (v saphena magna) with intact valves to connect the ventricle with the SSS. In his series of 15 patients, 7 deaths were reported. In the second half of the 20th century, clinical studies were published by

Sharkey P.C.[112] in 1965, Hash C.J.[114] in 1979, Wen H.L.[113] in 1982, and Bersnev V.P.[117] in 1989.

In the 21st century, 2 groups exploring VSS were recognized, with publications of retro-[12,118] and prospective[13-15] clinical studies. Ismail and his son Hassan El Shafei in Cairo, Egypt, and the Børgesen - Gjerris group, Rigshospitalet, Copenhagen, Denmark. Both groups reported excellent clinical results and few complications, not endeavoring the patient's life or functional integrity. Alone, apart from case reports or smaller series, no enthusiastic and wide implementation of the VSS was to be noticed in the neurosurgical community. Possibly, this was due to the necessity of operating on a dural venous sinus, with possibly life threatening complications such as air embolism, severe hemorrhage and postoperative venous sinus thrombosis. However, the prevalence of these complications was reported zero in recent literature review.

3.2.1 Retrograde Ventriculo-sinus Shunt (RVSS)

El Shafei, through experience with the retrograde ventriculojugular shunt, advocated the retrograde VSS. His arguments were convincing:

He had proven in a hydrodynamic study[119,120] that orientating the distal catheter of a VSS against the blood flow direction (i.e. retrograde) induced the benefits of the so called 'impact effect' at the catheter's end (Figure 55).

A catheter's distal end orientated against the direction of the blood flow, will have the creation of the impact effect at its end. Therefore, the static pressure at its distal end will equal the static venous pressure + the dynamic venous pressure according to Bernoulli's principle (

Table 13).

Table 13. Bernoulli's principle

[ρ is the fluid's density (kg/m^3); ΔP is differential pressure between a situation without blood flow and situation with blood flow and equals the dynamic pressure; Δv is the differential velocity of flow rates (m/s)].

$\Delta P = \rho \times (\Delta v)^2 / 2$

This impact effect is in a quadratic relationship to the blood flow velocity (as velocity at the catheters end drops to zero). According to El Shafei, this dynamic pressure increase at the catheter's end creates following advantages:

Reduction of shunt obstruction due to:

- At all time, the pressure inside the catheter, and - owing to the continuous CSF production and outflow - the pressure in the ventricles remains above the venous pressure (P_{venous}), eliminating conditions in favor of blood reflow.
- The constant positive differential pressure between the ICP and P_{venous} combined with the constant CSF production will create a constant CSF flow through the shunt, preventing internal shunt obstruction by blood or debris.
- The constant CSF outflow out of the catheter's end, will create a molecular CSF film around the external catheter surface, reducing or preventing blood - catheter contact. This should reduce the risk of thrombus formation on the catheter surface.
- In the impact zone the blood flow is laminar and swift, again reducing the risk of thrombus formation on a catheter. On the contrary, at the wake zone, the blood flow shows turbulences and stagnation, increasing the risk of thrombus formation.

Physiological CSF drainage

The combination of (a) constant positive differential pressure between the ICP and the P_{venous} and (b) the constant CSF production will create a constant CSF evacuation, as experienced in experimental studies op physiological CSF absorption[20].

Cost efficiency

Theoretically a shunt without valve is adequate. An one-way valve is not mandatory, as the combination of constant positive differential pressure and constant CSF production would exclude blood reflow. However, in case of disturbance of this delicate dynamic balance, e.g. a sudden ICP fall due to a lumbar puncture, the pressure difference is temporarily lost with, as a consequence, blood regurgitation and possible shunt obstruction[1].

3.2.2 SinuShunt®

Børgesen[13-15] and Gjerris have designed dedicated VSS devices, the SinuShunt®, with specific dural venous catheter and dedicated valve (Figure 36).

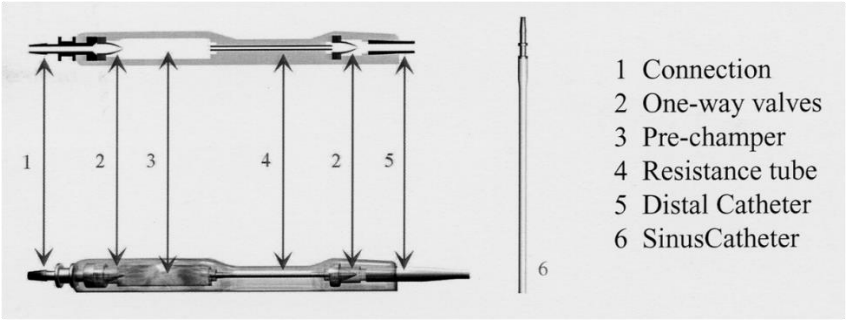

Figure 36. The SinuShunt® [source: Børgesen and Gjerris]

The technical drawing of the Børgesen and Gjerris SinuShunt® dedicated devices. The SinusCatheter (not on drawing) is made of medical grade silicone with outer diameter of 2,1 mm. The valve system is composed of 2 very low resistance one-way slit valves, designed to exert zero opening pressure. One valve is situated at the inlet, one at the outlet of the system (n° 2 on the drawing). In between the 2 slit valves, in serial order, a silicone prechamber (n° 3) enabling diagnostic 'pumping' or punctuation of the SinuShunt® valve, and a 'resistance tube' in titanium (n° 4) with well-defined length and diameter. Therefore the resistance tube's R_{out} equals the physiological R_{out} of 8 mm Hg / ml / min.

The SinuShunt® was developed to introduce the SinusCatheter with its tip in the direction of the blood flow, or antegrade. The SinusCatheter is implanted in one of the transverse sinuses, at its widest part, just proximal of its transition into the sigmoid sinus. It is indicated to drill a guiding groove in the skull's tabula externa, to keep the catheter orientated in the sinus center. The intravascular length of the SinusCatheter should be between 1,5 - 2 cm.

3.2.3 UZ Gent VSS prospective clinical study

We decided to opt for a study with the El Shafei RVSS for the following reasons:

1. The principle of impact effect preventing obstruction and providing near-physiological drainage was well studied and documented by El Shafei and a promising retrospective clinical study was published[11,118]. The SinuShunt® does not profit of the impact effect.
2. El Shafei studied and published on ventriculo-venous shunting since 1975[121,122]. He gradually evolved to the retrograde principle in 1985, implementing it into the ventricolo-jugular shunt[111,120,123,124] and in 2001 towards the retrograde ventriculo-sinus shunt (RVSS)[12]. Every adaptation on this path was based on both clinical experience and experimental work and seemed logical.
3. The RVSS did not request dedicated shunt devices. It was perfectly realizable with our standard practice shunt material. The SinuShunt required dedicated devices and - at that moment - an European prospective multicenter clinical study had started.
4. In 2004 - 2005 we performed the RVSS procedure as a rescue procedure in 4 patients with very complicated shunt history of both VA and VP shunts. The results were positive in 2 out of 4 and the procedures went technically well and complication-free.
5. Also nature uses the retrograde injection to maintain differential pressures.

On cerebral MR-scans the cerebrocortical veins can be observed making a turn to inject into the SSS opposite to the direction of the SSS blood flow. This retrograde injection is essential to maintain the cortical venous pressure elevated above the p_{SSS} (Figure 37 and Figure 38).

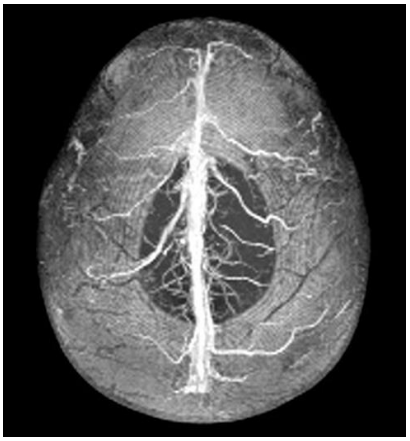

Figure 37. MR-venogram of cerebrocortical veins injecting into the SSS

In general, veins injecting anterior of the coronal sutures, inject in antegrade or perpendicular orientation. Veins injecting posterior of the coronal sutures, reject in a retrograde direction.

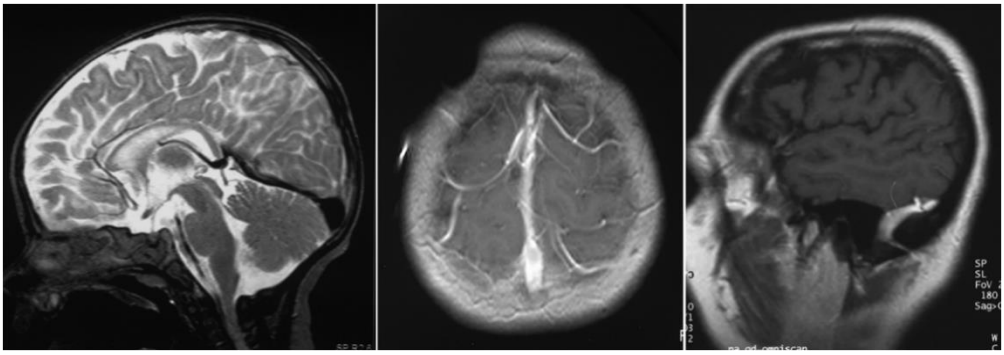

Figure 38. Deep cerebral veins making a turn

Not only the cortical veins but also the deep cerebral veins make a turn to inject in a retrograde manner to maintain elevated pressure. (left) the vein of Galen into the inferior sagittal sinus to form the straight sinus; (middle) the cortical veins into the SSS; (right) the communicating vein of Labé into the transverse-sigmoid sinus transition zone (as well as the superior petrosal sinus into the sigmoid sinus).

3.3 IBITECH – in vitro and numerical modeling of RVSS

The 'real' Ph. D. work started in 2006. After evaluation and presentation of our personal experience concerning the rescue RVSS procedures and of the VSS literature, we aimed at a monocentric prospective clinical RVSS study. Beforehand an experimental study had to verify the impact effect of the RVSS. At the Institute of Biomedical Technology (IBiTech) of Ghent University, prof. ir. Pascal Verdonck agreed to collaborate. Experimental (Figure 40, Figure 41, Figure 42, 43 and Figure 45) and numerical (computerized fluid dynamics or CFD) modeling of the VSS (Figure 49) were performed in 2006 - 2007 by ir. Koen Van Canneyt and ir. Jan Kips, under direct guidance of Edward Baert and ir. Guy Mareels, to fulfill their master thesis.

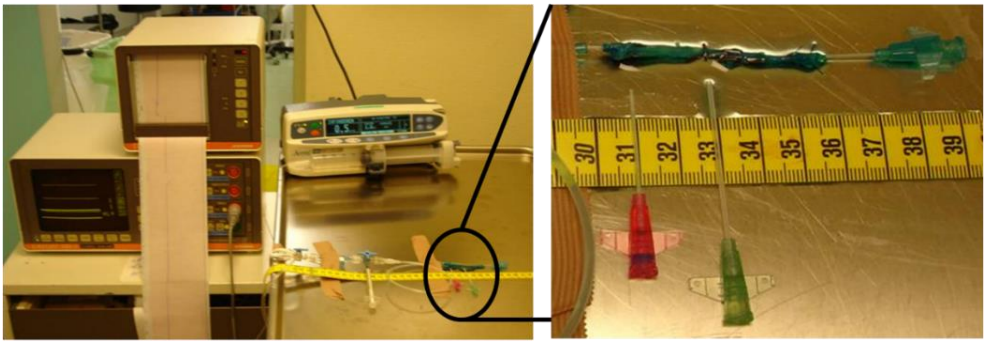

Figure 39. Setup cortical vein compliance testing + detail vein itself

In order to build experimental or numerical models, the knowledge of the cerebral cortical vein compliance was essential. [left picture] Overview of the experimental test setup of the cortical vein compliance; [right picture] detail of the vein itself

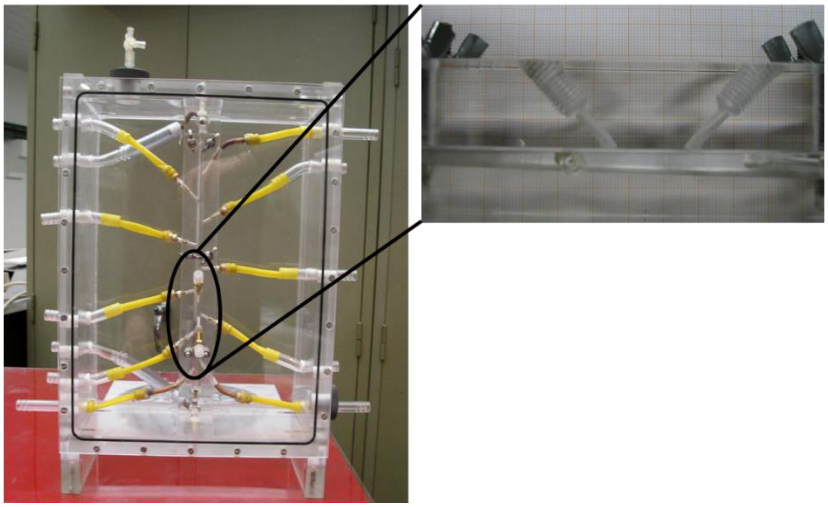

Figure 40. Detail of headbox and introduction ports

(Left) headbox part of the experimental model; (right) the introduction ports (with ante- and retrograde orientation) into the experimental SSS.

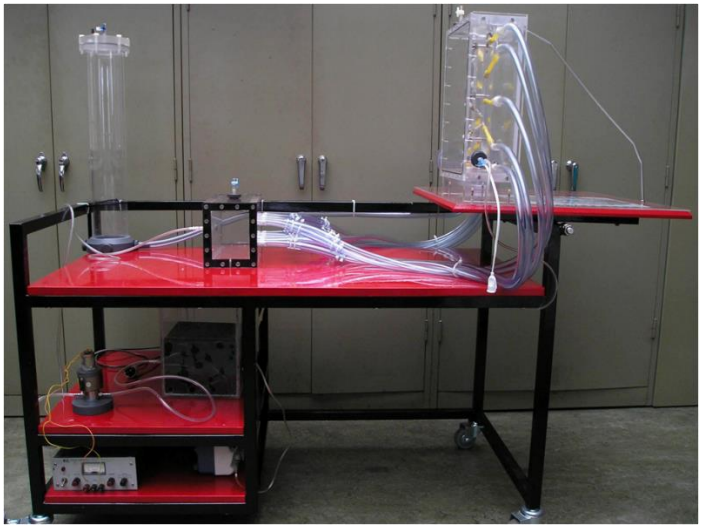

Figure 41. Headbox fixed on a tilting table

overview of the experimental model with the headbox (above right) fixed on a tilting table to mimic changes in posture.

3.3.1 MANUSCRIPT 1

EXPERIMENTAL AND NUMERICAL MODELING OF THE VENTRICULO-SINUS SHUNT (EL SHAFEI SHUNT)

K Van Canneyt[1*†], J Kips[1,2†], G Mareels[1], E Baert[3], D Van Roost[3] and P Verdonck[1]

[Proc Inst Mech Eng H., published, 2008;222(4):455-464]

[1]Institute Biomedical Technology (IBiTech), Ghent University, Ghent, Belgium
[2]Department of Pharmacology, Ghent University, Ghent, Belgium
[3]Department of Neurosurgery, Ghent University Hospital, Ghent, Belgium

[*]Corresponding author: Institute Biomedical Technology (IBiTech), Ghent University, De Pintelaan 185, Gent, B-9000, Belgium. email: Koen.VanCanneyt@UGent.be
[†]Both these authors contributed equally to this study
The manuscript was received on 29 January 2007 and was accepted after revision for publication on 1 October 2007.
DOI: 10.1243/09544119JEIM299

ABSTRACT

This study assesses malresorptive hydrocephalus treatment by ventriculo-sinus shunting with the shunt in the antegrade or retrograde position. First, an experimental model of the cerebral ventricles, the arachnoid villi, the cortical veins, and the superior sagittal sinus was built. For this purpose, the compliance of a human cortical vein was measured and then modelled by means of Penrose tubes. The dimensions of the superior sagittal sinus were determined in-vivo by measurements on magnetic resonance imaging scans

of 21 patients. Second, a numerical model of the cortical veins and the superior sagittal sinus was built. The numerical results were validated with the results from the experimental model. The experimental and numerical pressure difference between the intracranial pressure and the static sinus pressure was small (0–20 Pa) and corresponded to the theoretically expected values. No overdrainage was found in either the antegrade or the retrograde position of the shunt. Blood reflow was only found while mimicking lumbar puncture or changes in position with the experimental model (lowering the intracranial pressure or increasing the sinus pressure rapidly). Optimal results can be obtained with the shunt positioned in the most downstream half of the superior sagittal sinus. The experimental and numerical results confirm the potential of ventriculo-sinus shunting as therapy for malresorptive hydrocephalus patients. The ventriculo-sinus shunt thus proves to be a promising technique.

Keywords: experimental, numerical, ventriculo-sinus shunt, hydrocephalus, overdrainage, superior sagittal sinus

INTRODUCTION

In normal physiological conditions, cerebrospinal fluid (CSF) is drained to the superior sagittal sinus (SSS) via small granulations, the arachnoid villi. Malresorptive hydrocephalus occurs when the arachnoid villi are unable to drain enough CSF, and the intracranial pressure (ICP) rises. Standard therapy includes draining the CSF by a shunt from the cerebral ventricles to the peritoneum (ventriculo-peritoneal shunt) or the right atrium of the heart (ventriculo-atrial shunt). However, both shunt types are associated with major complications, one of them being siphonage[89,90,93,96,125]. This siphon effect, which develops when the patient assumes the erect position, can cause intraventricular hypotension and overdrainage[123].

A new type of shunt, the ventriculo-sinus shunt (VSS), was proposed by El Shafei and El Shafei[12]. Figure 42 shows the shunt connecting the cerebral ventricles to the SSS.

Major advantages of this VSS are its short length and the use of an anti-siphon effect caused by collapse of the internal jugular vein[111]. The VSS can be placed antegrade or retrogade (shunt tip with or against the direction of the SSS flow respectively). A potential drawback of all ventriculo-venous shunts (e.g. ventriculojugular and VSS) is (temporary) reflow. Reflow can be associated with blood stagnations, thus triggering thrombus formation. This can obstruct the shunt and make it useless.

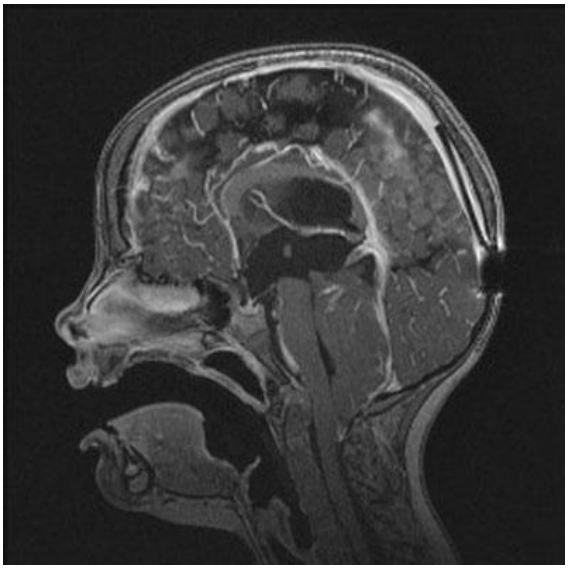

Figure 42. Magnetic resonance imaging scan of an in-vivo VSS

This study evaluates malresorptive hydrocephalus treatment by VS shunting. Overdrainage, reflow, and non-reflow conditions are assessed using an experimental and numerical model in order to have a detailed look at the flow and the pressures in the SSS, complementary to theoretical considerations and previous clinical studies.

The experimental model was constructed to study pressures on different locations associated with the insertion of a VSS in either the antegrade or the retrograde position. The ICP and the pressure in the SSS at the shunt tip were measured continuously. The transitional behaviour of the model towards steady state conditions and the steady state pressure difference between ICP and SSS pressure at the end of the shunt can be

evaluated with the shunt in both the antegrade and the retrograde position to assess the shunt performance in clinical practice. In addition to this transitional behaviour, an extra test was included to investigate the impact of a change in the patient's position from upright to lying or to mimic a lumbar puncture.

A numerical model was developed to support the experimental findings. The steady state ICP and SSS pressure at the shunt tip were measured to assess reflow or overdrainage. Furthermore, a parametric study was included to investigate the impact of the shunt location in the SSS and a different flowrate on the correct functioning of the VS shunt.

Finally, both the experimental and the numerical results are compared with theoretical considerations and with the conclusions and clinical results of El- Shafei and El Shafei[12].

MATERIAL AND METHODS

Experimental model

The experimental set-up is shown in Figure 43. It contains the human ventricles (A), the SSS (C), and the cerebral venous system (D). The human brain counts four cerebral ventricles, where the majority of CSF is produced and conserved. These ventricles are connected to the subarachnoid space around the brain tissue and in the spinal cord. Both the ventricles and the subarachnoid space are modelled as one CSF reservoir (Figure 43, A), and so the reservoir pressure corresponds to the ICP and the CSF pressure. The total compliance of the CSF reservoir was set at 0.008 ml/ Pa, corresponding to a pressure–volume index of 25 ml at 10 mmHg[71]. Compliance is set by use of a windkessel attached to the CSF reservoir (Figure 43, B). CSF is modelled as pure water.

Since the shunt is inserted in the SSS, which has a triangular cross-section, it is important to model this SSS geometry accurately. The proximal upstream entering veins lead antegrade into the SSS and the most downstream veins lead retrograde into the SSS[126,127]. The SSS can be seen as incompressible[128,129]. The length of the SSS and the

surface area were measured along the SSS on magnetic resonance images of 21 patients (between 47 and 68 years old). The SSS surface areas were measured in three different cross-sectional planes. These planes were chosen at the end of the SSS (confluens sinuum), at the coronal suture, and in the middle between coronal suture and the confluens sinuum. The beginning of the SSS was determined as the first point where the SSS was visible on magnetic resonance images. In the three planes, the base and height of the approximate triangular cross-sections were measured and the corresponding surface area was calculated. Additionally, the exact surface area of the SSS at the chosen locations was measured. Figure 44 shows the measured and calculated values, from the beginning (0 cm) to the confluens sinuum (28 cm). As can be seen in Figure 44, a geometry that fitted between the two values was used (an exception was made for the beginning of the SSS). The length of the measured SSS was 28.2 ± 1.7 cm. Consequently, a triangular profile was milled out of Plexiglas, 28 cm in length (Figure 43, C, and Figure 45).

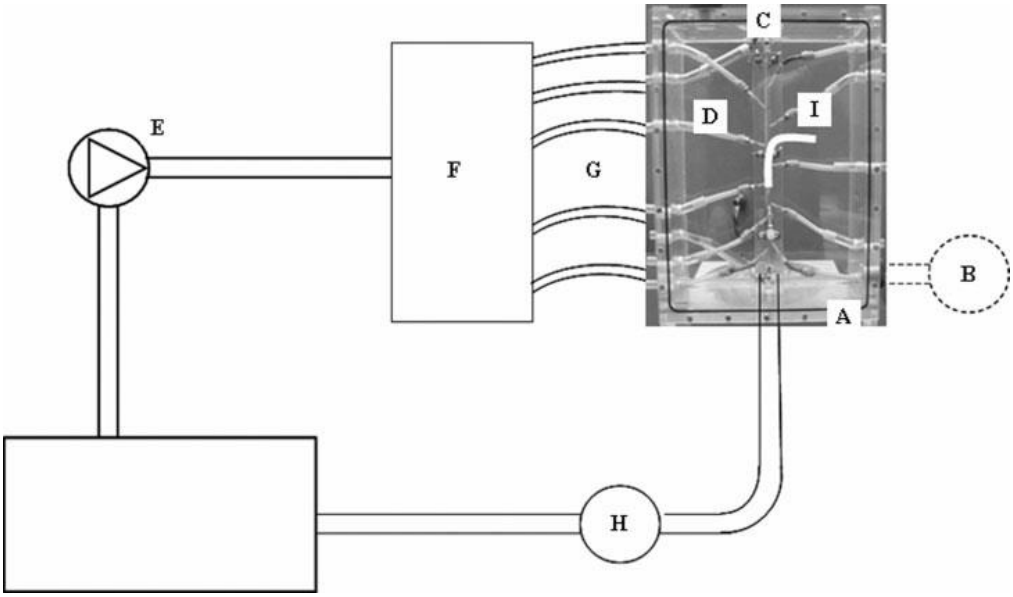

Figure 43. Experimental set-up

A, CSF reservoir; B, windkessel; C, SSS; D, Penrose tubes modeling cortical veins; E, pump; F, distributor; G, rigid tubes; H, pressure reservoir; I, VSS

In order to model the cortical veins physiologically, two parameters are particularly important, namely the inflow velocity of the blood from the veins in the SSS and the compliance of the veins. About 40 cortical veins flow into the SSS, each with an average diameter of 1.5 mm[126]. In the model, they are represented by ten veins with a diameter of 3 mm. This ensures that the inlet velocity in the SSS remains similar to the in-vivo situation. Second, a compliance measurement was performed on a human cortical vein (diameter, 1.5 mm; length, 2 cm) in order to quantify the magnitude of the compliance of cerebral veins.

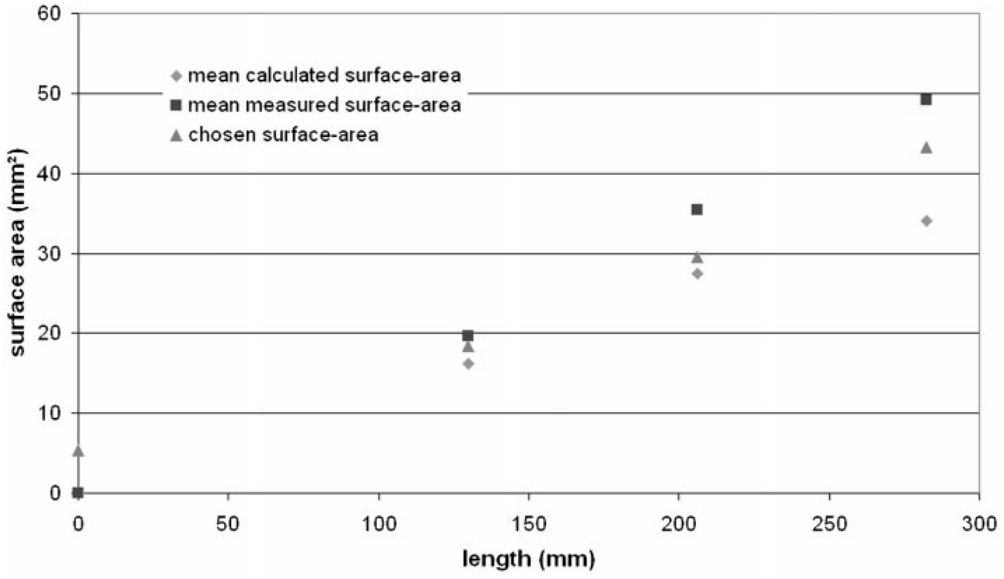

Figure 44. Dimensions of the SSS: in-vivo measurements

(more detail in fig. 4)

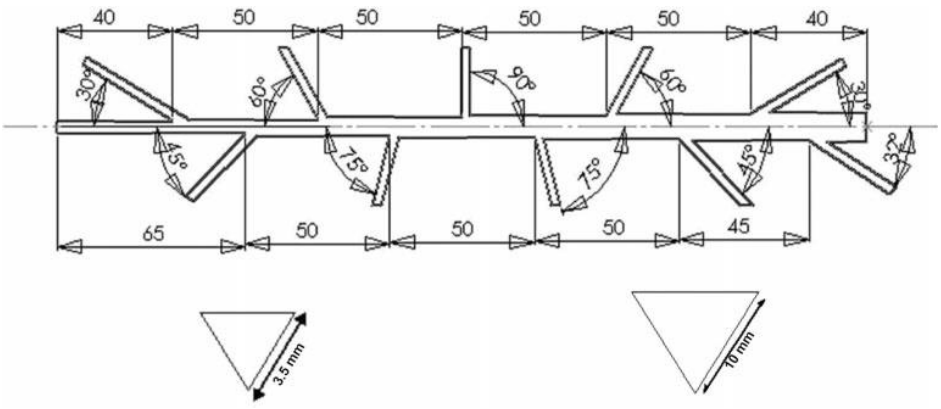

Figure 45. Detailed view of upstream and downstream

Dimensions (mm) of the chosen SSS: detailed view of upstream (left) and downstream (right) cross-sections

A syringe pump with a constant inflow of 0.5 ml/h generated a steady state pressure in the vein and compensated the permanent leakage. The compliance curve in Figure 46 was obtained with a syringe and a fluid-filled pressure transducer (type DT-XX, Becton Dickinson, Franklin Lakes, USA). Similar compliance tests were performed on different Penrose tubes in order to find the appropriate substitute material for the cortical veins. Finally, Penrose tubes of type 2 reference 473600 (8 mm diameter) were used. The compliance curve for this material is shown in Figure 47. Ten Penrose tubes of 5.1 cm length yield the same compliance as 40 cortical veins in-vivo (Figure 43, D). As mentioned above, a windkessel provided the additional compliance to match the physiological compliance of the CSF system.

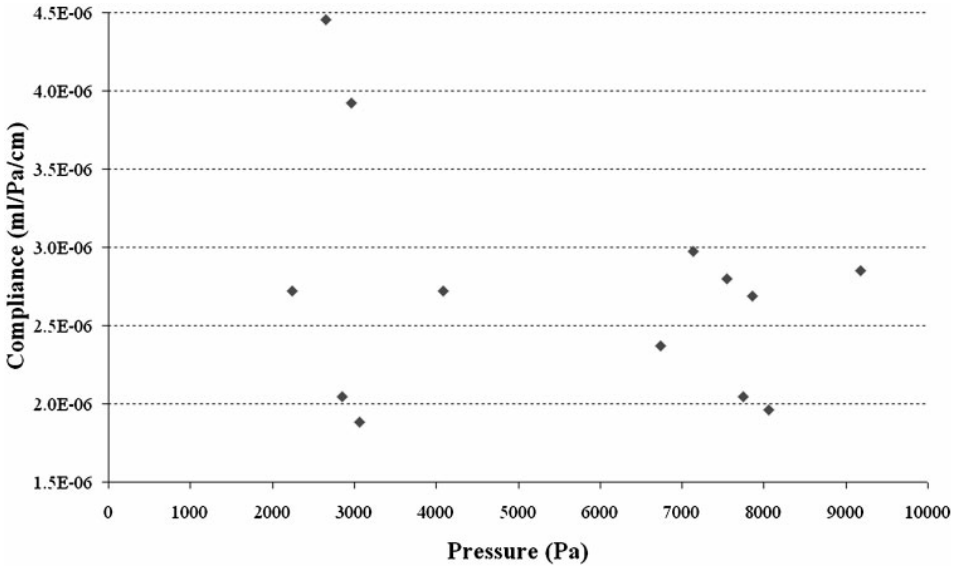

Figure 46. Scatter plot of cortical vein compliance (in-vivo)

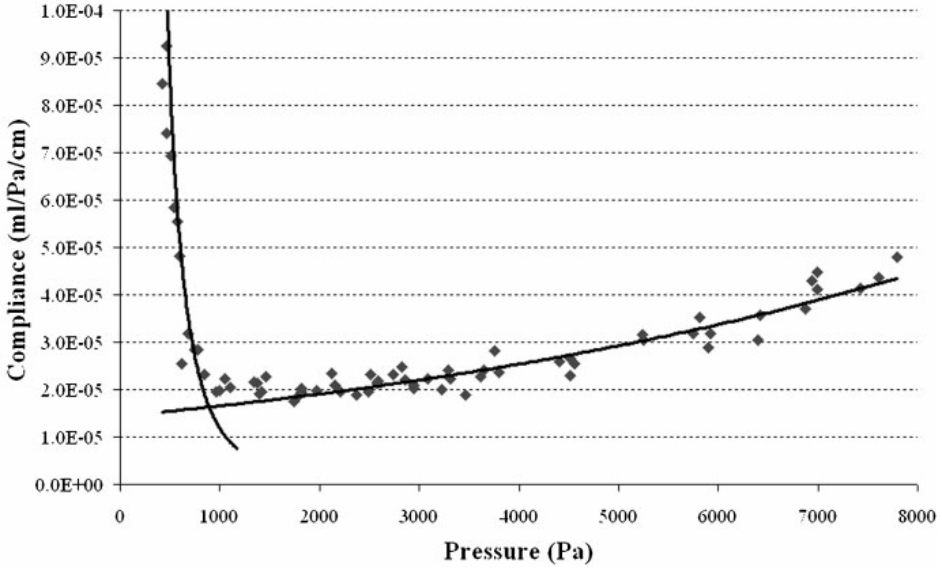

Figure 47. Compliance curve for the Penrose tube

100–900 Pa: compliance, 4006.3 $p^{-2.843}$(R2=0.8903); 2000–8000 Pa: compliance, 1.4 x 10^{-5} exp(10^{-4} p) (R^2=0.8906)

Blood is modelled by a 40 per cent glycerine–60 per cent water mixture with a mass density of 1103 kg/m^3 and a dynamic viscosity of 3.75 mPa s at 25 °C. A volumetric pump (200 ml/min) brings this mixture into a distributor, where it is divided over ten rigid tubes (Figure 43, E, F, and G). These tubes lead the mixture into the CSF reservoir where it flows into the SSS through the cortical veins, modelled by the Penrose tubes. The downstream pressure in the SSS is set by an adjustable-pressure reservoir which captures the glycerine–water mixture (Figure 43, H).

In the CSF reservoir, the CSF surrounds the cortical veins and the modelled SSS. The shunt has an internal diameter of 1.1 mm and an external diameter of 2.2 mm. To study an antegrade and a retrograde position, two entrances were made in the SSS at an angle of 45° (Figure 43, I). The antegrade shunt enters at 18 cm from the beginning of the SSS (upstream, smallest part). The shunt is placed 4 cm in the SSS so that the shunt tip is located 22 cm from the SSS beginning. For the retrograde set-up, the shunt was inserted at 20 cm and the shunt tip was at 16 cm from the beginning of the SSS.

During the tests, there was no extra CSF input in the system. The CSF pressure was raised to 3000 Pa and the pressure at the end of the SSS was fixed at 1000 Pa. The CSF pressure, corresponding to the ICP, and the pressure in the SSS were measured until they both stabilized. The pressure measured in the SSS is the static pressure in the SSS at the position of the shunt end. Since there is no CSF input, CSF flow through the shunt in the steady state condition will also be absent. This implies that the pressure in the CSF reservoir (ICP) is equal to the pressure in the shunt. Three tests for the retrograde set-up and three tests for the antegrade set-up were performed. Since small pressure differences are expected, differential water columns were used to perform pressure measurements.

To investigate the possibility of reflow of blood into the shunt, the pressure in the SSS was increased by 100 Pa, starting from steady state conditions. This was achieved by raising the downstream pressure reservoir[111], mimicking the change from the upright to

the lying position. Similarly, the ICP was lowered by 100 Pa, to mimic a lumbar puncture.

Numerical model

The numerical model focuses mainly on the flow in the SSS itself. For this reason, only the inlet veins, the SSS, and an outflow vein were constructed in a three-dimensional model with exactly the same geometry as the experimental model. Flow and pressure boundary conditions were equal to those in the experimental model, and again both the antegrade and the retrograde configurations were studied. Fluent 6.2 (Fluent Inc., Sheffield, UK) was used to solve numerically the steady state Navier–Stokes equations. The complete model consists of over 1.14×10^6 finite volume mesh elements. The veins and the shunt were meshed with a successive ratio of 1.015 towards the outflow in the SSS. The SSS was filled with approximately 800 000 triangular cells. As in the experimental model, the pressure differences between shunt and SSS at the end of the shunt were studied.

Additionally, a parameter study was conducted. A different blood flow rate in the SSS, 400 ml/min instead of 200 ml/min, was simulated in both the antegrade and the retrograde positions. The influence of the shunt position more upstream or downstream from the SSS was assessed by studying the velocity profile along the longitudinal axis of the SSS.

RESULTS

Experimental model

In the antegrade position, the static stabilization pressure in the CSF reservoir (ICP) is 3.3 ± 2.5 Pa below the pressure in the SSS; this is the static pressure in the SSS at the

position of the shunt end. In the retrograde set-up, the steady state ICP is 16.7 ± 2.5 Pa higher than the static pressure in the SSS. Figure 48 shows the result of one test with the antegrade shunt and one test with the retrograde shunt.

While manipulating the model and increasing the SSS pressure [by 100 Pa or 1 cm H_2O], simulating a person changing from upright to lying position[111], temporary reflow was observed until the pressure equilibrium was re-established. The same phenomenon of temporary reflow occurred when lowering the ICP, simulating a LP (100 Pa).

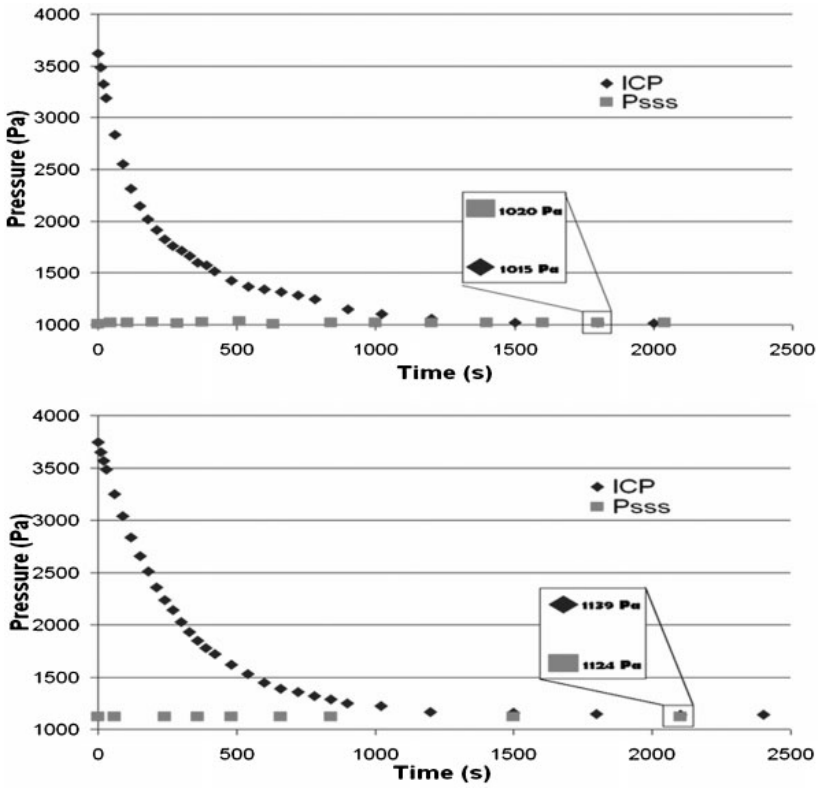

Figure 48. Steady state static pressure

ICP and sinus pressure Psss at the shunt tip [upper diagram, antegrade shunt; lower diagram, retrograde shunt]

Numerical model

In the antegrade numerical model, the ICP was 2 Pa lower than the static pressure in the SSS. With the shunt in retrograde position, the ICP was 13 Pa higher than in the SSS. Figure 48 shows the static pressure (Pa) in the SSS at the end of the shunt in both the antegrade and the retrograde positions.

When doubling the blood flowrate in the SSS (400 ml/min), the pressure difference in the antegrade model remained almost constant. In the retrograde position, the pressure difference increased to 51 Pa. The results are summarized in Table 14. Difference between the ICP and pressure Psss in the SSS at the shunt tip for both the antegrade and the retrograde set-up.

The maximum velocity profile in a sagittal cross-section of the SSS is shown in Figure 50. The maximum velocity rises in the first 10 cm of the SSS and remains almost constant in the last 18 cm.

DISCUSSION

As can be seen in fig. 49, the steady state static pressure in the retrograde shunt is higher than in the SSS. The total pressures in the SSS at the location of the shunt and inside the shunt are equal. Since there is no flow and consequently no dynamic pressure difference in the shunt, the static pressure in the shunt is equal to the total pressure in the SSS. As such, the static pressure in the shunt exceeds the static pressure in the SSS by the dynamic pressure in the SSS[12]. In other words, SSS blood flow stagnation at the shunt tip causes the static pressure in the shunt to rise by the amount of the dynamic pressure in the SSS, according to Bernoulli's principle: $\Delta p=\rho\,(\Delta v)^2/2$, with ρ the density (kg/m^3) and v the velocity (m/s). This effect was called the 'impact effect' by El Shafei and El Shafei[12].

At the position of the shunt tip, the blood velocity in the SSS is about 0.15 m/s. The CSF velocity in the shunt for steady state conditions is 0 m/s, corresponding to a pressure difference of 12.5 Pa. This is comparable with the experimental and numerical results: 16.7 Pa and 13 Pa respectively.

In the antegrade position, it can be theoretically expected that the ICP is lower than the static pressure in the SSS. El Shafei and El Shafei[12] described this as a 'wake effect'. Bernoulli's principle cannot be used here, which implies that no result can be calculated in an analytical way.

Table 14. Difference between the ICP and pressure Psss in the SSS at the shunt tip for both the antegrade and the retrograde set-up

	Difference (Pa) between the ICP and P_{SSS}		
Set-up	Experimental	Numerical	Numerical [SSS flow rate x 2]
Antegrade	-3.3 ± 2.5	-2	-2
Retrograde	16.7 ± 2.5	13	51

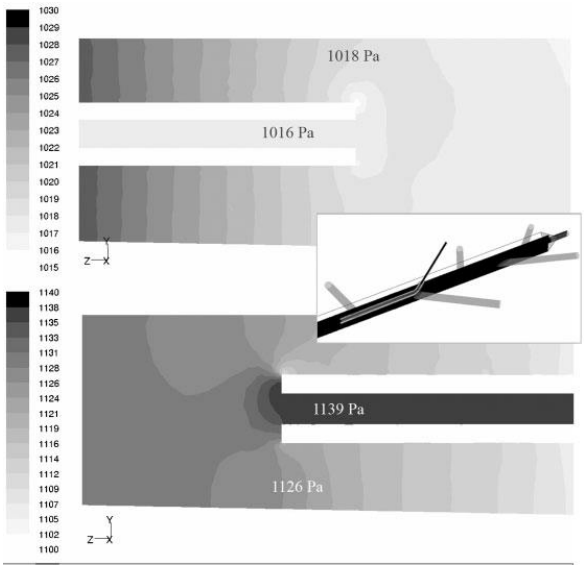

Figure 49. Numerical steady state static pressure (Pa) in the longitudinal plane

Upper diagram, antegrade shunt in the SSS; lower diagram, retrograde shunt in the SSS. The experimental and numerical results show that the values obtained for the pressure in the CSF reservoir are 3.3 Pa and 3 Pa respectively lower than in the SSS. The lower CSF pressure confirms the existence of the wake effect.

When doubling the SSS blood flowrate, the difference between the ICP and the SSS in the retrograde model changed quadratically with the blood flow velocity. This corresponds to the quadratic relationship between the pressure difference and blood flow velocity in the retrograde position according to Bernoulli's principle. In the antegrade position, the pressure difference remained constant, illustrating that an increased SSS flowrate does not trigger overdrainage.

In the numerical parameter study, the influence of the shunt position was studied in detail. Conclusions were made based on the velocity profile. When advancing more downstream in the SSS, the blood flowrate is higher and the surface area becomes larger. In the first 10 cm of the SSS, the velocity increased from 0.04 m/s to 0.15 m/s. In the last 18 cm, however, the mean velocity in the SSS remained almost constant.

Since the blood velocity has no influence on the difference between the ICP and the SSS pressure in the antegrade set-up (see increased SSS flow), it is clear that shunt position has no influence either.

In the retrograde set-up, however, the impact pressure will rise as the shunt is positioned more downstream in the first 10 cm of the SSS, to reach a more constant value in the last 18 cm. Therefore it seems recommendable for clinical practice to insert the shunt in the last 18 cm of the SSS (downstream part of the SSS).

In the first experiments, no reflow was observed in either numerical or experimental tests. As mentioned above, temporary reflow was only observed while rapidly lowering the ICP (mimicking lumbar puncture) or increasing the SSS pressure. Interestingly, recent clinical studies did not observe any temporary reflow[118]. The reason for this discrepancy could be the constant CSF flow through the shunt in in-vivo conditions. The physiological CSF production ratio is 0.35 ml/min, while there was no CSF production in the experiments. The difference between the pressure in the SSS at the position of the shunt tip and the pressure in the shunt tip will be approximately the same when CSF production is incorporated as without CSF production. Owing to the very

low CSF flow rates the change in impact or wake effect is negligible. However, the difference between the pressure in the CSF reservoir (ICP) and the pressure in the SSS at the shunt tip is increased by the pressure loss in the shunt. According to Poiseuille's law, this pressure drop can amount to 50–100 Pa, possibly explaining the higher capacity to withstand the natural pressure changes without reflow in clinical studies[118]. According to this study, however, an overall no-reflow configuration is not possible without any valve or other mechanical device.

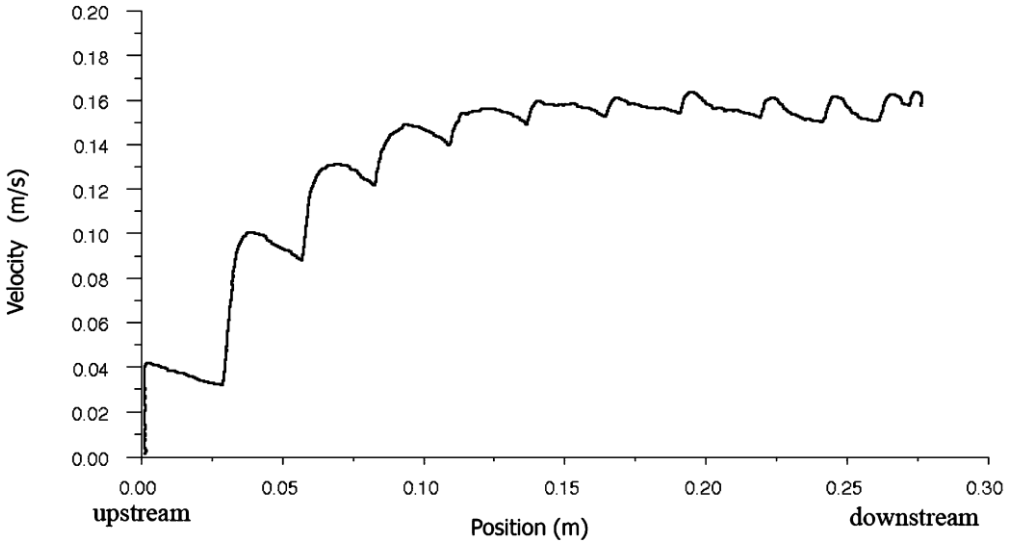

Figure 50. Maximal velocity distribution in the SSS (sagittal plane)

During the compliance measurement of the cortical vein, only one cortical vein with 2 cm length was measured. The use of this limited length can be discussed and is one of the limitations of the study. However, as the total imposed cerebral compliance was obtained from the literature[71], Figure 48 is expected to change only slightly when a more validated vein compliance is used.

A second limitation is the blood flow distribution over the cortical veins. The present authors did not find any relevant data in literature which describes the blood flow distribution along the human SSS. In both the experimental and the numerical models, the blood flow of 200 ml/min was distributed uniformly over the veins. This choice can lead to a velocity field in the modelled SSS that is different from the velocity field in the human SSS. Therefore, the recommendation of this study to insert the retrograde shunt in the last 18 cm of the SSS might have to be slightly adjusted as this distance depends on the inflow distribution in the SSS.

CONCLUSION

This study yields a predictive model to investigate VS shunting as a treatment for malresorptive hydrocephalus. The experimental measurements yield validation for the newly developed numerical model. According to the experimental and numerical tests, shunting the cerebral ventricles to the SSS is possible without permanent reflow, both in the antegrade and in the retrograde configurations. Nevertheless, in order to apply this technique clinically and given the small pressure differences, the fact that a pressure change in the system (e.g. sitting upright against lying down, or lumbar puncture) can cause a temporary reflow of blood in the shunt, should be taken into consideration. According to El Shafei and El Shafei[118] a simple one-way check valve with the least opening pressure can prevent this temporary blood reflow and should be implemented. The best clinical results are expected for a shunt positioned in the most downstream half of the SSS.

3.4 Prospective Clinical Study – 2011

With the hydraulic principles of VSS and of impact effect of RVSS being confirmed by the experimental and the numerical model, and with the clinical experience in the 4 RVSS rescue procedures performed in 2004 - 2005, we felt confident to aim for the prospective clinical RVSS study at the department of Neurosurgery, Ghent University Hospital.

According to the advices formulated in the publication on the experimental and numerical model, we decided to incorporate an one-way VLP valve and to position the end of the dural venous catheter in the most downstream half of the SSS.

Ethical Committee approval, no fault insurance, informed consents (pediatric and adult) were obtained. Approval was granted during the period 15/12/2010 - 15/12/2011, under registration number B67020109500.

3.4.1 MANUSCRIPT 2

TREATING HYDROCEPHALUS WITH RETROGRADE VENTRICULO-SINUS SHUNT
PROSPECTIVE CLINICAL STUDY

E. Baert, F. Dewaele, J. Vandersteene, G. Hallaert,
J-P. O. Kalala and D. Van Roost

[World Neurosurgery, accepted for publication 14/06/2018]

ABSTRACT

Background

Since the 1950's, hydrocephalus can be treated with cerebrospinal fluid shunts, usually to the peritoneal cavity or to the right cardiac atrium. However, due to their siphoning effect, these shunts lead to non-physiological cerebrospinal fluid drainage, with possible co-morbidity and high revision rates. More sophisticated shunt valve systems significantly increase costs and technical complexity and remain unsuccessful in a subgroup of patients. In an attempt to obtain physiological cerebrospinal fluid shunting, many neurosurgical pioneers shunted towards the dural sinuses, taking advantage of the physiological anti-siphoning effect of the internal jugular veins. Despite several promising reports, the ventriculo-sinus shunts did not yet become standard neurosurgical practice.

Methods

In this mono-centric prospective clinical study, we implanted the retrograde ventriculo-sinus shunt, as advocated by El Shafei, in 10 patients. This article reports on our operation technique and long-term outcome, including 4 patients in whom this shunt was implanted as a rescue.

Results

Implantation of a ventriculo-sinus shunt proved to be a feasible technique, warranting physiological drainage of cerebrospinal fluid. However, only in 3 out of 14 patients, functionality of the retrograde ventriculo-sinus shunt was maintained during more than 6 years follow-up. In our opinion, these shunts fail because present venous access devices are difficult to implant correctly and get too easily obstructed. After discussing possible causes of this frequent obstruction, a new dural venous sinus access device is presented.

Conclusion

An easy to implant and thrombogenic-resistant dural venous sinus access device needs to be developed before ventriculo-sinus shunting can become general practice.

KEYWORDS

hydrocephalus, ventriculo-sinus shunt, superior sagittal sinus, dural venous sinus access device

INTRODUCTION

In hydrocephalus (HC) the physiological evacuation of the cerebrospinal fluid (CSF) towards the dural venous sinuses is inhibited, either because of obstruction of its outflow from the cerebral ventricles towards the subarachnoid space ('obstructive' HC), or by limitation of either its subarachnoid space circulation or its absorption at the level of the arachnoid villi into the blood stream of the dural venous sinuses ('communicating' HC)[30,60-62,130].

The standard treatment of HC with ventriculo-peritoneal or ventriculo-atrial shunt (VPS, VAS) has a failure rate up to 50% in the first two years after implantation[94,95,131-133]. A major cause of shunt failure is over-drainage due to the siphoning effect of the CSF column in the vertically orientated catheter when a patient is in a sitting or standing position. By gravity, this CSF column creates aspiration like a piston falling in a cylinder. This siphoning leads to shunt-related intracranial hypotension and aspiration of the choroid plexus into the ventricular catheter. Intracranial hypotension causes headaches, nausea, vomiting, malaise and may lead to slit ventricle syndrome and even subdural haematoma. Aspiration of the choroid plexus is a main cause of shunt obstruction. In response, more sophisticated valves were developed, such as valves with programmable resistance, flow-regulating valves and anti-siphon devices. In spite of these, non-physiological CSF drainage and therefore non-physiological intracranial pressure (ICP) continue to be an issue in 5-10% of the shunted patients. Moreover, these devices increase the financial cost, technical complexity and vulnerability of CSF shunts.

A ventriculo-sinus shunt drains CSF to its natural absorption site, the superior sagittal sinus (SSS). Theoretically it reduces the risk of shunt failure in several ways[111,120]. First, excessive drainage is prevented by preservation of the natural, self-regulating anti-siphon effect of the internal jugular vein[111]. Therefore, there's no need for sophisticated valves or anti-siphon devices. Second, the shunt system is short, less complex and confined to the skull, which minimizes the risk of mechanical failure and infection.

Although a promising technique, early attempts were not successful due to thrombotic obstruction of the distal catheter positioned in the dural venous sinus (Gartner[134], Payr[10] and Dandy[30,61,62] at beginning of 20th century and Sharkey[112], Hash[114] and Wen[113] from 1960's till 1980's). I. El Shafei claimed that implanting a shunt's distal venous catheter with the tip directed against the blood flow ('retrograde') solves the thrombotic obstruction issue. Subtle hydrodynamic related advantages would prevent regurgitation of blood in the distal catheter and preserve the delicate pressure gradient between the dural venous sinus and the ventricles[120]. After extensive experimental and clinical work, El Shafei evolved from the retrograde ventriculo-jugular to the retrograde ventriculo-sinus shunt (RVSS) and reported excellent results in retrospective clinical studies, up to a shunt survival rate of 95% after a mean follow up of over 6 years[11].

In collaboration with the department of Hydraulics of Ghent University Civil Engineering, we implemented both a physical and numerical (computerized fluids dynamic or CFD) model of the RVSS[1]. These models supported El Shafei's experimental work on the hydrodynamic principles of the RVSS. Similar efforts were realised by S.E. Børgesen, F. Gjerris and A. Eklund leading to the development of the SinuShunt®, with an antegrade orientated dural venous sinus catheter[13-15,135].

Although inspired by the RVSS and the SinuShunt®, we wondered why, despite the potential advantages and the promising published clinical results, the RVSS nor the SinuShunt® are not implanted on a regular base worldwide. We realized that many neurosurgeons are reluctant to operate on the dural sinus, due to the risk of major haemorrhage, air embolism (AE) or sagittal sinus thrombosis (SST). Interestingly, none of the published clinical reports mentions these complications.

Therefore, we evaluated the RVSS in a mono-centric prospective clinical study for the treatment of communicating HC. This report summarizes the operation details and the follow-up of all 10 patients included in the study as well of the 4 patients in whom the RVSS was used as a rescue operation.

MATERIALS AND METHODS

Inclusion/exclusion criteria

Approval of Ghent University Hospital's Ethical Committee was obtained to include 'communicating' HC patients during the year 2011 (using an extensive informed consent and a no-fault insurance). Every patient was eligible to be included, without restriction concerning age. Exclusion criteria included: 1) pregnancy, 2) infectious, cardiovascular, haemostatic or severe internal diseases. Inclusion was on voluntary basis.

Surgical technique and materials

Every included patient had a pre-operative computed tomography (CT) and/or magnetic resonance imaging (MRI) scan of the brain. In some cases neuronavigation (NN) was applied (Medtronic, StealthStation® Treon™ AxiEm, Minneapolis, MN, USA). Standard preoperative clinical and serological/clotting examinations were performed.

Surgery was performed under general anaesthesia with tracheal intubation. The semi-sitting supine positioning was used, to retain the venous pressure in the SSS slightly positive. After shaving, washing and disinfection of the surgical region, proper sterile draping of the operating field and Tegaderm® (3M, St. Paul, MN, USA) on the scalp were applied to avoid cutaneous contact.

Two semi-circular scalp incisions and underlying burr holes were made: 1) a right or left parabregmatic and 2) a midline incision across the sagittal suture in the vertex region (in teenagers and adults about 10 cm posterior to bregma or about 3 cm anterior to lambda). In most patients, the SSS diameter starts to widen posterior to bregma and reaches a large and useful diameter halfway between bregma and lambda, with 3-5 mm width and 6-8 mm height internally. Through the parabregmatic burr hole a ventricular catheter (VC; anti-bloc right angle VC, Phoenix / Vygon S.A., Ecouen, France) was positioned in the frontal horn of the lateral ventricles. As promoted by El Shafei, two essential steps were taken maintaining the delicate pressure gradient between the ventricles and the SSS, in favour of the ventricles:

- The dura was perforated with a 2.0-2.5 mm wide round opening, applying monopolar coagulation on the VC's stylet (without the VC); during introduction, the 3 mm diameter VC was stretched on its stylet, narrowing it; once its position in the frontal horn reached, the stretching was released and the catheter re-expanded to its original diameter, creating a 'watertight' joint. If the closure seemed not watertight, a small amount of human fibrin glue was applied.
- The VC was kept blocked once positioned in a frontal horn. Any loss of CSF was compensated by an equivalent amount of intraventricular injection of physiological saline.

A one-way valve with 10 mm H_2O resistance (Codman precision Hakim valve, J&J, Raynham, MA, USA) was flushed, connected with its proximal end to the VC and positioned between the two incisions in the subgaleal layer. At the bottom of the sagittal suture's burr hole, the roof of the SSS was identified; if necessary the burr hole was widened laterally to have it in its centre. Then, a 3 mm wide and 1 cm long bevelled groove was punched out at the posterior border of the burr hole, in line with the trajectory of the SSS. This groove guided the catheter in the longitudinal direction of the SSS and prevented kinking. At the lateral border of this guiding groove, a 1 mm wide drill hole was made to apply a stabilizing polyfilament polyester wire around the sagittal sinus catheter (SSC, Phoenix / Vygon atrial catheter ref A03, pliant tip of 3.0 cm length and 1.3 mm outer diameter). In neonates, infants and toddlers, the skull bone was too thin to create this groove and was the SSC was stabilized with stitches through the periosteal layer. Once these steps performed, a longitudinal 4 mm slit incision was made in the roof of the SSS. With a venous hook, the slit incision was opened and lifted up to introduce the tip of the SSC into the lumen of the sinus. If no resistance was felt, the pliant tip was fully introduced until the thicker catheter part (outer diameter of 2.5 mm) fitted into the slit incision of the sinus roof. If resistance was experienced (septa within the sinus[114,136,137]) the catheter was retracted and reintroduced. In case of persistent resistance, the burr hole was extended and the catheter introduced through a new slit incision in the sinus roof. Catheter patency was checked firstly by aspiration of

blood and secondly by infiltration of saline without resistance. A small patch of absorbable gelatine sponge was applied on top of the catheter's passage through the sinus roof to control possible bleeding. Repetitive flushing of the SSC with saline was performed to prevent blood regurgitation. Only after having replenished the ventricular volume with saline through the VC, SSC and valve were connected. Wounds were rinsed with 1/10 Isobetadine Dermicum® / water solution and closed in separate layers.

Postoperative follow up

The postoperative follow up was based both on clinical and radiological examinations. In children under the age of 2 years, the clinical examination included head circumference, frontal fontanel tension, eye movement examination, evaluation of factors of wellbeing (eating versus intake refusal or vomiting; active versus passive/apathetic behaviour; visual contact versus absence of visual contact; laughing versus irritability or crying; motor functions). In older children and adults complaints of headache, nausea/vomiting, malaise, fatigue were noted. Clinically the Glasgow coma scale, axial stability, visual functions/eye movements and orientation were observed. Radiological examinations included X-ray to control integrity of shunt trajectory and CT or MR-scan to control position of VC and SSC, to prove patency of the SSS and to evaluate the ventricular dimensions and signs of trans-ependymal CSF drainage. All patients had pre- and postoperative MRI and/or CT scan. Three patients with obstructed SSC underwent digital subtraction angiography (DSA) of the cerebral veins or iodine contrast injection through the obstructed SSC under fluoroscopy, to investigate the mechanism of its occlusion.

RESULTS

Table 15. Results

Patients included in prospective group (1-10; white background) and in rescue group (11-14; grey background); age represents the age at the moment of the first RVSS operation [abbreviations used: patient (pat.), female (F), male (M), RVSS survival time (RVSS ST), HC after myelomeningocele closure (MMC), HC after neonatal sepsis (NNS), congenital HC (CONG), HC after chronic subdural hematoma treatment (CSH), HC after traumatic brain injury (TBI), HC after tumor resection (TR), HC after treatment of aneurysmal subarachnoid hemorrhage (ASAH), normal pressure hydrocephalus (NPH), HC because of obstructive malignant brainstem tumor (T), air embolism (AE), electromagnetic neuronavigation (EM NN), ultrasound (US), survival time (ST), obstruction (obstr.), reoperation (reop.)]

pat.	sex	age	HC aetiology	complication	guidance	RVSS ST	RVSS failure	RVSS reop.	result
1	F	6d	MMC	-	-	21d / 85d	SSC obstr.	Y	VPS
2	F	52d	NNS	-	EM NN	46d	SSC obstr.	N	VPS
3	M	84d	CSH	-	US Doppler	6y+	-	N	RVSS
4	F	293 d	CONG	-	EM NN	6y+	-	N	RVSS
5	M	16y	TBI	AE	EM NN	21d	SSC obstr.	N	VAS
6	M	36y	TR	-	EM NN	100d	SSC obstr.	N	VPS
7	F	55y	ASAH	-	EM NN	7d / 7d	SSC obstr.	Y	VAS
8	F	60y	ASAH	-	EM NN	12d / 7d	SSC obstr.	Y	VPS
9	M	63y	ASAH	-	EM NN	4d	SSC obstr.	N	VPS
10	M	86y	NPH	-	-	112d	SSC obstr.	N	VPS
11	F	3y	MMC	-	-	12y+	-	N	RVSS
12	F	15y	T	-	-	(68d)	T growth	N	death
13	F	16y	TR	-	US Doppler	14d	SSC obstr.	N	VAS
14	F	42y	TR	-	US Doppler	105d	SSC obstr.	N	VPS

The RVSS implantation was technically successful in all, with indisputable preservation of the watertight fitting of the dura around the perforating VC and with correct positioning and retrograde orientation of the SSC on the postoperative imaging. Locating exactly the midline of the SSS through a standard burr hole, was not always obvious. In some cases the burr hole needed to be extended; NN and US Doppler proved helpful.

Also, none of the patients suffered any CSF loss whatsoever (e.g.: leakage after closure of trepanation wound or of myelomeningocele), and all had sterile CSF with normal protein level and cell count.

In the prospective group, only 2 out of 10 patients benefited of a long lasting RVSS ST (Table 15). Both were young children and in both cases, the RVSS was successful without the need of reoperation (Figure 51).

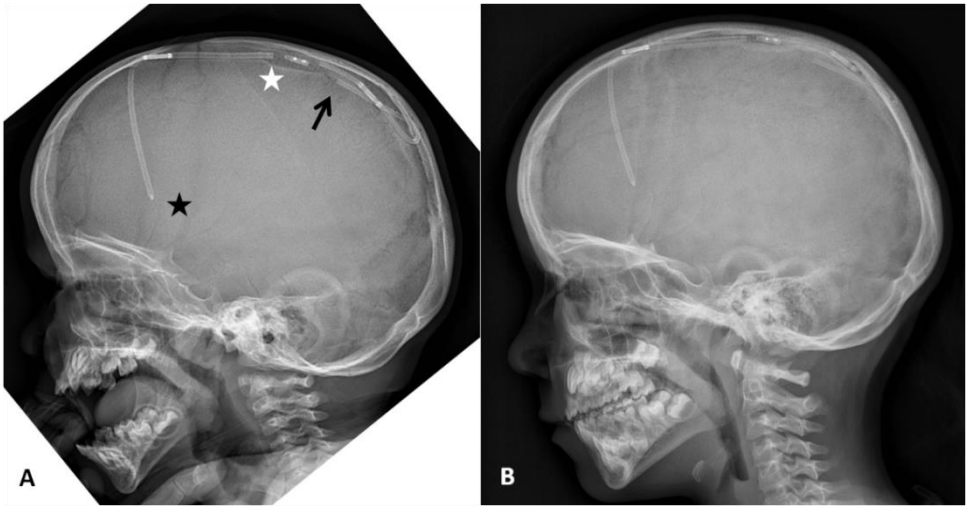

Figure 51. Postop images

Profile skull X-ray of patient 4 at 5 months postop (A) and 4 years 11 months postop (B). The black star indicates the tip of the VC, the white star the shunt valve and black arrow the tip of the SSC.

In the RVSS failure group (in all cases because of an obstructed SSC), 3 out of 8 patients underwent an operative revision of the obstructed SSC (Figure 54). None of the re-operated RVSS were lasting and all patients of the failure group were converted to a VPS or VAS. In all RVSS failures, the sinus catheter was removed when converting into a VAS or VPS.

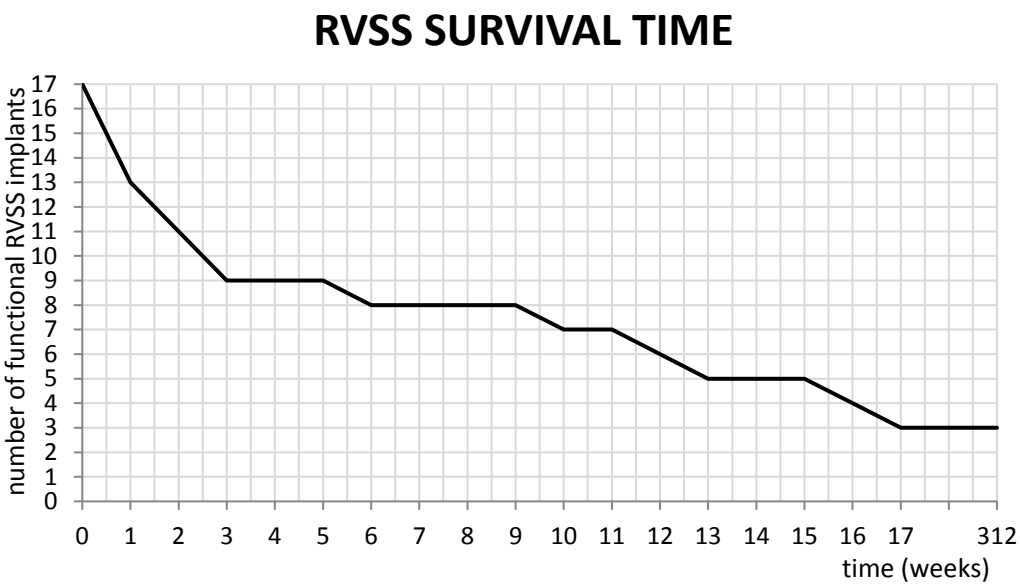

Figure 52. Kaplan-Meier graph

Displaying the survival time (time to clinical proof of block/obstruction) in 17 SSC implantations, on 14 patients (study + rescue group)

During surgery of a blocked SCC, visualisation of the catheter's tip inside de SSS was technically impossible. Prior to removal of a blocked SCC, we remarked that per-operative contrast injection demonstrated a sleeve around the catheter's tip; limited amount of contrast was leaking into the SSS, the rest oozed at the catheter's SSS introduction point, from between the SSC and its surrounding sleeve. This sleeve could be a thrombotic or an endothelial one, or a combination of both. We considered it medico-ethically unacceptable to open the SSS roof widely or to introduce a Fogarty

balloon catheter in order to remove the obstructed SSC together with its surrounding sleeve. Hence, the SSC was simply retracted out of the SSS and seemed – at close inspection – immaculate. In all 3 occasions of introduction of a new SSC through a slit incision at about 1 cm anterior to the former, the procedure remained uneventful.

In the rescue group, only in 1 out of 4 patients the RVSS remained undeniably functional. Doubtfully, one could include patient 12, as her HC control lasted until she died because of progressive malignant brainstem glioma. However, we considered a control period of 68 days too short to conclude. Patient 14 provided information concerning the physiological CSF drainage effect of the RVSS. 4 days before her RVSS surgery, she had an intraparenchymal ICP sensor implanted, being the bearer of a functional VAS with Integra OSV II valve but with ongoing intracranial hypotension in upright position. Her VAS was ligated 1 day before the RVSS surgery. Before ligation, her ICP ranged between 0 mm Hg in supine position to –15 mm Hg sitting or standing. After ligation, the ICP raised progressively up to 31 mm Hg. During the RVSS implant, the ICP dropped from 20 mm Hg to 11 mm Hg as the RVSS became functional. 2 Days later, her ICP ranged from 0 mm Hg in supine position to –7 sitting or standing and the clinical signs of intracranial hypotension had disappeared.

It is to note that none of the patients received anti-thrombotic drugs, except for patient 10. This patient was on prophylactic warfarin because of cardiac atrial fibrillation.

DISCUSSION

Despite small, this study gave answer to the questions about technical and operative feasibility, physiological CSF drainage, and long-term effectiveness of the RVSS.

In accordance with previous research[11,15,138], we consider the RVSS implantation an applicable procedure. In 17 procedures a single onset of AE was noticed by an acute drop in the end tidal CO_2 pressure from 34 mm Hg to 19 mm Hg. Applying fibrin glue, combined with mild Trendelenburg table tilting, immediately resolved the problem. In

none of the patients a SST occurred, in the short nor in the long term follow up (Figure 52). All bleedings were swiftly controlled with gentle gelatin sponge compression and – if necessary – extra anti-Trendelenburg tilt of the OR-table. We encountered no wound healing problems, infections and operation related morbidity nor mortality. No shunt related problems other than obstruction of the SSC have occurred.

In line with previous reports[11,15,138,139], we found that the RVSS restored a physiological intracranial pressure, as was noted above concerning patient 14. In the 3 patients with already more than 6 years lasting patency of the RVSS, absence of anamnestic, clinical and radiological signs of intracranial hypo- or hypertension was noted. In the infants, head circumference evolution stabilised on its percentile (Figure 53).

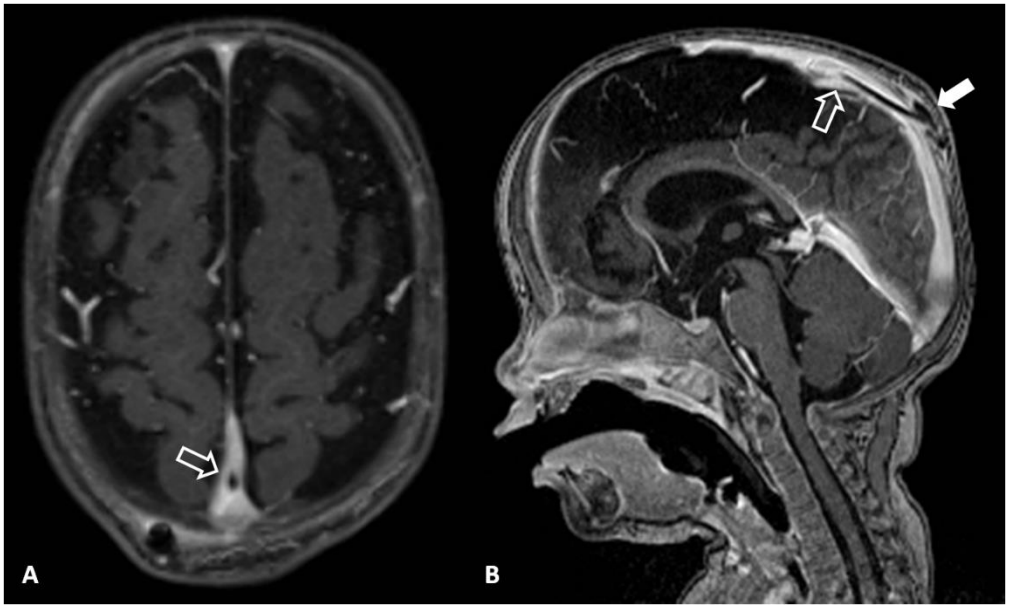

Figure 53. 1 month postop

Axial (A) and sagittal (B) T1 with IV gadolinium cerebral MRI of patient 4, 1 month postop. The open arrow indicates the tip of the SSC centrally in the SSS; the white arrow indicates the passage of the SSC through the roof of the SSS. The homogeneous contrast enhancement of the SSS excludes SST.

However, rapid and frequent obstruction of the SSC proved to be a major issue leading to the interruption of the study after the inclusion of 10 patients. DSA examination of 3 patients with an obstructed shunt, revealed an impeding sleeve around the distal catheter's tip (Figure 54). Although we were not able to harvest this sleeve for investigation, we suppose that it consisted of thrombus and/or of endothelial overgrowth.

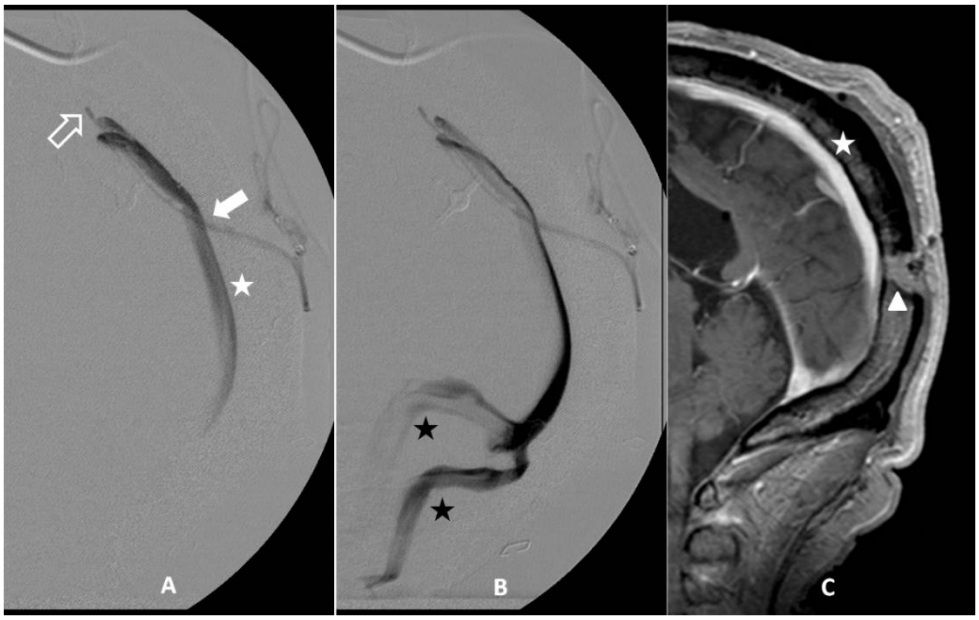

Figure 54. 4 months postop

(A) instantaneous and (B) few seconds later contrast enhancement of SSC and SSS during venogram (iodine contrast injection through the SSC), 4 months postop; (C) cerebral MRI, sagittal T1 with IV gadolinium, 2 months after removal of SSC

The open arrow indicates the tip of the SSC, the white star the SSS, the white arrow the passage of the SSC through the roof of the SSS, the black stars the transverse-sigmoid sinuses and the white triangle the burr hole above the SSS. Mark the homogeneous contrast enhancement of the sinuses.

These results contradict the hypothesis of El Shafei that retrograde implantation of the SSC solves the issue of thrombotic obstruction. According to El Shafei the beneficial

effect of the retrograde position relies on two advantages. Firstly, the blood flow 'hits' the draining CSF column and stagnates at the shunt tip. According to Bernoulli's principle, kinetic energy is converted to potential energy and the static pressure in the shunt rises by the amount of the dynamic pressure in the SSS. In other words, the ICP is kept above the pressure in the SSS. This effect is called the 'impact effect' by El Shafei[12,120,123]. This impact effect should preserve the delicate pressure gradient between the ventricles and the SSS, creating a continuous CSF outflow. Secondly, when the SSC is directed against the blood flow, CSF will be deflected and flow over the catheter's surface. According to El Shafei, the resulting 'CSF sleeve' protects against clot formation [120], reducing the blood-catheter-contact-surface and flushing away thrombus deposits (Figure 55).

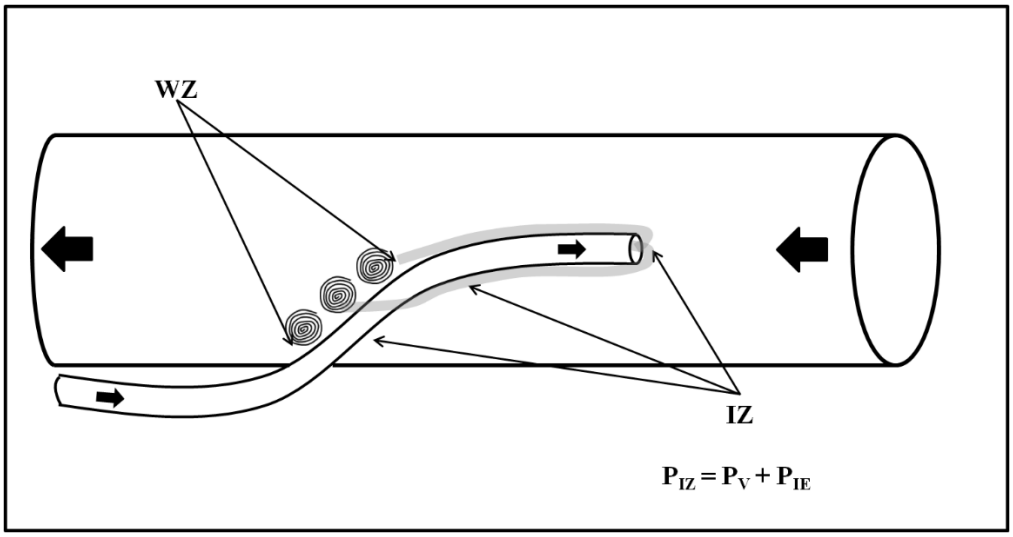

Figure 55. Drawing of retrograde orientated catheter in a vessel with laminar blood flow (big black arrows)

The CSF continuously streaming out of the catheter (small black arrow) creates a molecular CSF layer on the outside surface of the catheter (transparent grey zone) and gets accumulated in the stagnating and non-laminar blood flow at the wake zone (WZ) of the intravascular part of the catheter (spirals). The pressure at the impact zone (IZ, P_{IZ}) is the venous pressure (P_V) augmented by the dynamic pressure of the impact effect (P_{IE}) and equals the pressure inside the SSC.

The rapid and frequent obstruction in the failure group urged us to critically revise the hypothesis of El Shafei. We identified two factors that may promote clot formation and shunt obstruction:

- **Decentralised position of the SSC tip** – In the failure group, we noticed on the postoperative CT scan imaging that the tip of the SSC was not "centrally" positioned in the SSS, but rather 'laterally', with its tip against the vessel's wall (Figure 56). Despite our drilling of a guiding groove for the SCC, in accordance to the recommendations of Børgesen[14,15], this decentralised position of the SSC tip occurred in the majority of patients. We suspected that the lateral position of the SSC tip plays a major role in the frequent and rapid obstruction, as it has many disadvantages:
    - The velocity of the blood stream close to the wall of a blood vessel is very low. The velocity is at its maximum in the centre of the vessel. Therefore a tip against a vessel wall cannot benefit of the impact effect created by the retrograde orientation[1,139]. Also, low blood flow velocity predisposes to thrombus formation.
    - In a blood vessel, the concentration of red blood cells is at its highest in the centre of the vessel and at its lowest at the border. The opposite is true as to the clot forming factors of blood, plasma and platelets, which are at their highest concentration against the vessel wall[140].
    - A device in contact with the endothelial wall, stimulates both the endothelial growth and the clot forming cascade[107,141].

    Possible causes of the lateral position:
    - As SSS septa might block the passage of the SSC, they might also deviate the catheter's tip from its straight and central trajectory.
    - Both the RVSS and the SinuShunt® require a long distance SSC in the SSS. It is technically impossible to make sure that the tip of a long and flexible catheter is centrally positioned.

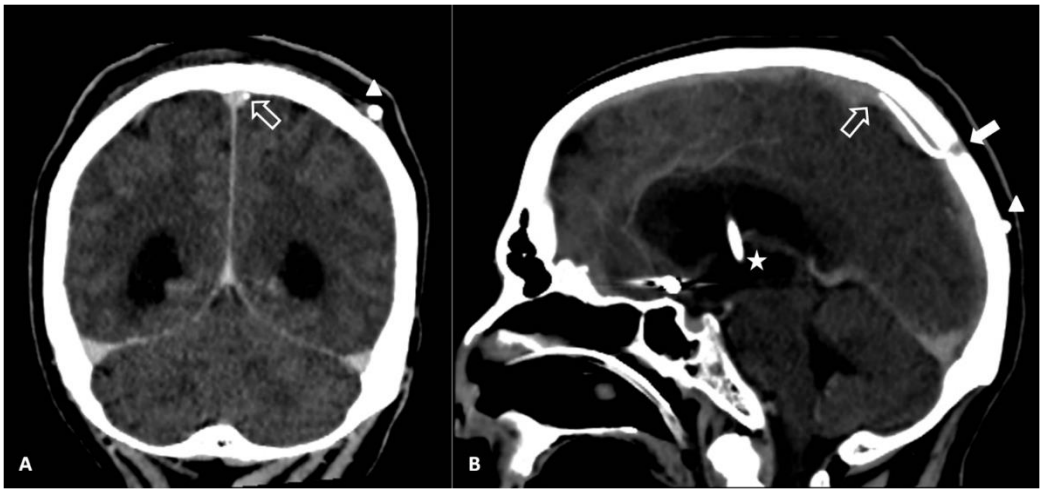

Figure 56. 14 days after the first SSC implantation

(A) coronal and (B) sagittal iodine IV cerebral CT scan of patient 8, 14 days after the first SSC implantation, just before the RVSS revision operation

The open arrow indicates the tip of the SSC, the white triangle the subgaleal trajectory of the RVSS, the white arrow the passage of the SSC towards the SSS through the burr hole, the white star the tip of the VC just passing through the foramen of Monro. Note the eccentric position of the tip of the SSC against the sinus wall and the homogeneous contrast enhancement of the sinuses.

- **CSF inducing blood clotting** – We suspected and proved in vitro, that CSF induces blood clotting[142]. In clinical practice, this can be observed by the rapid formation of membranes around the collection of a CSF leak, trying to encapsulate and to stop the leakage. CSF should reach a minimal concentration of about 5-9% to have a thrombogenic effect. Physiological concentrations of CSF in the SSS are far below 5%, as CSF inflow is approximately 0.35 ml/min for a blood flow of more than 200 ml/min[11,15,143]. However, in specific circumstances the coagulation enhancing effect of CSF could be problematic. Typical situations are contact between CSF and foreign material (molecular layer of continuous CSF outflow around tip of SSC) and accumulation of CSF in the stagnating non-laminar blood flow at the wake zone

of the SSC. Consequently the ‘protective’ CSF sleeve around the tip of the SSC might have turned out to be thrombogenic.

To address the above mentioned issues we proposed novel ‘dural venous sinus access device’ (DVSAD) prototypes (*Figure 57*).

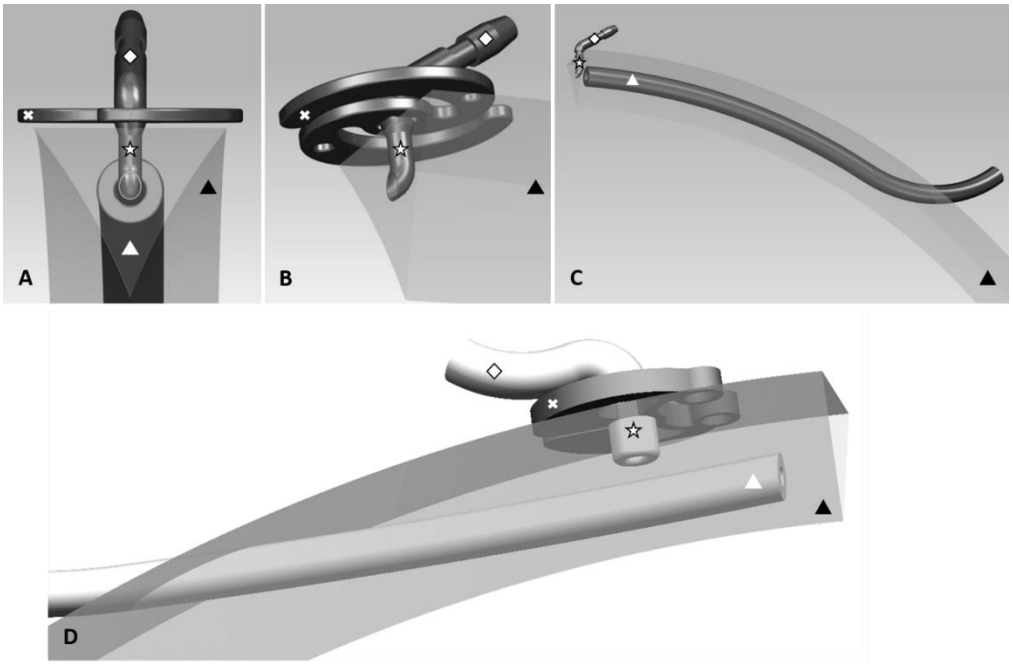

Figure 57. Drawings of the DVSAD prototypes

A, B and C represent the directional Tuohy tips capable of retrograde orientation. D represents the neutrally oriented tip. [intravascular tip (white star), epidural base plate (white X), connecting catheter (white diamond), standard SSC (white triangle) and SSS (black triangle)]

The device consists of a short intravascular tip with adaptable length, to determine the tip’s depth in the SSS centre. Its perpendicular introduction makes it easier to implant and the stabilizing epidural base plate secures its central position. Compared with a standard SSC, significant differences might reduce its thrombogenic capacities:

- Its tip will be in the centre of the SSS, where the blood flow’s velocity is maximal and the concentration of plasma factors and platelets at its lowest.

- It has a significantly reduced intravascular volume and surface. This minimalizes disturbance of the blood flow and creation of wake zone.
- The distal opening of the DVSAD has a retrograde either neutral (i.e. perpendicular to blood flow direction) orientation. As already mentioned, the retrograde orientation would benefit of the hydrodynamic impact effect but will create a larger surface of CSF-blood-catheter interface. The neutral orientation would reduce the contact surface between CSF and the intravascular tip as the CSF will be carried away immediately. It renounces the impact effect and will not be prone to the Venturi effect as the vessel's diameter is not narrowed.

The potential benefits of these DVSAD prototypes on surgical-technical domain and on prevention of thrombosis are currently being evaluated by in vitro and in-vivo animal models. In case of positive results we will proceed with a human prospective clinical study.

CONCLUSION

The prospective clinical trial with the RVSS as described by El Shafei was interrupted because of high failure rate due to blockage of the SSC. Nevertheless, operative feasibility and safety were proven, as was physiological drainage of CSF. Our goal to create a long-lasting and easily implantable RVSS remains. Therefore, the data obtained here formed the basis for a subsequent research project aiming at developing a new dural venous sinus access device (DVSAD), easily implantable, with its tip stabilized in the centre of the SSS and reduced thrombogenic characteristics.

CONFLICT OF INTERESTS

There are no competing interests to be reported.

CHAPTER 4. PROTOTYPING NOVEL 'DURAL VENOUS ACCESS DEVICE'

Nevertheless its operative feasibility and safety, its capacity of near-physiological / balanced CSF drainage in the treatment of HC, the poor results of RVSS survival did exclude continuation of the prospective clinical study and acceptance of the VSS as standard medical practice.

The decision was taken to carry on with the RVSS study, starting with the development of a newly designed dural venous access device (DVSAD), in order to prevent thrombus formation and rapid obstruction.

4.1 Concept

In the light of our observations during the clinical study, literature review and consultation of experts in the field of blood coagulation (prof. dr. Filip De Somer and dr. Anna Vantilborgh), the following characteristics for the DVSAD prototype were considered essential:

- Stable and central orientation of DVSAD's venous end (Figure 58).
- Easily and safely implantable
  A perpendicular way of introduction through the SSS roof, in combination with its epidural base plate, the introduction would be easy, the depth of introduction predetermined and stabilized. Because of its morphological aspect and its way of introduction, the DVSAD's nickname was the sinus-pushpin (sinus-punaise).

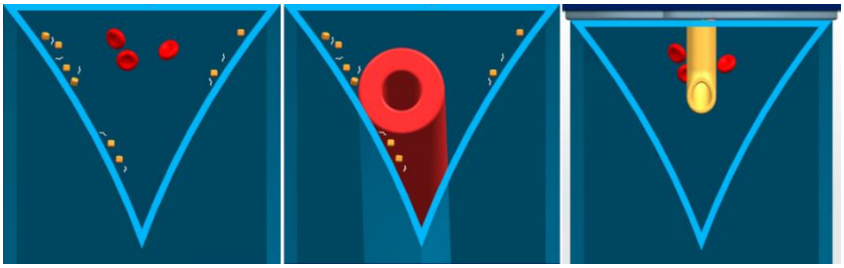

Figure 58. A cut through the triangularly shaped SSS

[left] In the center of a vessel, the concentration of RBC is relatively higher than at the edges of a vessel, where the concentration of platelets and clotting factors increases. [middle] In the failure group of the clinical RVSS study, the tip of the sinus catheter was adjacent to the SSS wall, where the concentration of platelets and clotting factors is high and the blood flow rate is slow. [right] The concept of the dural venous access device (DVSAD), with its tip at the center, perpendicular (to the vessel's wall or orientation) introduction into the vessel, its significantly reduced intravascular volume and surface and its epidural base plate.

- Minimal intravascular volume of DVSAD (Figure 59)
  The massive reduction of the DVSAD's intravascular volume compared to the standard silicone dural venous catheter should result in reduction of blood stream influence and of blood-material interface surface.
- Retrograde orientation of DVSAD's end
  Initially the retrograde orientation and subsequent impact effect remained an issue and the goal. This was obtained giving the DVSAD's end an orientable Tuohy-needle-like opening, to avoid a long distance intravascular segment.

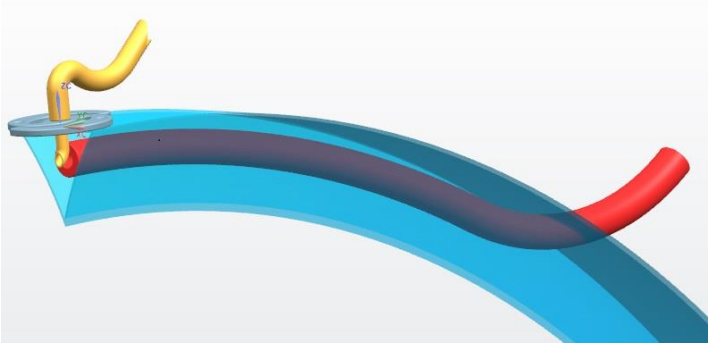

Figure 59. 3-D drawing of the new DVSAD concept

Intravascular volumes of DVSAD and standard silicone venous catheter compared.

4.2 Material selection – IOF and SI co-operation

At the start of our prototyping project, some questions needed to be responded: (a) Which raw material should be used to prevent thrombogenic activity? (b) Where / by who will the prototypes be developed and produced? (c) How will the prototyping project be financed?

On suggestion of dr. Frank Dewaele, we applied for an IOF (Industrieel OnderzoeksFonds) at the UGent. Consequently, in 2012 The IOF granted the project a StarrTT fonds (IOF11/StarTT/014) to enable us producing prototypes and having them tested in vitro. Considering the prototyping and production process, we contacted Stearable Instruments© (SI), a firm specialized in designing and developing dedicated medical devices. SI agreed to co-operate and fully support us.

We decided that prototypes would be made in various materials, with and without coating. In accordance with the thrombogenic results obtained during the in vitro experiment, the material of choice for further investigation would be determined. Initial prototypes were manufactured in:

- Nitinol; this nitinol-group was divided into a subgroup without and a subgroup with phosphoryl choline coating.
- Polyimide group; because of its inert behavior and resistance to heat, electrical conductance and chemical reactions.
- Control group with the standard medical degree silicone venous catheter.

4.3 Roller pump test

4.3.1 Selection of circulatory pump of in vitro model

In order to take final decision concerning the material selection and DVSAD design, before implementation in an eventual animal model study, in vitro tests were mandatory. Concerning the in vitro tests, the standard test for intravascular devices, the Chandler loop (Figure 60), was considered not fulfilling the following demands:

- The DVSAD should be tested in fresh human blood with a high flow rate comparable with the flow rate of up to 200 - 400 ml/min in the SSS.
- The in vitro set-up should allow injection of fluids through the tested DVSAD.

To obtain an in vitro test setup capable to meet these requirements, a non-occlusive roller-pump model was developed in co-operation with the Ghent University Hospital Cardiac Surgery experimental laboratory (Figure 61). The roller pump test setup, materials and results are written down in the following manuscript, 'A new dynamic model for in vitro evaluation of intravascular devices'.

Figure 60. Chandler loop set-up

Our Chandler loop set-up allowing infiltration of a fluid (in this case methylene bleu) through the 'DVSAD' perforating the silicone tube wall. Rotation was possible thanks to integrating the three way stop cock as a rotation axis. Only if a large air-bubble was allowed in the tube, 'blood flow' could be created, making this model inadequate for our experimental set-up. Therefore the Chandler loop option was quickly abandoned.

4.3.2 MANUSCRIPT 3

A NEW DYNAMIC MODEL FOR IN VITRO EVALUATION OF INTRAVASCULAR DEVICES

E J Baert[1], J Vandersteene[1], F Dewaele[1], A Vantilborgh[3], D Van Roost[1] and F De Somer[2]

[IJ of Artificial Organs, accepted for publication September 20, 2018]

Department of Neurosurgery[1],
department of Cardiac Surgery[2],
department of Hematology[3] of Ghent University Hospital, Belgium

An approval for the collection and use of human CSF and fresh whole blood was granted by the hospital's Ethical Committee and registered as EC/2016/0560.

ABSTRACT

Introduction: A dynamic model to evaluate thrombus formation on intravascular catheters *in vitro* is presented. The model enables fluid infusion, variation in the catheter orientation and variable flow conditions. It was applied on a catheter used to shunt cerebrospinal fluid (CSF) to a vein, a dural venous sinus, for the treatment of hydrocephalus.

Methods: Fresh human blood filled circuits were circulated in a non-occlusive roller pump. A catheter infused either with CSF, Ringer's lactate (RL) or no fluid (control) was inserted through each circuit's wall. Sixteen circuits (6 CSF, 6 RL, 4 control) ran

for 60 minutes. Qualitative assessment was performed by measuring viscoelastic properties of blood at the start and end of the experiment; quantitative evaluation of clot formation by scanning electron microscope.

Results: Average blood velocity was 79 mm/s, with a pressure wave between 5 and 15 mmHg. At the experiment's end, the infused fluid represented 5.88 % of the blood/infusion volume in the circuit. The control circuits showed no statistical difference between start and end for viscoelastic testing whereas both RL and CSF enhanced coagulation, most pronounced for the latter. Most thrombus material was observed on catheters in the CSF group. Clot formation was less pronounced on the surface of the catheter facing the blood flow.

Discussion: A dynamic model for intravascular catheter testing mimics better clinical conditions when evaluating blood material interaction. Catheter position, blood flow around the catheter and infusion fluid have all a potential impact on the hemocompatibility of a given catheter.

Key words: blood, cerebrospinal fluid, dynamic in vitro model, thrombogenicity, venous catheter

INTRODUCTION

Catheters are widely used to gain vascular access. Typical examples are peripheral and central venous catheters, arterial lines. However, blood-material interaction remains an issue and may lead to thrombotic complications[106,107,144-150]. As such good preclinical evaluation of catheters is mandatory to reduce potential risks for the patient.

A Chandler loop, an in vitro model to evaluate hemocompatibility and clot formation on intravascular devices[151], is often used for evaluation of catheters. It consists of a circular closed tubing filled with blood and a small amount of air. As the circular tube is rotated at a constant speed, the air bubble - which remains at the highest point -

generates a ‘blood flow’[152]. The set-up allows to evaluate catheter related factors such as biomaterial and design but does not allow to mimic several relevant in-vivo conditions that may influence thrombotic depositions. A first limitation is the flow rate. Catheters are often inserted in large vessels with resulting high flow rates. However, in a Chandler loop the flow rate is limited, as at higher rotation speeds, the air bubble starts to rotate in synchrony with the blood in the tubing[152]. A second limitation is related to the fact that the impact on the coagulation of the drugs or the infusion fluids administered through the catheter cannot be evaluated. One could overcome this limitation by inserting the catheter through the wall of the Chandler loop. A major disadvantage of this approach is that the catheter now has a fixed position, exposing it with each turn to the air in the air bubble. This exposure causes mechanical hemolysis, leucocyte induction, platelet activation and non-physiological shear forces that will significantly bias the results[152-154].

Animal models allow to evaluate relevant in-vivo conditions. However, animal blood is not completely comparable to human blood, which can influence the test results, especially when testing small bore catheters. As such, more vast results are obtained by using fresh human blood for the thrombogenic evaluation of medical devices[152,155,156].

In this study a dynamic model is proposed that overcomes many limitations of contemporary test methods. It can generate any required flow and allows to test a catheter while infusing fluids. In order to validate this dynamic model, it was used in this study to evaluate the venous catheter of a ventriculo-sinus shunt for treating hydrocephalus[11,15].

MATERIALS AND METHODS

Experimental set-up

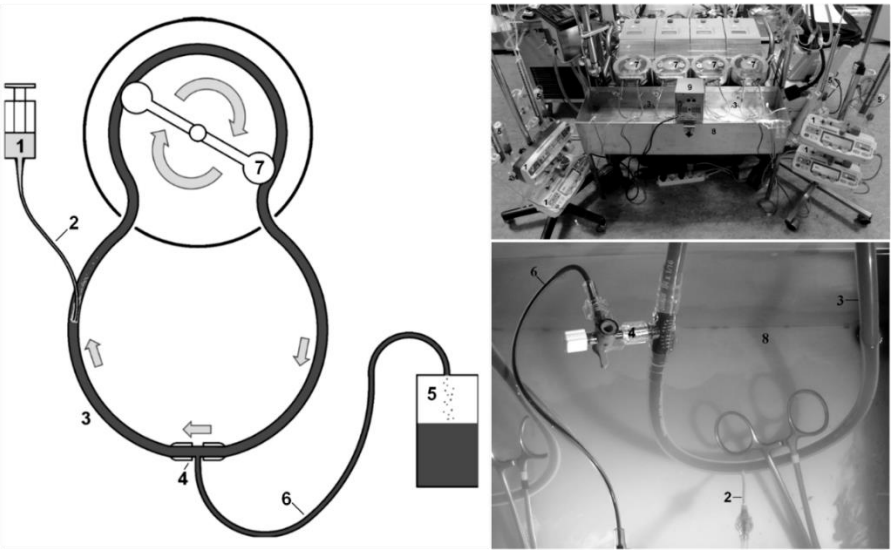

Figure 61. syringe pump injects the infusion fluid through a catheter

A syringe pump (1) injects the infusion fluid through a catheter (2) into the circuit (3) mimicking the blood vessel. The circuit's tube is closed by a T-formed connector (4) linked to dripping reservoir (5) through an overflow line (6) on which a pressure transducer can be connected. The overflow line compensates for the injected volume by draining an equal amount of the infusion fluid/blood mixture to the dripping reservoir. Blood flow is generated by a semi-occlusive roller pump (7). Depending on the rotational direction of the roller pump (round arrows) the blood flow (straight arrows) will be directed with or against the direction of the flow in the catheter (on the drawing the blood flow and the flow in the catheter have opposite directions). The circuit is submerged in a warm water bath (8) set at a temperature of 37°C (9).

The set-up of the dynamic model used to evaluate the venous catheter of the ventriculo-sinus shunt is shown in Figure 61. Specific characteristics of the in-vivo situation are the infusion of CSF through the intravenous catheter, the high blood flow and blood velocity[157] in the superior sagittal sinus (SSS) and the orientation of the intravenous catheter that is directed against the blood flow ('retrograde')[120].

Three groups were defined: a CSF infusion, a Ringer's lactate (RL) infusion and a no infusion (control, CTRL) group. In all groups, the circuit was filled with fresh whole human blood collected by standard venipuncture from two healthy donors and immediately heparinized with 0,7 IU/ml. The CSF used in the CSF group was obtained from a single patient with a ventriculo-external drainage. This CSF was sterile, biochemically normal and with a total protein concentration of 25,7 mg/dl. An approval for the collection and use of human CSF and fresh whole blood was granted by the hospital's Ethical Committee and registered as EC/2016/0560.

The CSF or RL was infused by a syringe pump (Ohmeda 9000, GE Healthcare, Madison, USA) at a rate of 2 ml/h. In the control group (no infusion) the catheter was purged with RL and subsequently closed at the extravascular end, in order to prevent backflow of blood.

The catheter was made of Tecothane (Lubrizol, TT-1074 A) with an internal diameter of 1,3 mm, a wall thickness of 0,6 mm and a total length of 30 mm. The catheter was inserted through the circuit's wall and 25 mm advanced into the lumen. The circuit consisted of 1m of ¼ inch phosphoryl choline-coated silicon tubing (LivaNova, Mirandola, Italy). After rinsing the circuit with RL, it was filled with the donor blood and closed by connecting both ends by a polycarbonate connector with a Luer lock. An overflow line, connected to the Luer lock port, allowed to compensate for the injected infusion fluid volume by draining an equal amount of the blood/infusion fluid mixture to a dripping reservoir. The reservoir's drip level is positioned 14 cm above the circuit which results in a pressure of 140 mm H_2O (10.3 mm Hg or 1373 Pa), representing a physiological pressure in the superior sagittal sinus in supine position[71]. In one circuit, a pressure transducer (DTXPlus; Argon; Bornem, Belgium) is connected to the Luer lock. A roller-pump (LivaNova, Mirandola, Italy) is set at 15 rounds per minute (RPM). A dynamic occlusion setting was used at 15 RPM with 75 % occlusion, resulting in a blood velocity of 79 ± 4 mm/s. The accuracy of the occlusion was validated by a calibrated cylinder. This non-occlusive setting is non-traumatic to blood[158].

The blood flow is opposite to the outlet of the catheter. The catheter's outlet is thus positioned 'retrograde' (Figure 62). All circuit's tubing outside the pump housing is submerged in a heated water bath to maintain blood temperature at 37 °C.

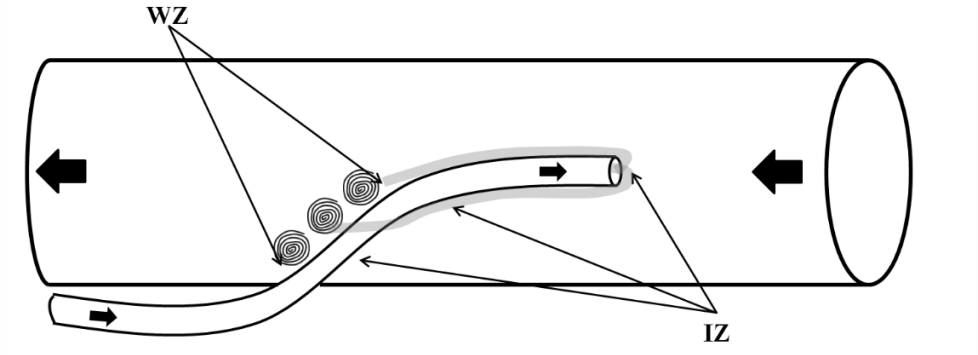

Figure 62. Retrograde position of the shunt's catheter in the vessel

The catheter is implanted against the blood flow. Two sides of the catheter are visualized: the impact zone (IZ) defined as the flank facing the blood flow and the wake zone (WZ) defined as the 180 degrees opposite flank (away from the incoming blood flow).

The concentration of the infusion fluid in the blood filled circuit (C_{inf}) depends on the infusion rate (Q), the outflow of the infusion fluid/blood mixture and the 'intravascular' volume (V_{tot}). The infused volume equals the drained volume, and the intravascular infusion fluid/blood mixture remains identical to the mixture drained to the dripping reservoir. By consequence, draining to the dripping reservoir doesn't change the ratio between blood and infused fluid in the circuit. The volume percentage of the infusion fluid ($V_{\%inf}$) at a given time (t) is given by the following formula:

$$\mathbf{C_{inf} = V_{\%inf} = t \times Q / (V_{tot} + t \times Q) \times 100\ \%}$$

The infusion rate was 2 ml / 60 min, the total intravascular volume 32 ml (volume circuit $= \pi \times r^2 \times l = \pi \times (0.635\ cm / 2)^2 \times 100\ cm$) and the duration of the test 60 minutes. Thus, at the end of the experiment the volume percent of the infusion fluid was:

60 min × 2 ml / 60 min / (32 ml + 60 min × 2 ml / 60 min) × 100 % = 5.88 %

For this experiment, a total of sixteen circuits (6 with infusion of CSF, 6 with RL and 4 CTRL) was used. Each circuit was circulated by a roller pump and, with exception of the control group, infused, during a period of 60 minutes. The experiment was performed in 4 separate runs of 4 circuits simultaneously (with 4 adjacent and identical roller pumps, fig. 1). Each run contained blood from the same donor and at least one circuit of each group (CSF, RL and CTRL).

A Sonoclot® Coagulation Analyzer (Sienco®, Inc., 7985 N. Vance Drive, Suite 104, Arvada, CO, 80003 USA) was used to evaluate changes in blood coagulation between the start and the end of the experiment. The Sonoclot® reports three values, activated clotting time (ACT, i.e. time to the end of the liquid phase or to the initiation of the fibrin monomers formation), clot rate (CR, i.e. speed and strength of polymerization of fibrin monomers into a fibrin gel) and platelet function (PF, i.e. clot retraction, speed and strength of the platelets adherence and retraction in the fibrin gel)[159].

After termination of the experiment, the catheter was cut out together with its surrounding circuit's wall, in order to prevent abrasion of deposits, and prepared for surface electron microscope (SEM) imaging (Figure 63).

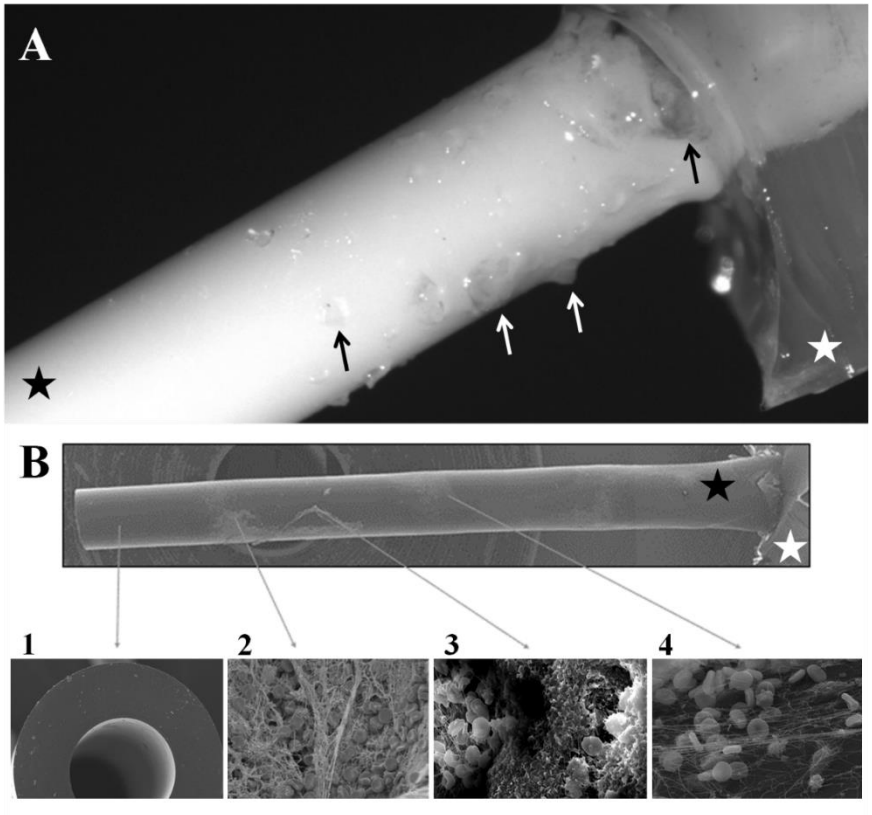

Figure 63. Stereophotographic image and SEM of a catheter

(A) stereophotographic image and (B) SEM of a catheter (black star) with its cut out circuit's wall (white star) and multiple deposits of coagulate on its surface (black and white arrows) Detailed SEM images of patterns of deposits recognized on the catheter's surface: detail (1), 70 × magnification, shows a smooth/'clean' surface at the tip. Details (2, 3, 4), 1500 – 2000 × magnification, demonstrate different clot patterns, combinations of fibrin network with captured red blood cells, thrombocytes and leucocytes.

Two sides of the catheter are visualized: the impact side, defined as the flank facing the blood flow and the wake-side, defined as the 180 degrees opposite flank, away from the incoming blood flow (Figure 62). The SEM images were corrected for projection effects by a script (MATLAB Simulink version 8.6) that applies the appropriate mathematical formulas to 'unroll' instead of project the three-dimensional cylinder onto a two-

dimensional plane, to prevent underestimation of the surface away from the center of the image (Figure 64). This method is described in detail elsewhere[160].

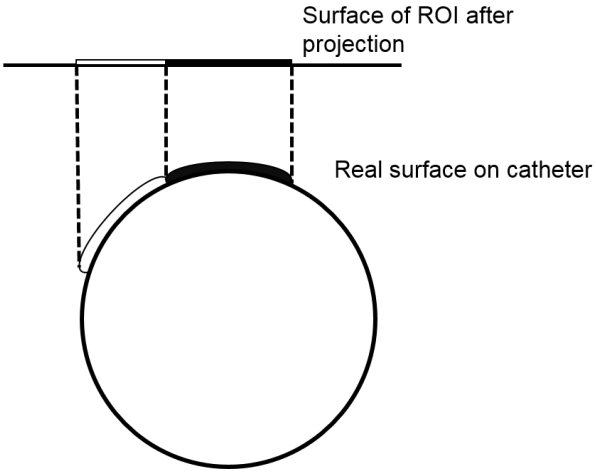

Figure 64. Bias due to 2D projection of a 3D surface of a cylindrical object
(ROI: region of interest)

Next, at each side of the catheter, the surface covered with clots was delineated (ImageJ for Windows, Version 150, available for download at https://imagej.nih.gov/ij/index.html) and expressed as a percentage of the visualized surface at the same side ($ratio_{clot}$). The amount of clot formation was evaluated by calculating the ratio between the surface of the catheter covered by coagulation debris and the total visualized surface.

$$\mathbf{ratio_{clot} = surface_{clot} / surface_{total}}$$

Statistical analysis

Statistical analysis was performed using a commercial software package (SPSS Statistics® 22 IBM Corp., Released 2013, IBM SPSS Statistics for Windows, Version 22.0, Armonk, New York, USA). Baseline Sonoclot® parameters were compared to those obtained at the end of the experiment by a non-parametric Mann-Whitney U test.

The amount of visualized catheter surface covered with clots is compared between the different infusion fluids (CSF, RL or CTRL) by a non-parametric Mann-Whitney U test. A one-sample t-test was used to evaluate differences in clot formation on impact and wake sides of the catheter.
Statistical significance is set at 5%.

RESULTS

Evaluation of the in vitro test-setup

The non-occlusive roller pumps generated an average blood flow of 141 ± 7.5 ml/min, resulting in a blood velocity of 79 ± 4 mm/s.
Thanks to the draining to the dripping reservoir, the pressure inside the circuit remained stabilized throughout the experiment. The pressure wave had a maximum ('systolic' pressure) of 15 mm Hg and a minimum ('diastolic' pressure) of 5 mm Hg. No leakage was observed during the experiment.

Coagulation parameters

Sonoclot® parameters are presented in table 1. Although a clear ACT prolongation was measured in both CTRL ($p = 0.285$) and RL ($p = 0.138$) infusion groups while it stagnated in the CSF group ($p = 1$), statistical evidence was not significant. On the other hand, the CR and PF increased significantly in both RL and CSF infusion groups, but not in the CTRL.

Table 16. comparison of the difference of ACT/CR/PF values

Comparison of the difference of ACT/CR/PF values before and after the experiments for CSF, RL and CTRL, grouped by infusion fluid, Asterisk: comparing the start and stop value (before and after the run) yielded a p-value < 0.05

	Infusion Fluid		
Parameter (median)	**CTRL**	**RL**	**CSF**
Δ ACT [s]	41.0	44.0	0.0
Δ CR	3.5	4.2*	6.3*
Δ PF	1.0	1.4*	2.3*

Evaluation of clot formation on the catheter surface

Clot formation, defined as red blood cells and platelets embedded in a fibrin network, was observed on the surface of all the catheters. It was explored if there was a difference in the amount of clot formation depending on blood donor (donor 1 versus donor 2), infusion fluid (CRTL versus RL versus CSF), or side of the catheter surface (impact versus wake side). The values of $ratio_{clot}$ for the different groups are shown in table.

$Ratio_{clot}$ did not differ between the two donors (P-value = 0.6). However, differences were found depending on the infusion fluid. The difference between RL and CSF are statistically significant (P-value = 0.009).

When the impact and the wake sides of the catheters were evaluated separately, $ratio_{clot}$ was higher on the wake side of the catheters (statistically significant, P-value = 0.008).

Table 17. Ratio between the catheter surface and the total catheter surface

The ratio between the catheter surface covered with clots and the total catheter surface depending on blood donor, infusion fluid and catheter side. Single and double asterisks: the difference between the marked parameters is statistically significant, $p < 0.05$

Parameter	$Ratio_{clot}$
Donor 1	0.45 ± 0.11
Donor 2	0.53 ± 0.14
CTRL	0.68 ± 0.15
RL	0.63 ± 0.14*
CSF	0.88 ± 0.05*
Impact	0.42 ± 0.08**
Wake	0.50 ± 0.09**

DISCUSSION

The presented in vitro experiment demonstrates that it is possible to mimic part of the in-vivo conditions to which intravascular catheters are subjected: infusion of fluids through a catheter, orientation and position of a catheter in a vessel and a realistic blood flow velocity and pressure. Mimicking "real world" conditions is important as we could clearly demonstrate that both the infusion fluid as the position of the catheter will influence catheter patency.

Our goal was to evaluate the impact of CSF infusion and of specific blood flow characteristics on the degree of thrombus formation on the venous catheter of an experimental ventriculo-sinus shunt to treat hydrocephalus. This shunt, draining CSF from the brain's ventricles towards a dural venous sinus consists out of 3 components. The proximal ventricular catheter and one-way valve are well accepted and routinely used components of CSF shunts. However, the distal venous catheter is prone to

thrombosis and more research is needed to optimize its design and to define the best polymer to attenuate blood-material interaction.

In our short-duration-experiment deposits were observed on the surface of each catheter at the end of the experiment. This is no surprise as protein adsorption takes place within minutes after blood exposure, even in the presence of small amounts of heparin. Once adsorbed the intrinsic coagulation cascade will be activated[155].

Although infusion volumes were small, significant differences were found in the amount of clot formation between catheters infused with RL versus CSF.

Both CTRL and RL infusion groups, had an increase in ACT and CR values. ACT reflects the time necessary till initial fibrin monomers formation and represents the intrinsic limb of the coagulation cascade. Increased post-experiment ACT values can be explained by deprivation of fibrinogen and consumption of clotting factors during the in vitro test. The CR value is a measure for the rate at which fibrin monomers are polymerized into fibrin. The CR value increases in all post-experiment blood samples. This can be explained by the formation of thrombin, due to the extracorporeal circulation of the blood[159].

When CSF is infused, ACT remains stable whereas both CR and PF increase significantly more than in RL and CTRL groups. This finding confirms the coagulation enhancing effect of CSF[142] which seems to compensate for the fibrinogen deprivation and the consumption of clotting factors due to the in vitro test.

The infusion of fluids proved to have an influence. There was a trend towards less clot formation in the RL group compared to the CTRL group. Thus, although CR and PF increased more in the RL group compared to the CTRL, less clot formation was observed on the RL catheters, indicating that the presence of a RL fluid sleeve did attenuate blood-catheter interaction and thrombogenicity. If CSF is infused, the ACT remains stable while the CR and PF both increase significantly more than in RL and

CTRL group. We observed significantly more clot formation in the CSF group compared to the others. The presence of a CSF sleeve seemed enhancing blood-catheter interaction and thrombogenicity.

Another important finding was the impact of catheter orientation in the vessel and the surrounding blood flow conditions. A significant lower number of deposits was seen on the impact side of the catheter compared to the 180 degrees opposite wake side. As blood streamlines hit the catheter surface they deflect and cause shear forces that might wash off deposits in an early stage. On the other hand downstream the catheter, laminar flow is disrupted resulting in eddy formation and local stagnation[12] both known to promote clot formation[120].

Strengths and weaknesses of the model

The usage of blood from different donors is a possible source of bias. This was attenuated by performing a control loop (without infusion of fluid) with each portion of donated blood and by distributing the different loops (RL, CSF and CTRL) equally between the donors.

The infusion of fluids results in hemodilution that may bias the results. The rate of 2 ml/h in combination with limited duration of 60 minutes for each circuit was chosen to minimize hemodilution and related blood coagulation disturbances[142]:

- By limiting the duration of the experiment and the infusion rate, the volume percentage of the infusion fluid was only 5,88 % at the end of the experiment. This is significantly lower than 9 – 11 % that is the known threshold for infusion fluids like CSF and RL to affect blood coagulation properties[161].
- In the non-hydrocephalic population, physiological drainage of CSF through the cranial venous sinuses measures about 20 ml/h. In the hydrocephalic patient, the required CSF drainage through a CSF shunt is highly patient dependent, from a few ml/h up to the full 20 ml/h. Also, CSF flow through a shunt fluctuates: e.g. the flow equals zero during periods of a pressure gradient between the ventricles and the

venous structures lower than the opening pressure of the shunt's valve and, vice versa, can attain milliliters per minute during a Valsalva maneuver. Therefore, we consider that the continuous CSF flow, even at a low level, as representative for the study of thrombogenic characteristics of a shunt's venous catheter.

The blood flow velocity of 79 ± 4 mm/s is below the average blood flow velocity reported in the SSS measured with phase-contrast cine MR imaging between 136 and 229 mm/s[157,162,163]. A lower velocity was preferred as we realize that this high velocity is only attained in the strict center of a circuit with laminar flow and its decline follows a parabolic curve once out of the center towards the margins. In real life conditions, rarely the catheter will be positioned in the strict center, and therefore its tip submitted to a significantly reduced blood velocity. This 'worst case scenario' seemed the better option. Easily, the roller pump set-up itself could generate a wide variety of physiological blood flow velocities, making this model adaptable for studying other intravascular catheters or devices.

The absence of the endothelium-catheter interaction is its main drawback, as is encountered in any other in vitro set-up.

SUMMARY

We present an in vitro experiment that better mimics some of the in-vivo conditions to which intravascular catheters are subjected. The set-up allows infusion of fluids, correct positioning and orientation of the catheter and generation of realistic blood flow conditions, to study the blood-fluid-catheter interactions. Adding these variables to the test set-up significantly influences catheter thrombotic capacity.

ACKNOWLEDGMENTS

None.

DISCLOSURES

There's no conflict of interest to report concerning the materials or methods used in this study or the findings specified in this paper.

This research was not funded by any external company or industry. All costs were covered by the Departments of Neurosurgery and Cardiac Surgery of the Ghent University Hospital, Ghent, Belgium.

4.3.3 Conclusions roller pump test on material selection

In the roller pump test different DVSAD types were compared with the control group of standard silicone venous catheter.

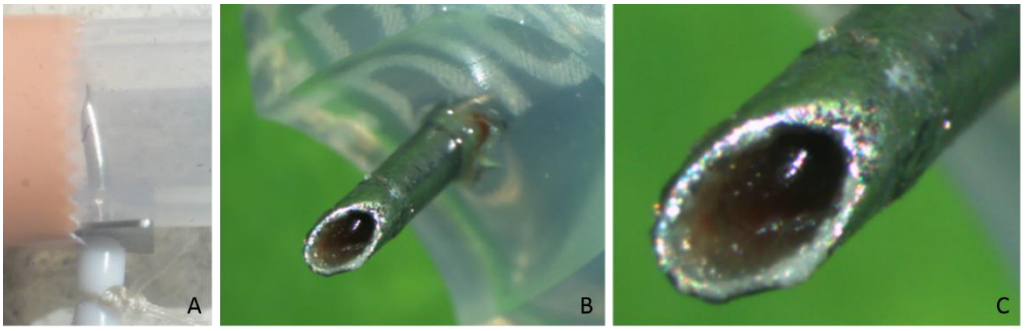

Figure 65. (Stereo)photography of nitinol DVSAD wiht Tuohy-needle-shaped end
(A) Photography of DVSAD just introduced through the loop's tubing wall, before filling it with blood; (B) stereophotography of DVSAD cut out with its surrounding tubing wall, at the end of the experiment; (C = magnification of B) clear thrombi deposits on the external surface and inside the end's aperture.

- A nitinol group (Figure 65 and Figure 68) was subdivided in 3 sections: (a) Tuohy-needle-shaped end, tested in retrograde orientation, (b) 45° angle cut end, also tested in retrograde orientation and (c) cross cut end, tested in perpendicular orientation in relation to the bloodstream. In the Tuohy-needle-shaped subdivision, a group with

and a group without phosphoryl choline coating were tested. All other DVSAD prototypes and control silicone catheters (Figure 66) remained without coating.

- Polyimide group (Figure 66), with cross cut ends.

Figure 66. Stereophotography or the polyimide DVSAD prototype

(Left) with its cut out loop wall and (right) in detail. Clear thrombus formation is noted on its blood contact surface and at or in its tip.

In order not to remove possible deposits or thrombi, both silicone control catheters and DVSAD prototypes were cut out of the loop tubes together with a surrounding part of the tubes wall, at the end of each roller pump session. All the devices were fixated and prepared for surface electron microscopic evaluation. Independent of the end's morphology and independent of the presence or absence of phosphoryl choline coating, the results were poor for both Nitinol and Polyimide prototypes. On both significant thrombus deposits were registered at the external device service and in the end's aperture. Only the silicone control group showed no or very limited deposits (Figure 67). As a consequence the nitinol and polyimide trajectories were abandoned.

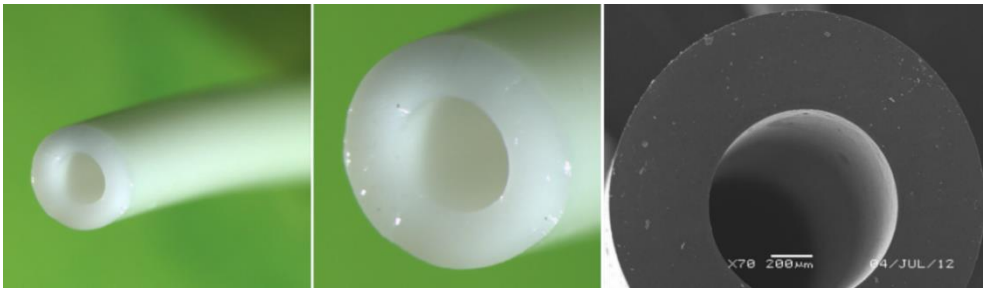

Figure 67. Ends of cut out controle silicone catheters

(Left and middle) stereophotography and (right) surface electron microscope of the silicone control catheter: minimal and very few thrombi deposits.

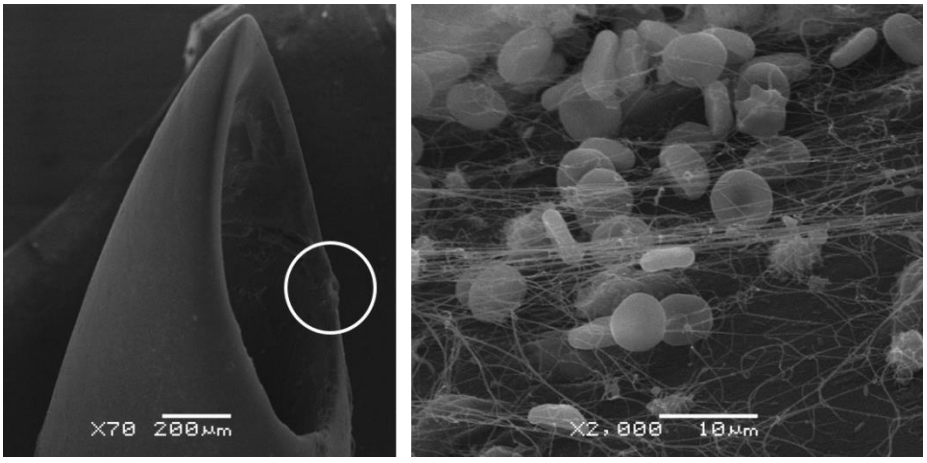

Figure 68. Electron microscopy confirming the thrombus formation

Surface electron microscopy confirming the thrombus formation on the tip of the nitinol phosphoryl choline coated DVSAD.

CHAPTER 5. ANIMAL IN-VIVO STUDY

5.1 Concept, material selection – IOF and SI co-operation

After the roller-pump in-vitro experiments with the initial DVSAD designs, following conclusions were made:

- The material of choice should definitely be medical grade silicone or polyurethane (PU). Literature and daily clinical practice indicating similar thrombogenic and biocompatibility for both polymers[156,164-168], the choice was made to start off with polyurethane. Reasons to choose polyurethane included the possibility to use pressure molding techniques or heated tip setting techniques to produce the prototypes. These techniques are not applicable with silicone, silicone devices need to be produced with pouring techniques or dipping techniques, which are difficult to get standardized. Polyurethane injection molding techniques would allow to produce prototypes in constant quality, greater design possibilities and difficulties at lower cost, once the injection mall manufactured (Figure 77). Also, polyurethane comes in a greater variety of qualities and of durometers, again increasing prototyping possibilities.
- The base plate, being extradural, will remain made of nitinol.
- The co-operation with SI and IOF concerning the VSS trajectory, will continue.

A new IOF fund was granted in 2013 - 2014 (F2012/IOF-Advanced/041) with the following goals / targets (Table 18):

- Production of DVSAD prototypes in medical grade polyurethane, using injection molding or tip-set techniques, in close co-operation with SI (Figure 69).
- Selection of an animal model, in co-operation with the faculty of Veterinary Medicine of UGent.

- Performing in-vivo animal model tests in co-operation with the faculty of Veterinary Medicine.
- Funding of a full-time scientific co-worker on the project (dr. Jelle Vandersteene).

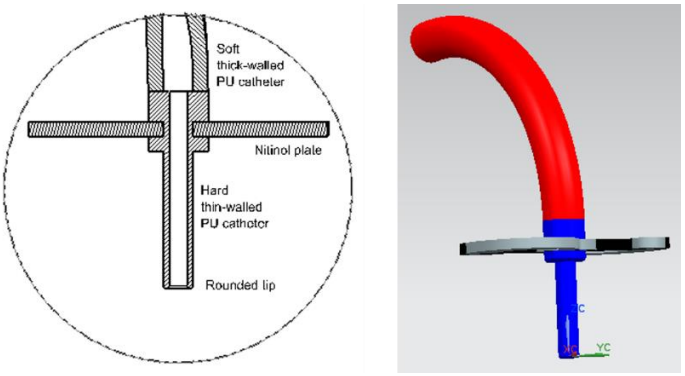

Figure 69. Technical and NSX drawings of the first prototype of animal DVSAD

Meanwhile, in co-operation with IOF, a patent design and search concerning the DVSAD was initiated. This finally resulted in a US patent granted August 2016 (manuscript 4).

Table 18. main targets of the advanced IOF Starr project

prototyping of implantable animal model adapted DVSAD
prototyping and production of implantable telemetric pressure sensor
prototyping of ventricular aiming device
in vivo tests of the VSS with DVSAD on animal hydrocephalus model

5.2 MANUSCRIPT 4

US009402982B2

(12) **United States Patent**
Baert et al.

(10) **Patent No.: US 9,402,982 B2**
(45) **Date of Patent: Aug. 2, 2016**

(54) **MINIMALLY-ADVANCING LUMINAL CATHETER**

(75) Inventors: **Edward Baert**, Melsen (BE); **Frank DeWaele**, De Pinte (BE)

(73) Assignees: **Steerable Instruments BVBA** (BE); **Universiteit Gent** (BE)

(*) Notice: Subject to any disclaimer, the term of this patent is extended or adjusted under 35 U.S.C. 154(b) by 179 days.

(21) Appl. No.: **14/241,488**

(22) PCT Filed: **Sep. 5, 2012**

(86) PCT No.: **PCT/EP2012/067334**

§ 371 (c)(1),
(2), (4) Date: **Feb. 27, 2014**

(87) PCT Pub. No.: **WO2013/034602**

PCT Pub. Date: **Mar. 14, 2013**

(65) **Prior Publication Data**

US 2014/0207044 A1 Jul. 24, 2014

Related U.S. Application Data

(60) Provisional application No. 61/531,312, filed on Sep. 6, 2011.

(30) **Foreign Application Priority Data**

Sep. 5, 2011 (EP) 11180066

(51) **Int. Cl.**
A61M 5/00 (2006.01)
A61M 27/00 (2006.01)
A61M 25/04 (2006.01)

(52) **U.S. Cl.**
CPC ***A61M 27/006*** (2013.01); ***A61M 25/04*** (2013.01)

(58) **Field of Classification Search**
CPC A61M 27/006; A61M 27/002; A61M 5/14276; A61M 2202/0464; A61M 2210/0693; A61M 2205/8287; A61M 25/04; A61B 5/031
USPC 604/8–10, 537
See application file for complete search history.

(56) **References Cited**

U.S. PATENT DOCUMENTS

3,492,996	A	2/1970	Fountain	
4,646,752	A	3/1987	Swann	
6,264,625	B1 *	7/2001	Rubenstein	A61M 27/006 604/537
2008/0262406	A1 *	10/2008	Wiener	A61M 25/04 604/8

FOREIGN PATENT DOCUMENTS

WO	2013034602	A1	3/2013

OTHER PUBLICATIONS

International Preliminary Report on Patentability for PCT/EP2012/067334. Dated Mar. 12, 2014. 6 pages.

* cited by examiner

Primary Examiner — Philip R Wiest
(74) *Attorney, Agent, or Firm* — Lathrop & Gage LLP; James H. Velema, Esq.

(57) **ABSTRACT**

The present invention relates to an implantable catheter (**100**) provided for insertion through a wall (**50**) of a dural venous sinus (**70**) in a subject, having a proximal (**20**) and distal end (**30**), comprising: —a tubular shaft (**10**) for insertion through the wall (**50**) of the venous sinus (**70**) into the sinus (**52**), provided with a shaft lumen (**12**) in fluid connection with a proximal port (**14**) at the proximal end and a distal port (**16**) at the distal end of the shaft (**10**), and —a stop element (**40**) disposed on an outer surface of the tubular shaft (**10**), configured to limit the depth of insertion of the tubular shaft (**10**) into the sinus.

19 Claims, 11 Drawing Sheets

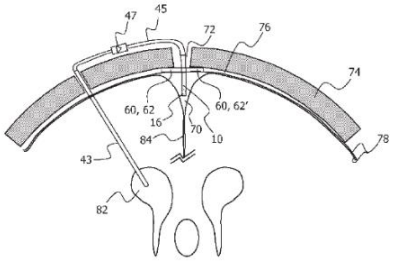

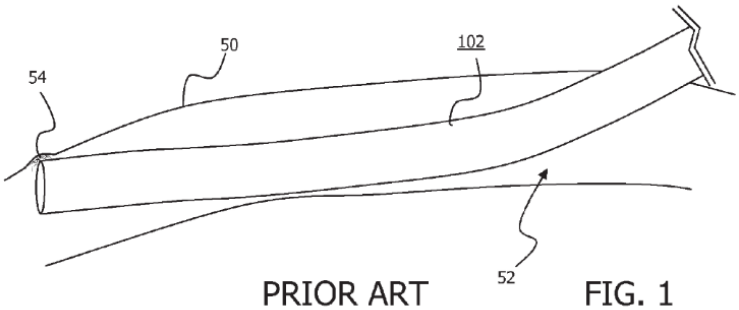

PRIOR ART FIG. 1

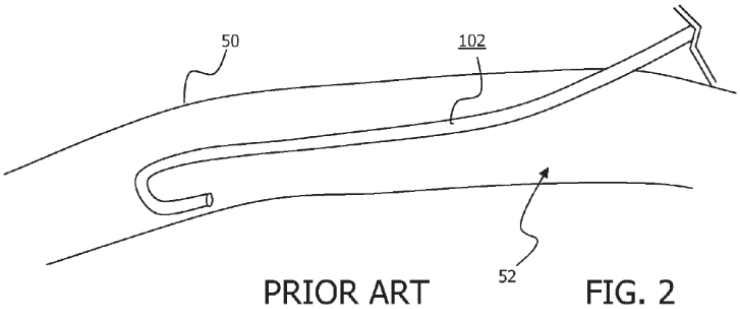

PRIOR ART FIG. 2

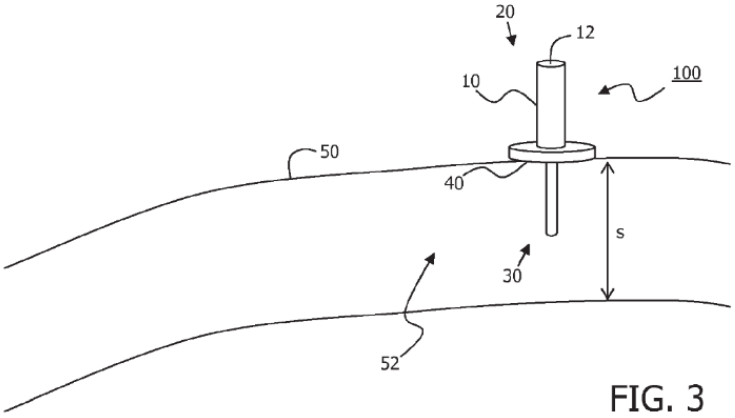

FIG. 3

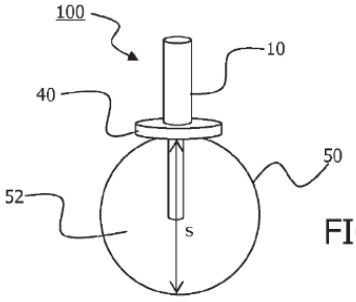

FIG. 3A

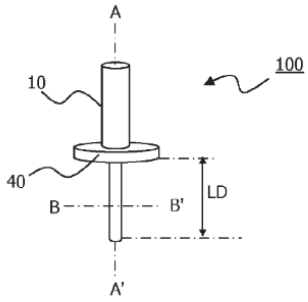

FIG. 4

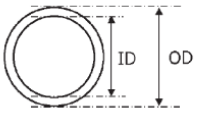

FIG. 4A

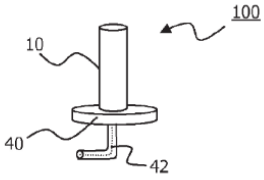

FIG. 4B

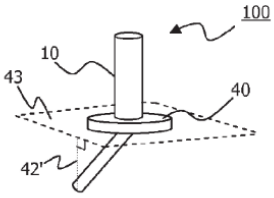

FIG. 4C

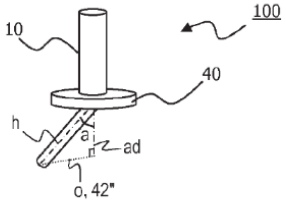

FIG. 4D

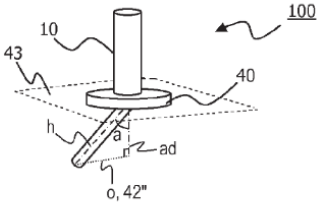

FIG. 4E

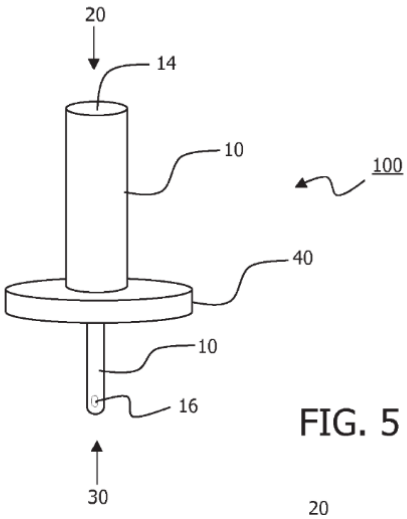

FIG. 5

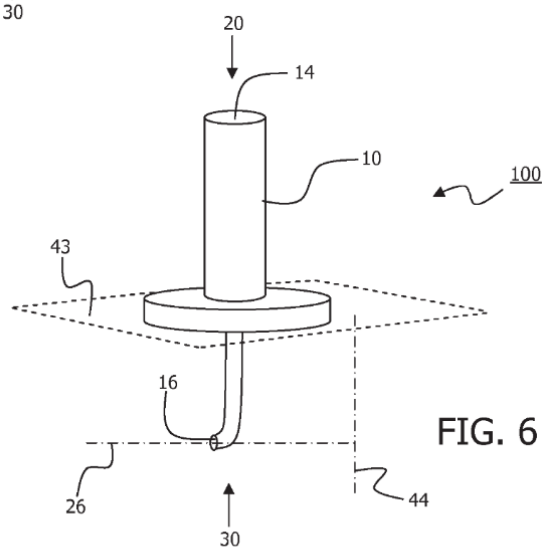

FIG. 6

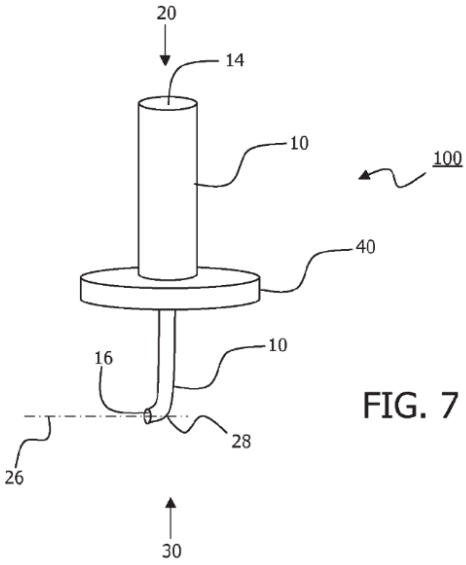

FIG. 7

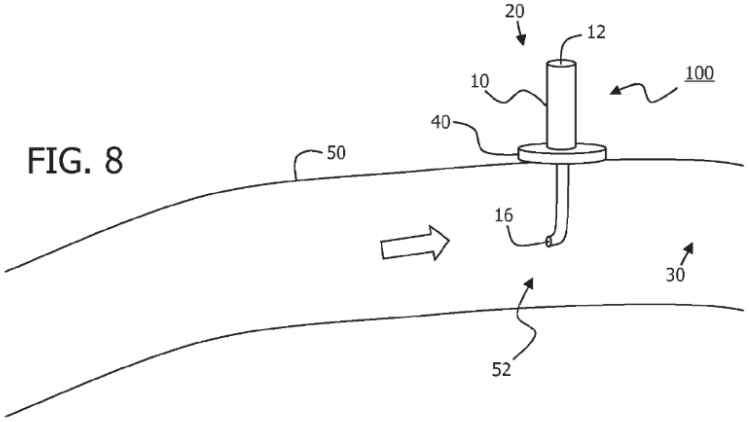

FIG. 8

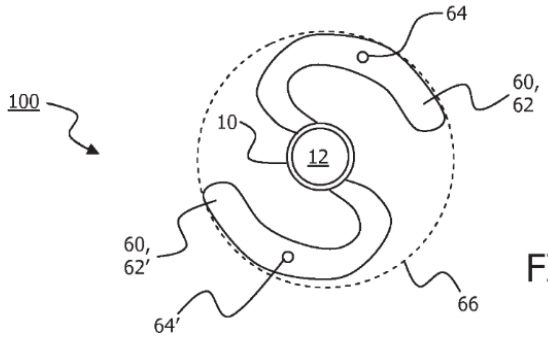

FIG. 9

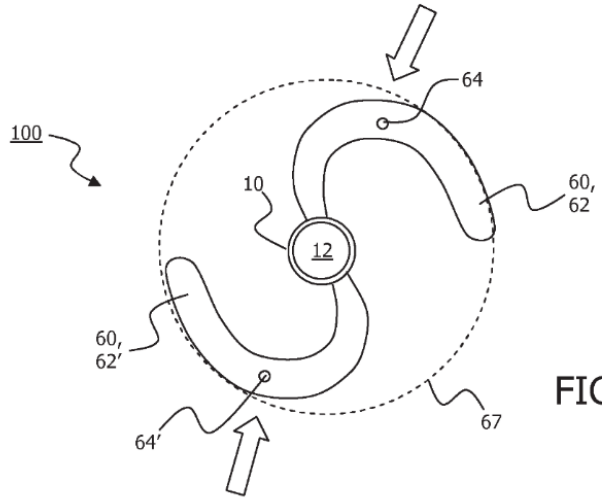

FIG. 10

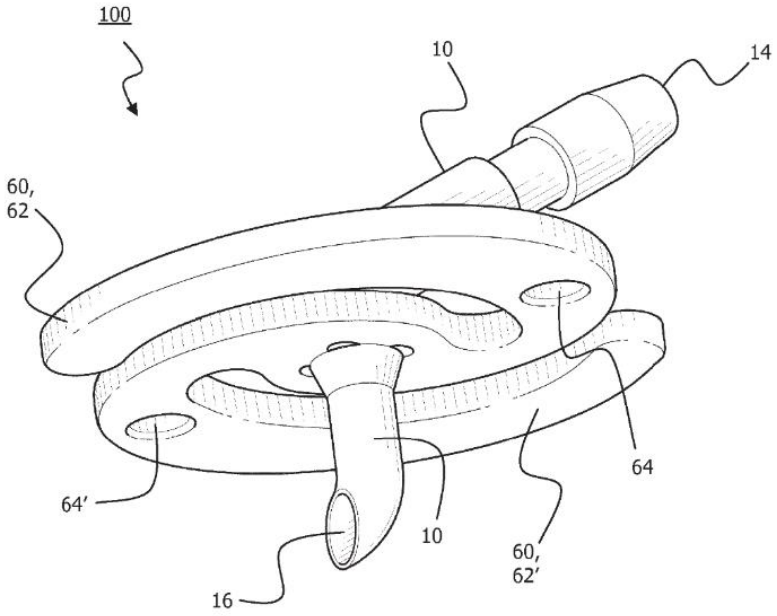

FIG. 11

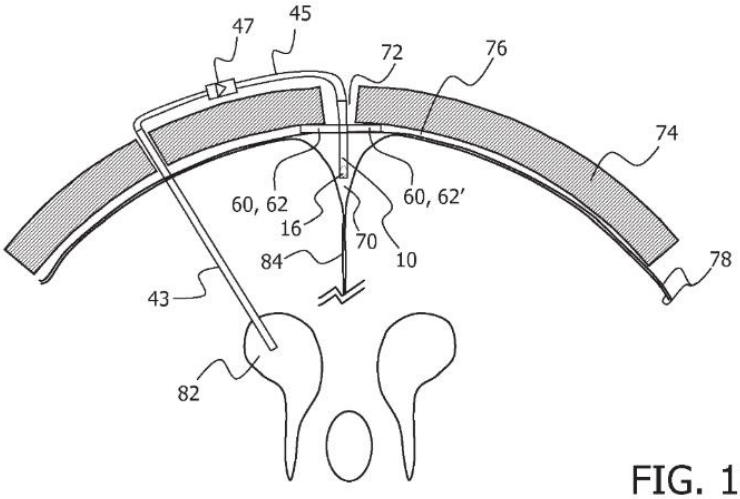

FIG. 12

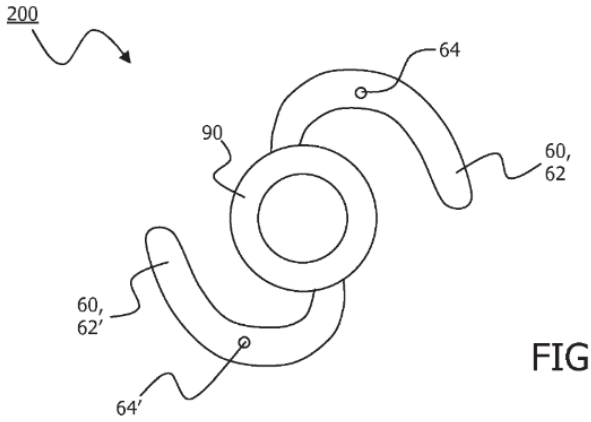

FIG. 13

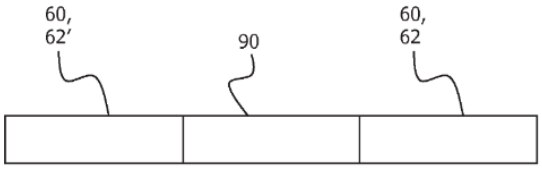

FIG. 13A

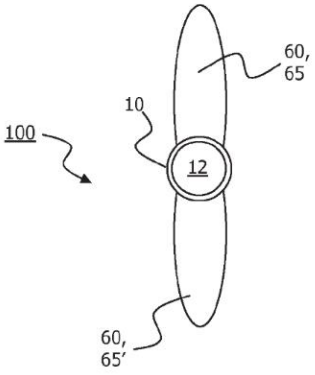

FIG. 14

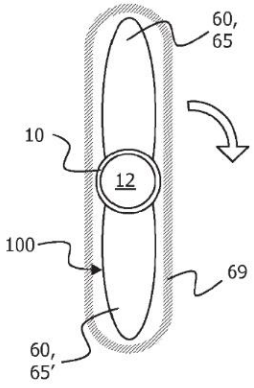

FIG. 14A

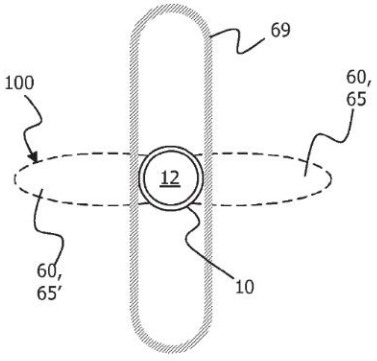

FIG. 14B

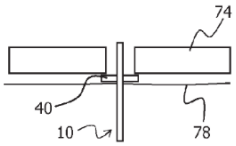

FIG. 15A

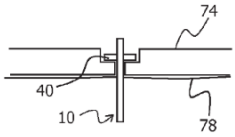

FIG. 15B

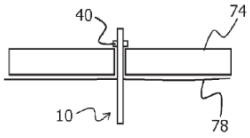

FIG. 15C

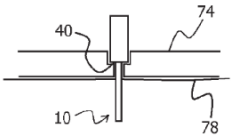

FIG. 15D

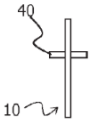

FIG. 16A

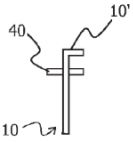

FIG. 16B

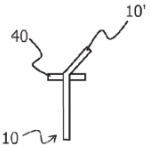

FIG. 16C

5.3 Selection of animal model

In co-operation with prof. dr. Paul Simoens, Veterinary Faculty of Ghent University, the animal model was selected (Figure 70). Canine, suidae (pig-like) and bovine models were excluded due to their huge frontal aerated sinuses running all over the cranial vault, except for the brachycephalic canine, in whom the anatomical structures are too small to perform VSS surgery, as is the case in the feline model. The primate model was considered too expensive, too diverse, and not realistic because of lack of experience with it at our university.

Figure 70. Selection of animal cadaver head

[left] equine (horse and pony) and caprine (goat and sheep) cadaver heads displayed for measuring and performing VSS surgery; [right] ventricle and sinus catheter introduced in the pony cadaver head, anatomically the ideal animal model.

The equine model model had a SSS of comfortable dimensions, similar to the human SSS, and quite large brain volume, making it a great animal model for our VSS study. However, for reasons of animal comfort and safety matters (both for the animal and for the humans working with the animal model), the caprine model with smaller SSS (Figure 71) was chosen. The ethics committee of the Faculty of Veterinary Medicine of Ghent University granted permission for the animal in vitro research into the caprine model.

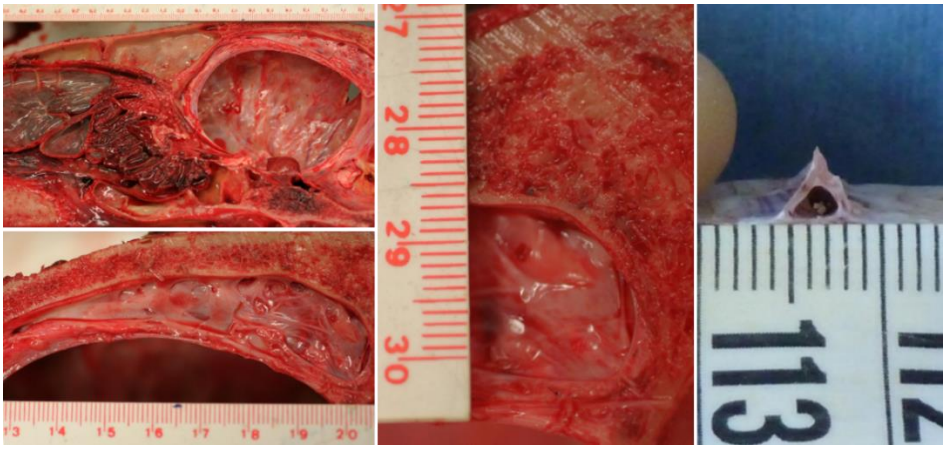

Figure 71. Anatomical differences in size between the equine and the caprine SSS

[3 left pictures] dimensions of the equine SSS, up to 7 cm long, 1,3 cm high and 6 mm wide; [right picture] dimensions of the caprine SSS, maximally 3 mm wide and high.

5.4 Technical challenges and solutions in the animal model

5.4.1 Housing, medical and anesthesiologic support

Thanks to the co-operation of the Veterinary Faculty, we were well supported considering operating theatre, anesthesia, general medical support and housing of the animals (Figure 72). Before an animal was included in the study, she remained 14 days in observation, to evaluate her general medical condition. During her stay, the animal lived in a stable together with her likes. Only in the immediate postoperative recovery phase, animals were put in isolation.

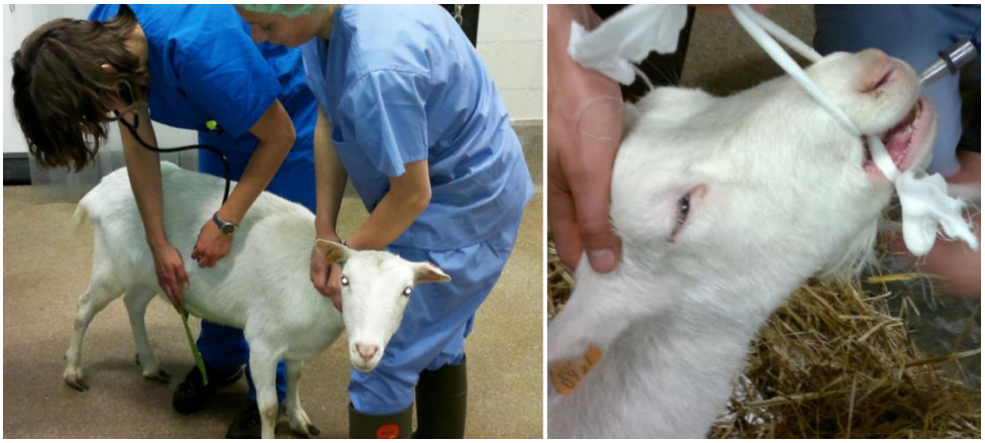

Figure 72. Start of a suboccipital puncture or operation day

[left] Just before anesthetic induction starts, a last medical check-up. [right] Directly after sedation and tracheal intubation, the animal is put on a bed of straw, for transport to the operation room or the CT scan.

5.4.2 Surgico-technical hurdles

5.4.2.1 Proper positioning on operation table

Considering the caprine model, not only the SSS and ventricular dimensions would prove challenging, we also needed to overcome many surgico-technical hurdles. How to position the animal in an appropriate way in order to make the VSS surgery possible, in order to prevent pressure lesions due to extended operation time? As in human neurosurgical practice, a head clamp seemed indicated. Due to the anatomy of the caprine skull, a dedicated head clamp had to be tailor-made, with 3-point pin fixation of the head on the maxillary bone structures. During surgery, tilting of the operation table could be necessary, to prevent air embolism, to prevent excessive blood loss (Figure 73).

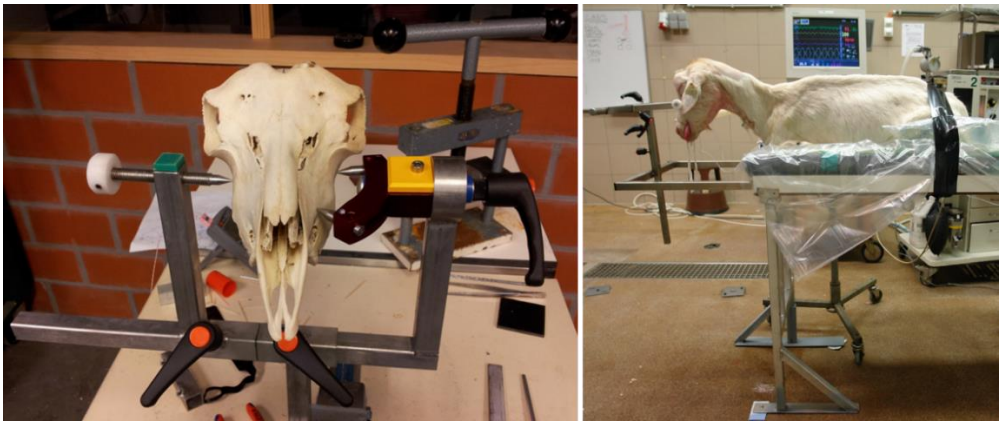

Figure 73. Tailor-made head clamp and operating table

[left] dedicated head clamp; [right] goat positioned on the cushioned operation table with tilting capability, head stabilized in head clamp, resting on her sternum / thorax and folded legs.

In none of the operated animals, wound infection or shunt infection was encountered. To prevent these, preoperative shaving / cleaning of the operated area and proper sterile draping of the operating field were routinely realized; surgical sterility precaution was put at the same level as in human medicine. No pressure ulcers were noticed, nevertheless some animals remained positioned for more than 4 hours.

5.4.2.2 Induction of hydrocephalus

Manuscript 5 gives detailed information on the HC induction technique and results. The decision was taken to use Kaolin infiltration to perform HC induction. The Kaolin infiltration was performed by sub-occipital puncture, always under fluoroscopic control (Figure 95). A subgroup received Kaolin infiltration in the pre-pontine region, the interpeduncular cistern. This was executed through a small bore catheter (Medtronic© Ascenda) pushed around the brainstem towards the intrapenduncular cistern under fluoroscopic control. In the other animals the Kaolin was injected into the cisterna magna, through the suboccipital puncture needle.

5.4.2.3 Guidance of ventricular catheter placement

Correct introduction of the ventricular catheter in the lateral ventricle depends on correct anatomical information and on a guiding device. The correct anatomical information was gathered by CT-scan, with the animal under general anesthesia (Figure 74). CT-scans were also performed to evaluate possible ventricular dilation after Kaolin injection and to control position of the ventricular catheter (more detailed in manuscripts 5 and 6).

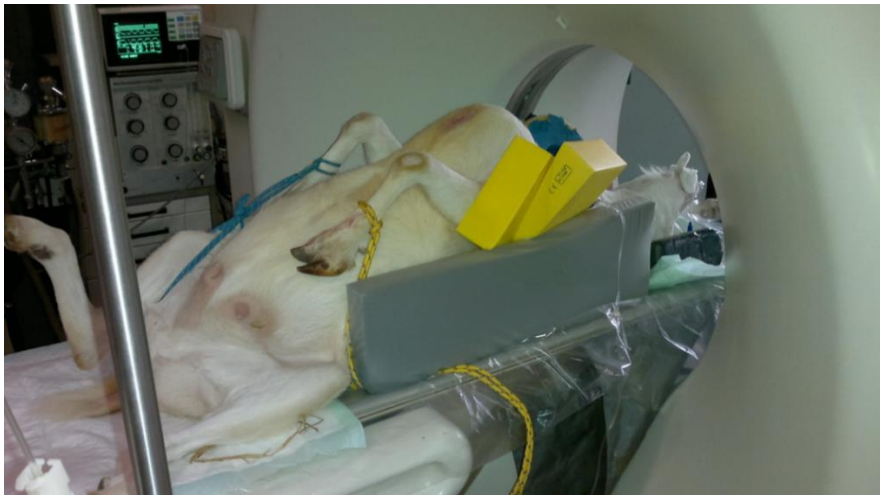

Figure 74. Goat scanned on the CT

If required by the study protocol, the sedated and ventilated goat is scanned on the CT, in horizontal position on the back.

Concerning the guiding, the use of a computed neuronavigation system or dedicated burr hole echo-doppler probe was not within our budget's limits. Therefore, an in-house guiding device was manufactured, to give direction at the moment of introduction of our ventricular catheter through the skull burr hole (Figure 75). Based on the preoperative CT-scan, the required angle and catheter length to target the frontal horn from a coronal suture burr hole was measured and subsequently programmed on the ventricular catheter aiming device.

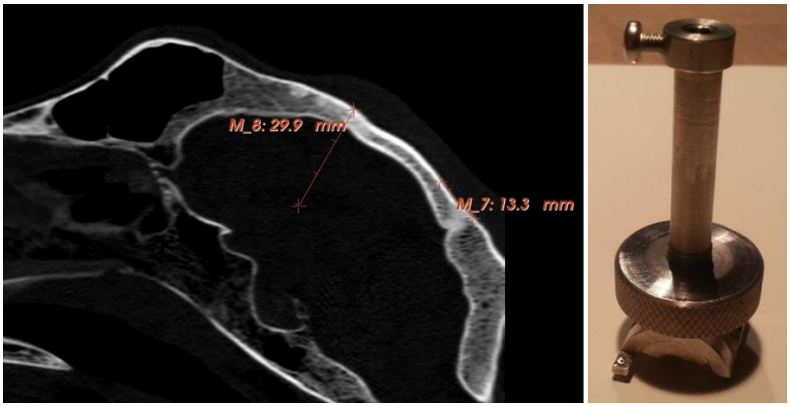

Figure 75. Home-made aiming device

[right] The home-made ventricular catheter aiming device, of which we could preset the angulation; was put on the skull at the burr hole. [left] Based on the preoperative CT scan, the required angle and catheter length to target the frontal horn of the lateral ventricle from a coronal suture burr hole were determined.

5.4.2.4 Measuring ICP

At the start of the animal in-vivo study, a telemetric implantable ICP sensor was produced, starting from an industrial telemetric sensor. On its pressure registering window, a nitinol cannula was fixed. On this nitinol cannula a standard silicone catheter for CSF shunts could be connected and the whole complex was made 'biocompatible' by covering it in a thick layer of medically approved silicone, using dipping technique (Figure 76).

Figure 76. Producing the telemetric ICP sensor

[left] the industrial telemetric sensor; [middle] nitinol cannula mounted on its pressure registering window; [right] 'biocompatible' sensor by covering it in a thick layer of medically approved silicone.

5.5 DVSAD_1 prototyping - production

The learning curve to design with NSX software, to perform computerized fluid dynamics on the drawn prototypes, to build stainless steel malls ready to apply injection molding techniques proved lengthy and was underestimated (Figure 77).

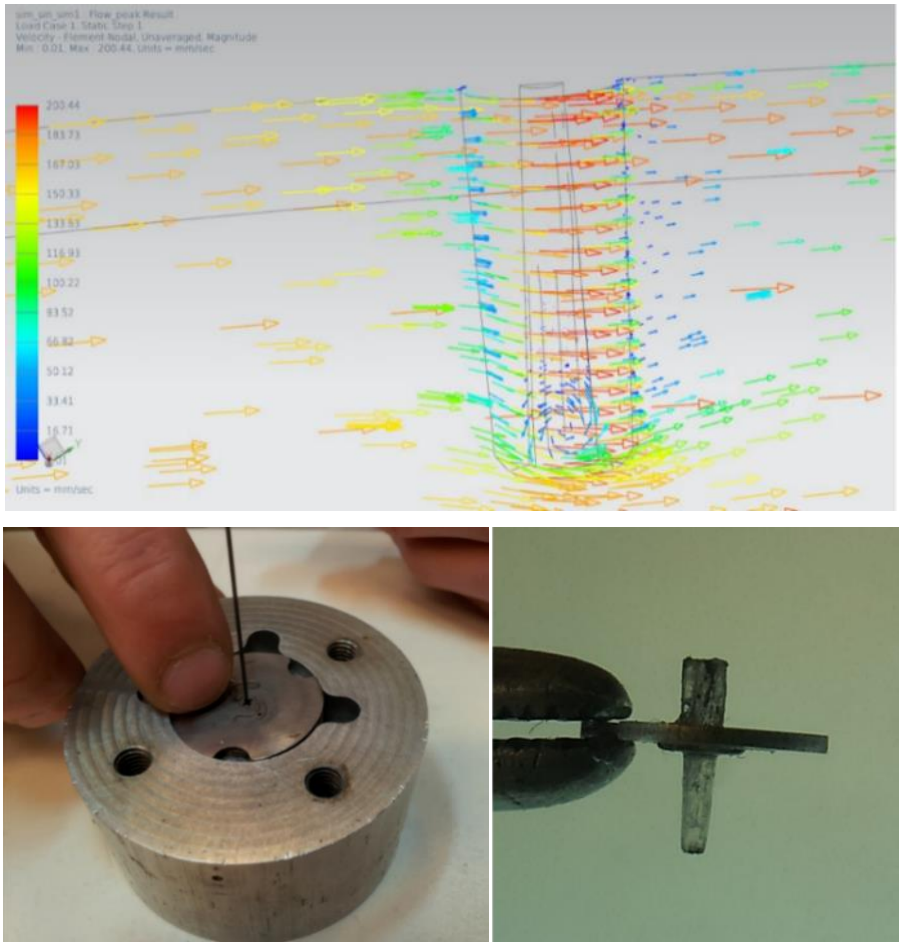

Figure 77. First phase of creating DVSAD implantable in animal model

[top] Computerized Fluid Dynamics model of DVSAD with perpendicular orientation of its cross cut end in relation to the blood flow direction; [bottom left] SI made stainless steel injection mall; [bottom right] the first animal DVSAD prototype.

After initial trials, gradually the design and production of the DVSAD_1 was realized (Figure 78).

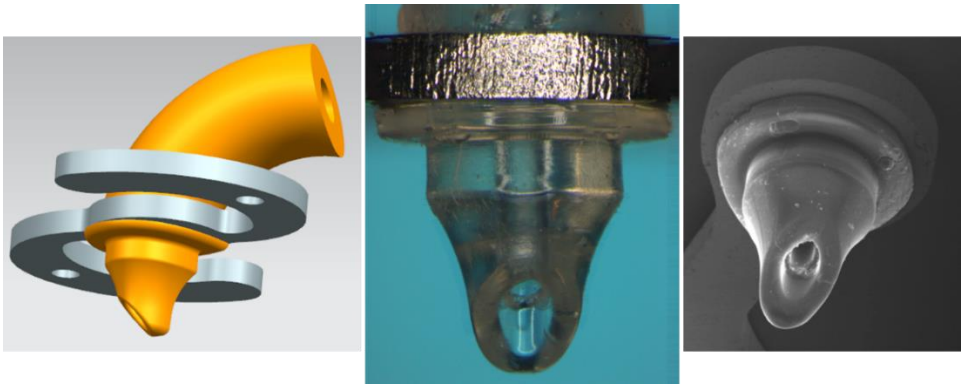

Figure 78. DVSAD_1

[left] NSX based drawing of DVSAD_1; [middle] stereophotography of produced DVSAD_1 in medical grade polyurethane and with nitinol base plate; [right] surface electron microscopic imaging of DVSAD_1 venous end, with a Tuohy-needle-like shape.

As mentioned above, the venous end and its more proximal tubing were made by medical grade polyurethane, the base plate was lasered out of a nitinol sheet (Figure 79).

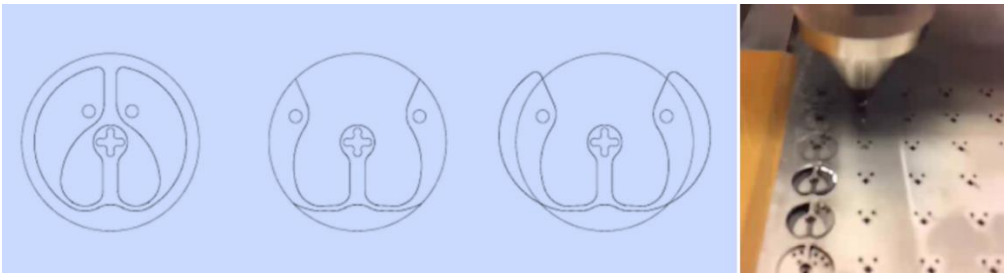

Figure 79. The nitinol DVSAD base plate

[left] NSX based drawing and [right] automated laser cutting of nitinol DVSAD_1 base plate

To obtain constant quality automated DVSAD production, Steerable Instruments© invested in an automated injection molding machine, the Cronoplast© Babyplast® (Figure 80).

Figure 80. The Babyplast®

Fully automatic hydraulic-driven micro-injection molding machine, the Babyplast® (source: Cronoplast© S.L., 08630 Abrera - Barcelona, Spain).

5.6 The executed in-vivo tests program on caprine model

5.6.1 Overview of the 5 phases of the caprine in-vivo tests

All the in in-vivo animal tests were performed from February 2013 - December 2013. This period is phased in 5 phases. These phases were not strictly designed beforehand. As unexpected results and problems emerged in initial phases, further phases were tailored to further investigate or answer those. In this section we give a short overview (Table 19) of the 5 phases, in further sections the scenario and results of each phase are discussed in detail.

The decision was taken to start with a **pilot study** (February - May) in which 3 goats were included. In this pilot study, a prepontine / interpeduncular Kaolin injection to induce HC was performed, the VSS was implanted with the DVSAD_1 prototype and with the telemetric ICP sensor.

In the second phase, the **first DVSAD study** (July - August), 3 goats were implanted with a VSS with different DVSAD prototypes, DVSAD_1 and DVSAD_2. These procedures were beforehand tried out on caprine cadaver heads.

The third and fourth phases, the **shortlasting HC study** (September) and the **longlasting HC study** (October), both studied the effect of Kaolin injection induced HC, in the cisterna magna; in the pilot study the Kaolin injection was interpeduncular. As the pilot study, each HC study included 3 goats. This means that in the whole caprine animal test a total of 9 goats were injected with Kaolin for HC induction.

In the fifth phase, the **second DVSAD study** (November - December), in 9 goats the VSS was implanted, in 3 of them with the standard retrograde silicone venous catheter, in 6 with the DVSAD_3 prototype.

Table 19. overview of 5 phases of caprine in-vivo model

PILOT STUDY prepontine Kaolin injection + DVSAD_1 VSS + sensor	FEB-MAY 2013 *3 goats*
FIRST DVSAD STUDY DVSAD_1 & _2 VSS	JULY-AUG 2013 *3 goats*
SHORTLASTING HC STUDY cisterna magna Kaolin injection	SEPTEMBER 2013 *3 goats*
LONGLASTING HC STUDY cisterna magna Kaolin injection	OCTOBER 2013 *3 goats*
SECOND DVSAD STUDY retrograde silicone VSS DVSAD_3 VSS	NOV-DEC 2013 *3 goats* *6 goats*
TOTAL	**21 goats**

5.6.2 Pilot study

In the pilot study, a combination of HC induction with Kaolin injection in the interpeduncular cistern + implantation of the VSS with the DVSAD_1 prototype + implantation and testing of the telemetric ICP sensor was performed in 3 goats. The goal was to take conclusions concerning (1) the technical feasibility of implantation of the DVSAD_1 prototype, (2) the ventricular catheter positioning in the frontal horn with the aiming device guidance, (3) the effect on HC development and clinical status of the goats following the interpeduncular cistern Kaolin injection and (4) the technical feasibility and added value of the implantation of the telemetric ICP sensor.

The scenario of the pilot study was strictly scheduled and is summarized in Table 20.

Table 20. Pilot study - scenario

DAY 0	CT under anesthesia + suboccipital puncture (ICP + Kaolin inj. – HC induction)
DAY 10	CT under anesthesia + suboccipital puncture (ICP) + sinusshunt with DVSAD_1 prototype + telemetric pressure sensor
DAY 30	CT under anesthesia + suboccipital puncture (ICP) + euthanasia + autopsy

The implantation of the DVSAD_1 wasn't without difficulties (Table 21). Its base plate was expected to stabilize the DVSAD_1 position and orientation thanks to the 'expanding wings' of the base plate in the epidural space under the bone edges of the burr hole. Due to variations in bone thickness, positional shifting forces were exerted by the expanding wings, requesting dural stitches to stabilize the DVSAD_1. Also, the mass effect of the base plate under the bone edges, created compression on the SSS, inducing partial obliteration. Even more cumbersome was the frequent obstruction encountered during the surgical procedure itself. At this initial phase we could not find a solid explanation for this per-operative obstruction. These factors increased operation duration significantly. During this pilot study, a totally unexpected VSS problem arose: once the fully implanted VSS was opened for functioning, a manifest and pulsatory blood regurgitation in the catheter between the shunt valve and DVSAD_1 was observed. We found out that this unexpected phenomenon was due to the dynamic P_{SSS} in combination with the compliance of the VSS shunt system (which is in the extra-cranial space), not only of the catheter's trajectory in between DVSAD_1 and valve, but also of the valve's housing, made of silicone walls. Subsequently, we reproduced this phenomenon in an in-vitro study with the blood filled loops in the non-occlusive roller pump set-up (Figure 81).

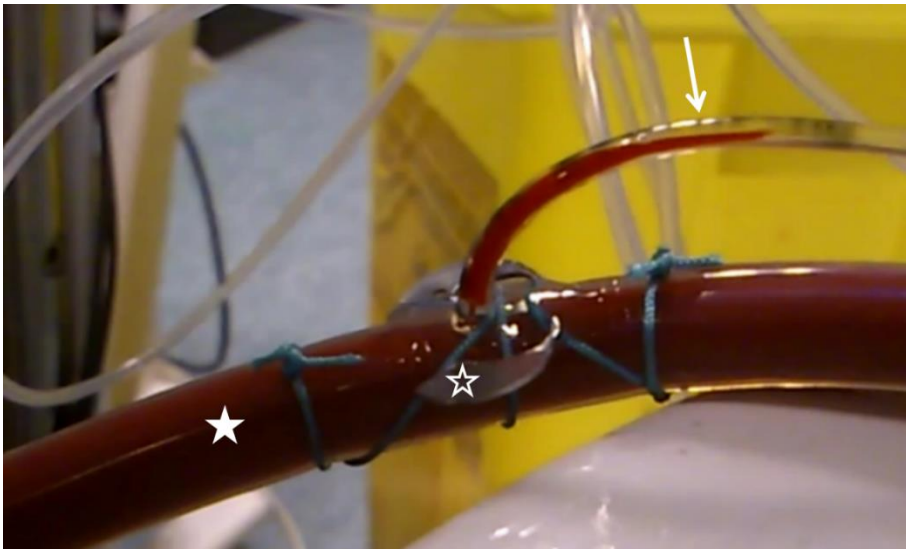

Figure 81. Roller-pump test of VSS compliance problem

Non-occlusive roller pump in vitro set-up with fresh human blood filled loop (solid white star), through the loop's wall the DVSAD_1 prototype with nitinol base plate (open white star) through which Ringer lactate is infused. Clearly a pulsatory blood regurgitation can be observed in the transparent catheter (white arrow) in between the DVSAS_1 prototype and the valve of the VSS.

Table 21. Pilot study - DVSAD_1 VSS implantation difficulties

Base plate related	1. SSS compression 2. DVSAD shift requesting stabilizing sutures
VSS compliance related	blood regurgitation causing VSS obstruction

Concerning the results of the use of the ventricular catheter aiming device, we concluded that these were very positive. The tool was a non-expensive home-made instrument, reusable. Control CT or cadaver dissections proved correct positioning of the ventricular catheters. During surgery (Figure 82), this guiding device proved to be time efficient, reducing the time required for the VC implantation. Subsequently, this aiming device was to be continued in future ventricular catheter implants.

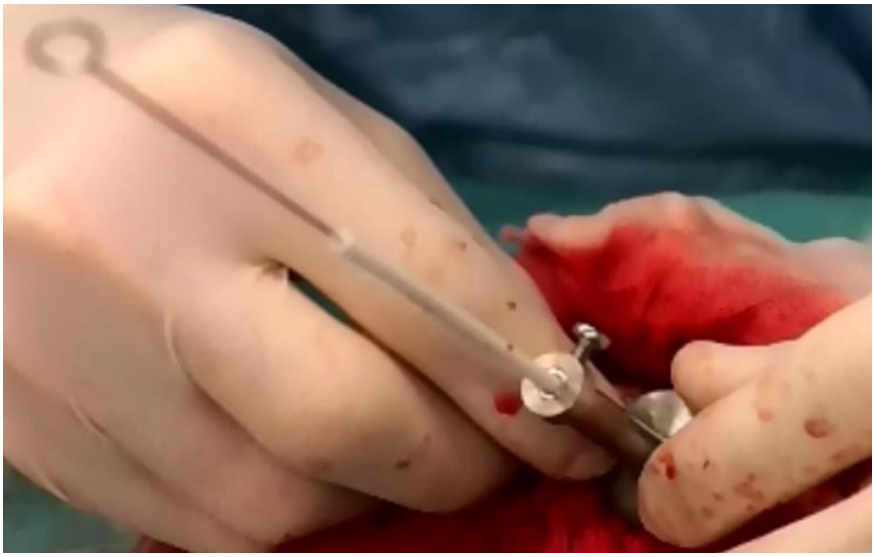

Figure 82. Guiding device with implanted frontal horn ventricular catheter

The results of the prepontine Kaolin injection into the interpeduncular cistern (Figure 95), were unsatisfactory (Table 22): they seemed not reproducible, complication rate was high and the postoperative discomfort of the Kaolin injection was not acceptable concerning animal welfare. Details about method and results have been written in the manuscript 5. We concluded that new Kaolin injection studies, the short- and long-lasting HC studies, were required. In these, the Kaolin dosage would be reduced from 4 to 3 ml and the site of injection would no longer be interpeduncular, but in the posteriorly located cisterna magna.

Table 22. Pilot study - interpeduncular Kaolin HC induction (250mg/ml - 4ml)

animal welfare	2/3 goats ill and uncomfortable - 1/3 goats death
HC induction	1/3 goats clear HC with ventricular dilatation 1/3 temporary ICP increase
conclusion	**HC induction not reproducible and with unacceptable impact on animal welfare**

This telemetric ICP sensor was implanted in the 3 pilot study goats, connected to their ventricular catheter of the VSS, via a T-connector (Table 23). Implantation proved technically feasible but increased operation time at least 30 min. The sensor did not create wound healing nor sterility problems. However, poor results of this telemetric ICP measurement (animals were not co-operative enough to obtain stable telemetric reading, the calibration of the sensors was not stable, the added value of this extra ICP measurement was very discussable / doubtful) led to its discontinuation. Therefore, the decision was taken to perform future ICP measurements with suboccipital puncture under sedation.

Table 23. Pilot study - results telemetric pressure sensor

PRO	technically feasible without complications
CONTRA	increased operation time doubtful telemetric reading / interference, non-co-operative goats non representative values / anxious & active animals
CONCLUSION	discontinuation of telemetric ICP sensor → suboccipital puncture

5.6.3 First DVSAD study

Because of the problematic DVSAD_1 implantation during the pilot study and in light of the problematic HC induction with interpeduncular Kaolin injection, a DVSAD study was scheduled to compare new DVSAD prototypes, without HC induction (Table 24). The focus was on ease of implantation of the DVSAD and control of the blood regurgitation thanks to decrease VSS compliance. The compliance reduction was realized by (a) reduction of catheter length between DVSAD and valve, (b) the use of polyurethane with increased durometer and (c) use of valves with reduced housing diameter and stiffer housing. DVSAD_1 (Figure 83) was compared with DVSAD_2 (Figure 84), which had a cross cut end and perpendicular orientation in relation to

bloodstream, in contrast with the Tuohy-needle-shape end of the DVSAD_1 and its retrograde orientation. Before and besides the implantation on 3 in-vivo models, numerous implantations were performed and routinely controlled on cadaver heads.

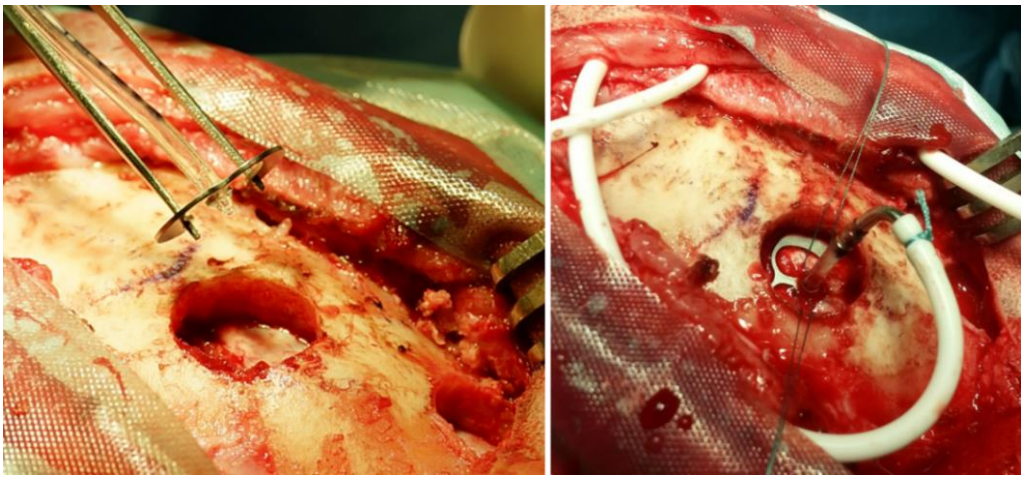

Figure 83. DVSAD_1 implantation

[left] The forceps is holding the wings of the DVSAD_1 base plate 'closed', while the DVSAD is going to be introduced in the SSS, through the sagittal prelambdoid burr hole. Note (1) the anteriorly orientated Tuohy-needle-like opening of the DVSAD_1 and (2) the coronal parasagittal burr hole prepared for the ventricular catheter introduction. [right] The DVSAD_1 has been implanted into the SSS and connected to the VSS valve with a silicone tube and metal (titanium) 90° connector to prevent kinking. The ventricular catheter has not been implanted yet.

Important conclusions from this study were:

1- No benefit was observed of the DVSAD_1 retrograde orientation compared with the cross cut and the DVSAD_2 perpendicularly orientated end considering blood regurgitation, clot formation, duration of patency. Hence, only in experimental hydraulic studies, the retrograde orientation of the DVSAD is of value; in the pulsatory in-vitro and in the animal in-vivo studies, the benefit of retrograde orientation is overruled.

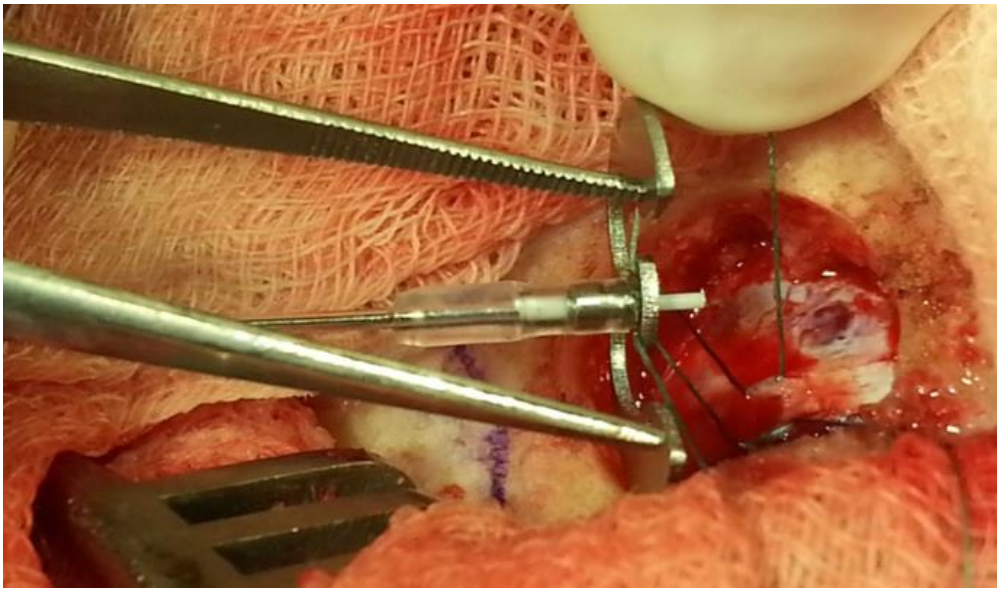

Figure 84. Introduction of the DVSAD_2 prototype into the SSS

Note (1) the straight cut end providing an opening perpendicular to the SSS blood stream direction and (2) the hanging-up stitches on each side of the opening in the SSS roof, in order to prevent or reduce the endothelial invagination and flap-formation with subsequent rapid covering an obstruction of the DVSAD aperture.

2- A second unexpected problem was recognized (Figure 85 and Figure 86): the manner of implantation of the DVSADs led to invagination of the venous sinus endothelium. The frequent DVSAD blockage during surgery, turned out to be caused by an endothelial flap, recovering the DVSAD's aperture.

Table 24. DVSAD study - protocol and results

DAY 0	comparison of DVSAD_1 (Tuohy end) and DVSAD_2 (cross cut end) • in VSS with reduced compliance • without Kaolin HC induction
DAY 5	Euthanasia and autopsy day 5 postop
RESULTS	• **no benefit of retrograde orientation / of impact effect** • **obstructive invagination of dural venous sinus endothelial wall**

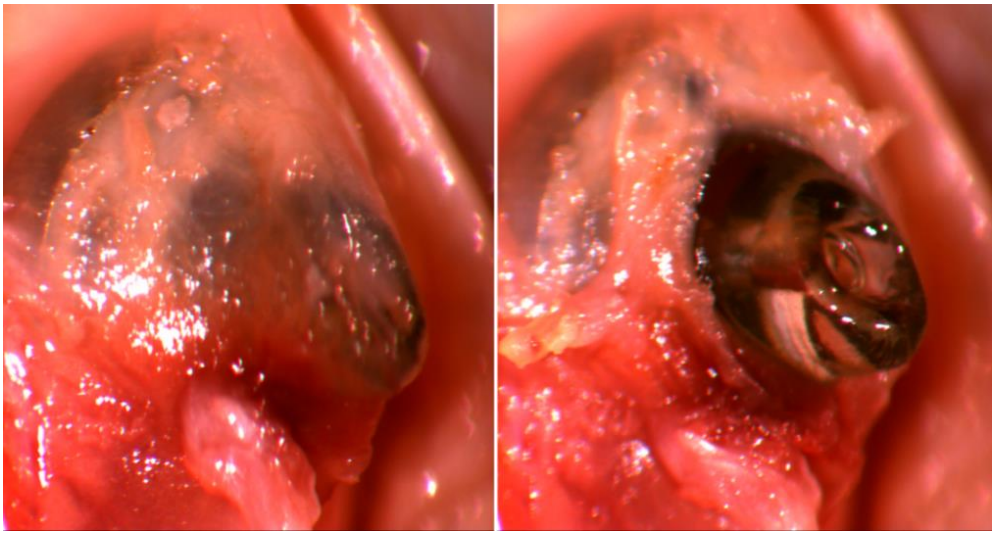

Figure 85. Stereophotographic cadaver study of the implanted DVSAD_1

One lateral wall of the SSS has been opened to visualize the through-the-roof implanted DVSAD inside the SSS. [left] Thick and evident endothelial covering of the DVSAD with obvious obstruction. [right] DVSAD_1 tip after removal of the endothelial covering.

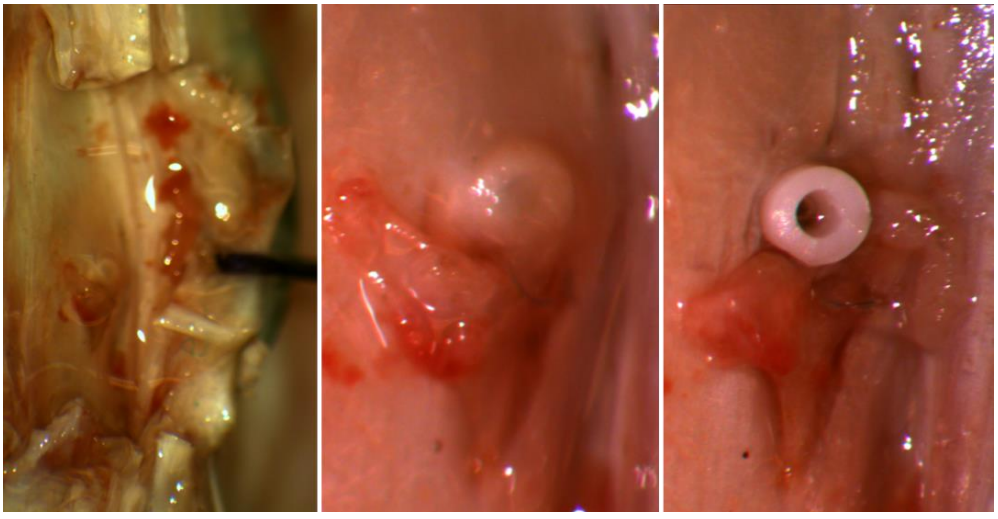

Figure 86. Stereophotography cadaver study of the implanted DVSAD_2

[left] on lateral wall of the SSS has been opened to visualize the through-the-roof implanted DVSAD inside the SSS. [middle] More zoomed in stereophotography of the DVSAD_2 tip covered by endothelial layer. [right] Visualiation of the tip after endothelial layer removal.

5.6.4 Short and long-lasting HC studies

To verify the results of the pilot study Kaolin HC induction, a new HC induction study, with two branches, was conceived: a short and a long-lasting branch. In both, the HC had to be induced by Kaolin injection, again with a concentration of 250 mg/ml, but with a reduced volume of injection, from 4 to 3 ml. Also, the injection site was changed. In both branches the injection was performed under fluoroscopy-controlled suboccipital puncture, and the aimed injection target was the cisterna magna. The cisterna magna injection is a more conventional and well-documented technique to induce HC in small domestic animals such as rats, canine and feline[169-171]. Both branches had a strict protocol, summarized in (Table 25).

Table 25. Short and long-lasting HC study, CM kaolin inj. - protocol

CM: cisterna magna; inj.: injection

	SHORT BRANCH	LONG BRANCH
DAY 0	suboccipital puncture under sedation - ICP measurement - CM Kaolin inj. (3ml, 250mg/ml)	suboccipital puncture under sedation - ICP measurement - CM Kaolin inj. (3ml, 250mg/ml)
DAY 10	suboccipital puncture under sedation - ICP measurement - euthanasia and autopsy	suboccipital puncture under sedation - ICP measurement
DAY 20		suboccipital puncture under sedation - ICP measurement
DAY 30		Suboccipital puncture under sedation - ICP measurement - euthanasia and autopsy

Two animals out of total of 9 died during the HC inducing experiments (3 goats of the pilot study with interpeduncular injection and 6 of the short- and long-lasting HC study with cisterna magna injection). One goat due to asphyxia after massive aspiration of gastric reflux during orotracheal intubation. A second goat due to complicated suboccipital puncture with subarachnoid and brainstem hemorrhage. In the remaining

goats (n=7), the kaolin injection provoked pronounced aseptic meningitis that caused HC in 6 out of 7 (86%) goats.

In the HC study goats (n=6) with reduced dose of 3ml of 250 mg/ml of Kaolin, the animals developed similar aseptic meningitis symptoms as in the pilot study, only milder of character. Nevertheless, the aseptic meningitis remained imposing an unacceptable impact on the animals' clinical status. The main symptoms included head pressing, spastic paresis of the legs, paddling, convulsions, apathy and dysphagia / loss of appetite.

The HC was characterized either by ventricular dilatation in 2/3 goats belonging to the interpeduncular cistern injection group, or by an increased ICP in the remaining 4/6 cisterna magna group (Figure 87). Manuscript 5, 'A Hydrocephalic Goat Experimental Model to Evaluate the Efficacy of HC Treatments', reports in detail the results and covers a comprehensive discussion concerning the different responses to Kaolin injection.

The results of Kaolin HC induction in both the groups with interpeduncular cistern and with cisterna magna injection, disappointed considering their added value to the project. As mentioned, in 86% the Kaolin injection HC induction was successful, but the clinical manifestations of the induced aseptic meningitis were ethically unacceptable and masked the clinical symptoms of the induced HC and possible clinical consequences of the surgical procedures. As a consequence, we decided to abort further HC induction during subsequent VSS animal in-vivo study.

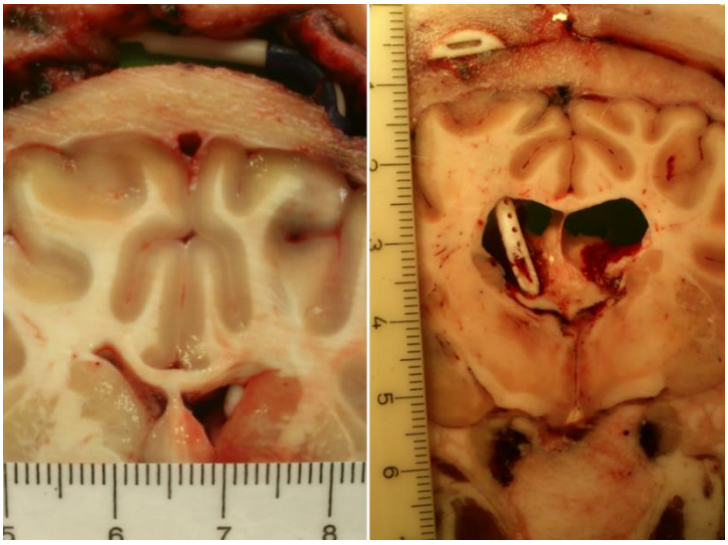

Figure 87. Cadaveric coronal cuts through the lateral ventricles the level of the foramina of Monro

[left] Note (1) the correct position of the ventricular catheter in the frontal horn and (2) the absence of ventricular dilatation despite increased ICP due to Kaolin injection. [right] Note (1) the correct position of the ventricular catheter in the frontal horn and (2) the ventricular dilatation due to Kaolin injection.

5.6.5 Second DVSAD study

The encountered problems with DVSAD_1 and DVSAD_2 prototypes during the pilot study (blood regurgitation due to compliance of VSS and dislocation of DVSAD due to side forces during opening of epidural wings of base plate) and the first DVSAD study (obstruction of the venous DVSAD ends due to invagination of dural venous sinus endothelium), urged to develop a new DVSAD_3 prototype. These observations led towards (1) a different implantation approach, a Seldinger-like technique combined with (2) a different DVSAD design, a DVSAD with a small and flexible barb (Figure 88), having the task to pull back the endothelial layer and to hold it fixed against the inside wall of the dural venous sinus.

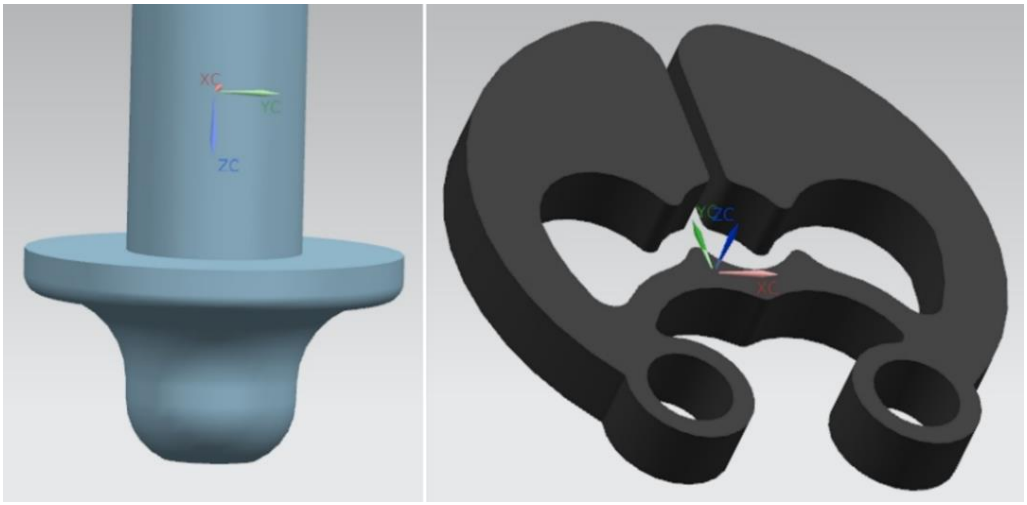

Figure 88. drawing of concept of the DVSAD_3 or barbed DVSAD

[left] technical drawing of venous end of DVSAD_3 with its flexible barb; [right] the sliding base plate, to secure the DVSAD epidurally.

The concept was to puncture the SSS roof with an angiocatheter needle, once clearly inside de SSS, to remove the needle and to use the angiocatheter as a guide and open window to introduce the DVSAD_3 vascular end. Inside the angiocath, the DVSAD_3 barb folds along the longitudinal axis and once the DVSAD_3 passed the angiocatheter's end, de barb unfolds or re-expands and the angiocatheter is retracted over the DVSAD. With the angiocath totally removed, the DVSAD is gently pulled back, its 'barb' hooking up to the perforated endothelium and pulling it against the dural sinus wall. To secure its stability, the sliding base plate is pushed over the DVSAD's proximal end towards its venous end until it reaches the epidural side of the SSS roof, thus securing the endothelial and dural SSS structures between the base plate and the intravenous barb. Again, prototypes were manufactured (Figure 89) and cadaver head try-outs were realized (Figure 90).

Figure 89. First prototype of the DVSAD_3

[left] photo of DVSAD_3 with its sliding base plate, apt for implantation in caprine model; [right] more detailed photo of venous tip of DVSAD_3, with flexible barb.

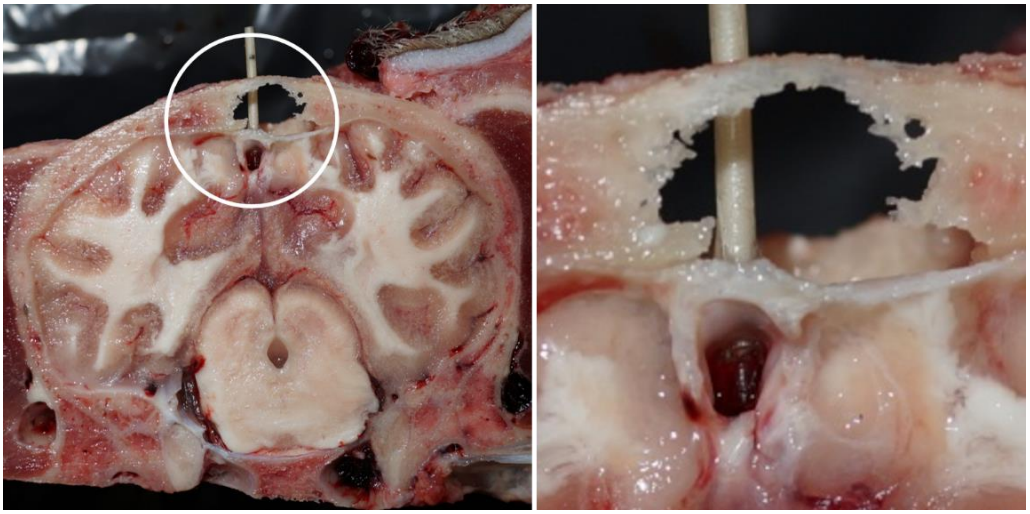

Figure 90. Cadaver study of the DVSAD_3

[left] Coronal cut showing DVSAD_3 introduced in the SSS, without endothelial invagination or covering. [right] More detailed photography of the position of the DVSAD_3 inside the SSS.

After promising tests on cadaver heard, a short lasting controlled in-vivo study was designed to evaluate the DVSAD_3 implantation technique and its results concerning obstruction by endothelial invagination or thrombi formation at its venous end. In the VSS with DVSAD_3 branch, 6 goats were included, in the control branch - VSS with

retrograde silicone venous catheter - 3. None of the goats received a Kaolin HC inducing injection (Table 26).

Table 26. Controlled VSS study

VSS: ventriculo-sinus shunt; DVSAD: dural venous sinus access device; P_{SSS}: pressure in superior sagittal sinus; VC: ventricular catheter

	VSS with DVSAD_3 group (n = 6) ***VSS with retrograde silicone catheter (n = 3)***
DAY 0	under anesthesia CT-scan → operation theatre • VSS implantation • pressure measurement DVSAD (P_{sss}) and VC (ICP)
DAY 10	under anesthesia CT-scan → operation theatre • ICP measurement and verification of patency • euthanasia and autopsy

In all animals surgical procedures were technically successful, without complications and with greater ease of introduction of the DVSAD_3 than the DVSAD_1 or DVSAD_2, thanks to its Seldinger-like technique (Figure 91). Also, the smaller epidural base plate did not compress the superior sagittal sinus and stabilized nicely the DVSAD_3. During surgery, both the DVSAD_3 and the control silicone catheter remained patent, we did not encounter episodes of (thrombotic or endothelial) blockage as we did with previous prototypes.

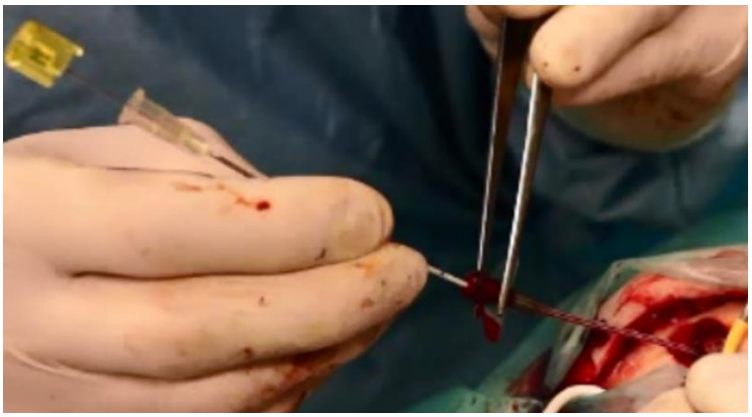

Figure 91. Insertion of the DVSAD_3 into the SSS

insertion of the DVSAD_3 into SSS through the angiocatheter during the in-vivo controlled VSS study.

However, at day 10, when controlling the patency, all silicone catheters and DVSAD_3 devices were blocked when testing. After euthanasia, immediate autopsy (Figure 92, 93, 94 and 103) proved thrombotic blockage at the venous sinus end of the devices in both groups. None of the animals suffered venous sinus thrombosis.

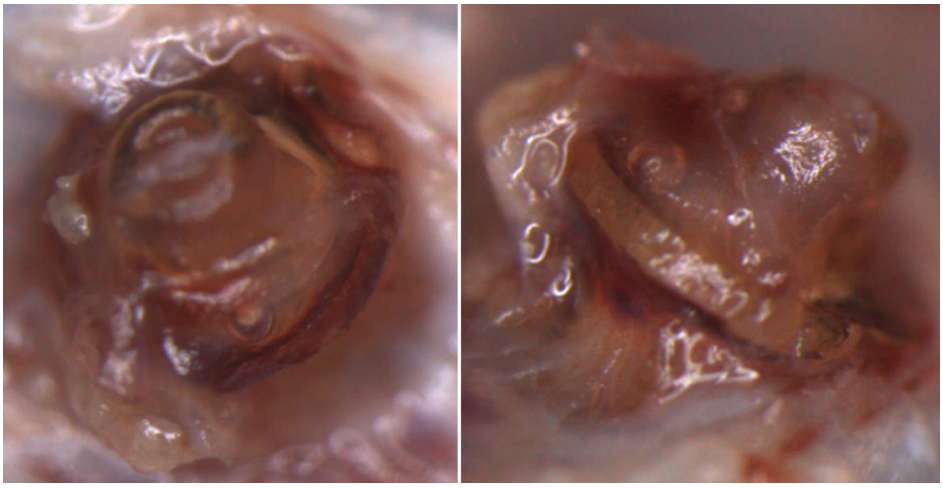

Figure 92. Stereophotography of postop cadaver study at the end of VSS study

Stereophotography of postop cadaver study at the end of the controlled VSS study, showing the DVSAD_3 nicely positioned within the SSS, without endothelial invagition but covered by thrombus. The barb is nicely positioned against the endothelium.

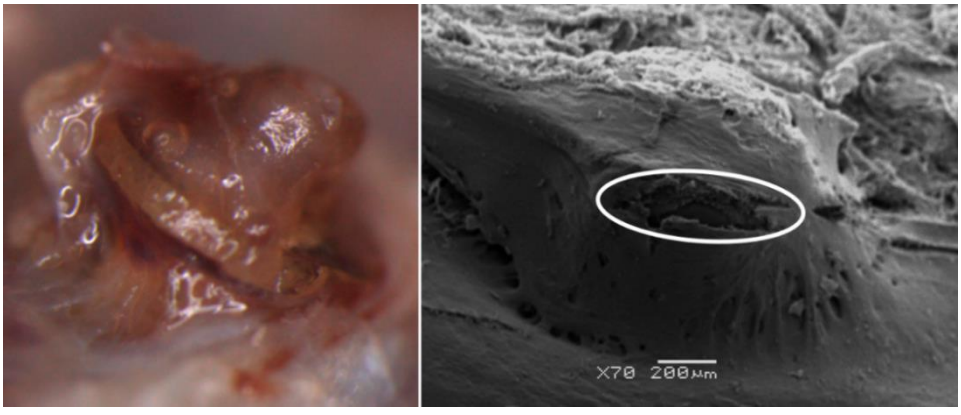

Figure 93. Images of the intravascular part of DVSAD_3

[left]stereophotography, [right] surface electron microscopy of intravascular part of DVSAD_3.

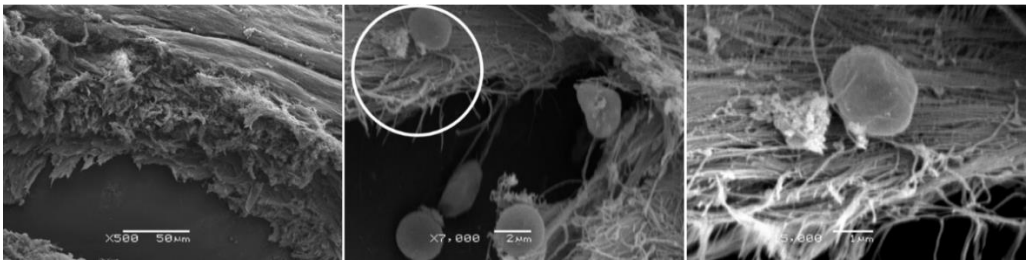

Figure 94. Magnifications of SEM figure

Magnifications of the previous SEM figure (white oval determined region at the barbed edge). [left] Magnification x500, [middle] magnification x7000 and [right] x 1500, proving that the DVSAD covering is not endothelial but only thrombotic, with typical fibrin polymer network with captured platelets and white and red blood cells.

This second DVSAD study concluded that **(a)** the DVSAD_3 prototype and its Seldinger-like introduction technique resolved the problematic endothelium invagination encountered with previous prototypes and **(b)** that this technique proved safe and straightforward, significantly reducing surgery related risk and operation time. **(c)** Considering the thrombotic obstruction problem, no difference was noted between the DVSAD_3 and the standard silicone catheter.

At last, as the animals were not injected with Kaolin, they did not suffer aseptic meningitis and their pre- and post-operative clinical conditions could be well monitored. We remarked a very swift postoperative revalidation, with return to normal activity and clinical status within first 24 - 48 u, without need of painkilling medication hereafter. This proves that the VSS surgical procedure is safe and with very swift recovery.

5.6.6 MANUSCRIPT 5

Manuscript 5 reports the hydrocephalus induction with Kaolin injection on the in-vivo caprine animal model. Rationale, techniques and results are discussed in detail.

A HYDROCEPHALIC GOAT EXPERIMENTAL MODEL TO EVALUATE THE EFFICACY OF HYDROCEPHALUS TREATMENTS

E. Baert[1], S. Schauvliege[2], J. Vandersteene[1], K. Vandevelde[2], F. Dewaele[1], F. De Somer[3], D. Van Roost[1]

[Veterinary Research Communications, submitted and under revision]

[1] Department of Neurosurgery, Ghent University Hospital, Belgium
[2] Faculty of Veterinary Medicine, Ghent University, Belgium
[3] Department of Cardiac Surgery, Ghent University Hospital, Belgium

---

ABSTRACT

Hydrocephalus (HC) is treated with ventriculo-peritoneal or ventriculo–atrial shunts, which have a failure rate of up to 50% in the first two years. A hydrocephalic large animal model is presented allowing evaluation of novel treatments. Hydrocephalus was induced in 9 female domestic dairy goats (Saanen breed) by injection of a 25 % kaolin in NaCl-H_2O solution into the interpeduncular cistern (IC) (n=3) or into the cisterna magna (CM) (n=6). A severe aseptic meningitis developed with the clinical expression of reduced food intake, refusing to stand, spasticity of the legs, pressing of the head and in some cases even seizures. Two out of 9 animals (22 %) died before HC could be diagnosed. Six of the remaining 7 animals (86 %) developed HC. The increase in intracranial pressure (ICP) was comparable between the two groups (9.3 mmHg to 15.1

mmHg). Two of the 3 animals of the IC group and none of the animals of the CM group developed ventricular dilatation. In contrast with other species, an outflow channel between the spinal central channel and the lumbo-sacral subarachnoid space (SAS) persists in goats. This channel prevents complete obliteration of the fourth ventricular outflow and thus the development of obstructive HC. This anatomical characteristic makes goats suited for the development of a model of non-obstructive HC. However, the kaolin injection provoked pronounced aseptic meningitis with unacceptable high clinical impact, which clearly overshadowed the resulting HC symptoms. The development of better tolerated techniques may be the subject of further research.

INTRODUCTION

HC, the progressive accumulation of CSF in the brain, can be caused by obstruction of the CSF flow within the ventricular system (obstructive HC), by an impeded CSF flow through the distal SAS or by damage to the normal resorption capacity (the two latter being non-obstructive, communicating or malresorptive HC)[172]. Obstructive HC is treated by an endoscopic third ventriculostomy, while the current treatment of non-obstructive HC consists of drainage of CSF to the peritoneal cavity or to the right cardiac atrium by a ventriculo-peritoneal or ventriculo-atrial shunt[90]. An important drawback of such shunts is siphoning: in a sitting or standing position of the patient, the CSF column within the catheter – through gravity – exerts suction, leading to shunt-related intracranial hypotension and aspiration of choroid plexus into the proximal catheter[173]. Intracranial hypotension causes headaches, nausea, vomiting and even subdural hematomas while aspiration of choroid plexus is a major cause of shunt obstruction at the level of the ventricular catheter[90]. The rate of shunt failure - necessitating surgical revision - remains as high as up to 50% in the first 2 years in the neonatal and pediatric group and in the first 5 years in the adult group, despite the usage of expensive programmable resistance valves, flow-regulating valves and anti-siphon devices[95]. A rationale for ongoing hydrocephalus research remains evident, as shunt failure throws a

high burden on physical, psychological and socio-economic functioning of the patient and at high macro-economic impact for society[174]. To evaluate current and novel treatment techniques a suitable animal model will be required[175]. A larger animal model is more suitable than canine or feline models described in earlier studies as the dimensions of larger brain ventricles allow the usage of shunt systems that are similar in size and design to their counterparts for human medicine[176]. A non-hydrocephalic goat model, allowing to evaluate whether a new technique for hydrocephalus treatment is feasible, safe and well tolerated, has been described in previous literature[175]. However, to evaluate the long term efficacy of any new solution, a hydrocephalic model will be unavoidable[175]. To approximate human treatment conditions, a model of non-obstructive HC is preferable.

This paper reports on the technique and results of the induction of hydrocephalus in goats by kaolin injection. Two different injection sites were evaluated: the interpeduncular cistern (IC)[177] and the cisterna magna (CM)[169-171].

ETHICAL COMMITTEE

All experiments in this study were approved and registered by the Ethical Committee of the Faculty of Veterinary Medicine of the Ghent University (EC2012/187, EC2013/66). Care and use of animals were in full compliance with the most recent national legislation (Belgian Royal Decree of 29 May 2013)[178] and European Directive (2010/63/EU)[179].

MATERIALS AND METHODS

Animals: selection, housing and medical treatment

The study was designed as a pilot study to identify a suitable hydrocephalic large animal model to evaluate HC. The species was selected based on anatomical characteristics. In pigs and cattle, an aseptic frontal access to the ventricles and superior sagittal sinus is impeded by the pronounced posterior extension of the frontal sinuses over the cranial vault. Remaining possible models were sheep, goats and horses or ponies. Finally, domestic dairy goats (Saanen breed) were chosen because of their manageability and short hair. All goats were bought from dairy goat farms, sold because of decrease of their milk production. They were 1 to 2 years old and weighted less than 60 kg. Only female goats were included to be able to house the animals in a large group stable, providing ample space to move and play and the possibility to socialize.

Since the investigation was a pilot study, small sample sizes were chosen. The study consisted of a cadaver study (6 goats) and an in-vivo study (9 goats). The studies were conducted serially and the goats were allocated to the different experiments in order of acquirement.

For the cadaver anatomical study, the goats were euthanized directly after arrival at the research facility. The remaining goats were admitted to the animal facility at least 10 days prior to the start of the study for acclimatization and health checks (clinical investigation, ultrasonography examination of abdomen and thorax, blood and feces analysis). These animals were housed in little groups (3-4 animals per cage). The cage measured 3 m x 4 m. The bedding consisted of straw and cage enrichment (an elevated platform) was present in all cages. Natural light was provided by translucent windows, and the cage temperature was kept between 15 and 20 °C. The animals were fed hay and water ad libitum, supplemented with 450 g nutritional pellets a day.

Clinical evaluation of the animals was performed twice daily. The evaluation consisted of objective (e.g. vital parameters, weight, food intake) and subjective (e.g. general impression, posturing) parameters.

All animals were fasted 24 h before surgery and received an intramuscular (IM) injection of 2.5 mg trimethoprim and 12.5 mg sulfadiazine/kg body weight (Borgal® 24%, Virbac, Barneveld, The Netherlands) starting one day prior to surgery and daily until 4 days after surgery. If needed, postoperative pain and fever were treated with 48 mg meloxicam subcutaneously (Metacam®, Boehringer Ingelheim, Germany).

Euthanasia was performed by intravenous (IV) administration of 50 mg/kg sodium pentobarbital 20% (Pentobarbital®, Kela, Hoogstraten, Belgium) after IV premedication with 0.3 mg/kg midazolam (Dormicum®, Roche Pharma, Brussels, Belgium), 0.1 mg/kg IV morphine (Morphine® HCL Sterop, Brussels, Belgium) and induction of anesthesia with 2-4 mg/kg IV propofol (Propovet®, Parsippany-Troy Hills, New Jersey, United States).

Anatomical cadaver study

After euthanasia, the goats were immediately frozen to -20 °C and decapitated. On a band saw the heads were cut in 1cm thick coronal slices. The slices were photographed with and without a scale bar. The contours of the ventricles and the brain were delineated at the level of the coronal suture and the ratio between the ventricular surface and the total brain surface was calculated using ImageJ software (ImageJ for Windows; National Institutes of Health, 9000 Rockville Pike, Bethesda, Maryland 20892, USA; Version 150, available for download at https://imagej.nih.gov/ij/index.html). ImageJ provides a tool to measure surface areas of a plain image in two dimensions. By delineating the periphery, ImageJ calculates the surface area as measured by the number of pixels of the selected surface.

In-vivo study

The day before the suboccipital puncture, the first three goats were anesthetized to perform a cranial computed tomography (CT) scan. This was not the case for the subsequent 6 goats.

For the suboccipital puncture, the goats were anesthetized and properly positioned. To reach the interpeduncular cistern (IC group, n = 3), the goats were positioned with the neck in a neutral position (Figure 95).

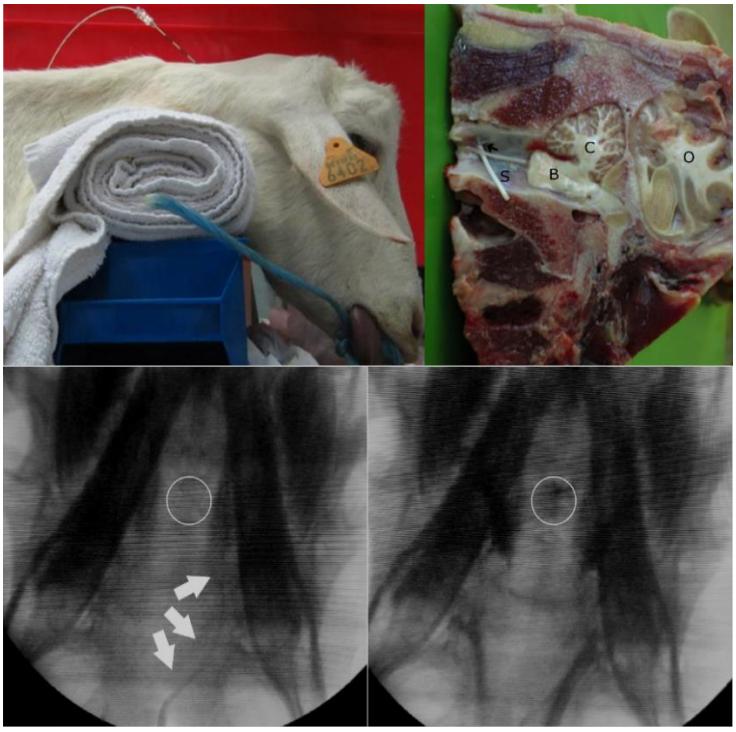

Figure 95. Suboccipital puncture to reach the interpeduncular cistern

[S: silicone catheter, B: brain stem; C: cerebellum; O: occipital cerebral lobe] Upper left: The anesthetized and ventilated goats were positioned prone with the neck in a neutral position, supported on a towel roll. A Tuohy needle was inserted through a small skin incision 3 cm caudal to the occipital protuberance and advanced under radioscopic guidance into the cisterna magna. Through this needle a catheter was inserted and advanced, still under radioscopic guidance,

around the brainstem to reach the interpeduncular cistern. Upper right: Sagittal slice through the cranio-cervical junction in the same goat. A white silicone catheter was inserted through the needle and left in place to mark the entry point into the cisterna magna (small black arrow). Lower left: fluoroscopic image showing the catheter curving around the brainstem (arrows) to end into to the interpeduncular cistern (circle). Lower right: image after test injection with iodine-contrast agent.

To reach the cisterna magna (CM group, n = 6), the goats were positioned with the neck in maximal flexion. A sterile surgical skin incision was made in the neck 3 cm caudal to the external occipital protuberance. Under radioscopic guidance a spinal needle (16 G) was advanced into the cisterna magna. A pressure transducer (DTXPlus; Argon; Bornem Belgium) was connected and the ICP measured. In the last 6 goats, the ICP measurement ran simultaneously with the central venous pressure (CVP) within the superior caval vein and the arterial partial pressure of carbon dioxide (P_{aCO2}) within the auricular artery using an anesthesia monitor (Datex Ohmeda S/5) and a blood gas analyzer (Radiometer ABL 5). A P_{aCO2} of 40-45 mmHg and a central venous pressure of 5-10 mmHg were targeted.

After adequate ICP registration, a catheter was advanced through the spinal needle to reach the IC in the first three goats. In these goats a spinal needle with a lateral opening (Tuohy needle, Ascenda® spinal intrathecal catheter; Medtronic©) was used for the suboccipital puncture. The Tuohy needle opening was turned to the right lateral side of the goat and, under radioscopic guidance, the spinal catheter was inserted through the needle and advanced around the brain stem to end into the interpeduncular cistern (Figure 1). In the 6 subsequent goats (CM group) the procedure below was performed directly through the spinal needle (with its tip in the CM). Thus in this group no catheter was inserted through the needle.

Once the final position reached, 3-4 ml CSF was evacuated and 1-3 ml of iodine-contrast (Omnipac®, GE Healthcare, Diegem, Belgium) was injected under fluoroscopic monitoring to verify the correct position of the catheter or needle respectively.

Subsequently, 4ml (IC group) or 3ml (CM group) of a solution of 250 mg kaolin per ml NaCl 0,7 % in H_2O was slowly injected (kaolin of Sigma Aldrich, Overijse, Belgium).

After kaolin infiltration, all 9 goats were scheduled on day +7, for ICP measurement conform the protocol described above. The 3 goats of the 4 ml kaolin IC group were scheduled for a cranial CT scan after the ICP measurement and to be euthanized afterwards. The 6 subsequent goats of CM group) were split into two groups: 3 goats were to be euthanized directly after the measurement on day +7, the remaining 3 goats were to be followed for 21 days to observe the natural history of the HC. The latter 3 goats were scheduled for ICP measurement and euthanasia on day +21. The protocol included a premature euthanasia in case the animal's condition were unbearable.

Statistics

The normal distribution of the parameters was assessed using QQ-plots and a Shapiro-Wilk test. An independent T-test was used to compare the increase in ICP between the IC and CM group. A paired T-test was used to analyze the increase in ICP (IC and CM group considered as one), and the ratio between the surface of the ventricles and the surface of the brain as measured on CT imaging. An independent sample T-test was used to evaluate whether there was a difference between the ratio of the ventricle to brain surface as measured during autopsy of non-hydrocephalic and hydrocephalic goats.

RESULTS

Anatomical cadaver study

The ratio between the ventricular surface and the total brain surface at the level of the coronal suture amounted to 0.026 (0.013-0.040).

Interpeduncular cistern group

In IC group (n=3) injected with 4ml of the kaolin solution, no specific problems were encountered during the procedure. In the first days after the injection, the goats were periodically paddling and experienced seizures. In between these episodes and after the first days, the main symptoms comprised a lowered, hanging head, head pressing, refusing to stand, foreleg stiffening and weakness, decreased reactivity and reduced food intake.

The ICP and the ventricular size before and days +7 are presented in Table 27.

The mean baseline ICP was 3.33 (0-7.13) mm Hg. The ICP increased only in one goat above the 95% confidence interval of the baseline values.

The ratio between the ventricular and brain surface increased from 0.030 (0.018-0.040) to 0.085 (0.00-0.29). This increase was statistically not significant (P-value 0.338). In two goats, the ventricular size increased above the 95% confidence interval of the baseline values.

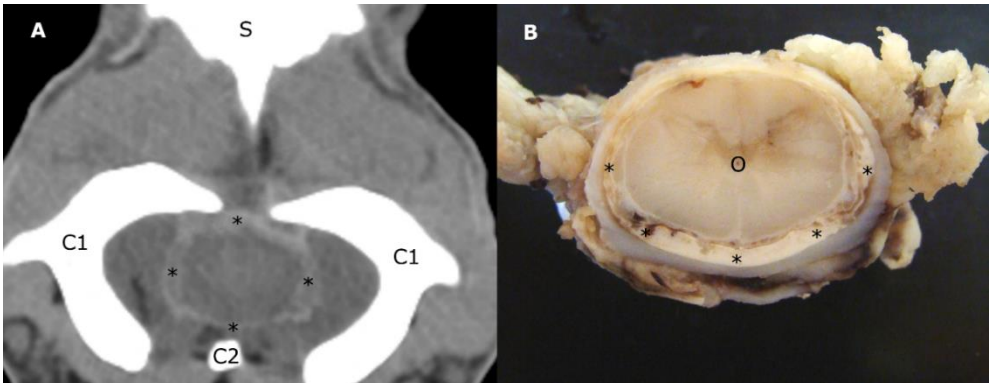

Figure 96. Kaolin distribution 7 days after injection into the prepontine interpeduncular cistern

A: Axial head-CT showing the hyperdense kaolin around the medulla spinalis (asterisks). S: skull; C1: atlas; C2: dens axis.

B: Transverse section through the upper medulla spinalis and meninges in the same animal. The kaolin deposition around the medulla can be seen (asterisks). Note the canalis centralis of the medulla spinalis (O).

In two goats, the cranial CT scan and the autopsy at day +7 showed deposits of kaolin predominantly anteriorly of the pons and medulla oblongata but also in the cisterna magna (Figure 96).

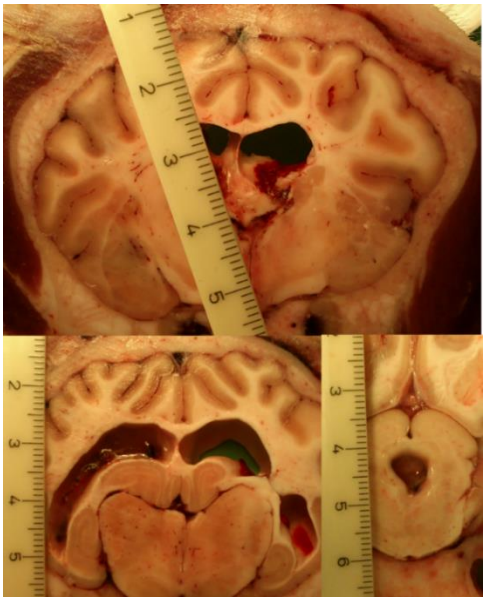

Figure 97. Obstructive HC

Coronal slices showing different parts of the ventricular system of the goat that developed pronounced obstructive hydrocephalus.
Top: rostral horns
Lower left: temporal horns
Lower right: aqueduct

One animal developed obstructive HC (Figure 97). In this animal kaolin was not predominantly observed anteriorly of the brain stem but in the fourth ventricle and along the olfactory nerve up to the olfactory bulb (Figure 98). In this specific goat, the ICP did not increase to a value above the upper limit of the 95% confidence interval of the baseline values.

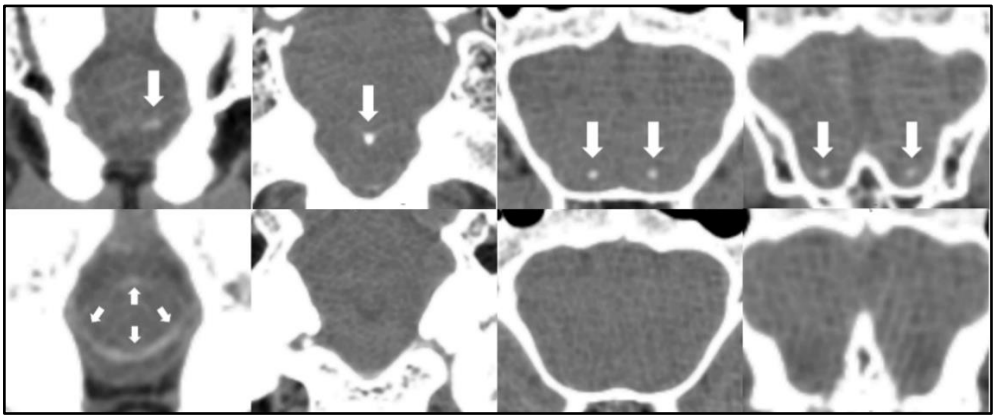

Figure 98. Axial CT images showing the distribution of kaolin

Axial CT images showing the distribution of kaolin (white spots indicated by the white arrows) in the animal that developed obstructive (upper row) versus non-obstructive (lower row) hydrocephalus. From left to right: level of the foramen magnum, level of the caudal fourth ventricle, level of the olfactory nerve, level of the olfactory bulb.

Cisterna magna group

In this group (n=6) with 3ml of the kaolin solution injection into the CM, no specific procedural problem but a single lethal anesthesiological complication was encountered. During orotracheal intubation, one goat suffered massive aspiration of gastric reflux and died shortly after the anesthetic induction due to asphyxia.

In the 5 surviving goats the ICP was measured by suboccipital puncture at day +7. In one, the suboccipital puncture was cumbersome and no clear ICP measurement obtained. After the puncture this goat appeared tetraplegic and had to be euthanized. The autopsy showed subarachnoid and brainstem bleeding. By consequence ICP measurements were obtained only in 4 out of 6 animals of the CM group.

The ICP values before and at day +7 are presented in Table 27.

Table 27. ICP (in mm Hg) and brain morphometric measurements at day 0 and day 7

Ventricles: ratio between ventricle surface and brain surface as assessed on a coronal slice at the level of the foramen of Monro. Asterisk: values increased above the upper limit of the 95% confidence interval of the baseline values. x: missing value /: value cannot be assessed.

Study ID	Group	ICP day 0	ICP day 7	Modality	Ventricles day 0	Ventricles day 7
1	IC	2	2	CT	0,032	0,177*
2	IC	3	18*	CT	0,024	0,024
3	IC	5	7	CT	0,031	0,055*
4	CM	16	x	Autopsy	/	x
5	CM	12	20*	Autopsy	/	0,030
6	CM	12	21*	Autopsy	/	0,043*
7	CM	14	x	Autopsy	/	0,018
8	CM	15	14	Autopsy	/	0,017
9	CM	16	24*	Autopsy	/	0,024

In the CM group, the mean baseline ICP increased from 13.8 (10.5-17.0) to 19.8 (13.0-26.4) mm Hg. The ICP increased to a value above the upper limit of the 95% confidence interval of the baseline values in 3 of the 4 animals.

In the IC group, the increase in ICP was almost equal to that of the CM group (6.0 and 5.7 mm Hg respectively; P-value 0.95).

All animals considered as a single group, the mean ICP increased from 9.3 to 15.1 mm Hg. The increase in ICP was statistically significant (P-value 0.036).

The due to pulmonary-aspiration-of-gastric-reflux deceased goat, and the euthanized post-puncture quadriplegic goat were divided into the 21 day follow-up group. Consequently, in only one goat the ICP could be measured at day +21. In this case, the ICP at day 0 of 16, increased to 24 at day +7 and attenuated to 18 mm Hg on day +21.

The ratio between the ventricular and brain surfaces was assessed during autopsy. This ratio did not differ between the 9 animals that were injected with kaolin and the 6 non-hydrocephalic animals of the cadaver study [0.027 (0.015-0.040) and 0.026 (0.13-0.040) respectively].

Histology

A histological sample of the dura adjacent to the kaolin deposits showed aseptic meningitis with granulomata formation. The granulomas consisted of kaolin containing macrophages (Figure 99).

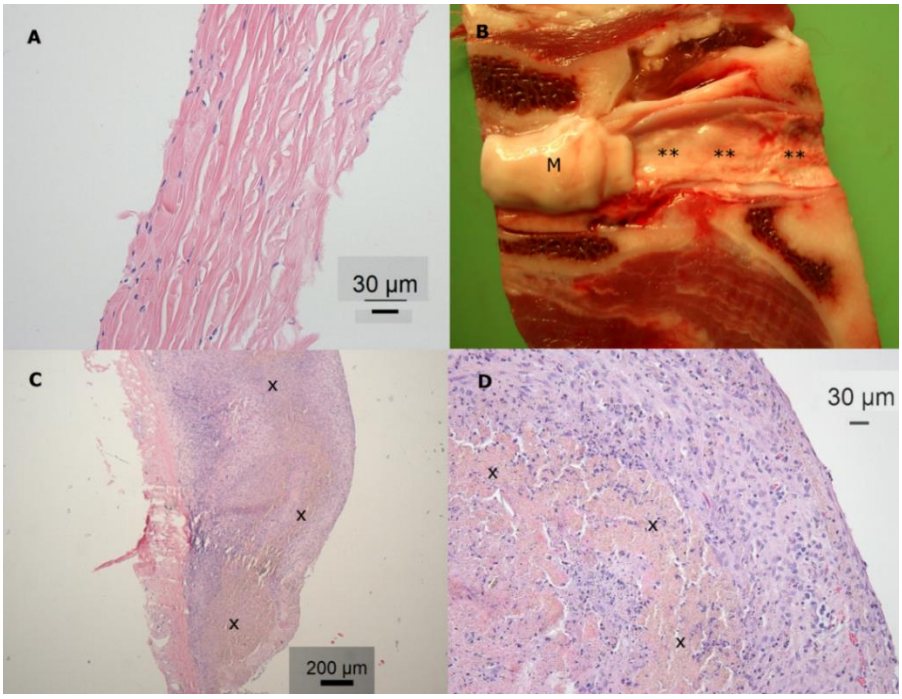

Figure 99. Histology of the dura after 7 days

A: Histological sample of normal dura; B: Sagittal section through the craniocervical junction showing the kaolin deposition and a thickened hyperemic aspect of the dura mater; C and D: Histological samples of the dura adjacent to the kaolin deposits showing aseptic meningitis with granulomata of kaolin containing macrophages [M: medulla oblongata; Asterisk: inflamed dura mater; x: granulomata]

The kaolin itself was observed in the SAS where it provoked perivascular inflammation. At the surface of the brain parenchyma, focal perivascular inflammatory infiltrates were observed (cuffing).

In the goats with increased ICP, the ependymal layer of the ventricles was flattened and denuded in some areas. Leukomalacia, focal hemorrhages and hyaline fluid were observed around the ventricular system. This is consistent with trans-ependymal resorption of CSF. The choroid plexus of the fourth ventricle was edematous.

DISCUSSION

Non-obstructive HC is treated with ventriculo-peritoneal or –atrial shunts, which have a high failure rate requesting reoperations at high individual and social security costs[95]. The aim of this study was to present a hydrocephalic goat model to endorse the development of novel techniques in the pursuit to moderate this failure rate. To approximate human treatment conditions, a model of non-obstructive HC was preferred. Two different techniques were evaluated: in the IC group (n=3), 4ml of a 25% kaolin solution was injected anteriorly to the brain stem to avoid occlusion of the fourth ventricle outflow[180]. In the subsequent CM group (n=6) 3ml of a 25% kaolin solution was injected into the cisterna magna, which is a more conventional and well-documented technique to induce HC in small domestic animals such as rats, canine and feline[169-171].

Two animals died during the experiment. One goat due to asphyxia after massive aspiration of gastric reflux during orotracheal intubation. A second goat due to

complicated suboccipital puncture with subarachnoid and brainstem hemorrhage. In the remaining goats (n=7), the kaolin injection provoked pronounced aseptic meningitis that caused HC in 6 out of 7 (86%) goats.

Hydrocephalus

The HC was characterized either by ventricular dilatation 2/3 goats belonging to the IC group, or by an increased ICP in the remaining 4/6 CM group goats).

Such a variable degree of ventricular dilatation within the same species and also in between species has been described in literature and probably relates to the pathophysiology of a kaolin induced HC: the aseptic meningitis combined with meningeal thickening and subarachnoid adhesions, impedes the normal CSF flow[169]. This may lead to acute obstructive or latent non-obstructive HC, depending on the location of the obstruction[169]. Acute or obstructive HC is due to obliteration of the fourth ventricle outflow and is characterized by a steep raise in ICP and clear ventricular dilatation[169,181]. Latent or non-obstructive HC is caused by a more downstream obstruction of the SAS space with reduction of the normal absorption capacity. It is characterized by a more gradual ICP increase and less pronounced ventricular enlargement[169,170,181]. Injection of kaolin into the basal cisterns probably causes a variable combination of both types and is not the most evident way to induce selectively obstructive or communicating HC. The variability of the ventricular dilatation within species can be explained by the variable obstruction of the fourth ventricular outflow, which was more pronounced in the animals that did develop ventricular dilatation in the current study.

Also, a variability of the ventricular dilatation in between species has been described. The ventricular dilatation in goats and sheep is less pronounced than described in other species[169,176,182]. Why a kaolin injection into the basal cisterns in goats and sheep produces such mild ventricular dilatation was not investigated. However, a similar issue was encountered in rabbits[183]. In contrast with most other species, goats, sheep and

rabbits have a persisting open outflow channel in common, between the central canal of the spinal cord and the lumbosacral subarachnoid space[183-186]. This channel enables CSF to bypass obstructed foramina of Luschka (goats have no median foramen of Magendie), thus eliminating the factor that contributes the most to the ventricular dilatation[183]. This persisting open outflow channel makes goats very suitable as a model of latent communicating HC.

Injection in the IC, which is more complicated to reach, does not present an advantage over the CM injection in the prevention of obstructive HC. It is striking that clear ventricular dilatation was only seen in the IC group, as kaolin was deliberately injected anteriorly of the brainstem to reduce the risk of obstruction of the fourth ventricular outflow. The ventricular dilatation was very pronounced (>300% of the original volume) in one. The distribution of kaolin in this goat suggests intraventricular injection, which is possible if the caudal medullary velum was perforated by the suboccipital puncture. Only in this goat, a kaolin plug was observed in the fourth ventricle. This plug obstructed not only the foramina of Luschka, but also the origin of the central canal at the obex. Interestingly in this goat, kaolin was also observed along the olfactory nerves and even in the olfactory bulb at lamina cribrosa level (Figure 98). In earlier studies, the nerve sheet of the olfactory nerve was found to drain up to 30% of the CSF towards the extra-cranial lymphatic system in sheep (which are very similar to goats)[187,188]. The kaolin around the olfactory nerve may have obstructed the latter absorption pathway. In this one goat, the escapes via both the central canal and the olfactory nerves were both obliterated. Thus, besides the SAS CSF flow and absorption in the SAS, also the lymphatic pathways for evacuation were obstructed.

The fact that no increased ICP was measured in the animals that developed ventricular dilatation may be explained by the location of the ICP measurement. With a fourth ventricular outflow obstruction, a gradient may develop between the intraventricular and extra-ventricular CSF compartments, causing the ventricles to dilate. Although such a pressure gradient was not observed in kaolin induced hydrocephalic dogs[169], it was

found in sheep[176], which are very similar to goats. By consequence the ICP measurements in the cisterna magna in this study may have led to underestimation of the intraventricular pressure in the goats that developed ventricular dilatation.

The natural evolution of the induced HC is unclear as only one animal was followed for an extended period of 21 days. After initial ICP increase at day +7, a spontaneous readjustment to upper limit values was noted at day +21. The reason for this finding, that was also described in previous literature, is not clear[169]. Possibly the existing alternative CSF absorption pathways 'grow on demand'.

Aseptic meningitis

The injection of 4ml kaolin in the interpeduncular cistern (n=3) provoked pronounced aseptic meningitis, which had an unacceptable impact on the animals' clinical status. The main symptoms included head pressing, spastic paresis of the legs, paddling, convulsions, apathy and aphagia / loss of appetite. In order to reduce animal suffering, the dose was lowered and in the subsequent animals (n=6) 3ml of the kaolin solution was injected. The latter protocol (dose and injection site) was based on previous literature on sheep[176]. The reduced dose provoked a milder, but still heartbreaking clinical picture. In both groups, the important discrepancy between the severity of the meningitis and the mildness of the HC made it difficult, if not impossible to adequately monitor the developing HC clinically.

The pronounced clinical impact of the aseptic meningitis was also a major issue in previous studies. Although kaolin injection into the cisterna magna seems to be relatively well tolerated by mice and rats[189,190], this is not the case for larger animals like dogs, ferrets and sheep[169,176,182]. In the latter species the clinical signs were comparable to those observed in the current study and the mortality rate - typically 30-40% - was even higher[169,182,191].

The very pronounced clinical impact of suboccipital kaolin injection should urge the development of techniques that do not rely on meningitis to produce hydrocephalus. The injection of a silicone elastomer into the interpeduncular cistern seems an option to consider[177].

CONCLUSION

In contrast to other species, an outflow channel between the spinal cord central channel and the lumbo-sacral subarachnoid space persists in goats. This anatomical characteristic may be especially convenient for the development of a model of communicating HC as it's protective against obstructive HC development.

Although the suboccipital kaolin injection was effective in producing communicating HC, it provoked a pronounced aseptic meningitis with devastating clinical impact, clearly overshadowing the resulting HC. The development of better tolerated techniques not-depending on reactive aseptic meningitis may be the subject of further research.

ACKNOWLEDGEMENT

We express our gratitude to professor Paul Simoens for his enthusiastic support during the full course of the study and the preparation of the manuscript.

DECLARATION OF CONFLICTING INTERESTS

The Authors declare that there are no conflicts of interest

FUNDING ACKNOWLEDGEMENT

This study was supported by an Industrial Research Fund (IOF) of the Ghent University.

5.6.7 MANUSCRIPT 6

Manuscript 6 reports on the validity of the non-hydrocephalic caprine in-vivo model to prototype and test ventriculo-sinus shunts. Rationale, techniques, anatomy and results are discussed in detail.

A NON-HYDROCEPHALIC GOAT EXPERIMENTAL MODEL TO EVALUATE THE VENTRICULO-SINUS SHUNT

J. Vandersteene[1], E. Baert[1], S. Schauvliege[2], K. Vandevelde[2], F. Dewaele[1], F. Desomer[3], D. Van Roost[1]

[Laboratory Animals, published, January 2018]

[1] Department of Neurosurgery, Ghent University Hospital, Belgium
[2] Faculty of Veterinary Medicine, Ghent University, Belgium
[3] Department of Cardiac Surgery, Ghent University Hospital, Belgium

---

ABSTRACT

The ventriculo-sinus shunt is a promising treatment for hydrocephalus. Currently, different shunt techniques exist, and it is not clear whether one is preferable. This pilot study reports on a non-hydrocephalic goat model (Saanen breed) that provides opportunities to evaluate and optimize several aspects of the ventriculo-sinus shunt technique. Analysis of the coagulation properties of 14 goats by a viscoelastic coagulation monitor showed that goats have a hypercoagulable state compared to humans. This property can be partially counteracted by antiplatelet drugs. During implantation of a ventriculo-sinus shunt, a pulsatile reflux of blood was observed. After

implantation, the animals recovered to their preoperative state, and none of them developed a superior sagittal sinus thrombosis. Evaluation of the shunts after 16 days showed an obstructing luminal clot. Several model-related factors may have promoted this obstruction: the absence of hydrocephalus, the hypercoagulability of caprine blood and the smaller dimensions of the caprine super sagittal sinus. However, the pulsatile reflux of blood, which is caused by the compliance of the shunt system distal to the valve, may have been an important factor as well. In conclusion, the non-hydrocephalic goat model limits animal suffering and simplifies the study protocol. This model allows researchers to evaluate their implantation technique and shunt hardware but not the efficacy of the treatment or shunt survival.

INTRODUCTION

Hydrocephalus, or the accumulation of cerebrospinal fluid (CSF) in the brain, is treated with ventriculo-peritoneal or ventriculo-atrial shunts. An important drawback of these techniques is siphoning, in which the CSF column within the catheter exerts suction through gravity when the patient is in a sitting or standing position. This effect leads to shunt-related intracranial hypotension and aspiration of the choroid plexus into the proximal catheter[173]. Intracranial hypotension causes headaches, nausea, vomiting and even subdural haematomas, while aspiration of the choroid plexus is a major cause of shunt obstruction[90]. Despite the usage of expensive resistance valves and anti-siphon devices, the rate of shunt failure—which requires surgical revision—remains as high as 50% in the first 2 years[95].

A more physiological, but still experimental, technique is the ventriculo-sinus shunt. This shunt drains CSF to a natural resorption site, such as the superior sagittal sinus, and theoretically reduces the risk of shunt failure in several ways[111,120]. First, excessive drainage of CSF is prevented by the natural, self-regulating anti-siphon effect of the IJV. Second, the shunt system is shorter, less complex and confined to the skull, which minimizes the risk of mechanical failure and infection[118].

The efficacy of the ventriculo-sinus shunt was evaluated in a few clinical studies[11,15,138,192]. Although the technique has been proven to be safe and effective[11,15,134,138,192], several issues and uncertainties persist[134]. First, authors do not agree on whether the tip of the shunt should be directed towards or against the direction of blood flow[134]. Second, problems with the implantation of the shunt system exceed 10% in most of the available studies[134,138]. A technical advance using the Seldinger technique was published, but this method was evaluated in only 1 patient[115]. Third, when the shunt system is correctly implanted, obstruction of the intravascular catheter remains an issue[15,138,192]. Based on their experience, different authors have proposed several prototypes of the ventriculo-sinus shunt with distinct features[5,13,193]. It is not clear which of these shunt systems would be preferable[134].

To optimize the implantation technique and to evaluate the different prototypes of the ventriculo-sinus shunt, an animal model would be an indispensable tool[194].

The only model described to date to evaluate a ventriculo-sinus shunt is a hydrocephalic dog model that used only two animals, and it has substantial shortcomings: the induction of hydrocephalus was not well-tolerated, and the implantation of the ventriculo-sinus shunt resulted in a thrombosis of the superior sagittal sinus[194]. The only way to prevent venous congestion and sinus thrombosis in a canine model is an extended miniaturization of the intravascular catheter to fit the small size of the superior sagittal sinus[194]. To facilitate the use of shunt systems that are similar in size and design to their human counterparts, a large animal model must be created[176]. A hydrocephalic sheep model to evaluate ventriculo-peritoneal shunts has been described in a previous study[176].

The purpose of this pilot study is to assess the suitability and feasibility of a goat model (specifically 'Saanen breed' goats, which are very similar to sheep) for evaluating the implantation technique and design of the ventriculo-sinus shunt. Since hydrocephalus is not required for addressing the research question, a non-hydrocephalic model was chosen.

The study consists of a cadaver anatomical study, an in vitro coagulation assay (Sonoclot Analyzer©) and an in-vivo study. The cadaver anatomical study describes the relevant surgical anatomy of the caprine brain ventricles and superior sagittal sinus. The in vitro coagulation assay analyses the coagulability of the caprine blood. The in-vivo study assesses the feasibility of the in-vivo implantation of a ventriculo-sinus shunt.

MATERIALS AND METHODS

Animals

The species was selected based on anatomical characteristics. In pigs and cattle, frontal access to the ventricles and superior sagittal sinus may be impeded by the pronounced caudal extension of the frontal sinuses. The remaining possible models included sheep, goats and horses or ponies. Ultimately, domestic dairy goats (Saanen breed) were chosen because of their manageability and short hair. All goats were purchased from dairy goat farms. The goats were 1 to 2 years old and weighed less than 60 kg. Only female goats were included because the more pronounced cornual processes of bucks could impede frontal ventricular access.

Since the investigation was a pilot study, small sample sizes were chosen. The study consisted of a cadaver study (9 goats), an in vitro coagulation assay (14 goats) and an in-vivo study (3 goats). Three of the 14 goats included in the in vitro coagulation assay were also used for the in-vivo study; thus, 23 goats were used in total. The studies were conducted serially, and the goats were allocated to the experiments in order of acquirement.

All experiments in this study were approved by the Ethics Committee of the Faculty of Veterinary Medicine of Ghent University (EC2012/187, EC2013/66, EC2013/129). The care and use of animals were in full compliance with the most recent national legislation

(Belgian Royal Decree of 29 May 2013)[178] and the relevant European Directive (2010/63/EU)[179].

For the cadaver anatomical study, the goats were euthanized directly after arrival at the research facility. The remaining goats were admitted to the animal facility at least 10 days prior to the start of the study for acclimatization and health checks (including clinical investigation, ultrasonography examination of the abdomen and thorax, and blood and faeces analyses). The animals were housed in small groups (3-4 animals per cage). The cage measured 3 x 4 m. The bedding consisted of straw, and cage enrichment (an elevated platform) was provided in all cages. Natural light was provided by translucent windows, and the cage temperature was maintained between 15 and 20 °C. The animals were fed hay and water ad libitum and supplemented with 450 g of nutritional pellets daily.

Clinical evaluation of the animals was performed twice daily using a clinical scoring system. This scoring system was developed by the authors in cooperation with the Department of Internal Medicine of the Faculty of Veterinary Medicine of Ghent University. The score consists of objective (e.g., vital parameters, weight, and food intake) and subjective (e.g., general impression and posturing) parameters, and it is based on existing pain scores[195,196]. A perfectly healthy animal without signs of distress will score 0, while a very ill animal with signs of unbearable suffering will score 21. A total score of 6, or a maximum score for one of the parameters, was the threshold for therapeutic action to alleviate suffering.

All animals fasted for 24 h before surgery and received an intramuscular injection of 2.5 mg trimethoprim and 12.5 mg sulfadiazine/kg body weight (Borgal® 24%, Virbac, Barneveld, The Netherlands) starting one day prior to surgery and daily until 4 days after surgery. If needed, postoperative pain and fever were treated with 48 mg meloxicam subcutaneously (Metacam, Boehringer Ingelheim, Germany).

Euthanasia was performed by intravenous administration of 50 mg/kg sodium pentobarbital (20%) (Pentobarbital, Kela, Hoogstraten, Belgium) after intravenous premedication with 0.3 mg/kg midazolam (Dormicum, Roche Pharma, Brussels, Belgium) and 0.1 mg/kg morphine (Morphine HCL Sterop, Brussels, Belgium). The anaesthesia was intravenous propofol 2-4 mg/kg (Propovet, Parsippany-Troy Hills, New Jersey, United States).

Cadaver anatomical study

After euthanasia, the goats were frozen at –20 °C and decapitated. The heads were sawed in coronal slices at approximately a 1-cm thickness. The superior sagittal sinus was inspected for septa or trabeculae and measured at the confluens sinuum and 1 cm rostral to the confluence. The rostral horns of the lateral ventricles were measured at the level of the coronal suture. A point on the coronal suture was determined where a catheter, which is inserted perpendicularly to the skull in the coronal plane, would enter the ipsilateral ventricle. The length of the intraventricular trajectory of a shunt placed in that manner was measured.

In vitro coagulation assay

The goats were anaesthetized on the morning of the operation in the operation theatre. Eight animals received 75 mg clopidogrel (Plavix, Sanofi, Machelen, Belgium) and 80 mg acetylsalicylic acid per orally (Asaflow, Takeda, Sint-Jans-Molenbeek, Belgium) starting the day before the procedure. Six goats did not receive any antiplatelet drugs. Three millilitres of CSF and 15 ml of venous blood (citrated with 0.129 mole Na3-Citrate/l, Terumo, Heverlee, Belgium) were obtained by a sub-occipital puncture and a venepuncture, respectively. The samples were stored at room temperature and processed within 60 min. Because tissue factor is a potent activator of the extrinsic coagulation pathway, the first 1 ml of CSF and 3 ml of blood were not used for analysis.

To assess the impact of CSF on coagulation, different concentrations of CSF were added to the blood samples (0 µl CSF/ml blood and 100 µl CSF/ml blood). Subsequently, the mixture was recalcified with 40 µl of 0.25 mol/l $CaCl_2$ and analysed by a Sonoclot Coagulation Analyser© (Sienco, Arvada, CO, USA).

The Sonoclot Analyser© was used in an in vitro method for the analysis of the coagulation process from the start of fibrin formation through polymerization of the fibrin monomer and platelet interaction and eventually to clot retraction and lysis. The system consists of an open-ended plastic probe, which vibrates vertically while immersed in a cuvette containing a 0.33-ml sample of whole blood, and the probe measures changes in the viscoelastic properties of whole blood during the clotting process. The curve or signature reflects the changes in viscoelasticity from a liquid to a solid state[197]. Three parameters are defined: the activated clotting time (ACT), clot rate (CR) and platelet function (PF). The ACT is an expression of how long the sample remains completely in the liquid phase and corresponds to the time necessary for fibrinogen to be converted to fibrin monomers. The CR is the slope of the second peak/plateau of the curve, which corresponds to the polymerization of fibrin monomers; a faster fibrin polymerization will be reflected by a steeper slope. The PF represents the attachment of platelets to fibrin and the retraction of the clot[197].

Statistical analysis was performed using SPSS Statistics® 22 (IBM Corp., Released 2013, IBM SPSS Statistics for Windows, Version 22.0, Armonk, New York, USA).

The distribution of the Sonoclot parameters was evaluated using QQ-plots and a Shapiro–Wilk test.

To evaluate the effect of CSF on blood coagulation, the goats were considered one group independent of antiplatelet drug administration. Each of the Sonoclot parameters of pure blood was compared to the blood-CSF mixture using a paired-sample T test.

The effects of antiplatelet drug administration on the Sonoclot parameters were evaluated by comparing the Sonoclot parameters of the goats that received antiplatelet drugs with the parameters of the goats that did not receive antiplatelet drugs. An independent sample T test was used. Statistical significance was set at 5%.

In-vivo study

Shunt implantation

A ventriculo-sinus shunt was implanted in 3 goats under general anaesthesia. The procedure started in the morning and was performed in the operation theatre. The animals received 75 mg clopidogrel (Plavix, Sanofi, Machelen, Belgium), 80 mg acetylsalicylic acid (Asaflow, Takeda, Sint-Jans-Molenbeek, Belgium) and 40 mg pantoprazole per orally (Pantomed, Takeda, Sint-Jans-Molenbeek, Belgium) starting 24 h before surgery until the end of the study.

A surgical plan was made based on a contrast-enhanced brain CT scan the day before surgery. As shown in Figure 100. Positioning and incision, the head of the animal was secured in a custom-built frame. Under sterile surgical conditions, a 10-cm midline skin incision was made that reached from 2 cm rostral to the coronal suture to 2 cm caudal to the lambdoid suture.

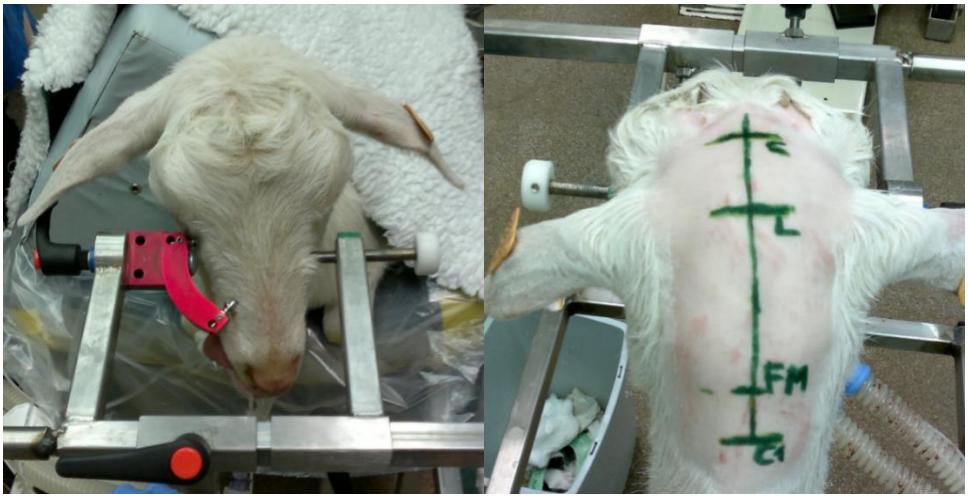

Figure 100. Positioning and incision

Left: the goats were positioned prone with the head slightly elevated and fixated in a custom-built head clamp. Right: a linear incision was made, starting 2 cm rostral to the coronal suture and ending 2 cm caudal to the lambdoid suture. The foramen magnum and the arch of the atlas were also marked as these are the anatomical references for a suboccipital puncture. [C: coronal suture; L: lambdoid suture; FM: foramen magnum; C1: atlas]

A hole was drilled approximately 18 mm to the right of the midline on the coronal suture, and another hole was drilled on the midline just rostral to the lambdoid suture. To introduce the ventricular catheter, an aiming device was used, which was similar to a device described in the literature[198].

This device was placed over the burr hole parallel to the sagittal plane and perpendicularly to the surface of the skull in the coronal plane. In the sagittal plane, the appropriate angle was set, and the ventricular shunt (Codman Hakim Ventricular Catheter, inner diameter (ID) 1.4 mm and outer diameter (OD) 2.7 mm) was inserted into the rostral horn of the right lateral ventricle. The correct position was confirmed by the outflow of CSF. The catheter was connected to a Codman Hakim very low pressure valve (Depuy Synthes - Codman Neuro, Raynham, Massachusetts) and obstructed by a clamp.

The superior sagittal sinus was then identified. The roof of the sinus was punctured with an 18G needle and/or incised with a surgical blade (n° 11). A peritoneal catheter (Codman Hakim Peritoneal Catheter, ID 1 mm and OD 2.2 mm) was introduced over a length of 3 cm in the superior sagittal sinus against the direction of blood flow.

The correct position of the sinus shunt was confirmed both by injection of a 0.9% sodium chloride solution and by aspiration of blood. The intravascular catheter was then connected to the valve after flushing the catheter with a 0.9% sodium chloride solution. The clamp was removed from the ventricular catheter, and the system was inspected for drainage of CSF to the sinus or reflux of blood to the catheter system.

In one goat, a spinal epidural catheter (Portex, Smiths-Medical, Hythe, United Kingdom, ID 0.55 mm and OD 1.03 mm), which was obliterated at its proximal end, was inserted in the superior sagittal sinus before implantation of the final catheter. After being inspected for blood reflux, the spinal epidural catheter was replaced by the final Codman Hakim peritoneal catheter.

Postoperative evaluation

Postoperatively, head computed tomography was acquired to verify the correct position of the shunt components and the patency of the superior sagittal sinus. The animals were evaluated daily until two weeks after the implantation. This follow-up period was chosen because full recovery or major complications, such as a superior sagittal sinus thrombosis or infection, are expected to manifest within this period. For clinical evaluation, the scoring system described above was used.

At the end of the follow-up period, the animals were anaesthetized, and the patency of the ventricular and intravascular catheters was assessed using water columns. At the end of this procedure, the animals were euthanized, and the superior sagittal sinus containing the intravascular catheter was explanted with the catheter left in place. The lateral wall of the superior sagittal sinus was opened to visualize the intravascular catheter. The correct position was verified, and the presence of clots was evaluated using a stereomicroscope. Subsequently, the catheters were removed along with the surrounding sinus wall, which was transversely cut in two equal parts and fixed in a HEPES buffer containing 2.5% glutaraldehyde solution (Sigma Aldrich, Steinheim, Germany). After fixation, the shunts were rinsed with a 0.9% sodium chloride solution, air-dried, mounted on aluminium pin mounts and sputtered with platinum particles.

The samples were then observed with a JEOL JSM-5600 LV scanning electron microscope (SEM) with the lumen facing the camera and evaluated at different magnifications.

RESULTS

Cadaver anatomical study

The mean weight of the animals was 45.3 kg (range 40-62 kg).

Table 28. Shows the dimensions of the superior sagittal sinus and the lateral ventricles.

Dimensions (mean values and 95% confidence intervals) of the superior sagittal sinus (SSS) and lateral ventricles. The dimensions of the superior sagittal sinus are expressed as latero-lateral x dorso-ventral distances. The dimensions of the ventricles are measured at the level of the coronal suture.

Variable	Dimension (mm)
SSS at confluence of sinuses	5.5 (4.0-7.0) x 6.0 (4.7-6.8)
SSS 10 mm rostral to confluence of sinuses	2.8 (2.3-3.3) x 3.3 (2.6-4)
Ventricle height	3.5 (2.6-4.4)
Bifrontal ventricular diameter	16.6 (14.4-18.9)
Intraventricular shunt trajectory	5.8 (4.6-7.0)
Centre of burr hole to midline	12.0 (11.0-13.0)
Dura to ependyma	18.9 (17.0-20.7)

The confluence had variable dimensions. The mean latero-lateral diameter was 5.5 mm, and the dorso-ventral diameter was 6 mm. As seen in Figure 101, the confluence frequently contains septa and trabeculae.

Ten millimetres rostral to the confluence, the cross section of the superior sagittal sinus has a triangular shape (Figure 101B). The mean latero-lateral diameter (base) was 2.8

mm, and the dorso-ventral diameter (height) was 3.3 mm on average. A septum was observed in only a few goats.

The mean height of the lateral ventricles at the level of the coronal suture was 3.5 mm. The mean bifrontal diameter at the same slice was 16.6 mm.

A burr hole at the coronal suture should be placed 12.0 mm lateral to the midline to ensure that a catheter inserted perpendicularly to the tabula externa of the skull will enter the rostral horn of the ipsilateral ventricle. Following this trajectory, the distance between the internal tabula of the skull and the dorsal ependyma of the rostral horn was 18.9 mm, and the intravascular trajectory was 5.8 mm (Figure 101C and Figure 101D).

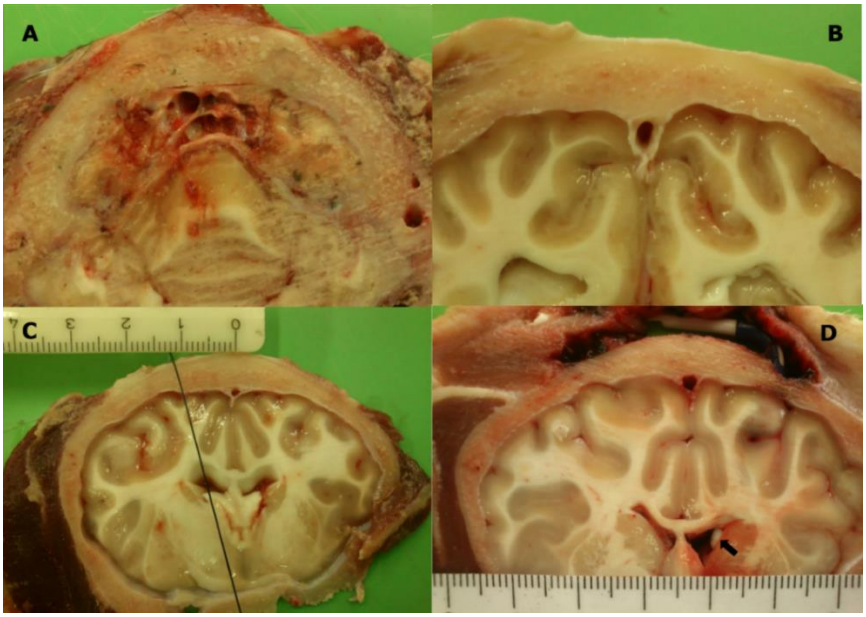

Figure 101. Anatomy of the caprine superior sagittal sinus and lateral ventricles.
A. septa in the confluence of sinuses. B: cross section of the superior sagittal sinus 1 cm rostral of the confluence of sinuses in the same animal. C: a catheter, inserted 12 mm lateral to the midline perpendicular to the tabula externa of the skull, will enter the ipsilateral rostral horn of the lateral ventricle. Figure 2d: the tip of the ventricle catheter is inserted in the rostral horn of the right lateral ventricle (arrow).

In vitro coagulation assay

A normal distribution was assumed because the Shapiro–Wilk test was not statistically significant for any Sonoclot parameter. The influence of the in vitro addition of CSF to pure blood and the oral administration of antiplatelet drugs on the ACT, CR and PF are shown in Table 29.

Table 29. Coagulation properties of goat blood.

The influence of in vitro addition of CSF to pure blood and oral administration of antiplatelet drugs on the ACT, CR and PF are shown (mean value and 95% confidence interval).

Variable	Activation time	Clot rate	Platelet function
	CSF		
0 µl CSF/ ml blood	130.4 s (113.2-147.7)	53.9 (44.7-63.1)	3.3 (2.7-3.8)
100 µl CSF/ ml blood	114.3 s (103.9-124.8)	65.5 (56.0-74.9)	3.3 (2.8-3.9)
P-value	0.006	0.009	0.734
	Antiplatelet drugs		
No antiplatelet drugs	108.8 s (88.2-129.3)	66.4 (54.3-78.6)	3.5 (2.4-4.7)
ASA + clopidogrel	146.7 s (124.9-168.4)	44.5 (34.7-54.4)	3.0 (2.2-3.9)
P-value	0.009	0.005	0.405

After the addition of 100 µl of CSF per millilitre of blood, the ACT shortened from 130 seconds to 114 seconds, and the CR increased from 54 units/min to 66 units/min. There was no significant impact on the PF.

After oral administration of antiplatelet drugs, the ACT increased from 109 seconds to 147 seconds, and the CR decreased from 66 units/min to 45 units/min. There was no significant impact on the PF.

In-vivo study

Shunt implantation. No specific obstacles were encountered during implantation of the shunt. When the transparent part of the Codman Hakim low pressure valve was inspected, spontaneous drainage of CSF to the superior sagittal sinus was observed directly after implantation of the shunt. Through the wall of the distal segment of the silicone catheter, a pulsatile reflux of blood to the shunt system was observed. This reflux disappeared after obliterating the catheter 1 cm proximally to its entrance in the superior sagittal sinus. No reflux was observed after introduction of a more rigid catheter with a smaller inner diameter.

Clinical score

The average clinical score of the 3 animals during the last 5 days before surgery was 1.5. The clinical score increased to 3.2 immediately after surgery and to 3.5 on the first postoperative day. The average clinical score normalized starting on the second postoperative day (average score between day 2 and 5 after surgery: 1.33).

Computed tomography imaging

Computed tomography imaging after surgery showed a correct position of the ventricle catheter in 2 animals. In the third animal, the ventricle catheter was positioned too deep and had no clinical consequences. The intravascular catheter was correctly positioned in all animals. The distal part was always located in the ventral angle of the triangular section of the sinus (Figure 102). Clinically and radiographically (contrast-enhanced CT), there were no indications of thrombosis of the superior sagittal sinus.

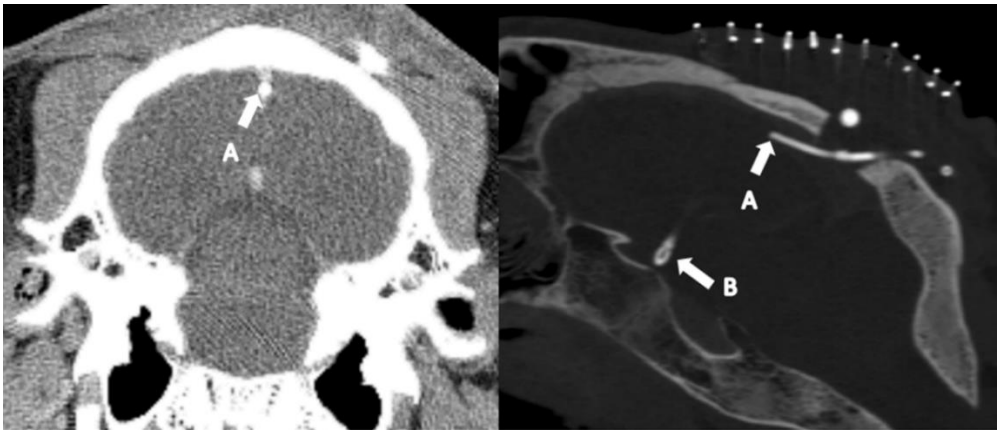

Figure 102. Position of the intravascular catheter in the superior sagittal sinus.
Coronal (top left) and sagittal (top right) computed tomography imaging of the caprine head showing the position of the intravascular catheter and the ventricular catheter. The intravascular catheter was always positioned in the basal tip (just above the falx) of the superior sagittal sinus. In this position the catheter touches the lateral walls of the sinus. The ventricular catheter was positioned to deeply in this animal, with the tip in the interpeduncular cistern. [A: intravascular catheter; B: ventricular catheter]

Assessment of shunt patency

The assessment of the shunt system after 16 days showed a patent ventricle catheter, but there was an obstructed vascular catheter in all animals.

Autopsy

Stereomicroscopic evaluation showed a correct position of the intravascular catheter in the three animals. However, the presence of a clot was visualized around all three catheters. This clot was situated at the site were the catheter enters the sinus and extended downstream (i.e., caudally) along the sinus roof (Figure 103A). The SEM evaluation of the lumen of the intravascular catheter showed the presence of an intraluminal clot in all catheters (Figure 103B).

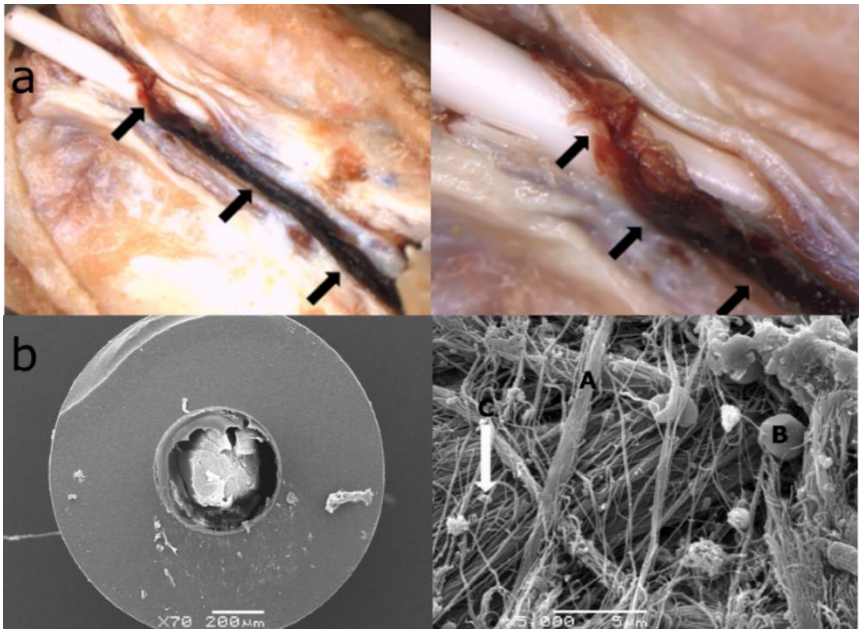

Figure 103. Microscopic evaluation of the intravascular catheter.

(a) evaluation with a stereomicroscope showed the presence of a clot (arrow) originating at the entry site of the catheters and extending downstream (i.e. caudally) along the sinus roof. (b) scanning electron microscopic views of the obstructed intravascular catheter. Left: SEM evaluation of a transverse section through the intravascular catheter showing the obstructing clot. Right: Higher magnification of the intraluminal clot showing fibrin network with red blood cells and platelets. [A: fibrin network; B: red blood cell; C: platelets]

DISCUSSION

Shunting CSF to its natural resorption site—the superior sagittal sinus—with a ventriculo-sinus shunt is a promising treatment for hydrocephalus[11,15,134]. Different authors have evaluated this shunt in clinical series[11,15,138]. Based on their experience, the authors have modified the technique and developed designated shunt hardware[5,13,115,193]. Currently, it remains unclear which technique or shunt system is ideal[134]. To maximize the chance of success, a ventriculo-sinus shunt should be optimized by evaluating and

combining the most valuable characteristics of the available techniques. This process requires a suitable animal model[194].

This pilot study reports on the characteristics and feasibility of a non-hydrocephalic goat model. The purpose of this model is to enable the evaluation and optimization of different implantation techniques and prototypes of the ventriculo-sinus shunt.

Strengths and limitations of the non-hydrocephalic caprine model

The implantation of a ventriculo-sinus shunt in goats has been found to be feasible and safe. The anatomy and dimensions of the caprine brain ventricles and superior sagittal sinus allow for the implantation of ventriculo-sinus shunts that are comparable in design and dimensions to shunts for human use[11]. These characteristics are in contrast to the previously described canine model, in which the implantation of a distal catheter with a comparable outer diameter resulted in venous congestion and sinus thrombosis[194].

Although the goat model resembles human anatomy, the dimensions of the caprine superior sagittal sinus are significantly smaller[199]. Depending on the prototype that will be tested, miniaturization of the shunt material might yet be necessary. The smaller superior sagittal sinus may also promote distal shunt obstruction, and the proximity of the sinus walls to the catheter tip may cause endothelial irritation and blood stasis, which are both known to enhance coagulation[141].

In contrast to previously described animal models[176,194], hydrocephalus was not induced in this study. Injection of Kaolin by a sub-occipital puncture, which is the best documented method for the induction of hydrocephalus, causes chemical meningitis[169]. This technique is associated with a high morbidity and mortality[169,176,182,191]. However, hydrocephaly is not required for the evaluation of the implantation technique and the design, dimensions and tolerance of current and potential new prototypes of the ventriculo-sinus shunt. The clinical impact of meningitis itself may even cloud the

assessment of the tolerance for the shunt system. Thus, the use of a non-hydrocephalic model is an important refinement because it simplifies the study protocol and drastically reduces animal suffering.

A major limitation of the non-hydrocephalic model is the impossibility to evaluate the efficacy and survival of the shunt system. The preserved physiological drainage of CSF causes the flow through the shunt system to be at least limited and inconsistent. This inconsistency leads to impaired clearing of fibrin deposits, which are known to result in catheter obstruction[200]. This obstruction partially explains why all implanted shunts were found to be obstructed after two weeks.

In addition to the absence of hydrocephaly, the coagulation properties of the caprine model may promote shunt obstruction. Sonoclot analysis showed that goats have a hypercoagulable state that is comparable to humans. Compared to normal human values[142], the ACT is 34% shorter, and the CR is 127% higher. This difference in coagulability was partly counteracted by administration of antiplatelet drugs, which reduced the relative difference in ACT to 11% and CR to 52%. The addition of CSF to blood enhances coagulation in humans[142]. This effect appears to be more pronounced in goats, which may further increase the risk of shunt obstruction.

Intra-operative evaluation of the ventriculo-sinus shunt

The current study shows that an intra-operative evaluation of the shunt system may be useful for clarifying the causes of shunt failure, even in the absence of hydrocephalus. One could observe a pulsatile reflux of blood to the shunt system despite the use of a competent one-way valve and a retrograde position of the shunt. This reflux is probably caused by a combination of the compliance of the silicone shunt system distal to the valve, the pressure pulsations in the superior sagittal sinus and the inertia of blood corpuscles that hit the CSF column at the distal shunt tip.

Pulsatile reflux of blood results in the development of a relatively static blood-CSF mixture in the distal shunt system. Both stasis of blood and the interaction with CSF promote clot formation, which finally results in shunt obstruction[142].

The reflux could be prevented by clamping the distal catheter close to its entrance in the superior sagittal sinus. In addition, reflux was not observed when a more rigid catheter with a smaller inner diameter was inserted in the sinus. Both manoeuvres reduce the compliance of the shunt system distal to the valve. These findings suggest that using a more rigid distal catheter with a smaller internal diameter may help prevent distal shunt obstruction.

CONCLUSION

The implantation of ventriculo-sinus shunts is feasible and safe in a non-hydrocephalic goat model. This model facilitates the intra-operative evaluation of the implantation technique, hardware and functions of the ventriculo-sinus shunt. The tolerance for the shunt system and possible postoperative complications can be monitored without interference of sequelae from the induction of hydrocephalus. However, in the absence of hydrocephalus, it is impossible to evaluate shunt efficacy and shunt survival. The development of a hydrocephalic goat model for this purpose may be used in future research.

ACKNOWLEDGEMENTS

We express our gratitude to professor Paul Simoens for his enthusiastic support during this study and preparation of the manuscript.

5.7 Roller pump test to evaluate CSF influence on blood coagulation

In our 2011 prospective clinical study, too frequently (in 10 of 14 patients or in 71 %) rapid thrombotic blockage of the dural venous sinus catheter end was encountered, which led to prototyping and in-vitro and animal in-vivo test of new dural venous access devices (DVSAD). But, also in the second DVSAD study of the caprine in-vivo animal study all (100 %) the DVSAD_3 and standard silicone ventriculo-sinus shunts were blocked within 10 days after their implantation. Nevertheless the efforts taken to optimize material selection, design, positioning / orientation and minimal invasive operation techniques, the chances of blockage by thrombus formation did not diminish, on the contrary.

We became aware that one essential question had not been addressed: 'Which is the influence of CSF on blood coagulation when mixed?' Does CSF decrease or enhance blood coagulability? We feared the latter, in the light of the above mentioned experiences. Although some authors mention that the presence of fibrinogen and tissue factor in CSF might activate the clotting cascade, literature review did not provide solid answer to this question. Therefore a study in which CSF and blood are confronted was indicated. The rationale, materials & methods and results have been discussed in detail in manuscript 7.

5.7.1 MANUSCRIPT 7

THE INFLUENCE OF CEREBROSPINAL FLUID ON BLOOD COAGULATION AND THE IMPLICATIONS FOR VENTRICULO-VENOUS SHUNTING

J. Vandersteene[1], E. Baert[1], G. Planckaert[2], T. Van Den Berghe[2], D. Van Roost[1], F. Dewaele[1], M. Henrotte[2] and F. De Somer[3]

[J. Neurosurgery, accepted for publication, January 2018]

[1] Department of Neurosurgery, Ghent University Hospital, Belgium
[2] Faculty of Medicine and Health Sciences, Ghent University, Belgium
[3] Department of Cardiac Surgery, Ghent University Hospital, Belgium

---

ABSTRACT

Object: The effect of CSF on blood coagulation is unknown. Enhanced coagulation by CSF may be an issue in thrombotic complications of ventriculo-atrial and ventriculo-sinus shunts. This study aims to assess the effect of CSF on coagulation and its potential effect on thrombotic events affecting ventriculo-venous shunts.

Methods: Two complementary experiments are performed. In a first static experiment, the effect on coagulation of different CSF mixtures is evaluated, using a viscoelastic coagulation monitor. A second dynamic experiment confirms the amount of clot formation on the shunt surface in a modified Chandler loop.

Results*:* CSF concentrations of 9% and higher significantly decrease the activated clotting time (ACT) (164.9 s at 0% CSF; 155.6 s at 9% CSF; 145.1 s at 32% CSF). Increased clot rates (CR) are observed starting at a concentration of 5% (29.3 at 0% CSF, 31.6 at 5% CSF; 35.3 at 32% CSF). The modified Chandler loop shows a significantly higher percentage of shunt surface covered with deposits when the shunts are infused with CSF instead of Ringer's lactate solution (90% versus 63%). The amount of clot formation at the side facing the blood flow or 'impact side', tends to be lower than at the side facing away from the blood flow or 'wake side' (71% versus 86%).

Conclusion*:* Addition of CSF to blood accelerates coagulation. The interaction CSF-blood-foreign material promotes clot formation which may result in thrombotic shunt complications. Further development of the ventriculo-venous shunt technique should focus on preventing CSF-blood-foreign material interaction and stagnation of CSF in wake-zones.

INTRODUCTION

The effect of CSF on blood coagulation is not well established. Some authors suggest that CSF may enhance hemostasis as it contains proteins such as fibrinogen and tissue factor that may activate the clotting cascade[201-203]. This prothrombotic status is an advantage in case of brain injury or subarachnoid hemorrhage but could be potentially harmful when CSF is shunted to the venous system as happens for the treatment of hydrocephalus[107].

Ventriculo-atrial shunts have a similar effectiveness and complication rate as ventriculo-peritoneal shunts[124,204-206]. However, thromboembolic complications are one of the reasons that most neurosurgeons reserve the former technique to patients in whom ventriculo-peritoneal shunts are contra-indicated or not successful[107].

Ventriculo-sinus shunts have several advantages over the classical ventriculo-peritoneal or ventriculo-atrial shunts. First, overdrainage is prevented by maintaining the natural, self-regulating anti-siphon effect of the IJV[111]. Second, the shunt system is shorter in length, less complex and confined to the skull, which minimizes the risk of mechanical failure and infection[4]. While some authors describe excellent long term results, others report that obstruction due to clot formation in and around the distal shunt tip remains an issue[11,207].

The impact of the CSF-blood-shunt interaction in this kind of thrombotic complications is still under debate. CSF, due to its composition, may enhance clot formation[201-203]. To attenuate clot formation some authors recommend to implant the ventriculo-sinus shunts with the tip opening directed against the blood flow ('retrograde') in order to deviate the CSF flow around the distal shunt tip. The resulting 'constantly renewing CSF sleeve' is believed to be protective against clot formation[11].

The present study assesses the impact of CSF on blood coagulation and the impact of CSF-blood-foreign material interaction on thrombotic shunt complications.

MATERIALS AND METHODS

Two complementary experiments are performed: a static experiment to evaluate the impact of CSF on the coagulability of blood and a dynamic experiment to assess the impact of CSF on clot formation on an intravascular shunt.

Static experiment

The study protocol is approved by the independent ethics committee of the Ghent University Hospital (registration number EC/2016/0560). Participation in the study is proposed to every patient – not threated with anticoagulants or antiplatelet drugs – undergoing a lumbar puncture (LP) or ventriculo-external drainage. CSF and citrated venous blood (0.109 mol trisodium citrate/L, Terumo, Heverlee, Belgium) are collected

from each patient. As the puncture itself may contaminate the first sample of each patient, these first samples are never used for the study. Immediately after the collection of at least a second sample from any selected patient, CSF is added to blood from the same patient in increasing concentrations (Table 30).

Table 30. Preparation of the 5 different blood-CSF mixtures

Mixture no.	1	2	3	4	5
Blood (µL)	900	900	900	900	900
Buffered Trisodium citrate 0.109 mole/L (µL)	100	100	100	100	100
Calcium solution (µL)	40	40	40	40	40
CSF (µL)	0	10	50	100	500
V% CSF (= V_{CSF}/V_{Total} x 100%)	0	0.952	4.587	8.772	32.468
V CSF / V blood (%)	0	1.111	5.556	11.111	55.555

The different blood-CSF mixtures are recalcified (40 µL of 0.25 mol/L CaCl2 solution) and analyzed by a Sonoclot® Coagulation Analyzer (Sienco®, Arvada, CO, USA). The Sonoclot® signature reflects the viscoelastic changes during the transition from liquid whole blood to a solid blood clot (Figure 104). It consists of the activated clotting time (ACT), the clot rate (CR) and the platelet function (PF).

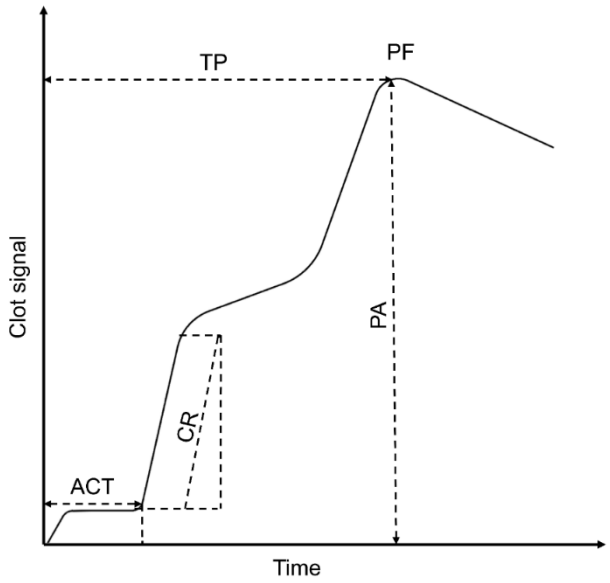

Figure 104. Sonoclot signature

The activated clotting time (ACT) is how long the sample completely stays in the liquid phase and corresponds to the time necessary for fibrinogen to be conversed to fibrin monomers. The clot rate (CR) is the slope of the second peak/plateau of the curve which corresponds to the polymerization of fibrin monomers: the faster the fibrin polymerization, the steeper the slope. The platelet function (PF) is determined by the time to the peak (TP), to which it corresponds inversely proportionally, and by the peak amplitude (PA) of the curve, to which it corresponds proportionally. It represents the attachment of platelets to fibrin and the retraction of the clot.

Dynamic in vitro experiment

The experimental setup, that is described in detail elsewhere[208], is shown in Figure 105.

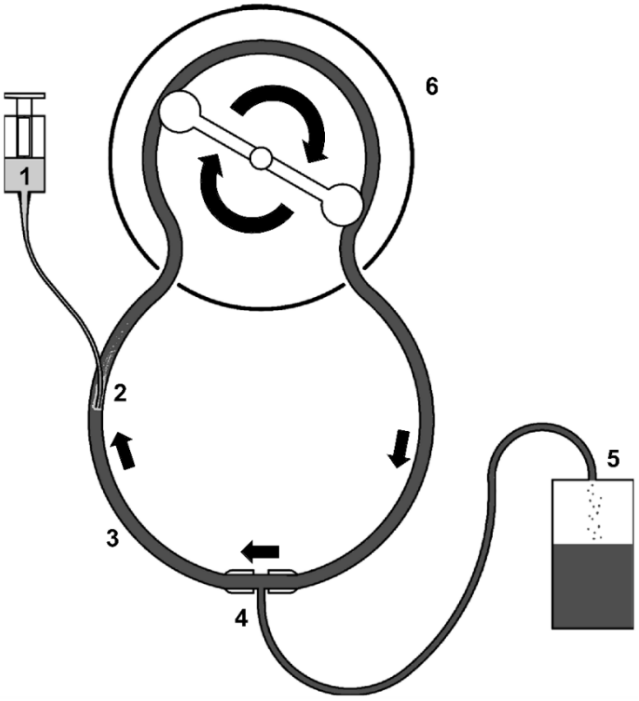

Figure 105. Setup of the dynamic experiment.

A silicone tube filled with blood simulates a blood vessel. Circulation of blood is achieved by a roller-pump. The tubing is partly submerged in a warm water bath to maintain a blood temperature of 37 °C. A catheter ('shunt') is inserted through the wall of the tubing and connected to a syringe pump. This pump simulates the hydrocephalic lateral ventricle and ensures infusion of CSF or RL. To compensate for the infused volume, an overflow tank is connected. 1 syringe and syringe pump, 2 shunt catheter, 3 silicone tubing filled with blood, 4 T-shaped connector, 5 dripping chamber, 6 roller-pump.

A roller-pump, set in a non-occlusive modus, circulates heparinized whole blood (collected from two healthy donors) through a phosphoryl choline-coated silicon tubing (LivaNova, Mirandola, Italy) that is partly submerged in warm (37°C) water. A syringe pump infuses a Ringer's lactate (RL) solution or CSF (collected from a patient with a ventriculo-external drainage) through a Tecothane (Lubrizol, Ohio, USA) catheter ('shunt') that is inserted through the wall of the tubing. The control shunts (no infusion) are purged with RL and subsequently closed at the extravascular end to prevent blood

from entering the lumen of the shunt. The infused volume is compensated by an overflow tank. The blood flow goes against the direction of the shunt insertion, the shunts are thus oriented 'retrograde' (Figure 106).

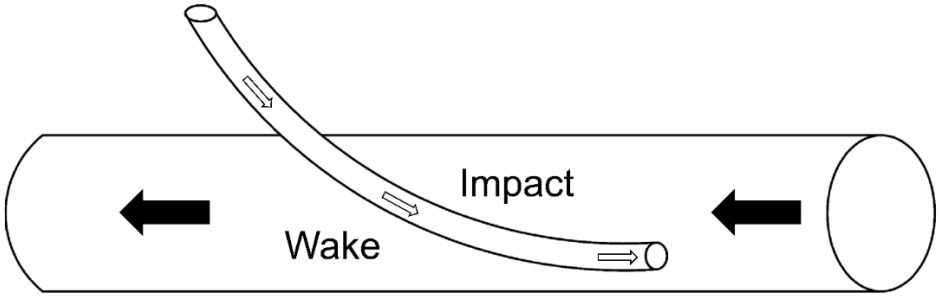

Figure 106. Shunt insertion in tubing and definition of impact and wake side.
The tip of the shunt is directed against the blood flow or 'retrograde'. The solid black arrows represent the direction of the blood flow in the tubing, whereas the white arrows represent the direction of the infusion of CSF or RL. The impact and wake sides of the shunt are defined relatively to the direction of the blood flow.

Each Chandler loop runs for 60 minutes. A total of 13 loops are performed (5 with CSF infusion, 5 with RL solution infusion, 3 without infusion).

The coagulability of the pure blood at the beginning of the experiment is compared to that of the infusion fluid - blood mixture at the end of the experiment by a Sonoclot® Coagulation Analyzer.

At the end of the experiment, the shunts are removed together with the surrounding tubing wall and prepared for scanning electron microscopic (SEM) evaluation. The samples are mounted in a horizontal position and analyzed with an 18-fold magnification. Two sides of the shunt are visualized: the impact side, defined as the flank facing the blood flow and the wake-side, defined as the 180 degrees opposite flank (away from the incoming blood flow).

SEM images are 2D projections of 3D cylindrical objects. As can be seen in figure 4, debris more distant from the image center present a smaller projection surface than debris closer to the midline section, although in reality both can have the same surface area.

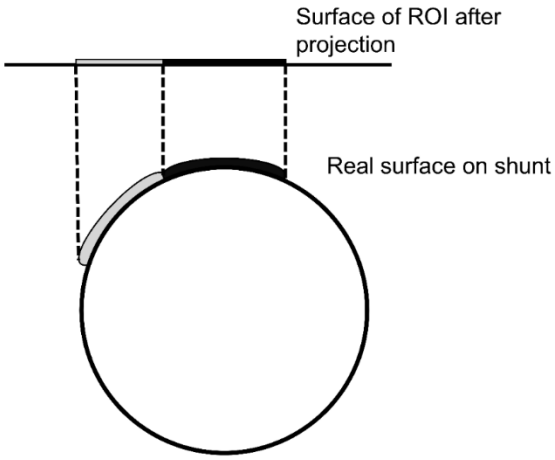

Figure 107. Bias due to 2D projection of a cylindrical object.

Two depositions that cover an equal true surface of the shunt are shown (black and light grey surface). On the projected scanning electron microscopic image, the outlined surface resembles only half as big as the solid surface due to 2D projection of the cylindrically shaped surface.

To correct for this bias, a specific script, written in MATLAB Simulink version 8.6 is executed. This script applies, to the projected surface areas, the appropriate mathematical formulas to simulate to 'unroll' the cylinder instead of 'project' it onto a two-dimensional plane.

At each side, the surface covered with clots is delineated (ImageJ for Windows, Version 150, available for download at https://imagej.nih.gov/ij/index.html) and expressed as a percentage of the visualized surface at the same side ($Ratio_{impact} = A_{clot\ impact}/A_{impact}$ x 100%; $Ratio_{wake} = A_{clot\ wake}/A_{wake}$ x 100%). Next, the total surface of the clots (impact side + wake side) is expressed as a percentage of the visualized total surface ($Ratio_{total} = (A_{clot\ impact} + A_{clot\ wake})/(A_{impact} + A_{wake})$ x100%)

Statistical analysis

Statistical analyses are performed in IBM® SPSS® Statistics 22.0 for Windows.

In the static experiment, a parametric paired two-sample t-test is used - after objectifying normality - to compare each of the Sonoclot parameters (ACT, CR and PF) of pure blood (0% CSF) with those of the different blood-CSF mixtures (1%, 5%, 9% and 32% CSF).

In the dynamic experiment, the Sonoclot parameters of the donor blood before the start of the experiment are compared to those of the blood-infusion fluid mixture after the experiment by a non-parametric Mann-Whitney U test. The amount of visualized shunt surface covered with clots is compared between the different infusion fluids (CSF, RL or no infusion fluid) by a non-parametric Mann-Whitney U test. A one-sample t-test is used – after objectifying normality – to evaluate if there is a difference between clot formation on the impact and the wake sides of the shunt ($Ratio_{impact}$ - $Ratio_{wake}$).

Statistical significance is set at 5%.

RESULTS

Static study

The characteristics of the study population are shown in table below.

Table 31. Study population characteristics

AD, Alzheimer's disease; APTT, activated partial thromboplastin time; CSF, cerebrospinal fluid; CVA, cerebrovascular accident; ELD, external lumbar drainage; FTD, frontotemporal dementia; INR, international normalized ratio; LP, lumbar puncture; MS, multiple sclerosis; N/A, information not available; NOSD, neuromyelitis optica spectrum disorder; PTT, prothrombin time; SAH, subarachnoid hemorrhage; VD, ventriculo-external drainage

Patient number	Age (years)	CSF sampling	Symptoms or suspected diagnosis	Blood platelets (10^3/μL)	Total protein (mg/L)	INR, APTT, PTT results
1	59	LP	FTD	201	38.6	Normal
2	59	LP	Cerebral palsy	201	50.0	Normal
3	43	LP	White matter lesions	227	25.2	Normal
4	29	ELD	CSF rhinorrhea	N/A	71.5	N/A
5	68	LP	NOSD	307	151.9	N/A
6	47	LP	Cognitive dysfunction	637	40.5	N/A
7	48	LP	Vasculitis	253	115.2	Normal
8	50	LP	CVA	183	58.1	Normal
9	61	VED	SAH	394	N/A	Normal
10	70	VED	SAH	413	N/A	Normal
11	68	LP	Neurosyphilis	178	41.4	Normal
12	70	LP	AD	105	N/A	Normal
13	39	LP	Narcolepsy	235	18.6	Normal
14	58	LP	AD	180	N/A	Normal
15	19	LP	MS	260	17.5	Normal

The results of the Sonoclot® coagulation analysis of the different blood-CSF mixtures are shown in Table 32.

Table 32. Results of the patient study and comparison of ACT/CR/PF values for different CSF concentrations in the blood-CSF mixtures.

*[ACT, activated clotting time; CR, clot rate; CSF, cerebrospinal fluid; PF, platelet function. *P < 0.05]*

	% of CSF				
Parameter	0.0	1.0	5.0	9.0	32.0
ACT (mean)	164.9	160.4	158.9	155.6*	145.1*
CR (mean)	29.3	30.9	31.6*	31.3*	35.3*
PF (mean)	3.7	3.8	3.3	3.5	4.1

CSF concentrations of 9% and higher significantly decrease the ACT and CSF concentrations of 5% and higher significantly increase the CR. No significant effect on the PF is found.

Dynamic in vitro experiment (modified Chandler loop)

Hemodilution

The concentration of the infusion fluid increases during the experiment and depends on the infusion rate trough the shunt and the evacuation of the infusion fluid-blood mixture by the overflow tank. The calculated concentration of the infusion fluid at the end of the experiment equals 5.88%, as each loop runs for 60 minutes, the total blood volume is 32 ml and the infusion rate is set at 2 mL/h[208].

Sonoclot® coagulation analyzer.

The differences of the Sonoclot® parameters after and before the experiment, grouped by infusion fluid, are shown in Table 33.

Table 33. Comparison of the difference of ACT/CR/PF values before and after the experiments for CSF, RL and CTRL, grouped by infusion fluid.

*[ACT, activated clotting time; CR, clot rate; CSF, cerebrospinal fluid; CTRL, control (no infusion fluid); med., median; PF, platelet function; RL, Ringer's lactate solution. *P < 0.05]*

	Infusion fluid		
Parameter	CSF	RL	CTRL
$ACT_{difference}$ (med.)	0.0	44.0	41.0
$CR_{difference}$ (med.)	6.3	4.2*	3.5
$PF_{difference}$ (med.)	2.3	1.4	1.0

The ACT is higher after the experiment in the RL and CTRL group. In the CSF group there is no difference (before - after) for the ACT. Both the CR and the PF increase during the experiment and this increase is more pronounced in the CSF group.

Differences in clot formation in function of infusion fluid. RL-infused shunts show less clots and CSF-infused shunts show more clots than control shunts. Table 34 shows the medians of the three ratios.

Table 34. Impact of the infusion fluid on the amount of clot formation on the different shunt surfaces

Impact of the infusion fluid on the amount of clot formation on the different shunt surfaces ($Ratio_{impact}$, $Ratio_{wake}$ or $Ratio_{total}$). The amount of clot formation tends to decrease when shunts are perfused with RL but tends to increase when shunts are perfused with CSF. Clot formation on CSF-perfused shunts is significantly higher than on RL-perfused shunts (marked with an asterisk). Statistical significance was also reached when the $Ratio_{wake}$ of CTRL shunts was

compared to that of CSF-perfused shunts (marked with a double asterisk). [CSF, cerebrospinal fluid perfused shunts; CTRL, control (no infusion fluid); med., median; RL, Ringer's lactate perfused shunts; $Ratio_{impact}$, total surface of clots on the impact side divided by the total visualized surface of the impact side of the shunt; $Ratio_{wake}$, total surface of clots on the wake side divided by the total visualized surface of the wake side of the shunt; $Ratio_{total}$, total surface of clots on the impact + wake side divided by the total visualized surface of the impact + wake side of the shunt]

	Infusion fluid		
Parameter	RL	CTR	CSF
$Ratio_{impact}$ (med.)	0.59	0.62	0.89*
$Ratio_{wake}$ (med.)	0.71	0.75	0.93**
$Ratio_{total}$ (med.)	0.68	0.73	0.90*

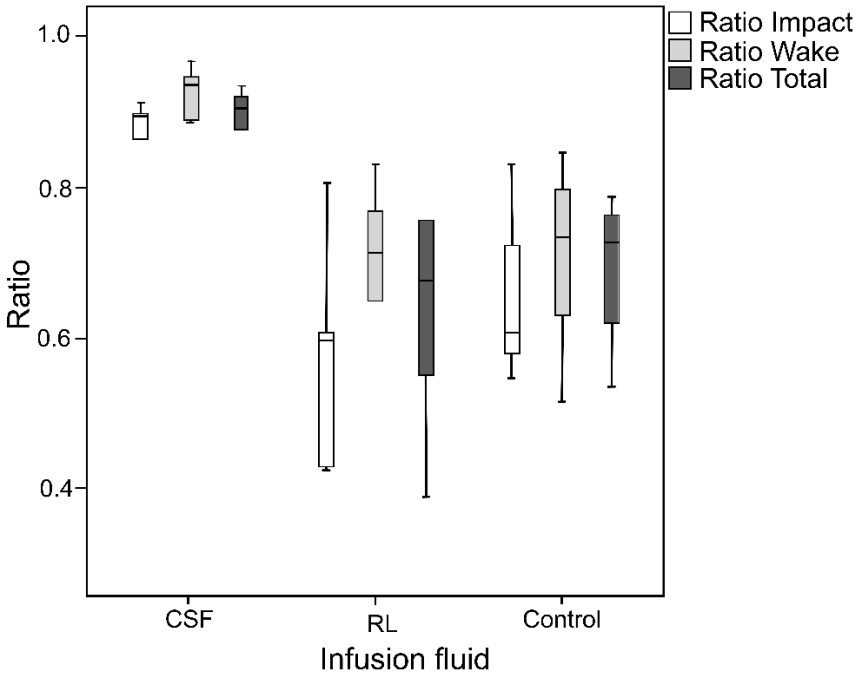

Figure 108. Boxplot of different ratios separated for infusion fluid.

For each infusion fluid the different ratios are displayed as a boxplot. A circle represents an outlier. $Ratio_{impact}$, total surface of clots on the impact side divided by the total visualized surface of the impact side of the shunt; $Ratio_{wake}$, total surface of clots on the wake side divided by the total visualized surface of the wake side of the shunt; $Ratio_{total}$, total surface of clots on the impact + wake side divided by the total visualized surface of the impact + wake side of the shunt); CSF, cerebrospinal fluid; RL, Ringer's lactate solution; CTRL, control group (no infusion fluid).

$Ratio_{impact}$, $Ratio_{wake}$ and $Ratio_{total}$ are significantly higher for CSF shunts in comparison with RL shunts. $Ratio_{wake}$ is significantly higher for CSF shunts in comparison to control shunts.

Orientation. Considering CSF and RL shunts to be one group, $Ratio_{impact}$ (med. = 0.71) tends to be lower than $Ratio_{wake}$ (med. = 0.86). The difference is statistically not significant (borderline: P = 0.067).

DISCUSSION

The effect of CSF on blood coagulation may be an issue in thrombotic complications of ventriculo-atrial and ventriculo-sinus shunts[107].

Ventriculo-atrial shunts have a similar effectiveness and complication rate as ventriculo-peritoneal shunts[15,204-206]. However, thromboembolic complications are one of the reasons that most neurosurgeons reserve the former technique for patients in whom ventriculo-peritoneal shunts are contraindicated or not successful[107]. The ventriculo-sinus shunt is a promising new treatment for hydrocephalus. However, obstruction due to clot formation in and around the distal shunt tip remains an issue[11,207].

To assess the effect of CSF on blood coagulation and the role of the CSF-blood-shunt interaction in distal shunt obstruction, two complementary experiments are performed.

The first experiment evaluates the effect of CSF on the thrombo-elastogram by analyzing different blood-CSF mixtures. The second, a modified Chandler loop, assesses the amount of clot formation on the shunt surface in more realistic conditions.

Influence of CSF on hemostasis

The first experiment shows that adding CSF to blood makes blood hypercoagulable. This is demonstrated by accelerated conversion from fibrinogen to fibrin after CSF addition and gradual shortening of the ACT. These effects become statistically significant at CSF concentrations of at least 5-9%. Interestingly the same critical concentration is found in the modified Chandler loop. The increase in CR and the higher platelet activation are most likely due to thrombin formation on the surface of the activated platelets[155] and is only found in the group where CSF was infused.

It is unclear which factors contribute to the influence of CSF on hemostasis. CSF contains coagulation proteins and tissue factor, a potent activator of the extrinsic coagulation pathway[209]. In healthy individuals, there is an imbalance between the CSF concentration of tissue factor and that of tissue factor pathway inhibitor, making CSF procoagulant. Apart from these clotting factors, immunoglobulins and other immunological factors like C3 can cause neuro-inflammation leading to a procoagulant state[201]. In pathological conditions, the concentration of coagulation proteins and the imbalance between tissue factor and tissue factor pathway inhibitor even increase, resulting in a more pronounced procoagulant effect of CSF[210]. Apparently, further research is necessary to elucidate this mechanism.

Based on our results we can endorse the finding of clinical series that under normal circumstances shunting CSF to the dural venous sinuses or superior vena cava will not lead to sinus or caval thrombosis[134,211]. Concentrations of CSF in the superior sagittal sinus and superior caval vein are below 5%, as CSF inflow is approximately 0.35 mL/min for a blood flow of more than 200 mL/min[11,15,143]. However, in specific

circumstances the coagulation enhancing effect of CSF can be problematic. Typical situations are contact between CSF and foreign material, accumulation of CSF in 'wake' zones and formation of a CSF-blood mixture in the distal shunt tip at higher than physiologically harmless concentrations.

Foreign material

Some authors implant the ventriculo-sinus shunt against the direction of the blood flow. CSF drained by a shunt in this position will flow along the shunt's surface resulting in a 'constantly renewing CSF sleeve' (Figure 109). This CSF sleeve is believed to protect against clot formation by preventing adherence of proteins and platelets to the foreign material's surface[11,120].

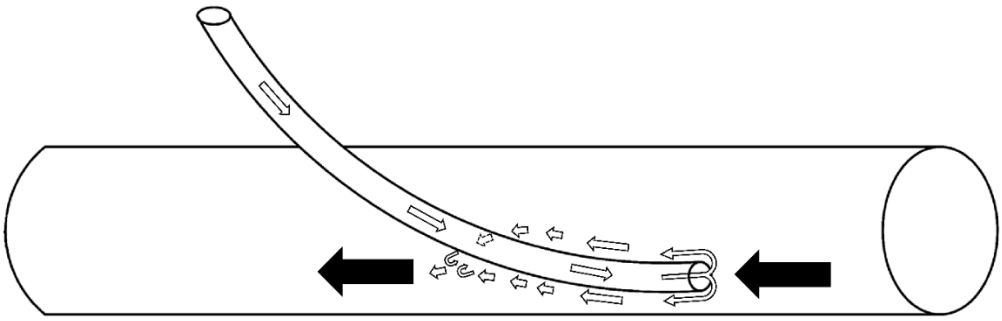

Figure 109. CSF sleeve effect

The white arrows represent the CSF 'sleeve'. This sleeve is formed by CSF draining along the shunt surface due to the blood flow that is oriented in the opposite direction. The solid black arrows represent the direction of the blood flow in the blood vessel.

The protective effect of a constantly renewing 'fluid sleeve' is confirmed by the reduced clot formation on RL-infused shunts compared to controls. However increased clot formation was observed on CSF-infused shunts. So, a CSF fluid sleeve is – contradictory to the protective effect of a fluid sleeve in general – harmful. The CSF

sleeve may promote adherence of thrombogenic proteins such as fibrinogen, fibronectin and globulins. Once adhered, these will attach platelets through the GPIIb/IIIa platelet receptor which mediates the further coagulation process[155,156].

Wake zones

A wake zone, characterized by a slow and non-laminar flow, develops directly distally to an object placed in the bloodstream (Figure 110)[120].

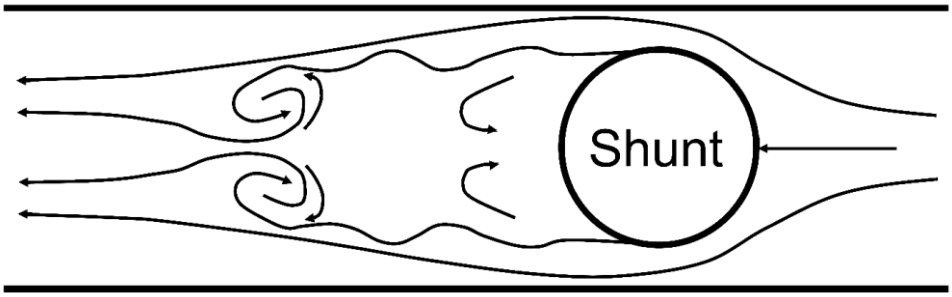

Figure 110. Hydrodynamic principles of flow past a cylindrical object.

When a cylindrical object is placed in the blood flow, blood will wrap around the object. When it reaches the broadest point of the object, blood will detach from the surface. At this point it will be dragged towards the wake side which causes a slow and non-laminar flow.

The current study endorses the hypothesis of previous literature that, due to the characteristic flow conditions, more clot formation occurs on the 'wake side' of a shunt[107,143]. This procoagulant effect may be reinforced when CSF is drained to a wake zone. The local slow and non-laminar flow may result in accumulation of CSF which promotes hemostasis.

Distal shunt tip

When blood regurgitates into the shunt system, it will become stagnant and the risk of intraluminal clot formation will be high[120]. The development of a blood-CSF mixture in the distal shunt system may even increase this risk further.

In the absence of a one-way valve, regurgitation of blood may occur due to a sudden increase of the pressure in the superior sagittal sinus or a decrease of the ICP (Valsalva maneuver or lumbar puncture respectively)[1,119].

Shunt material and design

Several shunt related factors, such as material and design, may have an influence on clot formation.

The shunt material should be bio- and hemocompatible. Silicone and polyurethanes are typical materials with a suitable profile[212]. In this study Tecothane, a non-coated aromatic polyether urethane is used. Although Tecothane is known to have a superior hemocompatibility[213], clot formation was visualized on the surface of all shunts. Different coatings may be used to further reduce the thrombogenicity of biomaterials[214]. Typical examples are phosphoryl choline and heparin[214,215]. Phosphoryl choline may counteract the procoagulant effect of CSF by preventing protein adhesion to the foreign material's surface[215,216]. Heparin eluting and non-eluting coatings exist[214]. Heparin eluting coatings have a limited duration of action and are developed to reduce clot formation in the acute setting[214]. There is good quality evidence that a heparin eluting coating - which has mainly been evaluated on central venous catheters in children – has no beneficial effect on catheter patency[217,218]. Heparin non-eluting coatings have theoretically a permanent antithrombotic effect and are known to reduce thrombus formation on vascular grafts and vascular stents[214]. In conclusion, both a phosphoryl choline and a heparin non-eluting coating may be useful to reduce the general

thrombogenicity of venous shunts and may also counteract the procoagulant effect of CSF.

Besides the material, also the shunt design might affect the amount of clot formation. The results of this study indicate that wake zones should be held as small as possible, contact between CSF and shunt material should be minimized and CSF should be prevented from entering the distal shunt tip. Wake zones can be reduced by reducing the volume of the intravascular catheter. Contact between CSF and shunt material can be minimized by not implanting the shunt retrograde. Ideally the distal shunt tip should be oriented perpendicular to the blood flow (neutral position). In this way CSF will not drain along the shunt surface nor will it drain to wake zones. CSF can be prevented from entering the distal shunt tip by using a one-way valve.

Strengths and limitations of the study

To our knowledge this is the first study to address the question as to how the interaction between CSF, blood and foreign material affects clot formation.

Especially the combination of a static and a dynamic experiment is a strong point of this study.

The static experiment is designed to minimize confounding factors. The blood and CSF come from the same donor to exclude possible immunological reactions due to incompatibility. The coagulation tests are not disturbed because there is no need for heparinization.

The dynamic experiment is designed to approximate the in-vivo situation. Special attention is paid to the flow conditions, the position of the shunt in the vessel and the infusion of CSF through the shunts.

However, not all the aspects of the in-vivo situation are modeled. The influence of the endothelium covering the wall of the blood vessel is maybe the most important factor that is not addressed. An intact endothelium counteracts coagulation, but when the endothelium is damaged or irritated, it releases thrombogenic factors[107,141]. Endothelial damage is unavoidable when the shunt is implanted. Irritation may occur at the insertion site of the shunt and at the shunt tip when positioned against the vessel wall.

Although the duration of the dynamic experiment is limited by the progressive dilution and degradation of blood products, clot formation is visualized on all shunts. This early-stage reaction consists of the adherence of proteins and platelets and is known to mediate the further coagulation process[155].

Over-dilution is avoided by maintaining the concentration of the infusion fluid beneath 6%, which is well below the concentration of 11% that is known to have an influence on hemostasis[161].

CONCLUSIONS

Adding CSF to blood enhances coagulability starting from a concentration of 5-9%. When CSF is shunted to the venous system, concentrations are generally below this critical threshold. However, in some specific situations CSF may concentrate, resulting in accelerated clot formation and shunt obstruction.

To prevent clot formation around the shunt tip (external shunt obstruction), contact of CSF with the outer shunt surface and accumulation of CSF in wake-zones should be avoided.

To prevent luminal clot formation (internal shunt obstruction), blood should be prevented from entering the shunt tip using an appropriate one-way valve.

DISCLOSURES

This research was not funded by any external company or industry. All costs were covered by the Departments of Neurosurgery and Cardiac Surgery of the Ghent University Hospital, Ghent, Belgium.

The authors report no conflict of interest concerning the materials or methods used in this study or the findings specified in this paper.

ACKNOWLEDGMENTS

Non

CHAPTER 6. DISCUSSION & FUTURE OF VSS PROJECT

6.1 The study path

This ventriculo-sinus shunt study took off in 2006, with the **experimental and numerical modeling of the hydrodynamic principles of cerebrospinal fluid and dural venous blood circulation**[2] . The modeling investigated their differential pressure balance and the effect on it when a cerebrospinal fluid shunt for the treatment of hydrocephalus is in place. The modeling validated the 'impact effect' when a retrograde ventriculo-sinus shunt is in place, as advocated by El Shafei[219]. As the differential pressure balance between the cerebrospinal fluid and dural venous blood proved delicate and the impact effect of the retrograde ventriculo-sinus shunt marginal, the modeling study advised to include a low resistance one-way valve and to introduce the dural venous sinus access device in the distal half of the superior sagittal sinus when treating hydrocephalus with a retrograde ventriculo-sinus shunt.

A **non-randomized monocentric prospective clinical trial**[3] was accomplished in 2011. In this trial, the retrograde ventriculo-sinus shunt was implanted in patients struck by communicating hydrocephalus. The trial proved appropriate cerebrospinal fluid drainage, also the technical feasibility and surgical safety. However, the rapid and frequent obstruction of the shunt's dural venous sinus catheter forced us to end the clinical trial after the inclusion of 10 patients. Only 2 of the 10 study-group-patients and 2 of the 4 rescue-group-patients enjoy a long-term shunt survival, 28,5 % of the patients.

A large intravascular volume or blood-material interface, a decentralized position of the dural venous sinus catheter end and damage-irritation of the vessel's endothelium were considered as potential causes of the rapid obstruction caused by either thrombosis or endothelial covering. Therefore, the concept of a new dural sinus access device was thought of. The Ghent University IOF (Industrieel Onderzoeksfonds) granted a StarrTT

project in 2012, to design and manufacture dural venous sinus access devices in different shapes and materials and to have them tested in a dynamic and non-occlusive roller-pump in-vitro setting[4]. In this test, the prototypes were introduced in a loop filled with fresh human blood while, through them, human cerebrospinal fluid was infused into the blood stream. Microscopic evaluation of the thrombotic deposits on the prototypes, showed a clear benefit for the use of silicone. Literature review[156,220-222] indicated similar results concerning biocompatibility, hemocompatibility and thrombotic activity for polyurethane compared with silicone. Also, polyurethane allowed us to produce prototypes with high pressure injection molding techniques or with high temperature tip-setting. These production techniques are not applicable to silicone. Silicone devices need to be produced by pouring or dipping techniques, which are much more difficult to control.

Continuation of the ventriculo-sinus shunt project was secured by IOF Advanced StarTT grant in 2013-2014. This funding allowed to continue with dural sinus access device prototype design and production, to implement these prototypes in a caprine in-vivo animal trial and to engage a full-time scientific co-worker.

The caprine animal in-vivo model[6,7] delivered important conclusions. (a) The compliance of the extracranial part of the ventriculo-sinus shunt combined with the dynamic pressure in the superior sagittal pressure, overwhelmed the impact effect of the retrograde orientation of a dural sinus access device. (b) In-vivo, dural sinus access devices with retrograde orientation showed no advantage compared with cross cut dural sinus access devices with perpendicular orientation, on the contrary. (c) Induction of hydrocephalus by Kaolin injection by suboccipital punction was effective in 85,7 % of the injected animals, but the severity of the reactive aseptic meningitis symptoms masked the clinical follow-up of the ventriculo-sinus procedure and of the hydrocephalus itself. Also, the induced hydrocephalus proved temporary. The scientific output of the hydrocephalus induction was not in balance with the animal suffering and therefore discontinued. (d) Dural sinus access devices with direct insertion of a short

intravascular trajectory, create invagination of the endothelial wall, causing rapid obstruction. (e) Dural sinus access devices introduced with a Seldinger-like technique and a barb to retract and stabilize the endothelial layer overcome endothelial invagination. Also their ease and safety of implantation is proven.

In 2016 a small but very interesting sideways experimental non-occlusive-roller-pump study was performed to evaluate the influence of CSF on blood coagulation activity[8] (see manuscript 7). Clinically, we suspected CSF of stimulating blood coagulation, e.g. as a CSF leak is encapsulated by membranes in a period of days. Also, in the non-occlusive-roller-pump study of 2012[4] (see manuscript 3), the Sonoclot® (Figure 111) ACT of the fresh human blood is increased in the CSF infused loops compared to the control and to the Ringer lactate infused loops. In the 2016 non-occlusive-roller-pump study, the influence of CSF on the blood coagulation was tested in 2 experiments, a static and a dynamic (in the roller pump). In the static test, a CSF/blood mixture with increasing CSF concentration was made, proving that adding CSF to blood makes blood hypercoagulable, due to accelerated conversion from fibrinogen to fibrin after CSF addition and consequently a gradual shortening of the ACT on the Sonoclot® analysis. These effects become statistically significant at CSF concentrations of 5-9%. Interestingly the same critical concentration is found in the dynamic test with the roller pump model. The dynamic test (with a control group, a Ringer lactate infusion group and CSF infusion group through a retrograde silicone catheter as advocated by El Shafei) proved the protective effect of a constantly renewing 'fluid sleeve' by the reduced clot formation on RL-infused catheters compared to controls. However increased clot formation was observed on CSF-infused catheters. So, in contradiction with the protective effect of a fluid sleeve in general, a CSF fluid sleeve proved increasing thrombus formation. The CSF sleeve may promote adherence of thrombogenic proteins such as fibrinogen, fibronectin and globulins.

6.2 Conflict with El Shafei and Børgesen results

As noted above, in the UZ Gent series of ventriculo-sinus shunt patients[3], only 28,5 % of long-term shunt survival was experienced. The reports of El Shafei[118] and Børgesen[14,15] mention up to threefold higher shunt survival rates, respectively 89 % and 77,8 % (Table 35).

At first sight, this huge shunt survival difference is not well explainable. However, many remarks can be made:

- El Shafei's population is much younger (60 % of patients with open fontanel and cranial sutures; mean age of total patient group of 5,4 y). It is well known that the development of ararchnoid villi and granulations lasts until the age of 18 months. However, the results in both the open and closed cranium groups are in the same range (84,8 % and 95,5 % success rates). This indicates that the high incidence of open cranium patients does not distort the results.
- El Shafei performed experimental work, of high quality and reported in detail, but it was limited to hydrodynamic modeling. No in-vitro experiments with blood/CSF and no animal in-vivo experiments were published.

Table 35. Comparison of published ventriculo-sinus shunt trials

[FU: follow-up; EU: European Union; NS: not specified; CONG: congenital; MMC: myelomeningocele; BM: bacterial meningitis; NPH: normal pressure HC; ASAH: acute subarachnoid hemorrhage; TR: tumor related; HC: hydrocephalus; EC: encephalocele; TBI: traumatic brain injury; VLP: very low pressure; SSS: superior sagittal sinus; TS: transverse sinus; m.: mean; obstr.: obstruction; SI: shunt infection; WI: wound infection; AE: air embolism; ICP: intracranial pressure; PSSS: superior sagittal sinus pressure; LP: lumbar puncture; CFD: computerized fluids dynamics; US: ultrasound; R_{out} and C_{out}: resistance and conductance to CSF outflow; T FU: technical follow-up; exp.: experiment; cath.: catheter]

	Sharkey 1965	*Hash 1979*	*Wen 1983*	*Børgesen 2004*	*El Shafei 2005*	*Baert 2018*
Number of patients	4 retrospect.	36 22 in FU retrospect.	52 17 in FU retrospect.	45 EU multicenter prospective	110 retrospect.	14 single-center prospective
Age	4w - 7m	10y - 80y	3m - 14y	NS	6w - 54 y	6d - 86y
Etiology of HC	1 CONG 1 MMC 2 BM	MIXED	MIXED	19 NPH 11 ASAH 7 TR 5 BM 3 HC (NS)	MIXED not MMC/EC	4 TR 3 ASAH 2 MMC 2 TBI 1 NPH 1 BM
Valve	slit	VLP	slit	SinuShunt	99 (90%) valveless 11 (10%) VLP	VLP
Orientation	antegrade	antegrade	antegrade	antegrade	retrograde	retrograde
Venous Sinus	SSS	SSS	SSS	TS	SSS	SSS
FU Period	7w - 3m m. 78d	m. 213d	1y - 6y m. 1788d	2d - 430d m. 223d	3m - 11y m. 1248d	4d - 12y m. 669d
Shunt Obstr.	1 (25%)	2 (9%)	9 (37,5%)	6 (13,3%)	10 (9%)	10 (71,4%)
Complication	1 (25%) death	2 (9%) SI	11 (21,1%) death 2 (3,8%) SI	3 (6,7%) SI 1 (2,2%) IVH	3 (2,7%) SI 8 (7,3%) WI 1 (0,9%) death	1 (7,1%) AE warning
T FU Postop.	NS	NS perop. ICP/P_{SSS} monitoring 5 (13,9%)	NS	CT / MR Evans' ratio	US-doppler Pourcelot index 10 (9%) CT-scan MR 20 (18%) MR-angio 10 (9%)	MR CT MR/CT-angio Angiography postop. ICP monitoring 1 (7,1%)
In-vitro Exp.	-	-	-	LP infusion (R_{out} / C_{out})	hydrodynamic	hydrodynamic + CFD dynamic blood/CSF
Animal Exp.	-	-	-	5 dogs 2mm silicone cath. in SSS during 21d	-	21 goats HC induction VSS implantation

- In his report, El Shafei doesn't note how many patients had pre- and postoperative CT / MR-scan or ultrasound-doppler examination. The accessibility of a neurosurgical center is less evident in Egypt than in Western Europe. As a result,

the indication and follow-up can be performed less profoundly. Only in 10 of sixty-six patients with open cranium, the ultrasound-doppler Pourcelot's index[223-225] (Table 36) was recorded in postoperative follow-up; in 20 of 110 patients a postoperative MR-scan, in 10 a postoperative MR-angiography. The frequency of postoperative neurosurgical outpatient consultation is not mentioned.

Table 36. Pourcelot's resistive index

[PSV: peak systolic velocity; EDV: end-diastolic velocity of cerebral arterial flow] An index above 0,8 in children with open cranium and above 0,65 in children with closed cranium suggests an elevated ICP.

Equation of Pourcelot's resistive index: PSV - EVD / PSV x 100

- Børgesen includes in his patient group a very large number of normal pressure hydrocephalus patients, namely 19 on 45 or 42,2 %. Diagnosis and follow-up of normal hydrocephalus patients specifically, remains up to now complex and doubtful. It is very difficult to measure their progression postoperatively, as their clinical picture is fluctuating, changes can be very subtle. The communication with the patient itself can also be seriously disrupted and often different care providers take part in the consecutive consultations of the outpatient clinic.
- Before the multicenter prospective study was performed, Børgesen had already included 73 patients in a monocentric setting at Rigshospitalet, Copenhagen. There is no clear report or publication about these results (retrospective or prospective?), except a publication on a pilot group of 18 patients[14].
- The follow-up in the SinuShunt trial is not long-term (from 2 d - 430 d with a mean of 223 d). No further long-term follow-up figures have been published and no ongoing SinuShunt studies can be found.
- To our knowledge, Børgesen published extensive hydrodynamic modeling experiments on CSF absorption and on the concept of the SinuShunt, but no blood/CSF in-vitro modeling was reported and the animal in-vivo study was limited.

In 5 dogs a 2 mm wide silicone catheter was implanted in the superior sagittal sinus for a period of 21 d.

- One could conclude that the surgical procedure was not performed 'lege artis' in the UZ Gent study group. However, all procedures were performed by the investigator himself, frequently assisted by an experienced member of the Neurosurgical senior staff. The researcher has extensive experience in CSF shunt operations, complex shunt problems are referred to him, pediatric and adult. The investigator assisted on a ventriculo-sinus shunt implantation performed by El Shafei Ismail at Cairo, Egypt. The general surgical quality seems OK as none of the patients suffered a complication of infection, shunt malposition, wound healing problems or any other. None of the valves or the ventricular catheters were blocked. Likewise in case of ventriculo-sinus shunt revisions and derivations into ventriculo-peritoneal or ventriculo-atrial shunt, none of the patients suffered a complication. This was also the case in all 21 operated and re-operated goats.
- 100 % of our patients had pre- and postoperative CT-scan and/or MR-scan, besides frequent outpatient clinic follow-up by the investigator (1 week postop - 4 weeks - every 2 months until 1 year, than every 4 months until 2 year and finally every year).
- In all clinical except the Børgesen and UZ Gent series, communicating and obstructive HC patients were mixed. In UZ Gent series, all patients suffered communicating HC.
- Discontinuation of ventriculo-sinus shunt projects may be an indication of a higher obstruction rate than published in different reports.

6.3 Strenghts and weaknesses

6.3.1 weaknesses

In both the clinical and caprine in-vivo trials, the numbers of patients included were small. With regard to the human study, it was ethically unacceptable to continue with

inclusion, as a clear indication of much more frequent obstruction than with standard CSF shunt therapy was already noticed in a group of 10 patients. Considering the caprine study, the IOF budget provided for the inclusion of 12 animals. Thanks to improvisation and economics, we were able to expand the group to 21. Although small in number, also in the caprine trial, the trends were very clear and representative.

CSF enhancing blood coagulation activity poses a threat to ventriculo-sinus shunts. It is essential to minimize CSF concentration and to omit any material-CSF-blood interface, as this only enhances thrombus deposits on the implanted device.

One could criticize the absence of pre- and postoperative ICP measurements in the patients with ventriculo-sinus shunts. We did not find it ethically correct to perform, because it would increase risks of infection and cause extra discomfort for the patient. Nevertheless, continuous ICP monitoring with parenchymal sensor was performed due to circumstances in a patient suffering from long-term and complex siphoning[3] (see manuscript 2). Her clinical evolution and these measurements support the near-physiological or balanced CSF drainage by a ventriculo-sinus shunt.

Continuing the ventriculo-sinus shunt study requires great budget and scientific/industrial efforts. The next level would be the prototyping / production of dural venous access devices appropriate to implant in a human trial. This demands industrial partners able to produce according EC level 3 criteria. New and extensive in-vitro studies with human blood and CSF and animal in-vivo studies will be required for the validation of the new devices and will be requested by the Federal Agency for Health and Medicines (FAGG) and the Ethics Committee before considering approval for clinical prospective studies. Finding the necessary budget to hire a full-time employee, to have prototypes produced according EC level 3, to finance the trials, will not be 'a piece of cake'.

6.3.2 strengths

The ventriculo-sinus shunt study has been gradually and logically built up, guided by literature review, ongoing results and conclusions. The group of investigators and co-workers was multidisciplinary, exceeded the level of 1 person, 1 medical service, 1 faculty. Also, many of the investigators followed the whole trajectory of the study, maintaining an overview.

The combination of clinical, in-vitro and in animal in-vivo studies unveiled several ventriculo-sinus shunt related problems not or merely mentioned in other study reports or literature, e.g. problematic central intravascular positioning of the dural sinus access device, coagulation enhancing effect of CSF, compliance of the extracranial part of the ventriculo-sinus shunt causing blood regurgitation powered by the dynamic intravascular pressure, danger of endothelium invagination during introduction. This increased insight is capable of guiding, fine-tuning further investigations and will increase their relevance.

In the caprine animal study, all dural sinus access devices used (prototypes and silicone catheters) are prone to blockage by thrombotic deposits and this within a period of 10 days. However, important considerations are to note. Most animals, also the caprine, have a significant faster and stronger clotting activity than humans (Figure 111). Thus, extrapolation of the thrombus formation results in goats to humans is premature. On the other hand, despite the augmented thrombus formation activity in goats, none developed a sinus thrombosis due to the ventriculo-sinus shunt insertion. Consequently, as encountered in the series of Sharkey[112], Hash[114], Wen[113], El Shafei[118], Børgesen[14,226] and UZ Gent[3], we consider the chance of this complication in humans as very improbable. Technical feasibility and operative safety can also be extrapolated to humans, because the caprine structures considered (superior sagittal sinus and ventricles) have only a half to a third of human sizes and are therefore more difficult to access and operate.

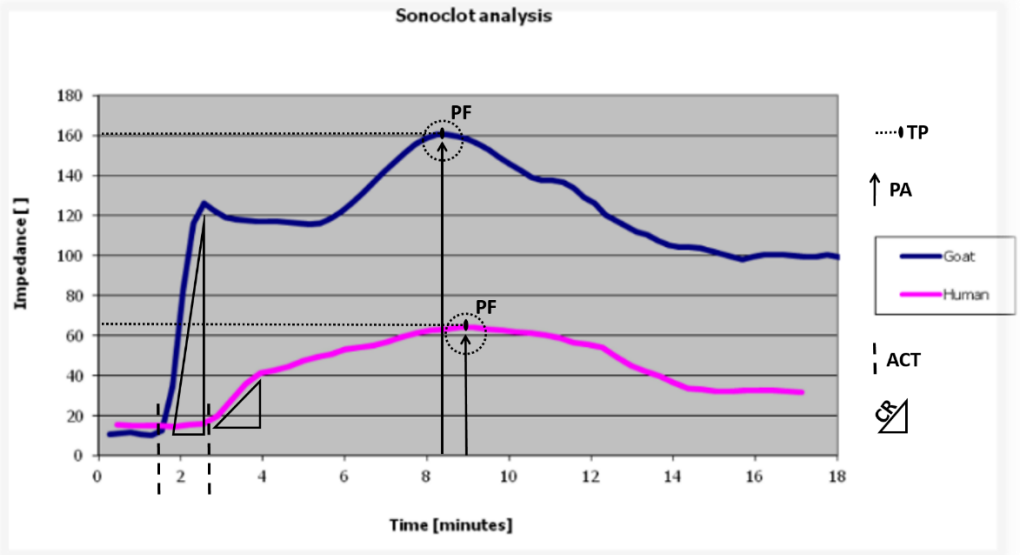

Figure 111. The Sonoclot® results of caprine and human fresh whole blood

[ACT] the activated clotting time measures (in seconds) the duration a fresh blood sample stays in the liquid phase. The ACT corresponds to the time necessary for fibrinogen to be conversed to fibrin monomers. [CR] the clot rate is the slope of the second peak/plateau of the curve which corresponds to the polymerization of fibrin monomers. The faster the fibrin polymerization, the steeper the slope. [PF] the platelet function is determined by [TP] the time to the peak, to which it corresponds inversely proportionally, and by [PA] the peak amplitude of the curve, to which it corresponds proportionally. The PF represents the attachment of platelets to fibrin and the strength of retraction of the clot.

6.4 Project's future

As operative feasibility and safety are proven, further efforts to develop a ventriculo-sinus shunt dural sinus access device remain worthwhile and should continue (Table 37). Proof of its capability of balanced or near-physiological CSF drainage is provided by in-vitro experiments and clinical trials. At present however, ventriculo-sinus shunt survival time is too short to use it as standard hydrocephalus treatment. Further scientific and clinical efforts should concentrate on ease and safety of implantation (although the DVSAD_3 Seldinger-like technique made significant progress), and on the problem of thrombotic reactivity of the infused CSF. The CSF should not come in contact with or form a molecular film around the dural sinus access device blood-contacting surface and the dural sinus access device material should inhibit clotting activation at its material/blood interface, by optimal material selection and/or coating.

Table 37. Steps to take in the continuation of the ventriculo-sinus shunt project

Non-occlusive roller-pump in-vitro study - With fresh human blood and CSF - Testing dural sinus access devices on morphology, material selection and coating
Prototyping the new dural sinus access device for human use taking into account - FAGG regulation (will animal in-vivo trials be requested?) - EC level 3 criteria
EC approval for new prospective clinical trial - Monocentric - Communicating hydrocephalus patients
Funding of project - Continuation of StarrTT trajectory with IOF? - Patents?

The present study also learned that multidisciplinary, inter-faculty co-operation is essential to obtain results. There's no doubt that a future project should be a group project.

The following considerations need to be taken into account in the development of a new dural sinus access device:

- The material should be silicone or medical degree PU and it could benefit of a coating, e.g. phosphoryl choline or heparin, reducing adherence of proteins, tissue or plasma clotting factors or platelets.
- The dural sinus access device should have minimal CSF or blood or CSF/blood contact and create minimal wake zones, factors facilitating thrombus formation which seem to be increased by a retrograde orientation. Advices are:
    - Minimal intravascular volume of the dural sinus access device.
    - Perpendicular orientation of the axis and end of the dural sinus access device (i.e. perpendicular in relation to the blood stream direction), to have the CSF flushed away without contacting its surface and keeping CSF out of reach of the wake zone.
    - Orientation and morphology of its end should reduce blood entering, causing stagnation and high concentration of CSF/blood mixture.
    - Compliance of the extracranial components of the ventriculo-sinus shunt need significant reduction to avoid blood regurgitation powered by the dynamic dural venous blood pressure.
- The use of a one-way valve will remain required.
- New in-vitro experiments, also with fresh human blood and CSF, will remain essential. Considering animal in-vivo study, one could question if these would be representative as is proven that CSF physiology, blood clotting activity and anatomy of animal models differ significantly from human.

CHAPTER 7. SYNTHESIS / SAMENVATTING

Since the 1950's, the standard treatment of communicating HC relies on the CSF shunt, deriving the CSF towards the peritoneal (ventriculo-peritoneal and lumbo-peritoneal shunt) or the right cardiac atrial (ventriculo-atrial shunt) cavity. Although saving many thousands a year worldwide, these shunts have the tendency of non-physiological CSF drainage. Once the patient's in an upright position, their vertically orientated fluid exerts a siphoning effect, creating intracranial hypotension. Although complex and sophisticated shunt valve systems are developed to compensate for this siphoning effect, these can never obtain the delicate regulating effect of the short-circuited anti-siphoning effect of the internal jugular veins provided by nature. Only a ventriculo-sinus shunt (VSS), a shunt deriving the CSF proximal of the internal jugular veins could obtain a physiological drainage. Several attempts to create a long-lasting VSS have been made worldwide since the beginning of the 20th century, but the Achilles heel of the VSS remains the frequent obstruction of its distal catheter in the dural venous sinus, due to thrombus formation.

This Ph. D. started in 2006 with experimental in vitro and numerical modeling of the retrograde ventriculo-sinus shunt as advocated by El Shafei. Retrograde orientation, i.e. the sinus catheter opening orientated against the direction of the blood flow, has hydrodynamic advantages of creating an impact effect developing a constant differential pressure (the intracranial pressure remaining higher than the venous pressure), and creating a potential antithrombotic continuous flow and film of CSF in the tip and on the surface of the sinus catheter. The experimental model confirmed the hydrodynamic properties and a monocentric prospective clinical study was performed in 2011. After the inclusion of 10 patients, the study was aborted because of frequent thrombotic obstruction of the VSS sinus catheter, only in 2 the VSS remained patent in the long-term. As no complications due to the VSS were encountered and its physiological CSF

drainage is proved, the decision was taken to continue with the development of a dedicated dural venous sinus device (DVSAD). Thanks to a UGent IOF StarrTT funding and the technical support of Steerable Instrument (SI), the first prototypes were tested in a new in vitro testing set-up, the non-occlusive-roller-pump, in 2012. These tests were important in the selection of the material of the intravascular part of the DVSAD, the decision was taken to continue with silicone or polyurethane. Meanwhile, in co-operation with the UGent faculty of Veterinary Medicine, the caprine species (goat) was chosen as a potential animal model. A new UGent IOF StarrAdvanced funding was granted and in 2013-2014 in-vivo studies on the caprine model were conducted considering Kaolin injection HC induction and implantation of 3 different DVSAD prototypes in hydrocephalic and non-hydrocephalic animals. The animal in-vivo tests showed that present VSS systems have a compliance facilitating blood regurgitation and that to prevent endothelial invagination during insertion of the DVSAD, a barbed DVSAD, safely and easily implantable using a Seldinger-like technique is required. The tests also proved that VSS shunting is a safe technique, but that thrombus formation at the DVSAD tip in the venous sinus remains an important issue. The retrograde orientation of the DVSAD did not prove to be beneficial above a the neutral orientation, oblique to the blood stream direction.

In 2016 new non-occlusive-roller-pump in vitro tests with human blood and CSF, proved that CSF mixed with blood increases significantly blood coagulation activity as from CSF concentrations of 5 % or more, both in static and dynamic conditions. Therefore, a retrograde orientation of the VSS sinus catheter proved not protective but inducing blood clot formation at its tip and intravascular surface. As a consequence the DVSAD design should have a minimal intravascular surface with minimal creation of blood flow wake zones, a perpendicular orientation avoiding CSF contact on its vascular surface, and a maximal prevention of blood regurgitation by the use of a one-way valve and by a reduced compliance of the VSS components. The DVSAD material should be silicone or polyurethane and coating preventing protein binding might be beneficial.

In conclusion, the VSS remains capable of balanced / near physiological CSF drainage in the treatment of communicating HC and is technically feasible and safe to implant, but its frequent obstruction due to thrombus formation prevents the VSS becoming standard medical practice. Consequently, further efforts to develop a dedicated DVSAD preventing clotting activation should continue to achieve optimal treatment of communication HC.

CHAPTER 8. ACKNOWLEDGEMENTS / DANKWOORD

Dit onderzoeksproject oversteeg de dienst neurochirurgie, het UZ Gent, de faculteit geneeskunde of de U Gent. Multidisciplinaire samenwerking met hemato-oncologie, cardiochirurgie, faculteit diergeneeskunde, faculteit burgerlijk ingenieur – hydraulica / Instituut voor Biomedische Technologie (IBiTech), alsmede externe partners zoals het Industrieel Onderzoek Fonds (IOF) en zeker de firma Steerable Instruments® (SI) bleek de sleutel tot voleindigen van dit ventriculo-sinus shunt project. Velen dienen dan ook te worden bedankt en vergeef mij indien ik onvolledig was.

Prof. em. dr. **Jacques Caemaert** geloofde in mijn vreemde carrièreswitch van psychiater tot neurochirurg-in-opleiding en heeft steeds innovatie binnen ons vakgebied gepromoot, zo ook het ventriculo-sinus shunt project toen het idee opborrelde in 2004. Binnen de dienst neurochirurgie zorgde mijn promotor prof. dr. **Dirk Van Roost** voor de standvastigheid van het project, de logistieke omkadering en de occasionele momenten zonder klinische opdracht, broodnodig voor wetenschappelijke concentratie en vlijt. Prof. dr. **Jean-Pierre Okito Kalala** en collega **Giorgio Hallaert** offerden zich frequent op met extra klinische taken, zodat wij periodiek met gerust gemoed de patiëntenzorg naar de achtergrond konden dringen. Collega dr. **Frank Dewaele** kan ik niet genoeg bedanken voor zijn aanhoudende stimulatie, innoverende invallen, opbouwende kritiek vanaf de begin- tot eindfase van dit doctoraat. Frank was de spin-in-het-web om succesvol coöperatieve banden te smeden met de vele actoren in dit project, zowel wetenschappelijk, logistiek, als financieel-budgettair. Sinds 2012 gooide collega dr. **Jelle Vandersteene** zich anderhalf jaar fulltime op het project en nadien tussen de klinische activiteiten in. Jelle's doorzetting en gestructureerd wetenschappelijke aanpak waren belangrijk voor het slagen van de prototypering, de dierproeven en de in-vitro proeven.

Dankzij IOF fondsen (StarTT in 2012 en Advanced_StarrTT in 2013) en budgettaire flexibiliteit van Dirk Van Roost en Giorgio Hallaert, kon Jelle als voltijds wetenschappelijke medewerker worden verloond. Het IOF zorgde niet alleen voor het budget. Planning van de 'targets to achieve', 'SWOT analyses' en voorbereidende alsmede debriefing presentaties zorgden voor realistische planning, activerende deadlines en realisatie van patenten. Bijzondere dank wensen wij te uiten aan prof. dr. **Patrick Dhaese**, dr. **Ewout Vansteenkiste**, ir. **Kris Bonnarens**, mr. **Bernadette Tuerlinckx**, dr. **Ingrid Merchiers**, prof. dr. **Patrick Vankwikkelberge**, en mr. **An Van den broecke**.

Het onderzoek startte met het akkoord van prof. ir. **Pascal Verdonck**, diensthoofd IBiTech, om een experimenteel en numeriek ventriculo-sinus shunt model te bouwen als eindwerk thesis van ir. **Koen Van Canneyt** en ir. **Jan Kips**, gesuperviseerd door ir. **Guy Mareels**. Ook in het verdere verloop van het project, konden wij frequent beroep doen op hun expertise, in raad en daad.

De in-vitro proeven met humaan bloed en hersenvocht waren niet mogelijk geweest zonder de logistieke ondersteuning van het Labo voor Experimentele Cardiochirurgie (dank aan prof. dr. **Guido Van Nooten**), wetenschappelijke ondersteuning van prof. dr. **Filip De Somer** en dr. **Anna Vantilborgh** en de ijver en bloeddonaties van meerdere collega's (Anna Vantilborgh, Frank Dewaele, Jelle Vandersteene, **Guillaume Planckaert** en **Thomas Van Den Berghe**). De kritisch-analytisch wetenschappelijke inzichten, de kennis van de bloedstollingsprocessen, de daadkracht en specialistische ondersteuning van Filip De Somer bleken van essentiële waarde tijdens de in-vitro proeven en het schrijven van de manuscripten.

Velen zetten zich vrijwillig en onbaatzuchtig in. Hierbij speciale dank aan prof. em. dr. **Romain Lefebvre**, diensthoofd Heymans Instituut voor Farmacologie UZ Gent, die mij als student geneeskunde liet proeven van experimenteel wetenschappelijk onderzoek en mij de nodige motivatie en logistieke ondersteuning gaf om de laatste loodjes, het schrijfwerk, van dit doctoraat met succes te voleindigen. Aan prof. em. dr. **Luc**

Calliauw, diensthoofd Neurochirurgie UZ Gent, die zich engageerde om mij onder 4 ogen verbaal aan te sporen. Aan **Ilse Noterman**, hoofd secretariaat Neurochirurgie UZ Gent; Ilse offerde vrijwillig vrije dagen en feestdagen op om mijn proefschrift van correcte en aansprekende lay-out en leesbare structuur te voorzien in Microsoft Word en Adobe InDesign, conform de vereisten van de drukkerij. Aan **Natalie Cockuyt**, instrumenterende en spoedverpleegkundige; Natalie instrumenteerde vrijwillig en onbezoldigd bij de vele operaties op geiten. Het ganse verpleegkundig en secretariaatsteam van de poliklinieken Neurochirurgie en Neurologie diende herhaaldelijk de poliklinische agenda's, operatieschema's aan te passen om tijd te creëren voor het wetenschappelijk proces; hierbij veel erkentelijkheid aan **Robert Van Severen**, **Jo Immegeers**, **Vera Barbier**, **Cynthia Keustermans**, **Annelies Van de Sype**, **Brenda Van Gerven**. In het operatiekwartier zorgden vele verpleegkundigen voor recuperatie van vervallen of niet gebruikte shunt onderdelen en het vereiste materiaal voor succesvolle shunt operaties; hierbij grote erkentelijkheid aan **Katy De Beck**, **Nadine De Bruyne**, **Irene De Meester**, **Andy De Brauwer**, **Marleen De Wachter**, **Aurelie Hesters**, **Ann Huylebroeck**, **Laura Sette**, **Gaëlle Vandenhende**, **Chris Vandergucht**, **Wim Verleyen**.

Onwennig en onbeslagen startten Jelle Vandersteene en ikzelf aan de dierenproeven. Prof. em. dr. **Paul Simoens**, hoogleraar anatomie faculteit diergeneeskunde UGent, en dr. **Kimberley Vandevelde** ondersteunden ons met welgemeend enthousiasme bij de selectie van het diermodel en de kadaverstudies doorheen het ganse caprine in-vivo model traject. Prof. dr. **Frank Gasthuys**, decaan faculteit diergeneeskunde, hield ons een kritische spiegel voor, zodat wij de dierenproeven met dierenrespect en zin voor realiteit aanvatten. Frank Gasthuys stelde voor ons een topteam samen om de ingrepen en zorg & hospitalisatie van de dieren lege artis uit te voeren. Dr. **Stijn Schauvliege**, vakgroep heelkunde en anesthesie van de huisdieren, zorgde voor optimale anesthesie gedurende urenlang aanslepende ingrepen. Dr. **Eva Pint** en dr. **Sofie Bhatti** waren onze steun voor de neurologische opvolging van de dieren. Voor de verwerking van het microscopisch materiaal, leerde prof. dr. **Wim Van den Broeck**, vakgroep Morfologie

faculteit Diergeneeskunde, ons de technieken van de surface electronen microscoop (SEM), hierin steeds bereidwillig bijgestaan door **Bart De Pauw** (technisch coördinator vakgroep Morfologie).

Zonder de technische en logistieke ondersteuning van Steerable Instruments® (SI) voor de conceptualisatie en fabricatie van sinus katheter prototypes hadden we nooit de nodige flexibiliteit, materiaalkennis en vaardigheden gekend om op korte termijn vele en steeds weer gemodificeerde prototypes van de DVSAD of sinus punaise te maken. Frank Dewaele, **Cyriel Mabilde** en **Bart Blanckaert** hebben zich steeds 100% ingezet en het ganse traject ondersteund, in vriendschap, als kritische onderzoekers, als innovators.

De jarenlange combinatie van drukke klinische activiteit en wetenschappelijk onderzoek heeft familiaal een hoge tol geëist. Mijn vader prof. dr. **Andre-Emmanuel Baert** bleef rotsvast in mijn slagen geloven. Mijn schoonouders, **Myriam Van Hoorebeeck** en dr. **Marc Fiers** bleven ons gezin onbaatzuchtig en liefdevol ondersteunen. Mijn echtgenote **Ellen Van Goethem** en de kinderen, **Reinhart**, **Robbrecht** en **Ophelia** hebben 's avonds vaker een lege dan een bezette stoel aan tafel of een lege plaats in bed ervaren. Ellen heeft het leeuwendeel van de zorgen en emoties van het gezin gedragen, mijn frequente afwezigheid opgevangen. Ophelia, nu 16 jaar, heeft haar ganse bewuste leven papa weten 'bezig zijn met zijn doctoraat'. Mijn belangrijkste taak bestaat eruit deze situatie naar een harmonieus evenwicht om te buigen.

CHAPTER 9. CURRICULUM VITAE of BAERT, Edward

Biographical data	*Name*	Baert
	First, middle names	Edward, Jozef Alfons
	Date of birth	October 28, 1967
	Place of birth	Gent (Ghent), Belgium
	Citizenship	Belgian
	Religion	Roman Catholic
	Spouse	Van Goethem, Ellen
	Children	Reinhart, Robbrecht & Ophelia
	Home address	Gaversesteenweg 642 B - 9820 Melsen (Merelbeke) Phone +32 9 2211524 Cell +32 486 868919
	Office address	Universitair Ziekenhuis Gent Dienst Neurochirurgie Corneel Heymanslaan 10 B - 9000 Gent
	Phone	+ 32 9 3322847
	e-mail	edward.baert@uzgent.be edward.baert@telenet.be
	Belgian RIZIV reg.	1-46483-84-170

Education	*1980-86*	Secondary school: Latin-Greek St-Barbara college, Gent
	1987-94	Medical Degree (doctor in de genees-, heel- en verloskunde), cum laude, Ghent University
Postgraduate training	*1994-95*	Diploma in Clinical Neurology Institute of Neurology, Queen Square, London
	1995	Advanced Critical Life Support qualification, King's College Hospital, London
	1997	Radioprotection in use of X-rays for medical and diagnostic purposes qualification, Ghent University; FANC reattribution for period 2017 - 2027
	22 Feb '01	Recognition and permission as medical specialist in Neurosurgery, Belgian federal government of Public Health
	30 Aug '01	Multiple Choice Examination of the EANS, European Association of Neurosurgical Societies, after completing 4 year sequence of the European Course in Neurosurgery
	13 Mar '06	FELASA C project leader certificate for animal experimental studies, Belgian federal government of Public Health
	20 Mar '15	Certificate of Fluorescence-guided tumor resection using Gliolan®, Ziekenhuis Oost-Limburg, Genk
Scientific experience	*'90 - '93*	Animal experimental studies on nervous regulation of the gastric motility with L-*NNA* and NO as neurotransmitters (Heymans Institute of Physiology, Ghent University - prof. Bogaert M. and prof. Lefebvre R.)

	'10 - '18	In vitro, animal and clinical experimental prototyping and surgery on ventriculo-*sinus* sagittalis shunts in the treatment of hydrocephalus
	28 Jun '18	Submission of Ph. D. at Universiteit Gent, Geneeskunde – Gezondheidswetenschappen, *Hydrocephalus and the ventriculo-sinus shunt: capable of physiological drainage but a challenge for standard practice because of the high degree of obstruction of the venous sinus catheter*
Clinical experience	*Apr - Sept '95*	SHO (senior house officer) in Neurology, King's College Hospital, London
	Oct '95 - Sept '96	ASO in Surgery and Orthopedics, AZ-Jan Palfijn, Gent
	Oct '96 - Jan '01	ASO in Neurosurgery, Ghent University Hospital
	Jan '01 - Feb '07	Resident Neurosurgy, Ghent University Hospital
	Mar '07 - present	Consultant Neurosurgery, Ghent University Hospital
Teaching experience	*Sept '01 - Jul '13*	Introduction in Neurosurgery (15 hours a year + examination) for Masters in Audiology, Ghent University
	Sep '08 - present	Introduction in Surgical Professions - Pediatric NS and Hydrocephalus, Masters in Medical Sciences, Ghent University

Special clinical interest and experience

- Pediatric Neurosurgery:
  oncology, vascular malformations, craniospinal malformations, craniosynostosis, traumatology, epilepsy surgery
- Hydrocephalus
- Endoscopic neurosurgery
- Neuromodulation in the treatment of pain and spasticity/dystonia

PUBLICATIONS

1. **Baert E**, Vandersteene J, Dewaele F, Desomer F, Vantilborgh A, Van Roost D, Desomer F. A new dynamic model for in vitro evaluation of intravascular devices. International Journal of Artificial Organs. Accepted on September 20, 2018.

2. Vandersteene J, **Baert E**, Schauvliege S, Vandevelde K, Dewaele F, De Somer F, et al. A non-hydrocephalic goat experimental model to evaluate a ventriculo-sinus shunt. Laboratory animals. 2018:23677217753976.

3. Cizmeci MN, Thewissen L, Zecic A, Woerdeman PA, Boer B, **Baert E**, et al. Bedside Ultrasound-Guided Percutaneous Needle Aspiration of Intra- and Extra-Axial Intracranial Hemorrhage in Neonates. Neuropediatrics. 2018;49(4):238-45.

4. Vandersteene J, **Baert E**, Planckaert GMJ, Van Den Berghe T, Van Roost D, Dewaele F, et al. The influence of cerebrospinal fluid on blood coagulation and the implications for ventriculo-venous shunting. Journal of neurosurgery. 2018:1-8.

5. Maenhoudt W, Hallaert G, Kalala JP, **Baert E**, Dewaele F, Bauters W, et al. Hydroxyapatite cranioplasty: a retrospective evaluation of osteointegration in 17 cases. Acta neurochirurgica. 2018.

6. **Baert EJ**, Dewaele F, Vandersteene J, Hallaert G, Kalala JO, Van Roost D. Treating Hydrocephalus with Retrograde Ventriculo-sinus Shunt: Prospective Clinical Study. World neurosurgery. 2018;118:e34-e42.

7. Vandersteene J, Van Den Berghe T, Planckaert G, De Somer F, **Baert E**, Van Roost D. A corrected method for analysing impurities on two dimensional projected images of cilindrical objects. 2017.

8. Ninclaus VG, Walraedt S, **Baert E**, Laureys G, Leroy BP, De Zaeytijd J. Diplopia as presenting sign of Turcot syndrome. International ophthalmology. 2017;37(1):275-8.

9. Opsomer D, Allaeys T, Alderweireldt AS, **Baert E**, Roche N. Intracranial complications of midline nasal dermoid cysts. Acta chirurgica Belgica. 2017:1-4.

10. **Baert E**, Dewaele F, inventors; Steerable Instruments Bvba, Universiteit Gent, assignee. Minimally-advancing luminal catheter. USA patent US 20140207044 A1. 2016 Aug 2, 2016.

11. Dewaele F, Kalmar AF, **Baert E**, Van Haver A, Hallaert G, De Mets F, et al. The use of the trendelenburg position in the surgical treatment of extreme cerebellar slump. British journal of neurosurgery. 2016;30(1):115-9.

12. Couvreur T, Hallaert G, Van Der Heggen T, **Baert E**, Dewaele F, Kalala Okito JP, et al. Endoscopic Treatment of Temporal Arachnoid Cysts in 34 Patients. World neurosurgery. 2015;84(3):734-40.

13. Dewaele F, Kalmar AF, De Ryck F, Lumen N, Williams L, **Baert E**, et al. A novel design for steerable instruments based on laser-cut nitinol. Surgical innovation. 2014;21(3):303-11.

14. Dhondt K, **Baert E**, Van Herzeele C, Raes A, Groen LA, Hoebeke P, Vande Walle J. Sleep fragmentation and increased periodic limb movements are more common in children with nocturnal enuresis. Acta Paediatr. 2014; Jun;103(6):e268-72.

15. Vanhauwaert D, Hallaert G, **Baert E**, Van Roost D, Okito JP, Caemaert J. Treatment of cystic craniopharyngioma by endocavitary instillation of yttrium(9)(0) radioisotope--still a valuable treatment option. Journal of neurological surgery Part A, Central European neurosurgery. 2013;74(5):307-12.

16. Hallaert G, **Baert E**, Van Roost D, Caemaert J . Endoscopic Treatment of Choroid Plexus Hyperplasia. World Neurosurgery, November 2013.

17. Hallaert G, Vanhauwaert D, Logghe K, Van den Broecke C, **Baert E**, Van Roost D, et al. Endoscopic coagulation of choroid plexus hyperplasia. Journal of neurosurgery Pediatrics. 2012;9(2):169-77.

18. Verbeek S, Verloo P, Verhelst H, **Baert E**, …, Van Coster R. P07.18 Cerebral Capillary Teleangiectasias. European Journal of Paediatric Neurology, May 2011.

19. Caemaert J, Dewaele F, Kalala Okito J-P, **Baert E**, Van Roost D. Endoscopic treatment of cerebral tumors. Surgical Neurology, November 2009.

20. Vanhauwaert D, **Baert E**, Hallaert G, …, Van Roost D. Split cord malformation type 1 (diastematomyelia): illustration of surgical technique. Surgical Neurology, January 2009.

21. **Baert E**, Dewaele F, Van Roost D, Caemaert J. Three dimensional methylacrylate and wax skull modeling preparing cranioplasty in the treatment of complex craniosynostosis and skull malformation. Surgical Neurology, January 2009.

22. Vanhauwaert D, Van den Broecke C, Hallaert G, **Baert E**, Van Roost D. Angiocentric glioma: a rare epilepsy-related neoplasm added to the 2007 WHO classification. Report of 2 cases. Surgical Neurology, January 2009.

23. Kalala Okito JP, **Baert E**, Vanhauwaert D, Caemaert J. Cystic craniopharyngioma treatment by stereotactic instillation of emitting radioisotopes (yttrium90). Surgical Neurology, January 2009

24. Idris Z, Hallaert G, Vanhauwaert D, Kalala Okito JP, **Baert E**, Van Roost D, Caemaert J. Frameless neuronavigation-guided endoscopic total en-bloc removal of a third ventricular colloid cyst: A case report on surgical technique. Minimally Invasive Neurosurgery, June 2008; PMID 18521790.

25. Van Canneyt K, Kips J, Mareels G, **Baert E**, Van Roost D, Verdonck P. Experimental and numerical modeling of the ventriculo-sinus shunt (El Shafei shunt). Proceedings of the Institution of Mechanical Engineers Part H-Journal of Engineering in Medicine (2008); PMID 18595357.

26. Vanhauwaert D, Kalala Okito J-P, **Baert E**, Hallaert G. Migration of pump for intrathecal drug delivery into the peritoneal cavity. Case report, Surgical Neurology, May 2008; PMID 18291481.

27. Vanhauwaert D, Hallaert G, Kalala Okito J-P, **Baert E**, Caemaert J. Recurrent brain abscess with Eikenella corrodens due to misdiagnosed aspirated foreign body. Surgical Neurology, August 2007

28. Dewaele F, Caemaert J, **Baert E**, Kalala Okito J-P et al. Intradural endoscopic closure of dural breaches in a case of post-traumatic tension pneumencephalus. Minimally Invasive Neurosurgery, July 2007; PMID 17882756

29. Vonck K, Dedeurwaerdere S, De Groote L, Claeys P, **Baert E**, Caemaert J, De Reuck J, Boon P. Indication and timing for pulse generator replacement in epilepsy patients treated with vagus nerve stimulation. J. Neurol., 2003, 250 (suppl. 2), 17.

30. Michielsen G, Boon P, **Baert E**, Caemaert J. New perspectives in epilepsy surgery. Eur. Surg. Res., 2003, 35, 279.

31. Vonck K, Boon P, Goossens L, Dedeurwaerdere S, …, **Baert E**, …, Williamson P. Neurostimulation for refractory epilepsy. Acta Neurol. Belg., January 2004; PMID 15008506.

32. Deherdt V, Boon P, Goossens L, Vonck K, Nieuwenhuis L, Paemeleire K, Meire V, Michielsen G, **Baert E**, Van Roost D. Are psychotic symptoms related to vagus nerve stimulation in epilepsy patients? Acta Neurol. Belg., Octobre 2003, 103, 170-175; PMID 14626698.

33. Caemaert J, **Baert E**. Intracraniale overdruk. Boek Neurologie / praktische huisarts-geneeskunde , January 2003, 191-208.

34. Michielsen G, Benoit Y, **Baert E**, Meire F and Caemaert J. Symptomatic Pineal cysts: Clinical Manifestations and Management. Acta Neurochir., April 2002, 144, 233-242.

35. Lefebvre RA, **Baert E**, Barbier AJ. Influence of N-nitro-L-arginine on non-cholinergic relaxation in the guinea-pig gastric fundus. Br. J. Pharmacol., June 1992, 106, 173-179; PMID 1504726.

REFERENCES

1. Van Canneyt K, Kips J, Mareels G, Baert E, Van Roost D, Verdonck P. Experimental and numerical modelling of the ventriculosinus shunt (El-Shafei shunt). *Proc Inst Mech Eng H.* 2008;222(4):455-464.

2. Van Canneyt K, Kips J, Mareels G, Baert E, Van Roost D, Verdonck P. Experimental and numerical modelling of the ventriculosinus shunt (El-Shafei shunt). *Proceedings of the Institution of Mechanical Engineers Part H, Journal of engineering in medicine.* 2008;222(4):455-464.

3. Baert EJ, Dewaele F, Vandersteene J, Hallaert G, Kalala JO, Van Roost D. Treating Hydrocephalus with Retrograde Ventriculosinus Shunt: Prospective Clinical Study. *World neurosurgery.* 2018;118:e34-e42.

4. Baert EJ, Vandersteene J, Dewaele F, Vantilborgh A, Van Roost D, De Somer F. A new dynamic model for in vitro evaluation of intravascular devices. *The International journal of artificial organs.* 2018:391398818806158.

5. Baert E, Dewaele F, Inventors; Steerable Instruments Bvba, Universiteit Gent, assignee. Minimally-advancing luminal catheter. US patent US 20140207044 A1. Aug 2, 2016, 2016.

6. Baert E, Schauvliege S, Vandersteene J, et al. A Hydrocephalic Goat Experimental Model to Evaluate the Efficacy of Hydrocephalus Treatment. In:2018.

7. Vandersteene J, Baert E, Schauvliege S, et al. A non-hydrocephalic goat experimental model to evaluate a ventriculosinus shunt. *Laboratory animals.* 2018;52(5):504-514.

8. Vandersteene J, Baert E, Planckaert GMJ, et al. The influence of cerebrospinal fluid on blood coagulation and the implications for ventriculovenous shunting. *Journal of neurosurgery.* 2018:1-8.

9. Pickard JD, Richards HK, Mendez RF, Joannides AJ. UK Shunt Registry, Draft Report 2017. In: Registry US, ed2017.

10. Payr E. Drainage der Hirnventrikel mittelst frei transplantirter Blutgefässe: Bemerkungen über Hydrocephalus. *Arch Klin Chir* 1908;87:801-885.

11. El-Shafei IL, El-Shafei HI. The retrograde ventriculovenous shunts: the El-Shafei retrograde ventriculojugular and ventriculosinus shunts. *Pediatr Neurosurg.* 2010;46(3):160-171.

12. El-Shafei IL, El-Shafei HI. The retrograde ventriculosinus shunt: concept and technique for treatment of hydrocephalus by shunting the cerebrospinal fluid to the superior sagittal sinus against the direction of blood flow. Preliminary report. *Childs Nerv Syst.* 2001;17(8):457-465; discussion 466.

13. Borgesen SE, Inventor; Sinu Shunt A/S, assignee. Device for the treatment of hydrocephalus. US patent US6283934 B12001.

14. Borgesen SE, Gjerris F, Agerlin N. Shunting to the sagittal sinus. *Acta Neurochir Suppl.* 2002;81:11-14.

15. Borgesen SE, Pieri A, Cappelen J, Agerlin N, Gjerris F. Shunting to the cranial venous sinus using the SinuShunt. *Childs Nerv Syst.* 2004;20(6):397-404.

16. Osaka K, Handa H, Matsumoto S, Yasuda M. Development of the cerebrospinal fluid pathway in the normal and abnormal human embryos. *Childs Brain.* 1980;6(1):26-38.

17. Knigge KM, Schock SA, Silverman AJ, et al. Role of the ventricular system in neuroendocrine processes: synthesis and distribution of thyrotropin releasing factor (TRF) in the hypothalamus and third ventricle. *Can J Neurol Sci.* 1974;1(1):74-84.

18. Vigh B, Manzano e Silva MJ, Frank CL, et al. The system of cerebrospinal fluid-contacting neurons. Its supposed role in the nonsynaptic signal transmission of the brain. *Histol Histopathol.* 2004;19(2):607-628.

19. Hiyama TY, Watanabe E, Okado H, Noda M. The subfornical organ is the primary locus of sodium-level sensing by Na(x) sodium channels for the control of salt-intake behavior. *J Neurosci.* 2004;24(42):9276-9281.

20. Cutler RW, Page L, Galicich J, Watters GV. Formation and absorption of cerebrospinal fluid in man. *Brain.* 1968;91(4):707-720.

21. Cserr HF. Physiology of the choroid plexus. *Physiol Rev.* 1971;51(2):273-311.

22. Sakka L, Coll G, Chazal J. Anatomy and physiology of cerebrospinal fluid. *Eur Ann Otorhinolaryngol Head Neck Dis.* 2011;128(6):309-316.

23. McComb JG. Recent research into the nature of cerebrospinal fluid formation and absorption. *J Neurosurg.* 1983;59(3):369-383.

24. Maren TH, Broder LE. The role of carbonic anhydrase in anion secretion into cerebrospinal fluid. *J Pharmacol Exp Ther.* 1970;172(2):197-202.

25. Davson H, Segal MB. The effects of some inhibitors and accelerators of sodium transport on the turnover of 22Na in the cerebrospinal fluid and the brain. *J Physiol.* 1970;209(1):131-153.

26. Pollay M, Hisey B, Reynolds E, Tomkins P, Stevens FA, Smith R. Choroid plexus Na+/K+-activated adenosine triphosphatase and cerebrospinal fluid formation. *Neurosurgery.* 1985;17(5):768-772.

27. Pollay M, Curl F. Secretion of cerebrospinal fluid by the ventricular ependyma of the rabbit. *Am J Physiol.* 1967;213(4):1031-1038.

28. Rall DP. Transport through the ependymal linings. *Prog Brain Res.* 1968;29:159-172.

29. Gur RE, Mozley PD, Resnick SM, et al. Magnetic resonance imaging in schizophrenia. I. Volumetric analysis of brain and cerebrospinal fluid. *Arch Gen Psychiatry.* 1991;48(5):407-412.

30. Dandy WE. Experimental hydrocephalus. *Ann Surg.* 1919;70:129-142.

31. Pollay M. The function and structure of the cerebrospinal fluid outflow system. *Cerebrospinal Fluid Res.* 2010;7:9.

32. Rekate HL, Brodkey JA, Chizeck HJ, el Sakka W, Ko WH. Ventricular volume regulation: a mathematical model and computer simulation. *Pediatr Neurosci.* 1988;14(2):77-84.

33. Edsbagge M, Tisell M, Jacobsson L, Wikkelso C. Spinal CSF absorption in healthy individuals. *Am J Physiol Regul Integr Comp Physiol.* 2004;287(6):R1450-1455.

34. Kido DK, Gomez DG, Pavese AM, Jr., Potts DG. Human spinal arachnoid villi and granulations. *Neuroradiology.* 1976;11(5):221-228.

35. Welch K, Friedman V. The cerebrospinal fluid valves. *Brain.* 1960;83:454-469.

36. Gjerris F, Borgesen SE. Current concepts of measurement of cerebrospinal fluid absorption and biomechanics of hydrocephalus. *Adv Tech Stand Neurosurg.* 1992;19:145-177.

37. Weed LH. Studies on Cerebro-Spinal Fluid. No. II : The Theories of Drainage of Cerebro-Spinal Fluid with an Analysis of the Methods of Investigation. *J Med Res.* 1914;31(1):21-49.

38. Weed LH. Studies on Cerebro-Spinal Fluid. No. III : The pathways of escape from the Subarachnoid Spaces with particular reference to the Arachnoid Villi. *J Med Res.* 1914;31(1):51-91.

39. Tripathi BJ, Tripathi RC. Vacuolar transcellular channels as a drainage pathway for cerebrospinal fluid. *J Physiol.* 1974;239(1):195-206.

40. Levine JE, Povlishock JT, Becker DP. The morphological correlates of primate cerebrospinal fluid absorption. *Brain Res.* 1982;241(1):31-41.

41. Bradbury MW, Cole DF. The role of the lymphatic system in drainage of cerebrospinal fluid and aqueous humour. *J Physiol.* 1980;299:353-365.

42. Johnston M, Zakharov A, Papaiconomou C, Salmasi G, Armstrong D. Evidence of connections between cerebrospinal fluid and nasal lymphatic vessels in humans, non-human primates and other mammalian species. *Cerebrospinal Fluid Res.* 2004;1(1):2.

43. Johnston M. The importance of lymphatics in cerebrospinal fluid transport. *Lymphatic research and biology.* 2003;1(1):41-44; discussion 45.

44. Jessen NA, Munk AS, Lundgaard I, Nedergaard M. The Glymphatic System: A Beginner's Guide. *Neurochemical research.* 2015;40(12):2583-2599.

45. Louveau A, Plog BA, Antila S, Alitalo K, Nedergaard M, Kipnis J. Understanding the functions and relationships of the glymphatic system and meningeal lymphatics. *The Journal of clinical investigation.* 2017;127(9):3210-3219.

46. Kuo PH, Stuehm C, Squire S, Johnson K. Meningeal Lymphatic Vessel Flow Runs Countercurrent to Venous Flow in the Superior Sagittal Sinus of the Human Brain. *Tomography (Ann Arbor, Mich).* 2018;4(3):99-104.

47. Wilson MH. Monro-Kellie 2.0: The dynamic vascular and venous pathophysiological components of intracranial pressure. *Journal of cerebral*

blood flow and metabolism : official journal of the International Society of Cerebral Blood Flow and Metabolism. 2016;36(8):1338-1350.

48. Ekstedt J. CSF hydrodynamic studies in man. 2 . Normal hydrodynamic variables related to CSF pressure and flow. *J Neurol Neurosurg Psychiatry.* 1978;41(4):345-353.

49. Borgesen SE, Gjerris F. The predictive value of conductance to outflow of CSF in normal pressure hydrocephalus. *Brain.* 1982;105(Pt 1):65-86.

50. Albeck MJ, Borgesen SE, Gjerris F, Schmidt JF, Sorensen PS. Intracranial pressure and cerebrospinal fluid outflow conductance in healthy subjects. *J Neurosurg.* 1991;74(4):597-600.

51. Avery RA, Shah SS, Licht DJ, et al. Reference range for cerebrospinal fluid opening pressure in children. *N Engl J Med.* 2010;363(9):891-893.

52. Jamjoom AAB, Joannides AJ, Poon MT, et al. Prospective, multicentre study of external ventricular drainage-related infections in the UK and Ireland. *Journal of neurology, neurosurgery, and psychiatry.* 2018;89(2):120-126.

53. Scheithauer S, Burgel U, Ryang YM, et al. Prospective surveillance of drain associated meningitis/ventriculitis in a neurosurgery and neurological intensive care unit. *Journal of neurology, neurosurgery, and psychiatry.* 2009;80(12):1381-1385.

54. Wang X, Dong Y, Qi XQ, Li YM, Huang CG, Hou LJ. Clinical review: Efficacy of antimicrobial-impregnated catheters in external ventricular drainage - a systematic review and meta-analysis. *Critical care (London, England).* 2013;17(4):234.

55. Davson H, Hollingsworth G, Segal MB. The mechanism of drainage of the cerebrospinal fluid. *Brain.* 1970;93(4):665-678.

56. Heisey SR, Held D, Pappenheimer JR. Bulk flow and diffusion in the cerebrospinal fluid system of the goat. *Am J Physiol.* 1962;203:775-781.

57. Katzman R, Hussey F. A simple constant-infusion manometric test for measurement of CSF absorption. I. Rationale and method. *Neurology.* 1970;20(6):534-544.

58. Czosnyka M, Whitehouse H, Smielewski P, Simac S, Pickard JD. Testing of cerebrospinal compensatory reserve in shunted and non-shunted patients: a

guide to interpretation based on an observational study. *J Neurol Neurosurg Psychiatry.* 1996;60(5):549-558.

59. Masserman JH. Cerebrospinal hydrodynamics. IV. *Clinical experimental studies Arch Neurol Psychiat (Chic).* 1934;32:523.

60. Rekate HL. The definition and classification of hydrocephalus: a personal recommendation to stimulate debate. *Cerebrospinal Fluid Res.* 2008;5:2.

61. Dandy WE, Blackfan KD. An experimental and clinical study of internal hydrocephalus. *Journal of the American Medical Association.* 1913;61(25):2216-2217.

62. Dandy WE, Blackfan KD. Internal hydrocephalus: an experimental, pathological and clinical study. *Am J Dis Child* 1914;8:406-482.

63. Sundstrom N, Malm J, Laurell K, et al. Incidence and outcome of surgery for adult hydrocephalus patients in Sweden. *British journal of neurosurgery.* 2017;31(1):21-27.

64. Atalay B, Yilmaz C, Cekinmez M, Altinors N, Caner H. Treatment of hydrocephalus with functionally isolated ventricles. *Acta neurochirurgica.* 2006;148(12):1293-1296; discussion 1296.

65. Spennato P, Cinalli G, Ruggiero C, et al. Neuroendoscopic treatment of multiloculated hydrocephalus in children. *Journal of neurosurgery.* 2007;106(1 Suppl):29-35.

66. Karsy M, Abou-Al-Shaar H, Bowers CA, Schmidt RH. Treatment of idiopathic intracranial hypertension via stereotactic placement of biventriculoperitoneal shunts. *J Neurosurg.* 2018:1-9.

67. Tarnaris A, Toma AK, Watkins LD, Kitchen ND. Is there a difference in outcomes of patients with idiopathic intracranial hypertension with the choice of cerebrospinal fluid diversion site: a single centre experience. *Clin Neurol Neurosurg.* 2011;113(6):477-479.

68. Nadkarni TD, Rekate HL, Wallace D. Concurrent use of a lumboperitoneal shunt with programmable valve and ventricular access device in the treatment of pseudotumor cerebri: review of 40 cases. *J Neurosurg Pediatr.* 2008;2(1):19-24.

69. Langfitt TW, Weinstein JD, Kassell NF, Gagliardi LJ. Transmission of Increased Intracranial Pressure. Ii. Within the Supratentorial Space. *J Neurosurg.* 1964;21:998-1005.

70. Langfitt TW, Weinstein JD, Kassell NF, Simeone FA. Transmission of Increased Intracranial Pressure. I. Within the Craniospinal Axis. *J Neurosurg.* 1964;21:989-997.

71. Marmarou A, Shulman K, LaMorgese J. Compartmental analysis of compliance and outflow resistance of the cerebrospinal fluid system. *J Neurosurg.* 1975;43(5):523-534.

72. Marmarou A, Shulman K, Rosende RM. A nonlinear analysis of the cerebrospinal fluid system and intracranial pressure dynamics. *J Neurosurg.* 1978;48(3):332-344.

73. Pudenz RH, Russell FE, Hurd AH, Shelden CH. Ventriculo-auriculostomy. A Technique for Shunting Cerebrospinal Fluid into the Right Auricle* Preliminary Report. *Journal of neurosurgery.* 1957;14(2):171-179.

74. Ransohoff J, 2nd, Hiatt RB. Ventriculo-peritoneal anastomosis in the treatment of hydrocephalus; utilization of the suprahepatic space. *Transactions of the American Neurological Association.* 1952;56(77th Meeting):147-151.

75. Ransohoff J. Ventriculo-pleural anastomosis in treatment of midline obstructional neoplasms. *Journal of neurosurgery.* 1954;11(3):295-298.

76. Rekate HL, Wallace D. Lumboperitoneal shunts in children. *Pediatr Neurosurg.* 2003;38(1):41-46.

77. Buchsbaum HW, Gallo AE, Jr. Polyneuritis, papilledema, and lumboperitoneal shunt. *Archives of neurology.* 1969;21(3):253-257.

78. Aoki N. Lumboperitoneal shunt: clinical applications, complications, and comparison with ventriculoperitoneal shunt. *Neurosurgery.* 1990;26(6):998-1003; discussion 1003-1004.

79. Decq P, Schroeder HW, Fritsch M, Cappabianca P. A history of ventricular neuroendoscopy. *World neurosurgery.* 2013;79(2 Suppl):S14 e11-16.

80. Hsu W, Li KW, Bookland M, Jallo GI. Keyhole to the brain: Walter Dandy and neuroendoscopy. *Journal of neurosurgery Pediatrics.* 2009;3(5):439-442.

81. Aarli JA. [Arne Thorkildsen and Thorkildsen's surgery]. *Tidsskr Nor Laegeforen.* 2000;120(30):3726-3727.

82. Eide PK, Lundar T. Arne Torkildsen and the ventriculocisternal shunt: the first clinically successful shunt for hydrocephalus. *J Neurosurg.* 2016;124(5):1421-1428.

83. Timothy W. Vogel, Biji Bahuleyan, Shenandoah Robinson, Alan R. Cohen. The role of endoscopic third ventriculostomy in the treatment of hydrocephalus. *Journal of Neurosurgery: Pediatrics.* 2013;12(1):54-61.

84. Caemaert J, Abdullah J, Calliauw L. A multipurpose cerebral endoscope and reflections on technique and instrumentation in endoscopic neurosurgery. *Acta Neurochir Suppl.* 1994;61:49-53.

85. Abdullah J, Caemaert J. Endoscopic management of craniopharyngiomas: a review of 3 cases. *Minim Invasive Neurosurg.* 1995;38(2):79-84.

86. Caemaert J, Abdullah J. Diagnostic and therapeutic stereotactic cerebral endoscopy. *Acta Neurochir (Wien).* 1993;124(1):11-13.

87. Caemaert J, Abdullah J, Calliauw L. Endoscopic diagnosis and treatment of para- and intra-ventricular cystic lesions. *Acta Neurochir Suppl.* 1994;61:69-75.

88. Caemaert J, Abdullah J, Calliauw L, Carton D, Dhooge C, van Coster R. Endoscopic treatment of suprasellar arachnoid cysts. *Acta Neurochir (Wien).* 1992;119(1-4):68-73.

89. Browd SR, Gottfried ON, Ragel BT, Kestle JR. Failure of cerebrospinal fluid shunts: part II: overdrainage, loculation, and abdominal complications. *Pediatr Neurol.* 2006;34(3):171-176.

90. Browd SR, Ragel BT, Gottfried ON, Kestle JR. Failure of cerebrospinal fluid shunts: part I: Obstruction and mechanical failure. *Pediatr Neurol.* 2006;34(2):83-92.

91. Hanak BW, Bonow RH, Harris CA, Browd SR. Cerebrospinal Fluid Shunting Complications in Children. *Pediatr Neurosurg.* 2017.

92. Chumas PD, Kulkarni AV, Drake JM, Hoffman HJ, Humphreys RP, Rutka JT. Lumboperitoneal shunting: a retrospective study in the pediatric population. *Neurosurgery.* 1993;32(3):376-383; discussion 383.

93. Drake JM, Kestle JR, Tuli S. CSF shunts 50 years on--past, present and future. *Childs Nerv Syst.* 2000;16(10-11):800-804.

94. Drake JM, Sainte-Rose C. *The shunt book.* Blackwell Science; 1995.

95. Kestle J, Drake J, Milner R, et al. Long-term follow-up data from the Shunt Design Trial. *Pediatr Neurosurg.* 2000;33(5):230-236.

96. Pudenz RH, Foltz EL. Hydrocephalus: overdrainage by ventricular shunts. A review and recommendations. *Surg Neurol.* 1991;35(3):200-212.

97. Acikbas SC, Akyuz M, Kazan S, Tuncer R. Complications of closed continuous lumbar drainage of cerebrospinal fluid. *Acta Neurochir (Wien).* 2002;144(5):475-480.

98. Hanlo PW, Cinalli G, Vandertop WP, et al. Treatment of hydrocephalus determined by the European Orbis Sigma Valve II survey: a multicenter prospective 5-year shunt survival study in children and adults in whom a flow-regulating shunt was used. *Journal of neurosurgery.* 2003;99(1):52-57.

99. Cochrane DD, Kestle J. Ventricular shunting for hydrocephalus in children: patients, procedures, surgeons and institutions in English Canada, 1989-2001. *Eur J Pediatr Surg.* 2002;12 Suppl 1:S6-11.

100. Hakim S. Hydraulic and Mechanical Mis-matching of Valve Shunts Used in the Treatment of Hydrocephalus: the Need for a Servo-valve Shunt. *Developmental Medicine & Child Neurology.* 1973;15(5):646-653.

101. Kiefer M, Eymann R, Meier U. Five years experience with gravitational shunts in chronic hydrocephalus of adults. *Acta Neurochir (Wien).* 2002;144(8):755-767; discussion 767.

102. Lund-Johansen M, Svendsen F, Wester K. Shunt failures and complications in adults as related to shunt type, diagnosis, and the experience of the surgeon. *Neurosurgery.* 1994;35(5):839-844; discussion 844.

103. Lundkvist B, Eklund A, Kristensen B, Fagerlund M, Koskinen LO, Malm J. Cerebrospinal fluid hydrodynamics after placement of a shunt with an antisiphon device: a long-term study. *J Neurosurg.* 2001;94(5):750-756.

104. Zemack G, Romner B. Seven years of clinical experience with the programmable Codman Hakim valve: a retrospective study of 583 patients. *Journal of neurosurgery.* 2000;92(6):941-948.

105. Kluge S, Baumann HJ, Regelsberger J, et al. Development of pulmonary hypertension in adults after ventriculoatrial shunt implantation. *Respiration.* 2009;78(1):30-35.

106. Pascual JM, Prakash UB. Development of pulmonary hypertension after placement of a ventriculoatrial shunt. *Mayo Clin Proc.* 1993;68(12):1177-1182.

107. Wilkinson N, Sood S, Ham SD, Gilmer-Hill H, Fleming P, Rajpurkar M. Thrombosis associated with ventriculoatrial shunts. *J Neurosurg Pediatr.* 2008;2(4):286-291.

108. Karabatsou K, Quigley G, Buxton N, Foy P, Mallucci C. Lumboperitoneal shunts: are the complications acceptable? *Acta Neurochir (Wien).* 2004;146(11):1193-1197.

109. Karakis I, Nuccio AH, Amadio JP, Fountain AJ, Jr. The Monro-Kellie Doctrine in Action: Posterior Reversible Leukoencephalopathy Syndrome Caused by Intracranial Hypotension from Lumboperitoneal Shunt Placement. *World neurosurgery.* 2017;98:868 e811-868 e815.

110. Khan F, Rehman A, Shamim MS, Bari ME. Factors affecting ventriculoperitoneal shunt survival in adult patients. *Surg Neurol Int.* 2015;6:25.

111. El Shafei IL, el-Rifaii MA. Ventriculojugular shunt against the direction of blood flow. I. Role of the internal jugular vein as an antisiphonage device. *Childs Nerv Syst.* 1987;3(5):282-284.

112. Sharkey P. Ventriculosagittal-sinus shunt. *Journal of neurosurgery.* 1965;22:362-367.

113. Wen H. Ventriculo-superior sagittal sinus shunt for hydrocephalus. *Surg Neurol.* 1982;17(6):432-434.

114. Hash C, Shenkin H, Crowder L. Ventricle to sagittal sinus shunt for hydrocephalus. *Neurosurgery.* 1979;4(5):393-400.

115. Samadani U, Mattielo JA, Sutton LN. Ventriculosagittal sinus shunt placement: technical case report. *Neurosurgery.* 2003;53(3):778-779; discussion 780.

116. Kuhnel K, Seifert V. [Erwin Payr and his contributions to neurosurgery]. *Zentralblatt fur Neurochirurgie.* 1998;59(1):27-35.

117. Bersnev VP, Khachatrian VA, Oliushin VE. [The treatment of hydrocephalus by ventriculosinustransversotomy]. *Zhurnal voprosy neirokhirurgii imeni N N Burdenko.* 1989(4):17-19.

118. El Shafei IL, El Shafei HI. The retrograde ventriculo-sinus shunt (El Shafei RVS shunt). Rationale, evolution, surgical technique and long-term results. *Pediatr Neurosurg.* 2005;41(6):305-317.

119. El Shafei HI, Hafez MA. Ventriculojugular shunt against the direction of blood flow. IV. Technical modifications and policy for treatment. *Childs Nerv Syst.* 1991;7(4):197-204.

120. El Shafei IL, el-Rifaii MA. Ventriculojugular shunt against the direction of blood flow. II. Theoretical and experimental basis for shunting the cerebrospinal fluid against the direction of blood flow. *Childs Nerv Syst.* 1987;3(5):285-291.

121. El Shafei IL. Ventriculovenous shunt to the proximal segment of a ligated neck vein. A new surgical technique for shunting the cerebrospinal fluid to the venous circulation (preliminary report). *Childs Brain.* 1975;1(5):311-323.

122. El Shafei IL. Ventriculo-venous shunt to the proximal segment of an occluded neck vein. A new method for shunting the cerebrospinal fluid to the venous circulation. *Surg Neurol.* 1975;3(5):237-244.

123. El Shafei IL. Ventriculovenous shunt against the direction of blood flow: a new approach for shunting the cerebrospinal fluid to the venous circulation. *Childs Nerv Syst.* 1985;1(4):200-207.

124. El Shafei IL. Ventriculojugular shunt against the direction of blood flow. III. Operative technique and results. *Childs Nerv Syst.* 1987;3(6):342-349.

125. Naradzay JF, Browne BJ, Rolnick MA, Doherty RJ. Cerebral ventricular shunts. *J Emerg Med.* 1999;17(2):311-322.

126. Lang J. *Teil - a - Übergeordnete Systeme.* Berlin: Springer; 2000.

127. Lazorthes G. *Vascularisation et Circulation de l'Encéphale.* Paris: Masson; 1975.

128. Cirovic S, Walsh C, Fraser WD. Mathematical study of the role of non-linear venous compliance in the cranial volume-pressure test. *Med Biol Eng Comput.* 2003;41(5):579-588.

129. Ursino M, Lodi CA. A simple mathematical model of the interaction between intracranial pressure and cerebral hemodynamics. *J Appl Physiol (1985).* 1997;82(4):1256-1269.

130. Rekate H, Nadkarni T, Wallace D. The importance of the cortical subarachnoidal space in understanding hydrocephalus. *J Neurosurg Pediatrics.* 2008;2:1-11.

131. Sainte-Rose C. Shunt obstruction: a preventable complication? *Pediatric neurosurgery.* 1993;19(3):156-164.

132. Sainte-Rose C, Hooven MD, Hirsch J-F. A new approach in the treatment of hydrocephalus. *Journal of neurosurgery.* 1987;66(2):213-226.

133. Sainte-Rose C, Piatt J, Renier D, et al. Mechanical complications in shunts. *Pediatric neurosurgery.* 1991;17(1):2-9.

134. Toma AK, Tarnaris A, Kitchen ND, Watkins LD. Ventriculosinus shunt. *Neurosurg Rev.* 2010;33(2):147-152; discussion 153.

135. Eklund A, Koskinen LO, Malm J. Features of the Sinushunt and its influence on the cerebrospinal fluid system. *J Neurol Neurosurg Psychiatry.* 2004;75(8):1156-1159.

136. Becker D, Jane J, Nulsen F. Investigation of sagittal sinus for venous shunt in hydrocephalus. *Surg Forum.* 1965;16:440-442.

137. Bonnal J, Brotchi J. Surgery of the superior sagittal sinus in parasagittal meningiomas. *J Neurosurg* 1978;48:935-945.

138. Oliveira MF, Teixeira MJ, Reis RC, Petitto CE, Gomes Pinto FC. Failed Ventriculoperitoneal Shunt: Is Retrograde Ventriculosinus Shunt a Reliable Option? *World Neurosurg.* 2016;92:445-453.

139. Frim D, Munshi I, Goumnerova L. Measurements of intraventricular pressure in a patient shunted from the ventricle to the internal jugular vein against the direction of the blood flow (El-Shafei shunt). *Childs Nerv Syst* 2001;17(7):379-381.

140. Aarts PA, van den Broek SA, Prins GW, Kuiken GD, Sixma JJ, Heethaar RM. Blood platelets are concentrated near the wall and red blood cells, in the center in flowing blood. *Arteriosclerosis.* 1988;8(6):819-824.

141. Van Hinsbergh VW. Endothelium role in regulation of coagulation and inflammation. *Semin Immunopathol.* 2012;34(1):93-106.

142. Vandersteene J, Baert E, Planckaert G, et al. Influence of cerebrospinal fluid on blood coagulation and the implications for ventriculo-venous shunts. *Journal of Neurosurgery, Accepted.* 2017.

143. Stagno V, Navarrete EA, Mirone G, Esposito F. Management of hydrocephalus around the world. *World Neurosurg.* 2013;79(2 Suppl):S23 e17-20.

144. Martyak M, Kabir I, Britt R. Inpatient Peripherally Inserted Central Venous Catheter Complications: Should Peripherally Inserted Central Catheter Lines Be Placed in the Intensive Care Unit Setting? *Am Surg.* 2017;83(8):925-927.

145. Seo TS, Song MG, Kim JS, et al. Long-term clinical outcomes of the single-incision technique for implantation of implantable venous access ports via the axillary vein. *J Vasc Access.* 2017;18(4):345-351.

146. Borretta L, MacDonald T, Digout C, Smith N, Fernandez CV, Kulkarni K. Peripherally Inserted Central Catheters in Pediatric Oncology Patients: A 15-Year Population-based Review From Maritimes, Canada. *J Pediatr Hematol Oncol.* 2018;40(1):e55-e60.

147. Chen K, Agarwal A, Tassone MC, et al. Risk factors for central venous catheter-related thrombosis in children: a retrospective analysis. *Blood Coagul Fibrinolysis.* 2016;27(4):384-388.

148. Kluge S, Baumann HJ, Regelsberger J, et al. Pulmonary hypertension after ventriculoatrial shunt implantation. *J Neurosurg.* 2010;113(6):1279-1283.

149. Vernet O, Rilliet B. Late complications of ventriculoatrial or ventriculoperitoneal shunts. *Lancet.* 2001;358(9293):1569-1570.

150. Piatt JH, Jr., Hoffman HJ. Cor pulmonale: a lethal complication of ventriculoatrial CSF diversion. *Childs Nerv Syst.* 1989;5(1):29-31.

151. Chandler AB. In vitro thrombotic coagulation of the blood; a method for producing a thrombus. *Lab Invest.* 1958;7(2):110-114.

152. van Oeveren W, Tielliu IF, de Hart J. Comparison of modified chandler, roller pump, and ball valve circulation models for in vitro testing in high blood flow conditions: application in thrombogenicity testing of different materials for vascular applications. *Int J Biomater.* 2012;2012:673163.

153. Thorsen T, Klausen H, Lie R, Holmsen H. Bubble-induced aggregation of platelets: effects of gas species, proteins, and decompression. *Undersea & hyperbaric medicine: journal of the Undersea and Hyperbaric Medical Society, Inc.* 1993;20(2):101-119.

154. Ritz-Timme S, Eckelt N, Schmidtke E, Thomsen H. Genesis and diagnostic value of leukocyte and platelet accumulations around "air bubbles" in blood after venous air embolism. *International journal of legal medicine.* 1997;111(1):22-26.

155. Hoffman M, Monroe DM, 3rd. A cell-based model of hemostasis. *Thromb Haemost.* 2001;85(6):958-965.

156. Xu LC, Bauer JW, Siedlecki CA. Proteins, platelets, and blood coagulation at biomaterial interfaces. *Colloids Surf B Biointerfaces.* 2014;124:49-68.

157. Gideon P, Thomsen C, Gjerris F, Sorensen PS, Stahlberg F, Henriksen O. Measurement of blood flow in the superior sagittal sinus in healthy volunteers, and in patients with normal pressure hydrocephalus and idiopathic intracranial hypertension with phase-contrast cine MR imaging. *Acta Radiol.* 1996;37(2):171-176.

158. Tamari Y, Lee-Sensiba K, Leonard EF, Tortolani AJ. A dynamic method for setting roller pumps nonocclusively reduces hemolysis and predicts retrograde flow. *ASAIO J.* 1997;43(1):39-52.

159. Sienco®. Sonoclot Coagulation & Platelet Function Analyzer with graphics Printer For In Vitro Diagnostic Use. Operator's Manual For Firmware Version 4.0 In: Arvada, CO 8003 USA2004: http://www.sienco.com/sonoclot-usa/020-1001_user_manual_r401.pdf. Accessed 2015 April 5.

160. Vandersteene J, Van Den Berghe T, Planckaert G, De Somer F, Baert E, Van Roost D. A corrected method for analysing impurities on two dimensional projected images of cilindrical objects. 2017.

161. Tobias MD, Wambold D, Pilla MA, Greer F. Differential effects of serial hemodilution with hydroxyethyl starch, albumin, and 0.9% saline on whole blood coagulation. *J Clin Anesth.* 1998;10(5):366-371.

162. Kuriyama N, Tokuda T, Yamada K, et al. Flow velocity of the superior sagittal sinus is reduced in patients with idiopathic normal pressure hydrocephalus. *J Neuroimaging.* 2011;21(4):365-369.

163. Hirabuki N, Watanabe Y, Mano T, et al. Quantitation of flow in the superior sagittal sinus performed with cine phase-contrast MR imaging of healthy and achondroplastic children. *AJNR Am J Neuroradiol.* 2000;21(8):1497-1501.

164. Seckold T, Walker S, Dwyer T. A comparison of silicone and polyurethane PICC lines and postinsertion complication rates: a systematic review. *The journal of vascular access.* 2015;16(3):167-177.

165. Wildgruber M, Lueg C, Borgmeyer S, et al. Polyurethane versus silicone catheters for central venous port devices implanted at the forearm. *European journal of cancer (Oxford, England : 1990).* 2016;59:113-124.

166. Teilmann AC, Falkenberg MK, Hau J, Abelson KS. Comparison of silicone and polyurethane catheters for the catheterization of small vessels in mice. *Lab animal.* 2014;43(11):397-403.

167. Adipurnama I, Yang MC, Ciach T, Butruk-Raszeja B. Surface modification and endothelialization of polyurethane for vascular tissue engineering applications: a review. *Biomaterials science.* 2016;5(1):22-37.

168. Xu LC, Siedlecki CA. Protein adsorption, platelet adhesion, and bacterial adhesion to polyethylene-glycol-textured polyurethane biomaterial surfaces. *Journal of biomedical materials research Part B, Applied biomaterials.* 2017;105(3):668-678.

169. Penn RD, Lee MC, Linninger AA, Miesel K, Lu SN, Stylos L. Pressure gradients in the brain in an experimental model of hydrocephalus. *J Neurosurg.* 2005;102(6):1069-1075.

170. Yamada H, Yokota A, Haratake J, Horie A. Morphological study of experimental syringomyelia with kaolin-induced hydrocephalus in a canine model. *J Neurosurg.* 1996;84(6):999-1005.

171. Catalao CHR, Shimizu GY, Tida JA, et al. Environmental enrichment reduces brain damage in hydrocephalic immature rats. *Childs Nerv Syst.* 2017;33(6):921-931.

172. M. Czosnyka, Whitfield P. Hydrocephalus. A Practical Guide to CSF Dynamics and Ventriculoperitoneal Shunts. *Advances in Clinical Neurosciences and Rehabilitation.* 2006;6(No. 3, (July/August 2006)): 14-17.

173. Tschan CA, Antes S, Huthmann A, Vulcu S, Oertel J, Wagner W. Overcoming CSF overdrainage with the adjustable gravitational valve proSA. *Acta Neurochir (Wien).* 2014;156(4):767-776; discussion 776.

174. Patwardhan RV, Nanda A. Implanted ventricular shunts in the United States: the billion-dollar-a-year cost of hydrocephalus treatment. *Neurosurgery.* 2005;56(1):139-144; discussion 144-135.

175. Vandersteene J, Baert E, Schauvliege S, et al. A non-hydrocephalic goat experimental model to evaluate a ventriculosinus shunt. *Laboratory animals.* 2018:23677217753976.

176. Johnston MG, Del Bigio MR, Drake JM, Armstrong D, Di Curzio DL, Bertrand J. Pre- and post-shunting observations in adult sheep with kaolin-induced hydrocephalus. *Fluids Barriers CNS.* 2013;10:24.

177. Eskandari R, Packer M, Burdett EC, McAllister JP, 2nd. Effect of delayed intermittent ventricular drainage on ventriculomegaly and neurological deficits in experimental neonatal hydrocephalus. *Childs Nerv Syst.* 2012;28(11):1849-1861.

178. Belgian Royal Decree of 29 May 2013 on the protection of animals used for scientific purposes. In. *Belgisch Staatsblad* 29 May 2013.

179. Directive 2010/63/EU of the European Parliament and the Council of 22 September 2010 on the protection of animals used for scientific purposes. In. *Official Journal of the European Union,* 22.09.2010.

180. James AE, Jr., Flor WJ, Bush M, Merz T, Rish BL. An experimental model for chronic communicating hydrocephalus. *J Neurosurg.* 1974;41(1):32-37.

181. DeFeo DR, Myers P, Foltz EL, Everett B, Ramshaw B. Histological examination of kaolin-induced hydrocephalus. Its implications in the therapy of animals with experimentally induced hydrocephalus. *J Neurosurg.* 1979;50(1):7O-4.

182. Di Curzio DL, Buist RJ, Del Bigio MR. Reduced subventricular zone proliferation and white matter damage in juvenile ferrets with kaolin-induced hydrocephalus. *Exp Neurol.* 2013;248:112-128.

183. Torvik A, Murthy VS. The spinal cord central canal in kaolin-induced hydrocephalus. *J Neurosurg.* 1977;47(3):397-402.

184. Barbone R, Bortolami R. *Anatomie comparée des mammifères domestiques.* Vol 6 Neurologie I Système nerveux central: Vigot Freres, Editeurs; 2004.

185. Bradbury MW, Lathem W. A flow of cerebrospinal fluid along the central canal of the spinal cord of the rabbit and communications between this canal and the sacral subarachnoid space. *J Physiol.* 1965;181(4):785-800.

186. Gonzalez-Darder J, Barbera J, Cerda-Nicolas M, Segura D, Broseta J, Barcia-Salorio JL. Sequential morphological and functional changes in kaolin-induced hydrocephalus. *J Neurosurg.* 1984;61(5):918-924.

187. Boulton M, Flessner M, Armstrong D, Hay J, Johnston M. Determination of volumetric cerebrospinal fluid absorption into extracranial lymphatics in sheep. *Am J Physiol.* 1998;274(1 Pt 2):R88-96.

188. Silver I, Kim C, Mollanji R, Johnston M. Cerebrospinal fluid outflow resistance in sheep: impact of blocking cerebrospinal fluid transport through the cribriform plate. *Neuropathol Appl Neurobiol.* 2002;28(1):67-74.

189. Bloch O, Auguste KI, Manley GT, Verkman AS. Accelerated progression of kaolin-induced hydrocephalus in aquaporin-4-deficient mice. *J Cereb Blood Flow Metab.* 2006;26(12):1527-1537.

190. Del Bigio MR, Kanfer JN, Zhang YW. Myelination delay in the cerebral white matter of immature rats with kaolin-induced hydrocephalus is reversible. *J Neuropathol Exp Neurol.* 1997;56(9):1053-1066.

191. Cardoso EJ, Lachat JJ, Lopes LS, Santos AC, Colli BO. Changes caused by hydrocephalus, induced by kaolin, in the corpus callosum of adult dogs. *Acta Cir Bras.* 2011;26 Suppl 2:8-14.

192. Baert E, Dewaele F, Vandersteene J, Hallaert G, Kalala J-PO, Van Roost D. Treating Hydrocephalus with Retrograde VentriculoSinus Shunt. Prospective Clinical Study. *Journal of Neurosurgery, submitted.* 2017.

193. Shafei ILE, Shafei HIE, Inventors; Google Patents, assignee. Device for implantation of retrograde ventriculo-sinus shunt. US patent US7998103 B2. Aug 16, 2011, 2011.

194. Pinto FC, Becco R, Alho EJ, et al. The Retrograde Ventriculosinusal Shunt in an Animal Experimental Model of Hydrocephalus. *Pediatr Neurosurg.* 2016;51(3):142-148.

195. (IACUC IACaUC. Institutional Animal Care and Use Committee (IACUC). 2011. Guideline Humane Intervention and Endpoints for Laboratory Animal Species. In:2011.

196. Holton L, Pawson P, Nolan A, Reid J, Scott EM. Development of a behaviour-based scale to measure acute pain in dogs. *Vet Rec.* 2001;148(17):525-531.

197. Hett DA, Walker D, Pilkington SN, Smith DC. Sonoclot analysis. *Br J Anaesth.* 1995;75(6):771-776.

198. Thomale UW, Knitter T, Schaumann A, et al. Smartphone-assisted guide for the placement of ventricular catheters. *Childs Nerv Syst.* 2013;29(1):131-139.

199. Andrews BT, Dujovny M, Mirchandani HG, Ausman JI. Microsurgical anatomy of the venous drainage into the superior sagittal sinus. *Neurosurgery.* 1989;24(4):514-520.

200. Goossens GA. Flushing and Locking of Venous Catheters: Available Evidence and Evidence Deficit. *Nurs Res Pract.* 2015;2015:985686.

201. Conti A, Sanchez-Ruiz Y, Bachi A, et al. Proteome study of human cerebrospinal fluid following traumatic brain injury indicates fibrin(ogen) degradation products as trauma-associated markers. *J Neurotrauma.* 2004;21(7):854-863.

202. Cook MA, Watkins-Pitchford JM. Epidural blood patch: a rapid coagulation response. *Anesth Analg.* 1990;70(5):567-568.

203. Khodadoust AA, Stark WJ, Bell WR. Coagulation properties of intraocular humors and cerebrospinal fluid. *Invest Ophthalmol Vis Sci.* 1983;24(12):1616-1619.

204. Lam CH, Villemure JG. Comparison between ventriculoatrial and ventriculoperitoneal shunting in the adult population. *Br J Neurosurg.* 1997;11(1):43-48.

205. McGovern RA, Kelly KM, Chan AK, Morrissey NJ, McKhann GM, 2nd. Should ventriculoatrial shunting be the procedure of choice for normal-pressure hydrocephalus? *J Neurosurg.* 2014;120(6):1458-1464.

206. Vernet O, Campiche R, de Tribolet N. Long-term results after ventriculoatrial shunting in children. *Childs Nerv Syst.* 1993;9(5):253-255.

207. Oliveira MF, Teixeira MJ, Norremose KA, et al. Surgical technique of retrograde ventricle-sinus shunt is an option for the treatment of hydrocephalus in infants after surgical repair of myelomeningocele. *Arq Neuropsiquiatr.* 2015;73(12):1019-1025.

208. Baert E, Vandersteene J, Dewaele F, Desomer F, Vantilborgh A, Van Roost D. A new non-occlusive roller pump model for in vitro evaluation of intravascular devices. *Acta Biomaterialia.* Submitted, 2017.

209. Fareed J, Callas DD, Hoppensteadt D, Bermes EW, Jr. Tissue factor antigen levels in various biological fluids. *Blood Coagul Fibrinolysis.* 1995;6 Suppl 1:S32-36.

210. Van Dreden P, Hue G, Dreyfus JF, Woodhams B, Vasse M. Procoagulant phospholipids and tissue factor activity in cerebrospinal fluid from patients with intracerebral haemorrhage. *Adv Hematol.* 2014;2014:576750.

211. Yavuz C, Demirtas S, Caliskan A, et al. Reasons, procedures, and outcomes in ventriculoatrial shunts: A single-center experience. *Surg Neurol Int.* 2013;4:10.

212. Borow M, Crowley JG. Evaluation of central venous catheter thrombogenicity. *Acta Anaesthesiol Scand Suppl.* 1985;81:59-64.

213. Boswald M, Lugauer S, Bechert T, Greil J, Regenfus A, Guggenbichler JP. Thrombogenicity testing of central venous catheters in vitro. *Infection.* 1999;27 Suppl 1:S30-33.

214. Biran R, Pond D. Heparin coatings for improving blood compatibility of medical devices. *Adv Drug Deliv Rev.* 2017;112:12-23.

215. Murphy E, Lu J, Lewis A, Brewer J, Russell J, Stratford P. Characterization of Protein Adsorption at the Phosphorylcholine Incorporated Polymer− Water Interface. *Macromolecules.* 2000;33(12):4545-4554.

216. De Somer F, Francois K, van Oeveren W, et al. Phosphorylcholine coating of extracorporeal circuits provides natural protection against blood activation by the material surface. *Eur J Cardiothorac Surg.* 2000;18(5):602-606.

217. Anton N, Cox PN, Massicotte MP, et al. Heparin-bonded central venous catheters do not reduce thrombosis in infants with congenital heart disease: a blinded randomized, controlled trial. *Pediatrics.* 2009;123(3):e453-458.

218. Pierce CM, Wade A, Mok Q. Heparin-bonded central venous lines reduce thrombotic and infective complications in critically ill children. *Intensive Care Med.* 2000;26(7):967-972.

219. El-Shafei IL, El-Shafei HI. The retrograde ventriculosinus shunt: concept and technique for treatment of hydrocephalus by shunting the cerebrospinal fluid to the superior sagittal sinus against the direction of blood flow. Preliminary report. *Child's nervous system : ChNS : official journal of the International Society for Pediatric Neurosurgery.* 2001;17(8):457-465; discussion 466.

220. Sevastianov VI, Parfeev VM. Fatigue and hemocompatibility of polymer materials. *Artificial organs.* 1987;11(1):20-25.

221. Hugoni L, Montano-Machado V, Yang M, Pauthe E, Mantovani D, Santerre JP. Fibronectin adsorption on surface-modified polyetherurethanes and their differentiated effect on specific blood elements related to inflammatory and clotting processes. *Biointerphases.* 2016;11(2):029809.

222. Major TC, Brisbois EJ, Jones AM, et al. The effect of a polyurethane coating incorporating both a thrombin inhibitor and nitric oxide on hemocompatibility in extracorporeal circulation. *Biomaterials.* 2014;35(26):7271-7285.

223. Chadduck WM, Crabtree HM, Blankenship JB, Adametz J. Transcranial Doppler ultrasonography for the evaluation of shunt malfunction in pediatric patients. *Child's nervous system : ChNS : official journal of the International Society for Pediatric Neurosurgery.* 1991;7(1):27-30.

224. Goh D, Minns RA. Intracranial pressure and cerebral arterial flow velocity indices in childhood hydrocephalus: current review. *Child's nervous system : ChNS : official journal of the International Society for Pediatric Neurosurgery.* 1995;11(7):392-396.

225. Goh D, Minns RA, Hendry GM, Thambyayah M, Steers AJ. Cerebrovascular resistive index assessed by duplex Doppler sonography and its relationship to intracranial pressure in infantile hydrocephalus. *Pediatric radiology.* 1992;22(4):246-250.

226. Borgesen SE, Pieri A, Cappelen J, Agerlin N, Gjerris F. Shunting to the cranial venous sinus using the SinuShunt. *Child's nervous system : ChNS : official journal of the International Society for Pediatric Neurosurgery.* 2004;20(6):397-404.